PB86-111705

# Evaluation of Pilot-Scale Air Pollution Control Devices on a Refuse and Coal-Fired Boiler

PEDCo-Environmental, Inc., Cincinnati, OH

Prepared for

Environmental Protection Agency
Cincinnati, OH

Oct 85

**U.S. Department of Commerce**
**National Technical Information Service**
**NTIS**

PB86-111705

EPA/600/2-85/121
October 1985

# EVALUATION OF PILOT - SCALE AIR POLLUTION CONTROL DEVICES ON A REFUSE AND COAL-FIRED BOILER

by

Fred D. Hall, John M. Bruck, Dione N. Albrinck
PEDCo Environmental, Inc.
Cincinnati, Ohio 45246

Contract No. 68-03-2509

Project Officers

Michael I. Black
and
Robert A. Olexsey
Alternative Technologies Division
Hazardous Waste Engineering Research Laboratory
Cincinnati, Ohio 45268

HAZARDOUS WASTE ENGINEERING RESEARCH LABORATORY
OFFICE OF RESEARCH AND DEVELOPMENT
U. S. ENVIRONMENTAL PROTECTION AGENCY
CINCINNATI, OHIO 45268

REPRODUCED BY
NATIONAL TECHNICAL
INFORMATION SERVICE
U.S. DEPARTMENT OF COMMERCE
SPRINGFIELD, VA. 22161

## TECHNICAL REPORT DATA
*(Please read Instructions on the reverse before completing)*

| | | |
|---|---|---|
| 1. REPORT NO.<br>EPA/600/2-85/121 | 2. | 3. RECIPIENT'S ACCESSION NO.<br>PB8 6 111705/AS |
| 4. TITLE AND SUBTITLE<br>EVALUATION OF PILOT-SCALE AIR POLLUTION CONTROL DEVICES ON A REFUSE & COAL-FIRED BOILER | | 5. REPORT DATE<br>October 1985 |
| | | 6. PERFORMING ORGANIZATION CODE |
| 7. AUTHOR(S)<br>F.D. Hall, J.M. Bruck, D.N. Albrinck | | 8. PERFORMING ORGANIZATION REPORT NO. |
| 9. PERFORMING ORGANIZATION NAME AND ADDRESS<br>PEDco,Inc.<br>Cincinati, Ohio 45246 | | 10. PROGRAM ELEMENT NO. |
| | | 11. CONTRACT/GRANT NO.<br>68-03-2509 |
| 12. SPONSORING AGENCY NAME AND ADDRESS<br>Hazardous Waste Engineering Research Laboratory<br>Office of Research and Development<br>U.S. EPA<br>Cincinnati, OH 45268 | | 13. TYPE OF REPORT AND PERIOD COVERED<br>Project Report 6/77-6/80 |
| | | 14. SPONSORING AGENCY CODE<br>EPA/600/12 |

15. SUPPLEMENTARY NOTES
Michael Black, P.O.; Robert A. Olexsey (513) 569-77717

16. ABSTRACT

This project report describes the operation of pilot-scale air pollution control devices to gather data on air pollution efficiency versus several different operating parameters on various waste-as-fuel combustion processes. It also includes a test of a full scale fabric filter used to control dust emissions. The refuse-derived fuel is burned, along with pulverized coal, in a suspension-fired boiler. The pilot device testing program involved the evaluation of pollutant removal efficiency of a mobile electrostatic precipitator (ESP) and a mobile scrubber.

17. KEY WORDS AND DOCUMENT ANALYSIS

| a. DESCRIPTORS | b. IDENTIFIERS/OPEN ENDED TERMS | c. COSATI Field/Group |
|---|---|---|
| | | |

| | | |
|---|---|---|
| 18. DISTRIBUTION STATEMENT<br>RELEASE TO PUBLIC | 19. SECURITY CLASS *(This Report)*<br>UNCLASSIFIED | 21. NO. OF PAGES |
| | 20. SECURITY CLASS *(This page)*<br>UNCLASSIFIED | 22. PRICE |

EPA Form 2220-1 (Rev. 4-77) PREVIOUS EDITION IS OBSOLETE

## NOTICE

This document has been reviewed in accordance with U.S. Environmental Protection Agency policy and approved for publication. Mention of trade names or commercial products does not constitute endorsement or recommendation for use.

# FOREWORD

Today's rapidly developing and changing technologies and industrial products and practices frequently carry with them the increased generation of solid and hazardous wastes. These materials, if improperly dealt with, can threaten both public health and the environment. Abandoned waste sites and accidental releases of toxicand hazardous substances to the environment also have important environmental and public health implications. The Hazardous Waste Engineering Research Laboratory assists in providing an authoritative and defensible engineering basis for assessing and solving these problems. Its products support the policies, programs and regulations of the Environmental Protection Agency, the permitting and other responsibilities of State and local governments and the needs of both large and small businesses in handling their wastes responsibly and economically.

This project report entails the operation of pilot-scale air pollution control devices on a suspension-fired boiler burning pulverized coal and refuse-derived fuel. The pilot-scale devices tested were a mobile Electrostatic precipitator, a mobile scrubber, and a fabric filter.

The information contained herein will be of interest to those designers or users who are contemplating or working with a system similar to the Ames system. Requests for further information regarding the production and utilization of refuse-derived fuel should be directed to the Thermal Destruction Branch, HWERL, Cincinnati,

David G. Stephan, Director
Hazardous Waste Engineering Research Laboratory

# ABSTRACT

This project report describes the operation of pilot-scale air pollution control devices to gather data on air pollution efficiency versus several different operating parameters on various waste-as-fuel combustion processes. It also includes a test of a full scale fabric filter used to control dust emissions. The refuse-derived fuel is burned, along with pulverized coal, in a suspension-fired boiler. The pilot device testing program involved the evaluation of pollutant removal efficiency of a mobile electrostatic precipitator (ESP) and a mobile scrubber.

## CONTENTS

Page

Figures vii
Tables xi
Acknowledgment xii

1. Introduction 1

2. Facilities 5

3. Experimental Test Plan 9

3.1 Emission Characterization 9
3.2 Engineering aspects of control technique evaluation 13

4. EPA Pilot Air Pollution Control Equipment 23

4.1 Mobile ESP 23
4.2 Mobile scrubber 28
4.3 Pilot fabric filter 32

5. Presentation of Results 43

5.1 Fuel analysis 43
5.2 Mobile ESP 46
5.3 Mobile scrubber 61
5.4 Pilot fabric filter 75

6. Quality Assurance 99

6.1 Reference methods 99
6.2 Calibration procedures 99
6.3 Performance audits 102
6.4 Sample integrity 104
6.5 Data validation 104
6.6 Source representativeness 105

7. Test Summary 115

7.1 Mobile ESP 116
7.2 Mobile scrubber 117
7.3 Pilot fabric filter 119
7.4 Overall evaluation 122

CONTENTS (continued)

| | | Page |
|---|---|---|
| 8. | References | 124 |
| Appendix A | Sampling and Analytical Procedures | A-1 |
| Appendix B | Report on Analyses of Particulate Emissions From a Coal-Refuse Derived Fuel (RDF) - Fired Boiler | B-1 |
| Appendix C | Evaluation of the Performance of Mobile Air Pollution Control Devices | C-1 |
| Appendix D | Halide and Trace Metal Emissions From RDF Construction | D-1 |

# FIGURES

No. Page

2-1 Ames Power Plant Layout 7

3-1 Schematic of the IERL/RTP Mobile Control Devices at Ames, Iowa 14

3-2 Schematic of the Pilot Fabric Filter at Ames, Iowa 15

4-1 Plan View of Mobile ESP 25

4-2 ESP Cross Section 26

4-3 ESP Section Rollout 27

4-4 Flow Rectification on Inlet Ductwork 29

4-5 Schematic Plan of EPA Mobile Scrubber Unit 31

4-6 Mobile Scrubber Flow Diagram 33

4-7 Operational Characteristics of Medium Size Venturi Throat 34

4-8 Pilot Fabric Filter Operators Log 38

4-9 Pilot Fabric Filter Maintenance Checklist 40

4-10 Pilot Fabric Filter Multipoint Strip Chart - July 13, 1979 41

4-11 Pilot Fabric Filter Opacity Strip Chart - July 13, 1979 42

5-1 RDF Density and Ash Content in Fuel Measured Over Selected Test Periods 47

5-2 Particulate Removal Efficiency as a Function of Specific Collection Area 57

5-3 Lead Concentration as a Function of RDF Input 58

FIGURES (continued)

| No. | | Page |
|---|---|---|
| 5-4 | Lead Composition as a Function of RDF Input | 60 |
| 5-5 | Mobile Scrubber - Primary Device - Particulate Removal Efficiency as a Function of Venturi Throat Pressure Drop | 68 |
| 5-6 | Particulate Concentration as a Function of RDF Input | 69 |
| 5-7 | Lead Concentration as a Function of RDF Input | 72 |
| 5-8 | Mobile Scrubber - Secondary Device - Particulate Concentration as a Function of Venturi Throat Pressure Drop | 74 |
| 5-9 | Mobile Scrubber - Secondary Device - Particulate Removal Efficiency as a Function of RDF Input | 76 |
| 5-10 | Particulate Removal Efficiency as a Function of RDF Input | 83 |
| 5-11 | Particulate Removal Efficiency as a Function of Fabric Filter Pressure Drop | 88 |
| 5-12 | Uncontrolled Lead Concentration as a Function of RDF Input | 89 |
| 5-13 | Cadmium Concentration as a Function of RDF Input | 90 |
| 5-14 | Copper Concentration as a Function of RDF Input | 91 |
| 5-15 | Zinc Concentration as a Function of RDF Input | 92 |
| 5-16 | Iron Concentration as a Function of RDF Input | 93 |
| 5-17 | Chloride Concentration as a Function of RDF Input | 95 |
| 5-18 | Fluoride Concentration as a Function of RDF Input | 96 |
| 5-19 | Sulfur Oxide Emissions as a Function of RDF Input | 98 |
| 6-1 | Calibration Setup | 101 |
| 6-2 | Calibration Data Sheet | 101 |

FIGURES (continued)

| No. | | Page |
|---|---|---|
| 6-3 | Properly Constructed Type S Pitot Tube | 103 |
| 6-4 | Mobile ESP and Fabric Filter Slipstream Nozzle Detail | 108 |
| 6-5 | Slipstream Isokinetic Ranges for Each Mobile Device Operating Range (Velocity at Point of Slipstream/Velocity in Main Duct) | 110 |
| 6-6 | Slipstream Nozzle Details | 114 |

## TABLES

| No. |  | Page |
|---|---|---|
| 1-1 | PEDCo Resource Recovery Site Visit Summary | 3 |
| 2-1 | Characteristics of Boiler No. 7, Ames Municipal Power Plant | 6 |
| 3-1 | Sampling and Analytical Plan | 12 |
| 3-2 | Mobile ESP Test Plan--Operating Matrix | 17 |
| 3-3 | Mobile Scrubber Test Plan--Operating Matrix | 19 |
| 3-4 | Pilot Fabric Filter Test Plan--Operating Matrix | 22 |
| 5-1 | Average Fuel Analyses - Mobile Scrubber and ESP Test Runs Only | 44 |
| 5-2 | Average Fuel Analyses - Mobile Fabric Filter Test Runs Only | 45 |
| 5-3 | Differences in Elemental Composition Between Coal and RDF Fuel Samples From ESP and Scrubber Tests Only | 48 |
| 5-4 | Boiler No. 7 Operating Conditions During Mobile ESP Tests | 49 |
| 5-5 | Mobile ESP Operating Conditions | 51 |
| 5-6 | Mobile ESP Emission Concentrations | 52 |
| 5-7 | Boiler No. 7 Operating Conditions During Mobile Scrubber Testing | 62 |
| 5-8 | Mobile Scrubber Operating Conditions | 63 |
| 5-9 | Mobile Scrubber Emission Concentrations | 64 |
| 5-10 | Boiler No. 7 Operating Conditions During Fabric Filter Test Runs | 77 |

## TABLES (continued)

| No. | | Page |
|---|---|---|
| 5-11 | Mobile Fabric Filter Operating Conditions | 79 |
| 5-12 | Particulate Removal Efficiency as a Function of Test Group | 82 |
| 5-13 | Mobile Fabric Filter Emission Concentrations | 85 |
| 6-1 | Results of Randomly Splitting and Spiking Samples for Analysis | 106 |
| 6-2 | Isokinetic Comparison of Each Slipstream | 109 |
| 6-3 | Same-Day Comparisons Mobile ESP/Scrubber Inlet Particulate Concentrations | 112 |

# ACKNOWLEDGMENT

This report was prepared by PEDCo Environmental, Inc., under EPA Contract No. 68-03-2509. The PEDCo Project Director was Mr. Timothy W. Devitt, and Project Manager was Mr. Fred D. Hall. The principal authors were Ms. Diane N. Albrinck and Mr. John M. Bruck, with assistance from several members of PEDCo's technical staff, especially Ms. Carolyn Kulwicki and Ms. Mary Taft.

# SECTION 1

# INTRODUCTION

Under contract to the U.S. Environmental Protection Agency (EPA), PEDCo Environmental, Inc., conducted a sampling and analysis program at the Ames, Iowa, refuse-derived fuel (RDF) and coal co-firing facility. This program was conducted as part of Federal Contract Number 68-03-2509, "Air Pollution Control Technology Development for Waste-as-Fuel Processes."

The project included the operation of pilot-scale air pollution control devices to gather data on air pollution control efficiency versus several different operating parameters on various waste-as-fuel combustion processes. It also included a test of a full-scale fabric filter used to control dust emissions from the Ames RDF processing facility. (The results of this task are reported under separate cover.[1])

This report covers the results of operating, sampling, and analytical efforts in conjunction with the pilot-scale device programs at Ames, Iowa. This successfully operating co-firing facility processes municipal solid waste for resource recovery and preparation of RDF. The RDF is subsequently burned, along with pulverized coal, in a suspension-fired boiler.

Early in the project (1977-1978), PEDCo visited several waste-as-fuel facilities considered as candidate sites for this program. Table 1-1 summarizes these visits and presents the status of each site at the time of the visit. This table does not represent an up-to-date status report.

The Ames site was chosen primarily because of the cooperation of city officials, Iowa State University, and EPA personnel. Other advantages included the availability of data from previous and ongoing studies, high reliability of preprocessing and utility operations, and the limited facility modifications required.

The pilot device testing program at Ames involved the evaluation of pollutant removal efficiency of a mobile electrostatic precipitator (ESP) and a mobile scrubber obtained through a program-sharing agreement.

It also involved the evaluation of a pilot fabric filter constructed under this program.

All the pilot devices were slipstreamed on the flue gas from Boiler 7, a suspension-fired boiler that co-fires pulverized coal and RDF. Actual operation and testing of the devices took place in two stages. The mobile ESP and scrubber were evaluated in October and November 1978. The pilot fabric filter was installed and tested in June and July 1979.

Section 2 describes the facilities, Section 3 presents the test plan, Section 4 describes the EPA mobile devices, Section

TABLE 1-1. PEDCo RESOURCE RECOVERY SITE VISIT SUMMARY

| Generic technology | Plant location | Preprocessing product | Preprocessing emissions control | RDF combustion equipment | Combustion emission control device |
|---|---|---|---|---|---|
| Co-firing | Ames, Iowa | Fluff | Baghouse system | Pulverized coal and stoker-boiler | ESP |
| | Chicago (SW) | Fluff | Baghouse system | Pulverized-coal boiler | ESP |
| | Columbus, Ohio | Shredded waste | None | Stoker-boiler | Cyclone |
| | Hagerstown, Md. | Pellets | None | Stoker-boiler | Cyclone |
| | Milwaukee, Wis. | Fluff | Baghouse system | Pulverized-coal boiler | ESP |
| Mass burn | Chicago (NW) | Bulky items removed | Not applicable | Incinerator/boiler | ESP |
| | Harrisburg, Pa. | Bulky items removed | Not applicable | Incinerator/boiler | ESP |
| | Nashville, Tenn. | Bulky items removed | Not applicable | Incinerator/boiler | ESP |
| | Saugus, Mass. | As-received refuse | Not applicable | Incinerator/boiler | ESP |
| | Hamilton, Ontario | Pulverized refuse | None | Incinerator/boiler | ESP |
| | Braintree, Mass. | As-received refuse | Not applicable | Incinerator/boiler | ESP |
| Pyrolysis | South Charleston, W. Va. | Shredded waste | None | Open burner | None |
| Other | Fairmont, Minn. | Shredded waste | None | Incinerator/boiler | Wet scrubber |
| | Houston, Texas | Shredded waste | Baghouse | Cement kiln (co-fired with gas) | Wet scrubber |
| | Minneapolis, Minn. | Dewatered sludge | None | Multihearth sludge incinerator | None |

5 presents results of the tests, Section 6 discusses quality assurance, and Section 7 summarizes the report.

The appendixes contain sampling and analytical procedures and special reports from Brehm Laboratory and Midwest Research Institute, which discuss chemical analyses of particulate samples and evaluation of performance of the mobile ESP and scrubber, respectively.

## SECTION 2

## FACILITIES

The Ames Power Plant is owned and operated by the Ames Municipal Electric System. It is situated in the business area of the city, which is in Story County, Iowa. The Ames Solid Waste Recovery System (adjacant to the power plant) is a continuously operating system that processes municipal solid waste (MSW) for use as supplemental fuel in the Ames Power Plant.

The solid waste plant is capable of processing 136 Mg/day (150 tons/day) of "as received" MSW. A storage bin, which lies between the solid waste plant and the power plant, is capable of storing 454 Mg (500 tons) of RDF.[1] Operations at the processing plant consist of two stages of shredding, ferrous metal recovery, two stages of screening, and air density separation.

Suspension-fired Boiler No. 7 was used throughout the test program. The unit, which was installed in 1968, burns pulverized coal and RDF with a tangential firing mechanism. Table 2-1 presents the design and operating characteristics of this boiler.[2]

Figure 2-1 shows the complete power plant layout. The pilot device testing area is just northeast of the Unit No. 7 addition. This location provided direct access to slipstream ductwork from the boiler breeching that carries "uncontrolled" flue gas. All

TABLE 2-1. CHARACTERISTICS OF BOILER NO. 7, AMES MUNICIPAL POWER PLANT

| | |
|---|---|
| Manufacturer | Engineering combustion |
| Installation date | 1968 |
| Steam pressure/temperature | 490°C (900°F)/59,800 cm W.G. (23.500 in. W.G.) |
| Nominal steam output capacity | 160 Mg/h (360,000 lb/h) |
| Furnace pressure | Balanced draft |
| Dust collection equipment | American electrostatic precipitator |
| Heat input at nominal capacity | 460 GJ/h (436 x $10^6$ Btu/h) |

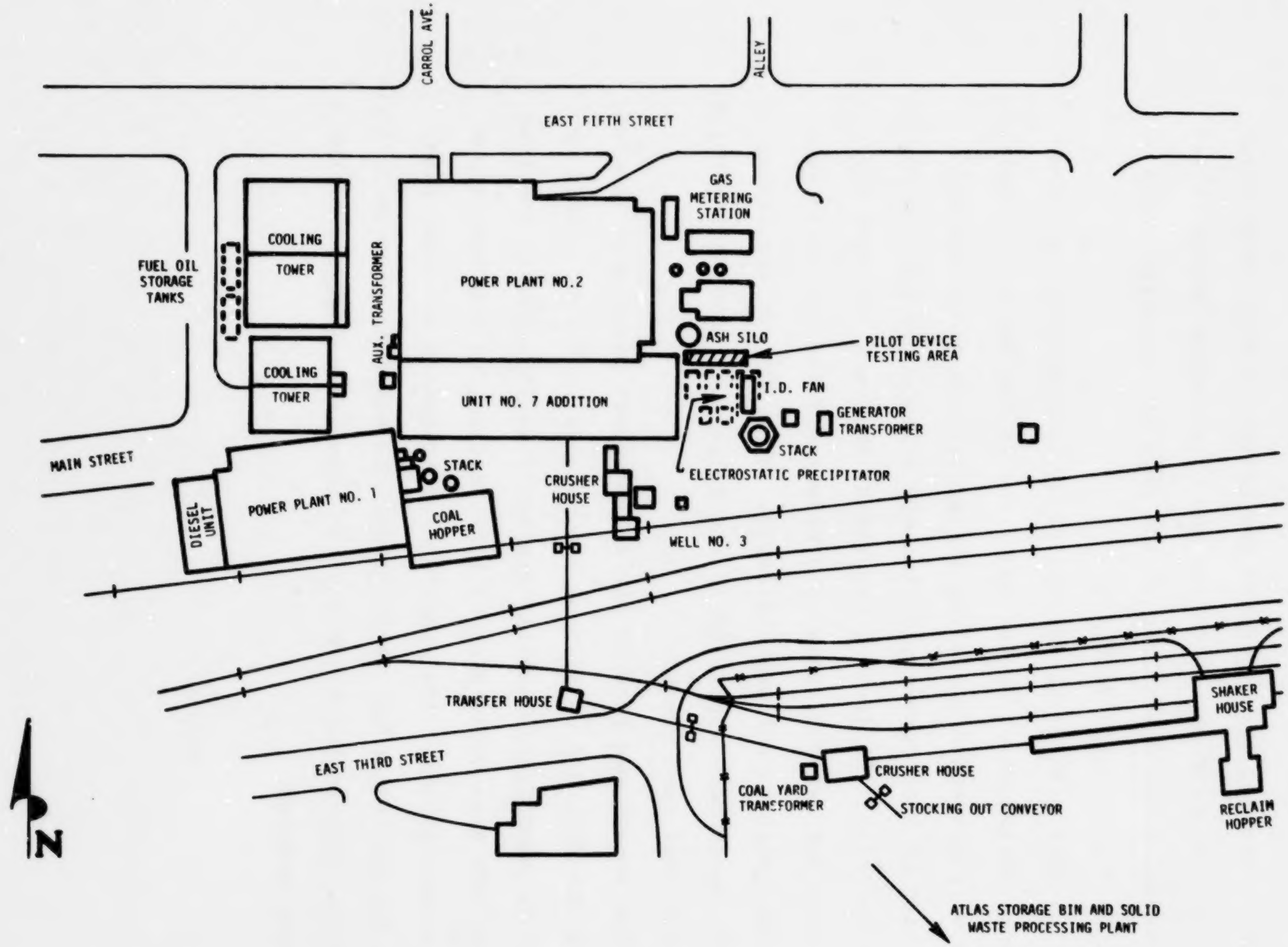
CARROL AVE.
ALLEY
EAST FIFTH STREET
GAS METERING STATION
FUEL OIL STORAGE TANKS
COOLING TOWER
AUX. TRANSFORMER
POWER PLANT NO.2
ASH SILO
PILOT DEVICE TESTING AREA
I.D. FAN
GENERATOR TRANSFORMER
COOLING TOWER
UNIT NO. 7 ADDITION
STACK
ELECTROSTATIC PRECIPITATOR
MAIN STREET
STACK
CRUSHER HOUSE
DIESEL UNIT
POWER PLANT NO. 1
COAL HOPPER
WELL NO. 3
TRANSFER HOUSE
SHAKER HOUSE
EAST THIRD STREET
CRUSHER HOUSE
COAL YARD TRANSFORMER
STOCKING OUT CONVEYOR
RECLAIM HOPPER
N
ATLAS STORAGE BIN AND SOLID WASTE PROCESSING PLANT

Figure 2-1. Ames power plant layout.

the pilot devices were operated and tested in this area; this included the scrubber, which was the only device tested while slipstreaming gas downstream of the main ESP in addition to treating uncontrolled flue gas.

The test program objectives required extensive baseline testing, during which no RDF was fired in the boiler. Baseline tests were attempted while the RDF processing plant was not operating or when capacity of the RDF storage bin was too low to allow cofiring. As testing proceeded, however, RDF runs were made when RDF was available, and baseline coal-only tests were performed when no RDF was available. When RDF was available, utility personnel cooperated to the fullest in maintaining boiler load and fuel feed rates.

The volumetric flow of RDF to the power plant over the test period was recorded as part of the data on each run. Based on operating experience, utility engineers would estimate the feed rate of RDF that would yield a high, medium, or low heat input over a test period. The exact RDF contribution to total heat input to the boiler was later calculated based on volumetric flow readings taken in the field and the laboratory analysis of RDF and coal samples.

# SECTION 3

# EXPERIMENTAL TEST PLAN

This section outlines and defines many of the details of the original testing and evaluation plans that were to be applied to the slipstream pilot devices installed on Boiler 7. These tasks can be broadly classified as having two general objectives:

1. To determine the physical and chemical character of emissions from these sources and the effectiveness of each control technology in the control of these emissions.

2. To evaluate the engineering aspects of the use of each control technology in this application, in sufficient detail to provide an accurate design basis for full-scale systems.

The actual test program differs slightly from the original test plan as outlined in this section.

## 3.1 EMISSION CHARACTERIZATION

The primary project objective was to characterize specific pollutant removal efficiencies of each control device under a set of variable conditions, including boiler load, RDF input, and specific device operating parameters. It was assumed that any full-scale installation of these control devices would have to operate with the varying flue gas temperatures and fluctuating flue gas compositions normally encountered in a coal- and RDF-fired boiler. The experimental plan developed was to monitor and measure these two factors, not to modify or control them.

The following characteristics of the inlet and outlet gas streams from each device were to be measured simultaneously:

Total particulate
Halides (chloride, fluoride, and bromide)
Sulfur oxides
Elemental composition of particulate
Selected trace metals
Oxygen
Carbon dioxide

Other gas stream characteristics were also measured in accordance with EPA Reference Methods 2, 3, 4, and 5. Appendix A explains the sampling and test methods used.

In addition to samples of controlled and uncontrolled flue gas, various grab samples also were taken. All 1-liter grab samples were taken concurrently with emissions testing in the event that the analytical data of discrete test runs were compared and evaluated by individual test. The grab samples included unpulverized coal, RDF, unfiltered scrubber liquor, mobile ESP ash, and fabric filter ash.

The unpulverized coal sample (1 liter) was taken at one of the two coal integrators on the main control room level. At this point the coal is about 5 minutes away from entering the boiler. A coal sample taken at this location is assumed to be representative of the total flow of coal to the boiler during a test period.

It is important to note that the Ames utility purchases coal from two suppliers, one in Iowa and one in Colorado. The Iowa coal is less expensive, but it contains a higher sulfur content than the western coal. To comply with the applicable sulfur dioxide ($SO_2$) emission regulation, the utility attempts to burn a 55/45 (Iowa/Colorado) mix.

The RDF samples were taken at the Atlas storage bin, at a point in the "air-vey" system less than 1 minute away from the boiler. The sample [0.028 $m^3$ (1 $ft^3$)] was weighed and recorded, and then halved and quartered until it fit into a 1-liter container.

During each mobile scrubber test run, a sample of unfiltered scrubber liquor was taken from the tank on top of the mobile scrubber trailer. This tank was used as the point for lime addition for pH control.

Ash was obtained from collection hoppers of the mobile ESP and fabric filter during corresponding test runs of each device. Table 3-1 summarizes the sampling and analytical plan.

Acurex operated the mobile ESP and scrubber under contract to AEERL/RTP. PEDCo was responsible for the operation of the pilot fabric filter. PEDCo and Acurex simultaneously tested the mobile ESP and scrubber for separate programs. Testing of the pilot fabric filter was performed solely by PEDCo.

Except for the elemental analyses, all data reported herein resulted from PEDCo's sampling and analytical efforts. Spark source mass spectrometry (SSMS) was used to give a qualitative and semiquantitative elemental analysis of the particulate

## TABLE 3-1. SAMPLING AND ANALYTICAL PLAN

| Sample stream | Collection technique | Chemical species and other parameters determined | Analysis method | Sampling and analysis responsibility |
|---|---|---|---|---|
| Air | | | | |
| Inlet/outlet | Grab | $O_2$ | Fryrite | PEDCo/Acurex |
| | | $CO_2$ | Fryrite | PEDCo/Acurex |
| | SST[a] Source sampling train | Total particulate | EPA Method 5 | PEDCo/Acurex |
| | | Pb, Sb, Cd, Fe, Cu | AAS[b] | PEDCo |
| | | Cl | c | PEDCo |
| | | Br | c | PEDCo |
| | | F | EPA Method 13B | PEDCo |
| | | Inorganic elements | SSMS[d] | PEDCo/Acurex/Brehm[e] |
| | | $SO_2$ | EPA Method 6 | Acurex |
| | | Particle size distribution | Cascade impactor | Acurex |
| Solid | | | | |
| Coal/RDF | Grab/composite | Density[f] | Gravimetric | PEDCo |
| | | Pb, Sb, Cd, Fe, Cu | AAS | PEDCo |
| | | Cl | c | PEDCo |
| | | Br | c | PEDCo |
| | | F | EPA Method 13B | PEDCo |
| | | Inorganic elements | SSMS | PEDCo/Brehm[e] |
| | | Fuel characterization | Ultimate and proximate | PEDCo |
| ESP ash | Grab[g] | | | PEDCo/Acurex |
| Fabric filter ash | Grab[g] | | | PEDCo |
| Liquid | | | | |
| Scrubber liquor | Grab[h] | | | PEDCo |

---

[c] Specific ion probe/titration with $AgNO_3$ or $Hg(NO_3)_2$.

[d] SSMS = spark source mass spectrometry.

[e] Brehm Laboratory - Wright State University.

[f] Only RDF was measured.

[g] Stored for future reference.

[h] Sent to Montgomery Engineering.

[a] SST = source sampling train.

[b] AAS = atomic absorption spectrometry.

collected from Method 5 sampling during mobile ESP and scrubber testing. Particulate samples that were analyzed with SSMS were taken by Acurex concurrently with PEDCo test runs. The SSMS analysis was performed by Brehm Laboratory of Wright State University; their report on these analyses is included as Appendix B. Section 5 presents further discussion and interpretation of these data.

## 3.2 ENGINEERING ASPECTS OF CONTROL TECHNIQUE EVALUATION

All the mobile devices were slipstreamed ahead of the main ESP, and thus drew uncontrolled flue gas and operated as primary control devices. The mobile scrubber was also operated for roughly half the program during the slipstreaming of gas downstream from the main ESP, which simulated operation of an ESP and scrubber in series. In this operating mode, the scrubber is referred to as a secondary device. Figure 3-1 is a schematic of the mobile device setup at Ames during utilization of the IERL/RTP equipment. Figure 3-2 is a schematic of the mobile fabric filter equipment.

The operating parameters of each control device were modified independently to determine their relative impact on specific pollutant removal efficiency. The specific modifications that were made for each device during the test program are discussed in following subsections.

The remainder of this section is divided into discussions of the test plans for each device. Section 4 presents a more detailed discussion of the operating capabilities of each device.

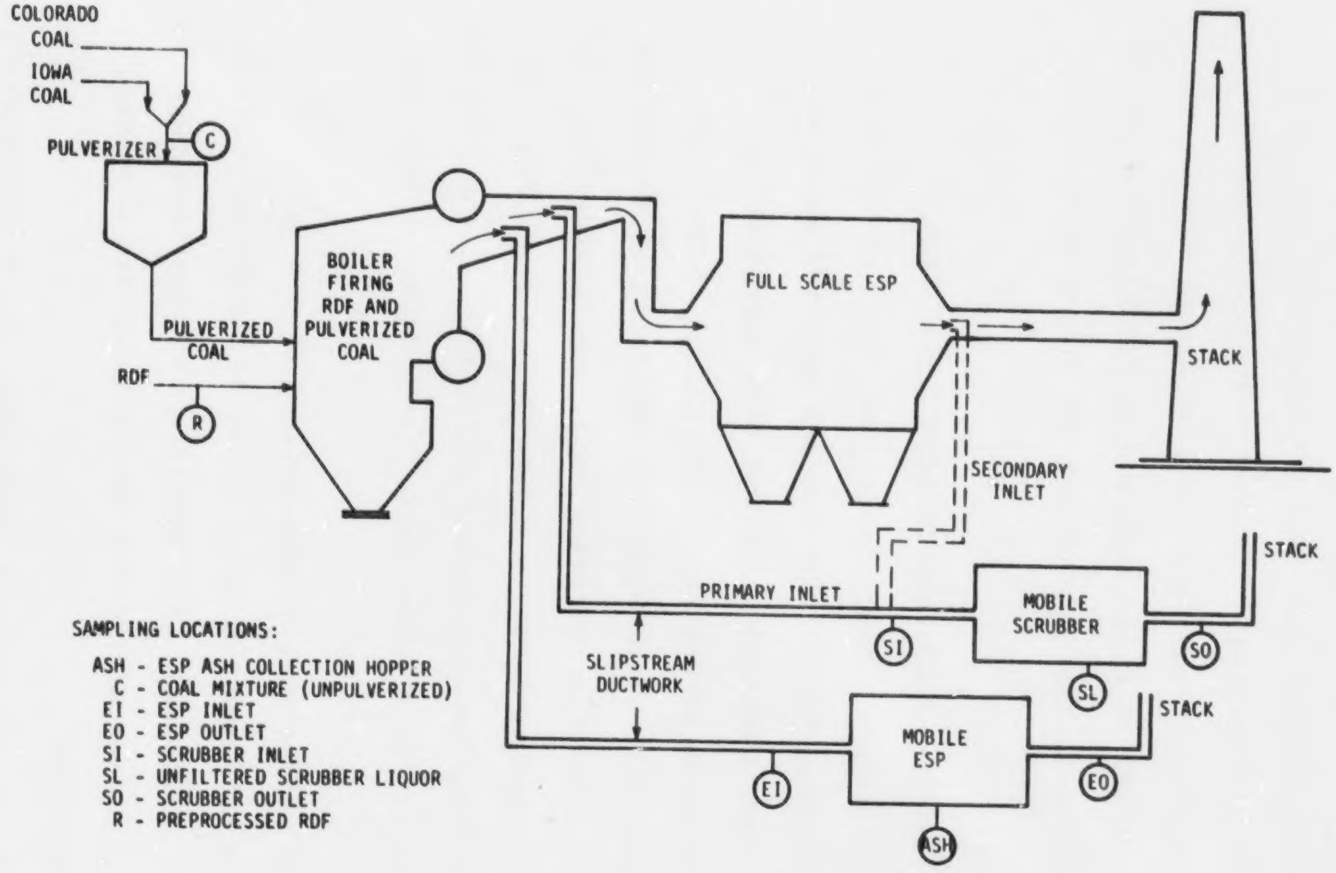
COLORADO COAL
IOWA COAL
PULVERIZER
C
PULVERIZED COAL
RDF
R
BOILER FIRING RDF AND PULVERIZED COAL
FULL SCALE ESP
STACK
SECONDARY INLET
PRIMARY INLET
SLIPSTREAM DUCTWORK
MOBILE SCRUBBER
STACK
SI
SL
SO
MOBILE ESP
STACK
EI
EO
ASH
SAMPLING LOCATIONS:
ASH - ESP ASH COLLECTION HOPPER
C - COAL MIXTURE (UNPULVERIZED)
EI - ESP INLET
EO - ESP OUTLET
SI - SCRUBBER INLET
SL - UNFILTERED SCRUBBER LIQUOR
SO - SCRUBBER OUTLET
R - PREPROCESSED RDF

Figure 3-1. Schematic of the AEERL/RTP mobile control devices at Ames, Iowa.

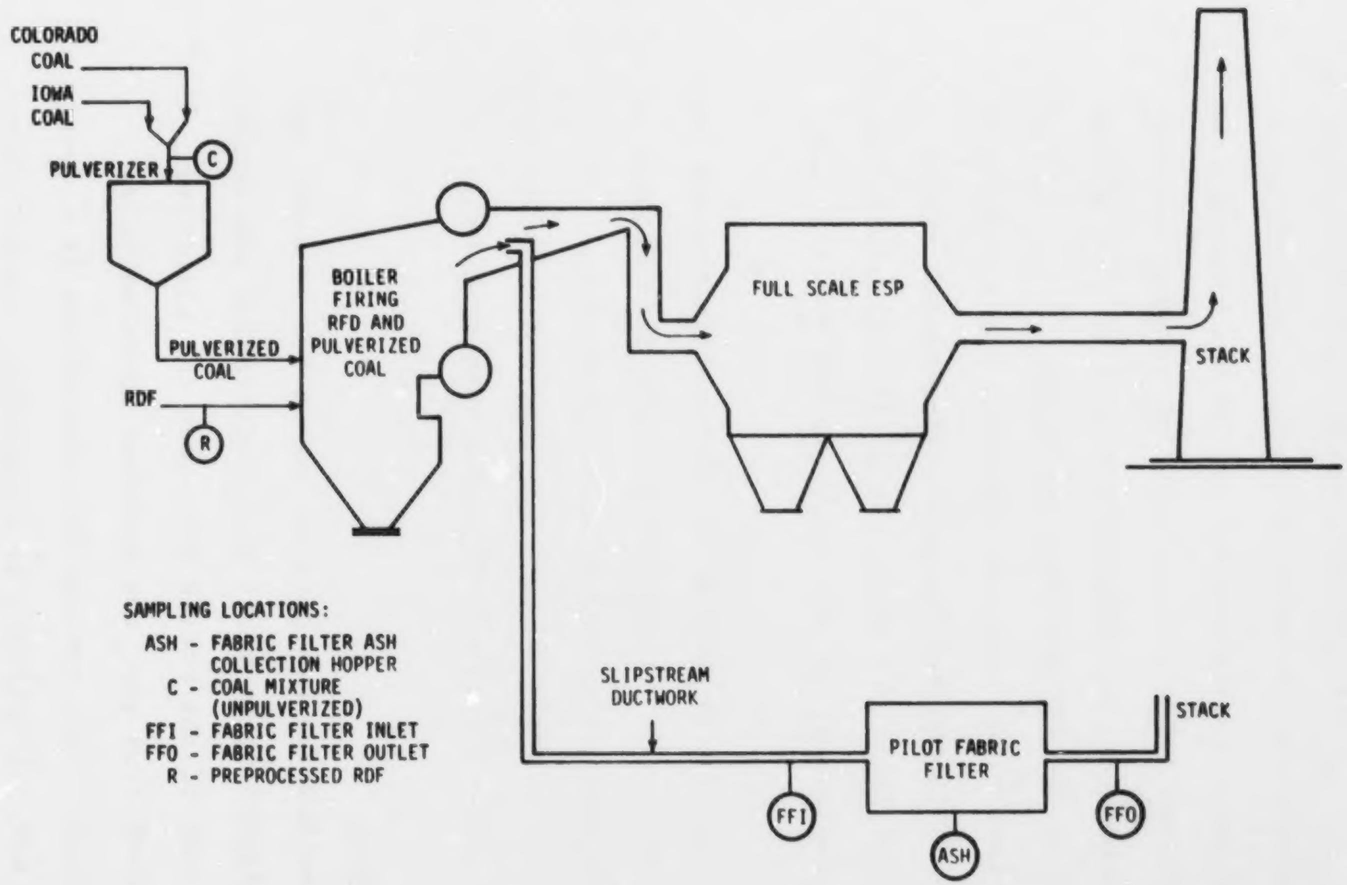
COLORADO COAL
IOWA COAL
PULVERIZER
C
PULVERIZED COAL
RDF
R
BOILER FIRING RFD AND PULVERIZED COAL
FULL SCALE ESP
STACK
SLIPSTREAM DUCTWORK
FFI
PILOT FABRIC FILTER
ASH
FFO
STACK
SAMPLING LOCATIONS:
ASH - FABRIC FILTER ASH COLLECTION HOPPER
C - COAL MIXTURE (UNPULVERIZED)
FFI - FABRIC FILTER INLET
FFO - FABRIC FILTER OUTLET
R - PREPROCESSED RDF

Figure 3-2. Schematic of the pilot fabric filter at Ames, Iowa.

### 3.2.1 Mobile ESP

The operating parameter of primary concern in the operation and testing of the mobile ESP was the specific collection area (SCA), which represents the ratio of the total collection area per unit volume of gas. Theoretically, the higher the SCA, the greater the particulate collection, within, of course, normally accepted design values for this application (7.3 to 27.3 $m^2$ per 1000 $m^3$/min or 130 to 500 $ft^2$ per 1000 $ft^3$/min).

The original test plans required operating the boiler at a coal-only baseline condition and various coal-plus-RDF conditions. The matrix in Table 3-2 shows the different conditions of mobile ESP and boiler operation that were planned for the test program.

Completion of the entire mobile ESP test matrix was not possible. Startup of the unit was delayed for some time because of failure in some structural supports that required repair. The RDF plant also had an untimely shutdown period, which forced more coal-only baseline tests and fewer RDF tests than originally scheduled.

### 3.2.2 Mobile Scrubber

Mobile scrubber testing was carried out in two separate operational phases, depending on where the slipstreamed gas originated. As in the case of the mobile ESP, when the slipstream contained uncontrolled flue gas, the scrubber operated as a primary control device. When the device received gas from downstream of the main ESP, it operated as a secondary control device.

TABLE 3-2. MOBILE ESP TEST PLAN--OPERATING MATRIX

| ESP operating condition | Coal only | Coal plus RDF |
|---|---|---|
| SCA = up to 10.9 $m^2$ per 1000 $m^3/h$ (200 $ft^2$/1000 acfm) | 1 test | 1 test |
| SCA = 16.4 $m^2$ per 1000 $m^3/h$ (300 $ft^2$/1000 acfm) | 5 tests | 5 tests |
| SCA = 21.9 $m^2$ per 1000 $m^3/h$ (400 $ft^2$/1000 acfm) | 3 tests | 3 tests |
| SCA = 27.3 $m^2$ per 1000 $m^3/h$ (500 $ft^2$/1000 acfm) | 1 test | 1 test |

The secondary phase of testing was considered of lower priority in the overall mobile scrubber testing program.

Pressure drop was modified to determine the impact on specific pollutant removal efficiencies. As described in more detail later in this report, pressure drop ($\Delta P$) was controlled by increasing or decreasing flow rate through the device until the desired $\Delta P$ setting, 25.4 to 76.2 cm W.G. (10 to 30 in. W.G.), was obtained. This procedure was not expected to have the significant impact on evaluation of performance that the data analysis will later indicate.

The liquid-to-gas ratio (L/G), the amount of scrubber liquid injected into the venturi throat per unit gas volume, was to be held constant throughout the test program. The gas flow rate was adjusted first to correspond to the desired pressure drop (10, 20, or 30 in. W.G.). The scrubber liquor flow rate was then adjusted to correspond to the incoming gas flow rate. Because each affects the other, an iterative procedure was used to adjust each parameter to its respective value, which produced an L/G value of 2.0 liters/m$^3$ (15.0 gal/1000 ft$^3$).

As with the mobile ESP, this test plan also required operating the boiler at the coal-only baseline condition and at coal-plus-RDF conditions. Table 3-3 presents the test matrix developed before testing.

### 3.2.3 Pilot Fabric Filter

A number of design and operational characteristics affect the performance of a fabric filter. The variable characteristics

TABLE 3-3. MOBILE SCRUBBER TEST PLAN--OPERATING MATRIX

| | Coal only | Coal plus RDF |
|---|---|---|
| Primary device | | |
| ΔP = 25.4 cm W.G. (10 in. W.G.) | 2 tests | 2 tests |
| ΔP = 50.8 cm W.G. (20 in. W.G.) | 1 test | 1 test |
| ΔP = 76.2 cm W.G. (30 in. W.G.) | 2 tests | 2 tests |
| Secondary device | | |
| ΔP = 25.4 cm W.G. (10 in. W.G.) | 2 tests | 2 tests |
| ΔP = 76.2 cm W.G. (30 in. W.G.) | 2 tests | 2 tests |

of the waste gas stream were considered in the unit design, and were discussed previously. At a constant flow rate, only five other variables influence the operation of the fabric filter. These are:

### Type of Filter Fabric--

A consideration in the overall test program was to evaluate both the physical properties and the filtering performance of various types of high-temperature filter fabric. Schedule limitations allowed the evaluation of only one fabric. The fabric selected for the test program was woven fiberglass with a graphite/silicone finish (Criswell Style 446-COF tri-temp finish).

### Method of Cloth Cleaning--

The equipment provided with the pilot fabric filter allowed four types of fabric cleaning: reverse air (RA), mechanical shake (MS), RA + MS simultaneously, and RA + MS sequentially. This plan was designed to evaluate any differences between two cleaning methods, reverse air and reverse air/mechanical shake simultaneously.

### Air-to-Cloth Ratio--

Air-to-cloth ratio, which defines the loading of the filter, is expressed as actual cubic meters of gas passing through each square meter of cloth each minute. Two air-to-cloth ratios are considered in this test plan: 0.46 $m^3$/min per $m^2$ (1.5 acfm/$ft^2$) and 0.91 $m^3$/min per $m^2$ (3.0 acfm/$ft^2$).

Degree of Cleaning--

The degree of cleaning is a measure of how completely the filter is cleaned during each cleaning cycle. It is recognized that a completely cleaned filter captures fewer particulates than one that is partially coated with fine solids. Although this action is recognized, its affect has not been quantified. The procedure was developed to provide a repeatable consistent basis for evaluation of the degree of cleaning. Its effect on filter performance was outlined before the tests, but the procedure was aborted because the pressure drop measuring equipment malfunctioned.

Frequency of Cleaning--

This variable, which is known to influence total removal of particulates from the flue gas stream, is defined as a measure of how dirty the filter is allowed to get before it is cleaned. For simplicity of subsequent data analysis, the intent was to use a timing mechanism to initiate cleaning throughout the program. The pressure drop, however, would be assigned an upper limit. When the limit was reached, the fabric filter would initiate a cleaning cycle regardless of the timed frequency status. Frequency of cleaning is discussed further in Section 4.

Table 3-4 shows the matrix for the fabric filter operational conditions versus the boiler fuel ratio. It is important to note that the fabric filter was available for roughly twice as much "in-field" testing as the other two mobile control units.

## TABLE 3-4. PILOT FABRIC FILTER TEST PLAN--OPERATING MATRIX

| | Coal only | Coal plus RDF |
|---|---|---|
| Air to cloth = $0.46\ (m^3/min)/m^2$ | | |
| RA[a] only | 6 tests | 6 tests |
| RA + MS[b] | 6 tests | 6 tests |
| Air to cloth = $0.91\ (m^3/min)/m^2$ | | |
| RA only | 6 tests | 6 tests |
| RA + MS | 6 tests | 6 tests |

[a] Reverse-air cleaning.

[b] Reverse-air and mechanical shaking.

# SECTION 4

# EPA PILOT AIR POLLUTION CONTROL EQUIPMENT

This section summarizes design and operating details of the three pilot devices that were used in the waste-as-fuel testing program in Ames, Iowa. The mobile scrubber and ESP are owned and indirectly operated by AEERL at Research Triangle Park, North Carolina. The pilot fabric filter is owned and indirectly operated by HWERL at Cincinnati, Ohio. Information contained herein is abstracted from design, operation, and maintenance manuals and from reports on tests that have been performed with this equipment.

The mobile units were designed to be as small as possible and still provide pollutant control data indicative of full-size systems. Under ideal conditions, all three units could slipstream the same source and provide completely comparable data.

Regional and local contractors were hired to connect heavy inlet ductwork and assemble the larger components of each device. The slipstream tie-in for each device was also made by these contractors.

## 4.1 MOBILE ESP

Southern Research Institute (SRI) designed the ESP unit for the EPA, and the Naval Surface Weapons Center (NSWC) at Dahlgren, Virginia, fabricated it. The following is a list of specific design criteria and features.

- The unit and working areas are located in two separate 12-m (40-ft) semitrailers. (See Figure 4-1.)
- Maximum operating temperature is 538°C (1000°F). (Normally operates at a much lower temperature.)
- Capacity is 85 $m^3$/min (3000 $ft^3$/min).
- Maximum system pressure drop is 180 cm (70 in.) W.G.
- A power supply of 480 volts is required.
- Transformers supply variable secondary voltage.
- Gas treatment velocity is 1.5 m/s (5 ft/s).
- The ESP consists of five sections [total length 6.1 m (20 ft)]. (Figures 4-2 and 4-3 show the layout of a single section.)
- Maximum operating voltage is 50 kV.
- Total power consumption is 2.5 kW/unit.
- Ductwork is 15 m (50 ft) long, made of stainless steel and covered with 0.3 m (11 in.) of insulation. Each 2.4-m (8-ft) section is fitted with six 235-W heaters to minimize heat loss through ducting.
- Total weight of the ESP van is about 20,000 kg (44,000 lb).
- Thermocouples are used for high- and low-temperature cutoff.

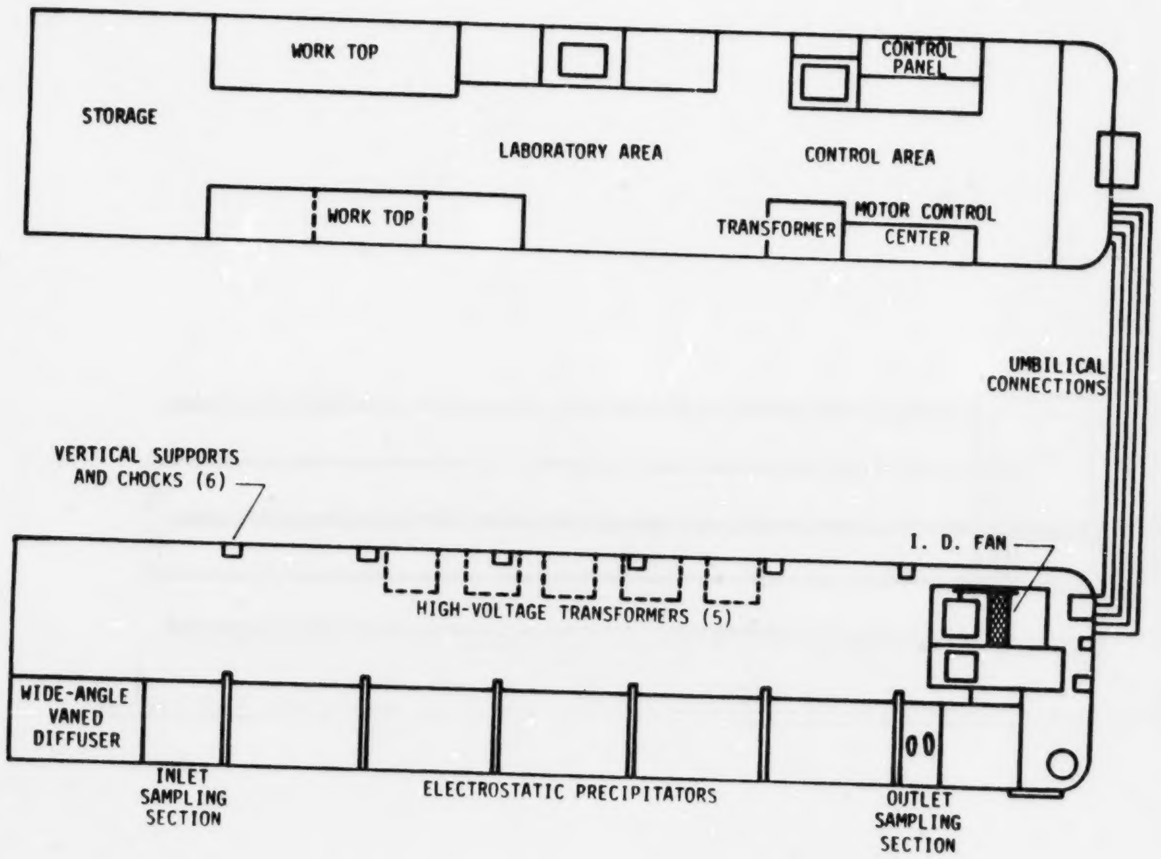
WORK TOP
CONTROL PANEL
STORAGE
LABORATORY AREA
CONTROL AREA
WORK TOP
TRANSFORMER
MOTOR CONTROL CENTER
UMBILICAL CONNECTIONS
VERTICAL SUPPORTS AND CHOCKS (6)
I. D. FAN
HIGH-VOLTAGE TRANSFORMERS (5)
WIDE-ANGLE VANED DIFFUSER
INLET SAMPLING SECTION
ELECTROSTATIC PRECIPITATORS
OUTLET SAMPLING SECTION

Figure 4-1. Plan view of mobile ESP.[2]

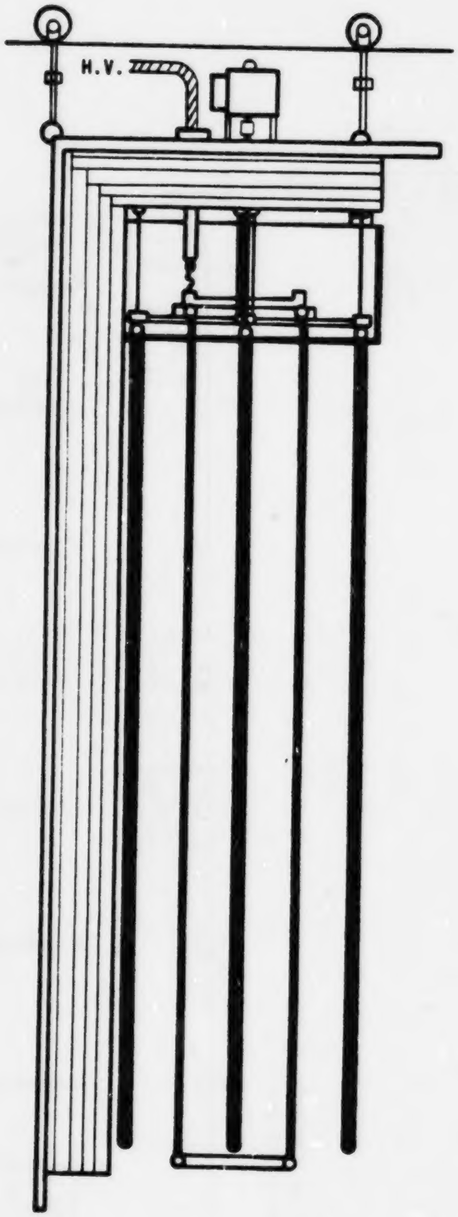

Figure 4-2. ESP cross section.[2]

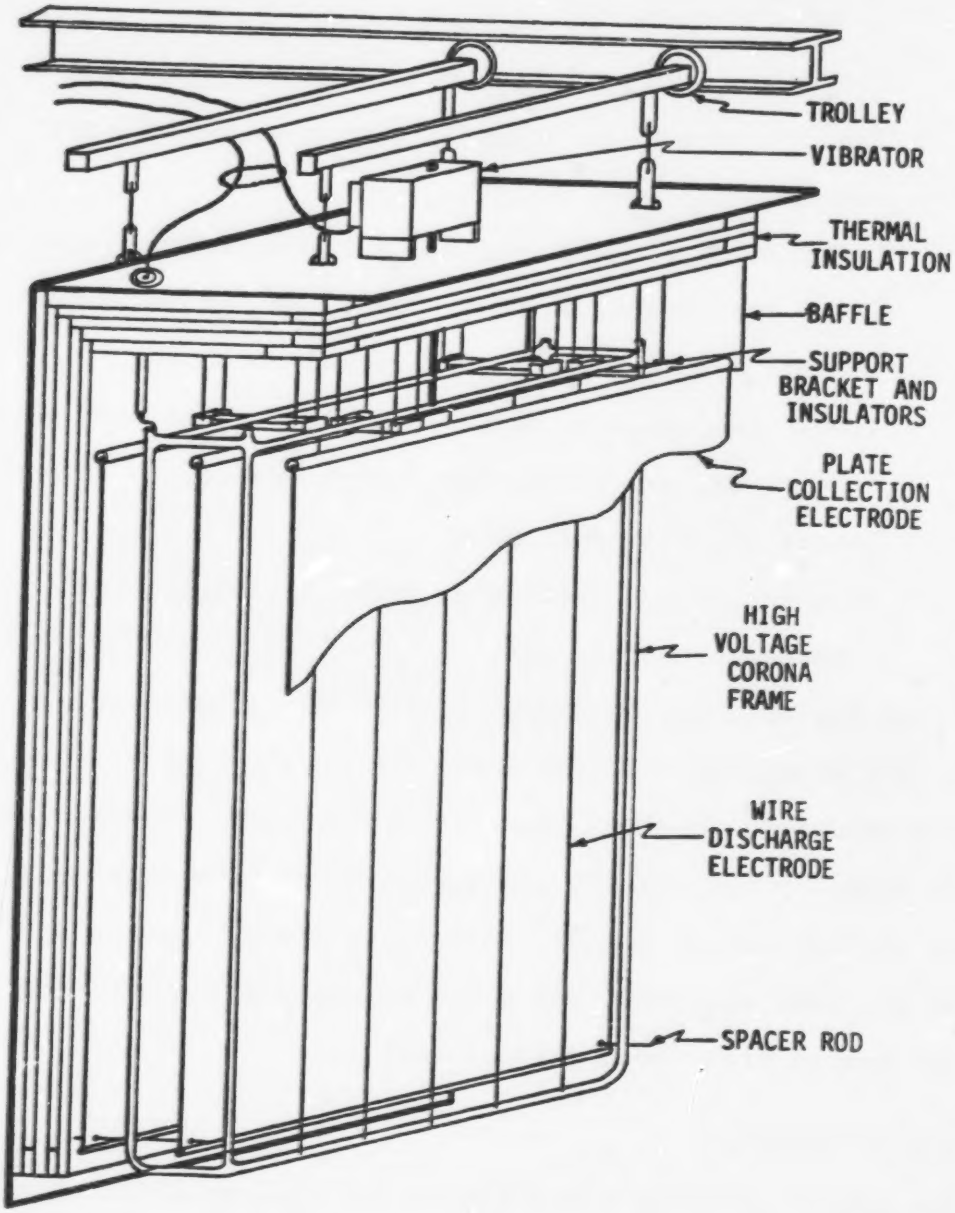
TROLLEY
VIBRATOR
THERMAL INSULATION
BAFFLE
SUPPORT BRACKET AND INSULATORS
PLATE COLLECTION ELECTRODE
HIGH VOLTAGE CORONA FRAME
WIRE DISCHARGE ELECTRODE
SPACER ROD

Figure 4-3. ESP section rollout.[2]

- A flow rectifier (see Figure 4-4) is used to insure a regular velocity profile at the ESP inlet.
- The unit has a stainless steel ID fan (insulated and liquid-cooled) and equipped with high-temperature cutoff.
- A trough-type ash hopper and a 13-cm (5-in.) screw conveyor are located under the van. Ash is conveyed through a gate valve to a disposal container.
- Electrical rappers, situated at the top of each collection plate, are controllable with respect to frequency, intensity, and cycle time.
- Five transformer/rectifier (T/R) sets are located underneath the ESP van.

Since the original shakedown of the mobile ESP system, ambient air inleakage has been a problem on a number of occasions. Improper welds, loose screw conveyor mounts, and insufficient packing around probe collars and access doors have been identified as high inleakage areas. Before and midway through the testing program, operators performed an audible check of the unit and sealed areas suspected of leaking.

## 4.2 MOBILE SCRUBBER

The mobile scrubber was designed for determination of the effectiveness of removing particulates from dirty industrial or utility flue gas streams. During 1973 and 1974, NSWC designed and constructed this unit in Dahlgren, Virginia. The following is a list of specific design criteria and features.

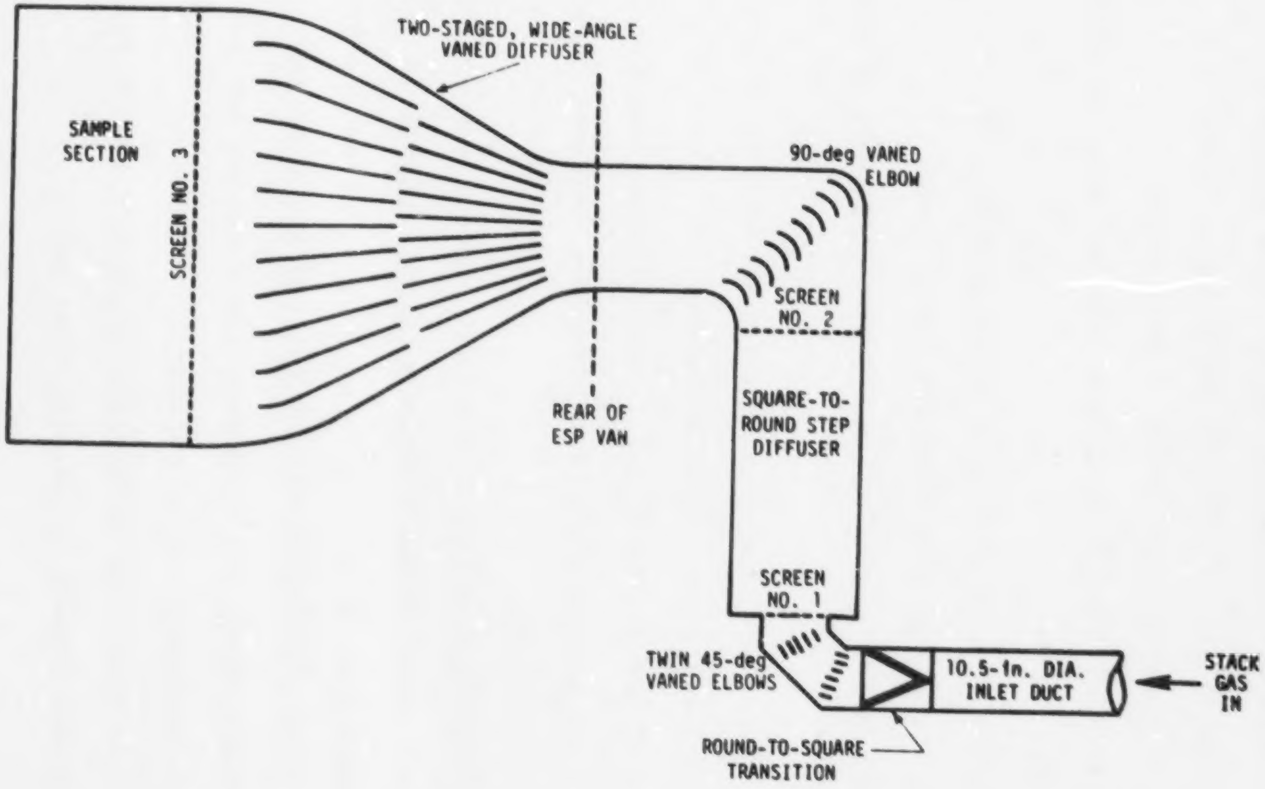
TWO-STAGED, WIDE-ANGLE VANED DIFFUSER
SAMPLE SECTION
SCREEN NO. 3
90-deg VANED ELBOW
SCREEN NO. 2
REAR OF ESP VAN
SQUARE-TO-ROUND STEP DIFFUSER
SCREEN NO. 1
TWIN 45-deg VANED ELBOWS
10.5-in. DIA. INLET DUCT
STACK GAS IN
ROUND-TO-SQUARE TRANSITION

Figure 4-4. Flow rectification on inlet ductwork.[2]

- The unit is housed in a 12.2-m (40-ft) semitrailer, which includes mechanical equipment, controls, and a small area of laboratory space. (See Figure 4-5.)
- It operates as a sieve tray with three trays or a venturi scrubber with three throat sizes.
- Maximum gas flow is 14 $m^3$/min (500 $ft^3$/min) at 177°C (350°F).
- Operating pressure drop is 0-254 cm W.G.
- The unit is equipped with two 20-hp fans.
- The scrubbing liquor system operates closed- or open-loop.
- The closed liquid system is equipped with gravity, deep-bed filter for solids removal.
- The unit has a 1700-liter (450-gal) water supply tank with a pH monitor; pH is adjusted by chemical (usually lime) treatment.
- High-temperature cutoff switches protect the system against temperatures exceeding 450°C (850°F) in inlet ductwork and 180°C (350°F) in tray tower or venturi.
- A presaturator (spray-type) located ahead of the scrubbers cools and saturates the incoming hot gas. (This component may be bypassed.)
- A baffle-type mist eliminator minimizes liquid and solid entrainment in exiting flue gas.

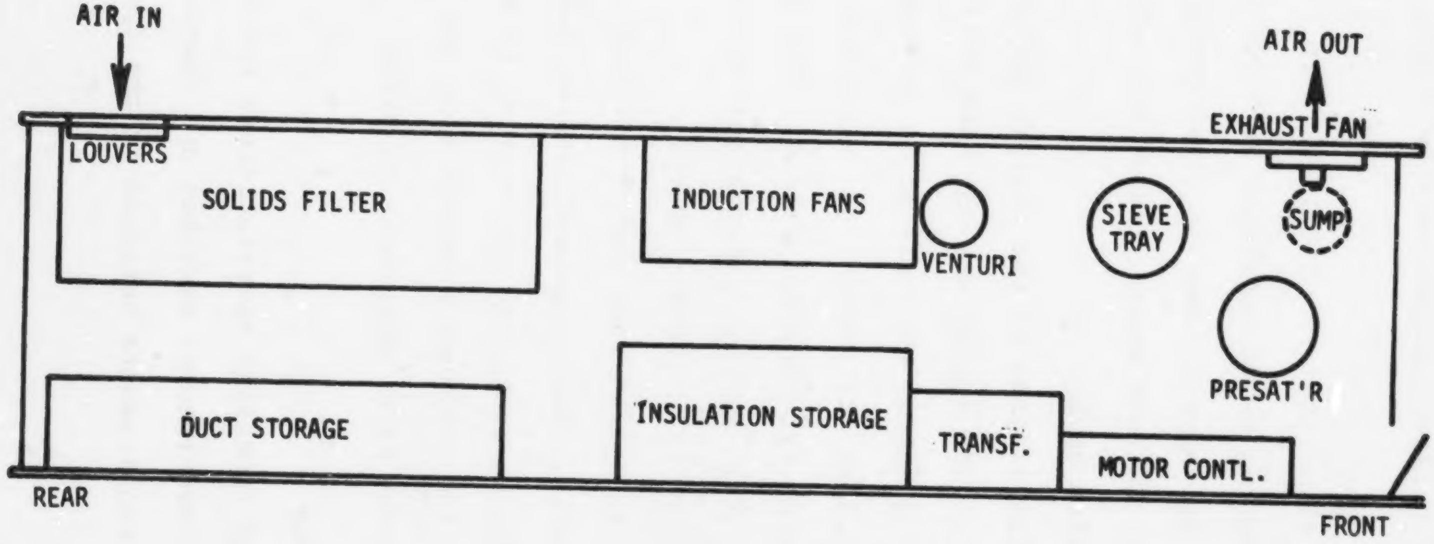
AIR IN
AIR OUT
EXHAUST FAN
LOUVERS
SOLIDS FILTER
INDUCTION FANS
VENTURI
SIEVE TRAY
SUMP
PRESAT'R
DUCT STORAGE
INSULATION STORAGE
TRANSF.
MOTOR CONTL.
REAR
FRONT

Figure 4-5. Schematic plan of EPA mobile scrubber unit.[3]

- Flow nozzles and rotameters measure all necessary gas and liquid flow rates; outputs may be visual or strip-charted.
- The unit has 91 m (300 ft) of 0.15-m (6-in.) diameter stainless steel ductwork insulated with 0.076 m (3 in.) of Fabrifax; Epitherm is used to cover ductwork heaters.
- There are four heaters assemblies on the inlet ductwork, 1720 watts each.

Figure 4-6 is a flow diagram of the venturi scrubber unit. The sieve tray portion of the system was not used during any of the tests. The venturi scrubber consists of an interchangeable throat section and a cyclone for centrifugal separation of large liquid and solid particles from the gas stream. The same throat, 6.0 cm (2-3/8 in.) diameter, was used throughout the test program. The throat was constructed of stainless steel.

Figure 4-7 shows the operational characteristics of the medium-size venturi throat. The crosshatched area indicates conditions that existed during operation and testing in Ames. The graph also illustrates the variable pressure drop and flow rate ranges while L/G ratio was held relatively constant.

## 4.3 PILOT FABRIC FILTER

PEDCo prepared the technical specifications for the pilot fabric filter, and a subcontractor designed and fabricated it. The general technical requirements outlined in the specification are listed below.

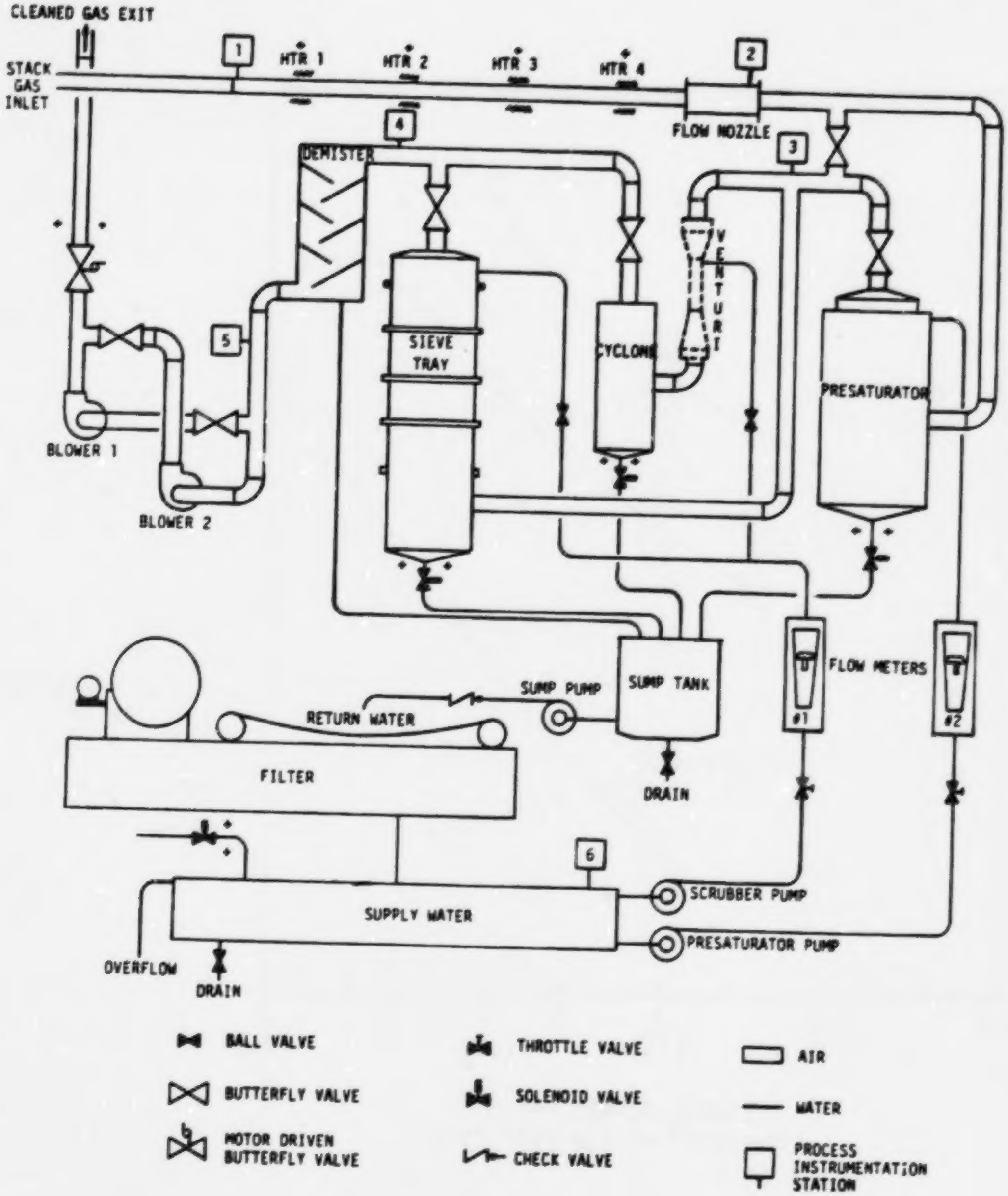
CLEANED GAS EXIT
STACK GAS INLET
1
HTR 1
HTR 2
HTR 3
HTR 4
2
FLOW NOZZLE
3
4
DEMISTER
5
SIEVE TRAY
CYCLONE
VENTURI
PRESATURATOR
BLOWER 1
BLOWER 2
FLOW METERS
#1
#2
SUMP PUMP
SUMP TANK
RETURN WATER
FILTER
DRAIN
6
SCRUBBER PUMP
SUPPLY WATER
PRESATURATOR PUMP
OVERFLOW
DRAIN
BALL VALVE
BUTTERFLY VALVE
MOTOR DRIVEN BUTTERFLY VALVE
THROTTLE VALVE
SOLENOID VALVE
CHECK VALVE
AIR
WATER
PROCESS INSTRUMENTATION STATION

Figure 4-6. Mobile scrubber flow diagram.[3]

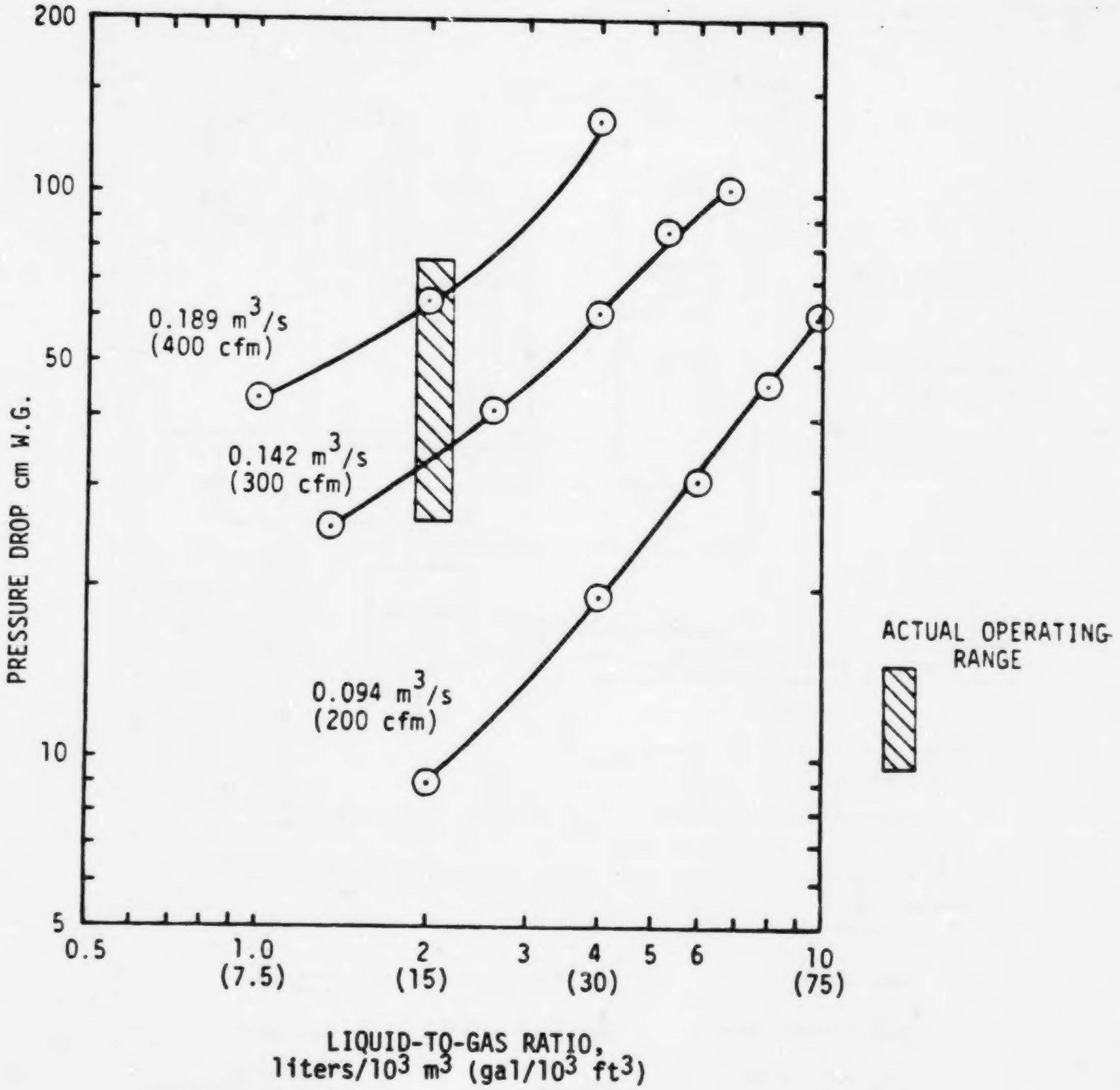

Figure 4-7. Operational characteristics of medium size venturi throat.[3]

- It must be capable of continuous uninterrupted operation.
- High-temperature, corrosion-resistant coating must be on all carbon steel interior surfaces.
- Required capacity is 85 $m^3$/min (3000 acfm) at 204°C (400°F).
- The unit contains three compartments.
- Air-to-cloth ratio is 0.46 $m^3$/min per $m^2$ (1.5 $ft^3$/min per $ft^2$) for all compartments.
- Air-to-cloth ratio is 0.91 $m^3$/min per $m^2$ (3.0 $ft^3$/min per $ft^2$) when one compartment is cleaning; this excludes reverse-air flow.
- The unit must withstand temperature excursions up to 260°C (500°F).
- Leakage of air into the unit is less than 1.4 std. $m^3$/min (50 scfm).
- Heat loss across the unit must be minimal: 7.6-cm (3-in.) fiberglass insulation with cover plates; hopper heaters to maintain 107°C (225°F) with ambient air at -18°C (0°F) and no heat addition from flue gas.

After startup and shakedown of the unit, the leakage and hopper heater capabilities were found to be out of the desired range. A review of inlet/outlet flow rate measurement data confirmed leakage in excess of 1.4 std. $m^3$/min (50 scfm). All attempts were made throughout the subsequent test programs to hold inleakage to a minimum.

The hopper heaters were not capable of maintaining the minimum temperature requirement; however, whenever possible, they were used to avoid acid condensation within the unit.

Other specific design features were as follows:

- A power supply of 240/480 V is required. Transformer rewiring is possible to accommodate either voltage.
- Control panel and working areas are located in a separate 6.6-m (20-ft) trailer.
- Thermocouples and instrumentation provide high- and low-temperature cutoff.
- Automatic flow control and recording system with flow rectifier are provided.
- There is an opacity monitor and recorder at the device outlet.
- Cleaning mechanism is variable reverse-air/mechanical-shake type.
- Unit has pressure drop transmitter and recorder.
- There is a variable-cleaning-cycle initiation sequence.
- Cleaning frequency and dwell times are all variable.

All instrumentation was operable throughout the program, with the exception of the differential pressure transmitter. Problems with proper calibration that were encountered from startup were never rectified despite numerous attempts. All reported pressure differential data were obtained by manually reading a slack U-tube manometer with static pressure taps attached to the inlet and outlet manifolds of the fabric filter.

Figure 4-8 shows the Operators Log. These forms were used throughout the test program to record the operating condition of the fabric filter system.

Several operating conditions were measured and recorded automatically. A multipoint recorder received input from a number of thermocouples and from the flow-measuring device located just upstream of the outlet sample point. An example of the multipoint strip chart record is shown in Figure 4-10. This particular time period included a reverse-air/mechanical-shake cleaning cycle. The record also shows a corresponding drop in temperature in the fabric filter interior and at the stack. The drop in flow rate is due to increased pressure drop from two-compartment operation without a proportional decrease in flow rate. The flow rate decreases automatically because the upper fan capacity limit is reached at the increased pressure loss.

Opacity of the stack gas is also measured optically and recorded. An example strip chart of opacity readings, corresponding to the multipoint strip chart shown in Figure 4-10, is shown in Figure 4-11.

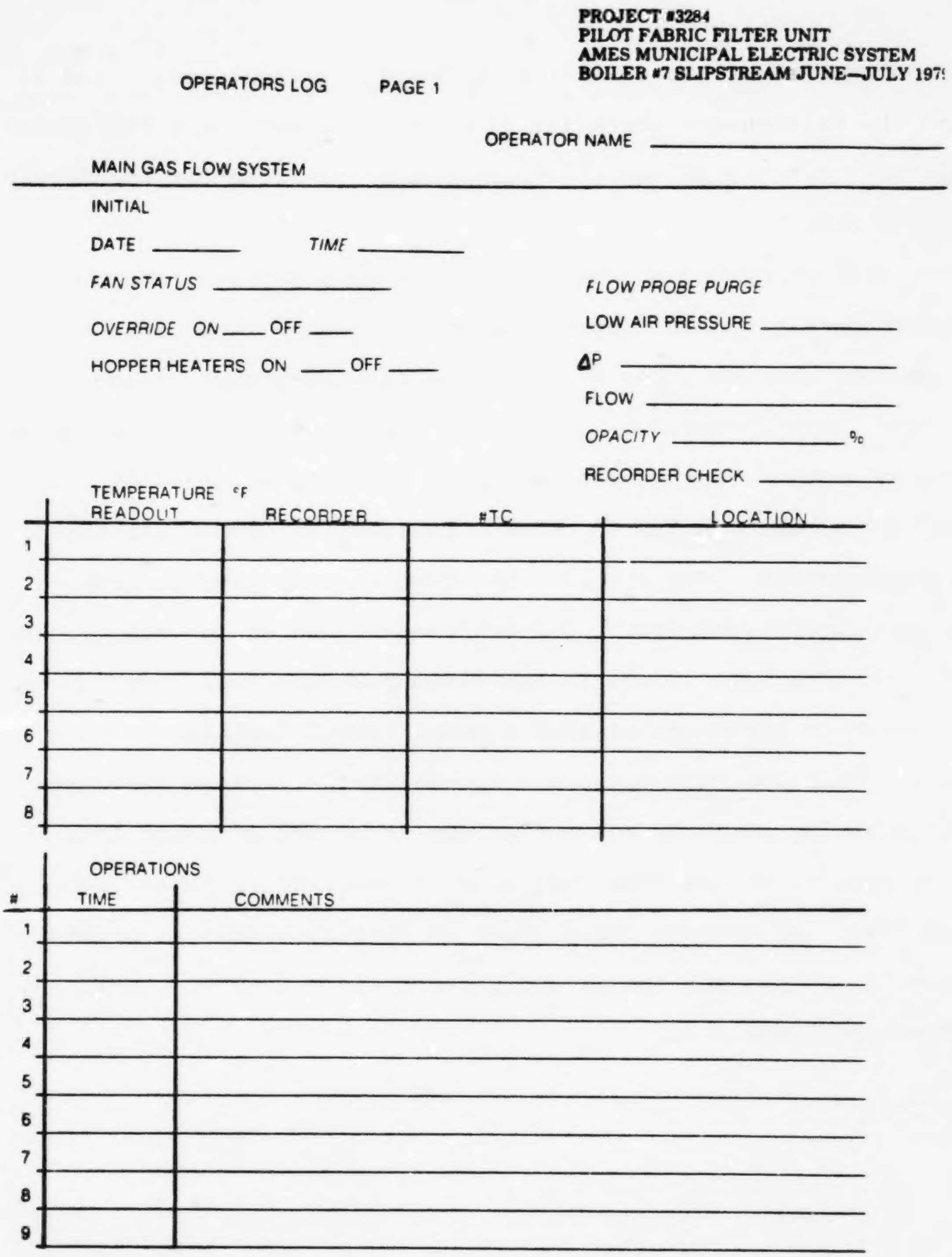

**PROJECT #3284**
**PILOT FABRIC FILTER UNIT**
**AMES MUNICIPAL ELECTRIC SYSTEM**
**BOILER #7 SLIPSTREAM JUNE—JULY 197**

OPERATORS LOG PAGE 1

OPERATOR NAME ____________

MAIN GAS FLOW SYSTEM

INITIAL

DATE ______ *TIME* ______

*FAN STATUS* ____________

*OVERRIDE* ON ____ OFF ____

HOPPER HEATERS ON ____ OFF ____

*FLOW PROBE PURGE*

LOW AIR PRESSURE ____________

$\Delta P$ ____________

FLOW ____________

*OPACITY* ____________ %

RECORDER CHECK ____________

| | TEMPERATURE °F<br>READOUT | RECORDER | #TC | LOCATION |
|---|---|---|---|---|
| 1 | | | | |
| 2 | | | | |
| 3 | | | | |
| 4 | | | | |
| 5 | | | | |
| 6 | | | | |
| 7 | | | | |
| 8 | | | | |

| # | OPERATIONS<br>TIME | COMMENTS |
|---|---|---|
| 1 | | |
| 2 | | |
| 3 | | |
| 4 | | |
| 5 | | |
| 6 | | |
| 7 | | |
| 8 | | |
| 9 | | |

Figure 4-8. Pilot fabric filter operators log.

**PROJECT #3284**
**PILOT FABRIC FILTER UNIT**
**AMES MUNICIPAL ELECTRIC SYSTEM**
**BOILER #7 SLIPSTREAM JUNE—JULY 1979**

OPERATORS LOG PAGE 2

OPERATOR NAME ____________________

CLEANING CYCLE SYSTEM

INITIAL

DATE __________ TIME __________ ΔP HIGH __________

# CYCLES ______ HRS RUNNING ____

CLEANING MODE R S R&S

SIM _____ SEQ _____

CYCLE INITIATED BY OFF _____ TIME _____ PRESS _____

CLEANING TIMES (MIN) FREQUENCY __________

DWELL __________

CLEANING __________

PRESSURE ACTUATOR SET (%) _____ x 20 = _____ IN WATER

| | REVERSE AIR FAN | SHAKER MOTORS | | | OUTLET DAMPERS | | | REVERSE AIR INLET DAMPERS | | |
|---|---|---|---|---|---|---|---|---|---|---|
| | | 1 | 2 | 3 | 1 | 2 | 3 | 1 | 2 | 3 |
| OFF | | | | | | | | | | |
| MANUAL | | | | | | | | | | |
| AUTOMATIC | | | | | | | | | | |

OPERATIONS

| # | TIME | COMMENTS |
|---|---|---|
| 1 | | |
| 2 | | |
| 3 | | |
| 4 | | |
| 5 | | |
| 6 | | |
| 7 | | |
| 8 | | |
| 9 | | |

Figure 4-8. Pilot fabric filter operators log (continued).

**PROJECT #3284**
**PILOT FABRIC FILTER UNIT**
**AMES MUNICIPAL ELECTRIC SYSTEM**
**BOILER #7 SLIPSTREAM JUNE—JULY 1979**

MAINTENANCE CHECKLIST

DATE

OPERATOR NAME ______________

MAIN FAN
OPERATING ________
BEARINGS CHECK ________
TIME ________
LUBRICATION ________
DATE SCHEDULED ________
COMMENTS

REVERSE AIR FAN
OPERATING ________
BEARINGS CHECK ________
TIME ________
LUBRICATION ________
DATE SCHEDULED ________
COMMENTS

SHAKERS
MOTORS OPERATING #1 ________ #2 ________ #3 ________
TIME ________
ASSEMBLIES OPERATING #1 /// =2 /// =3 ///
BEARINGS CHECK #1 ________ =2 ________ =3 ________
COMMENTS

DAMPERS
REVERSE AIR =1 ________ =2 ________ =3 ________
TIME ________
OUTLET =1 ________ =2 ________ =3 ________
COMMENTS

SCREW CONVEYOR ASH COLLECTION
SCREW MECHANISIM & MOTOR ______________
TIME ________
COMMENTS

| | TIME | | | WEIGHT | | |
|---|---|---|---|---|---|---|
| DRUM # | INITIAL | FINAL | NET | GROSS | TARE | NET |
| | | | | | | |
| | | | | | | |
| | | | | | | |
| | | | | | | |

Figure 4-9. Pilot fabric filter maintenance checklist.

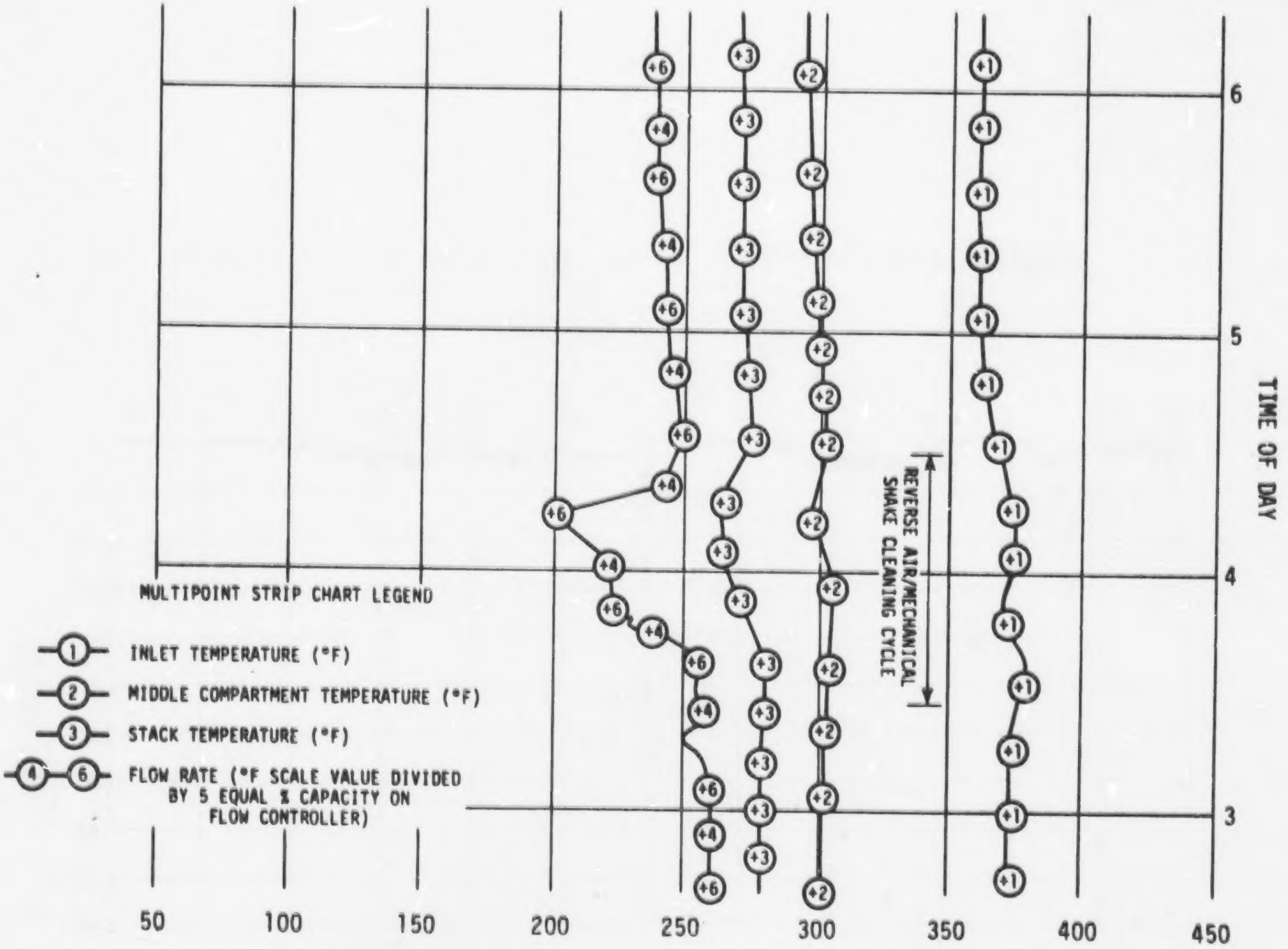

Figure 4-10. Pilot fabric filter multipoint strip chart - July 13, 1979.

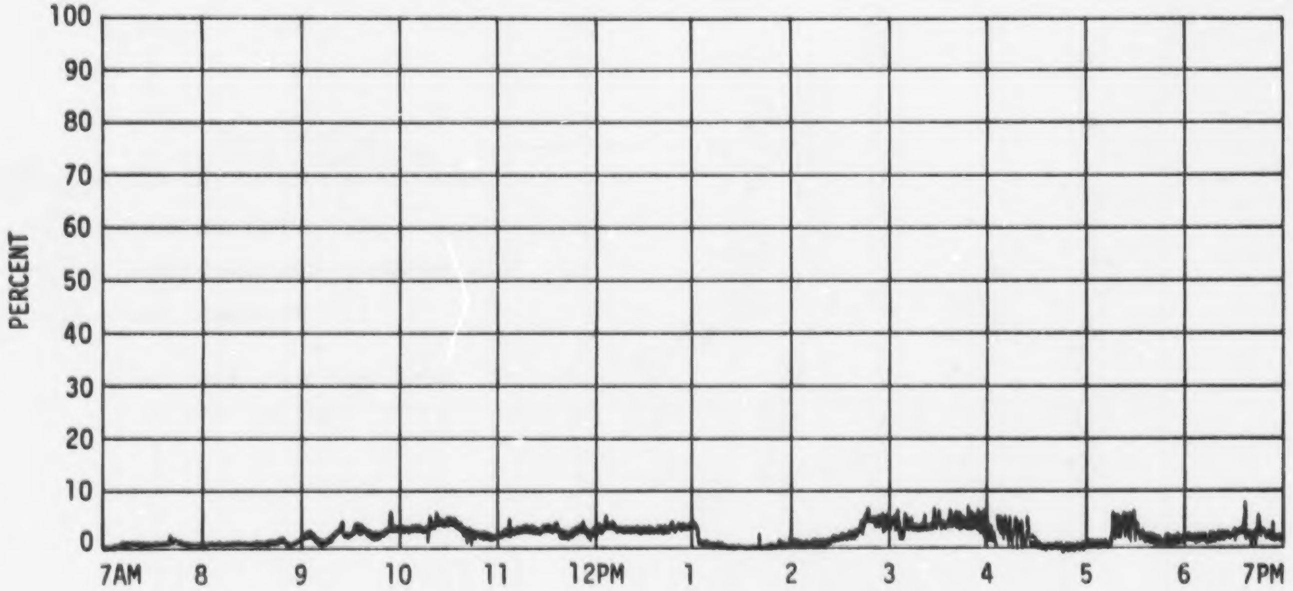

Figure 4-11. Pilot fabric filter opacity strip chart - July 13, 1979.

# SECTION 5

# PRESENTATION OF RESULTS

The results of sampling and analytical efforts presented in this section are organized according to fuel analysis and the control device tested. This section is supplemented by Appendixes B, C, and D, which are special analytical and evaluative reports prepared by Brehm Laboratory of Wright State University and Midwest Research Institute. These three reports apply only to the mobile ESP and scrubber test series. They are presented as typical of the various types of data analyses that could be performed on the Ames data. An exhaustive analysis of all the data obtained from the Ames test program is beyond the scope of this report.

## 5.1 FUEL ANALYSIS

Section 3 discussed the fuel sampling methodology for each test run. Table 5-1 presents the results of proximate and ultimate analyses of fuel samples taken during mobile scrubber and ESP testing, and Table 5-2 presents the results of the same analyses of fuel samples taken during pilot fabric filter testing.

It is interesting to note that the RDF sampled and analyzed contained less moisture than coal. The difference in fuel value is due primarily to the high ash and oxygen contents of RDF. The

## TABLE 5-1. AVERAGE FUEL ANALYSES - MOBILE SCRUBBER AND ESP TEST RUNS ONLY

(values in weight percent except as shown)

| | Coal[a] | RDF[a] |
|---|---|---|
| Fuel as received | | |
| Proximate analysis | | |
| Water | 16.13 | 13.25 |
| Ash | 9.27 | 12.78 |
| Volatile matter | 36.54 | 61.36 |
| Fixed carbon | 38.06 | 12.61 |
| Heating value, MJ/kg<br>(Btu/lb) | 23.68<br>(10,180) | 15.45<br>(6,644) |
| Dry fuel | | |
| Ultimate analysis | | |
| Ash | 11.06 | 14.83 |
| Carbon | 73.53 | 50.31 |
| Hydrogen | 1.38 | 3.97 |
| Oxygen[b] | 9.73 | 30.37 |
| Sulfur | 3.13 | .38 |
| Nitrogen | 1.17 | .14 |
| Heating value, MJ/kg<br>(Btu/lb) | 28.21<br>(12,130) | 17.80<br>(7,654) |

[a] Average of selected grab samples from Atlas storage bin.

[b] Calculated by difference.

## TABLE 5-2. AVERAGE FUEL ANALYSES - MOBILE FABRIC FILTER TEST RUNS ONLY
(values in weight percent except as shown)

| | Coal[a] | RDF[a] |
|---|---|---|
| Fuel as received | | |
| Proximate analysis | | |
| Water | 16.06 | 5.74 |
| Ash | 15.96 | 9.64 |
| Volatile matter | 31.53 | 70.57 |
| Fixed carbon | 36.50 | 14.05 |
| Heating value, MJ/kg | 21.25 | 17.38 |
| (Btu/lb) | (9,122) | (7,460) |
| Dry fuel | | |
| Ultimate analysis | | |
| Ash | 18.92 | 10.23 |
| Carbon | 61.81 | 46.83 |
| Hydrogen | 4.13 | 6.16 |
| Oxygen[b] | 9.60 | 36.17 |
| Sulfur | 4.38 | .27 |
| Nitrogen | 1.16 | .34 |
| Heating value, MJ/kg | 25.32 | 18.44 |
| (Btu/lb) | (10,869) | (7,913) |

[a] Average of selected grab samples.

[b] Calculated by difference.

fuel quality of RDF improved over the entire testing period as a result of effective process modifications in the RDF preparation facility. Improvements in fuel quality refer to lower moisture and ash content and higher available heat per kilogram. Figure 5-1 shows the measured values of ash contents of selected fuel samples and RDF density over the indicated test periods.

Elemental analysis, by spark source mass spectrometry (SSMS), was performed on composite coal and RDF samples. Appendix B discusses these analyses in detail. Table 5-3 presents a review of the fuel analysis portion of the information in this appendix. It shows the relative differences in elemental composition of the two types of fuel. Copper, lead, zinc, cadmium, and iron compositions were determined through atomic absorption techniques which is a quantitatively more accurate analytical technique than SSMS (but is, however, more expensive). Detailed elemental analysis was not performed on the fuel sampled during the pilot fabric filter test series.

## 5.2 MOBILE ESP

The mobile ESP was operated between October 18 and December 1, 1978, and 18 runs were tested. The data shown in Table 5-4 are boiler operating conditions during the ESP test series. Numbers 10 through 19 are excluded in the test number sequence to indicate that the mobile ESP did not operate during the first 4 weeks of November. Further, it is apparent from the last column (% RDF) that fewer RDF runs and more coal-only tests were

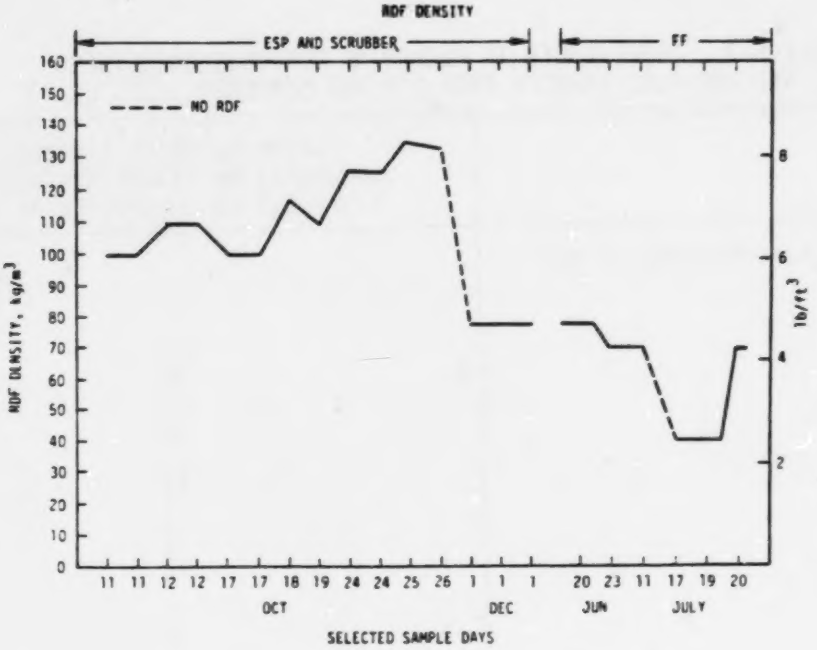

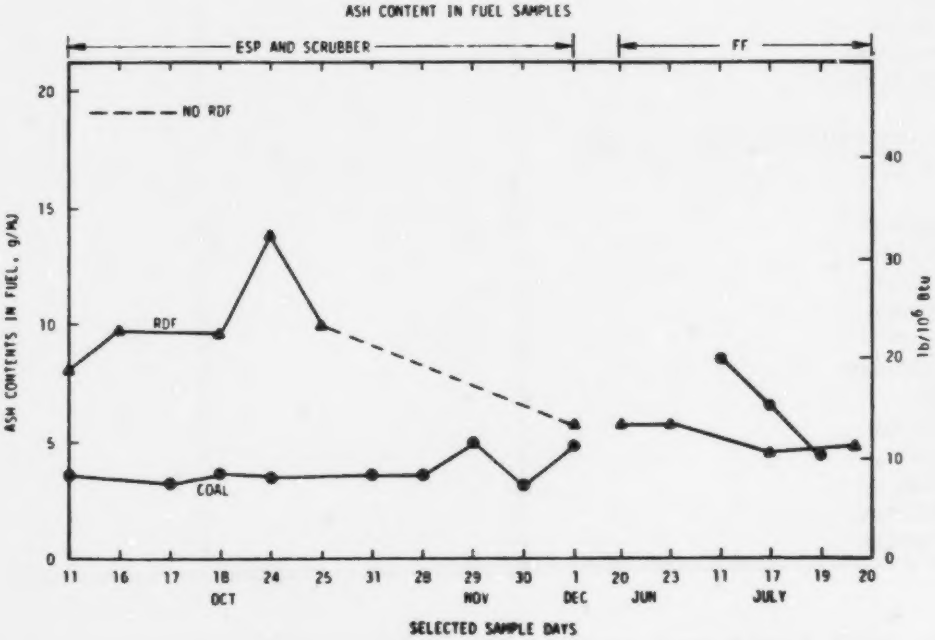

Figure 5-1. RDF density and ash content in fuel measured over selected test periods.

## TABLE 5-3. DIFFERENCES IN ELEMENTAL COMPOSITION BETWEEN COAL AND RDF FUEL SAMPLES FROM ESP AND SCRUBBER TESTS ONLY[a]

| | Factor by which elemental concentration in RDF differs from elemental concentration in coal |
|---|---|
| Elements more concentrated in RDF than in coal | |
| Copper[b] | 120 |
| Lead[b] | 40 |
| Bromine | 25 |
| Fluorine | 25 |
| Zinc[b] | 10 |
| Manganese | 10 |
| Antimony | 5 |
| Chromium | 5 |
| Cobalt | 5 |
| Chlorine[c] | 4 |
| Rubidium | 4 |
| Tin | 3 |
| Barium | 3 |
| Silver | 3 |
| Cadmium[b] | 2 |
| Titanium | 2 |
| Strontium | 2 |
| Phosphorus | 2 |
| Elements less concentrated in RDF than in coal | |
| Vanadium | 50 |
| Beryllium | 25 |
| Scandium | 7 |
| Yttrium | 6 |
| Sulfur[d] | 5 |
| Molybdenum | 5 |
| Iron[b] | 4 |
| Thallium | 3 |
| Nickel | 2 |
| Cerium | 2 |
| Lanthanum | 2 |
| Zirconium | 2 |

[a] Based on spark source mass spectrometry analysis unless otherwise stated.

[b] Based on atomic absorption spectrometry.

[c] Based on wet chemistry analytical methods.

[d] The initial determination of sulfur concentration might have been low by a factor of 3-10 because of high organic content, which necessitated low-temperature ashing of the samples.

## TABLE 5-4. BOILER NO. 7 OPERATING CONDITIONS DURING MOBILE ESP TESTS

| Date | Test No. | Time | Power generation rate, MW/h | Coal flow, kg | Coal[a] input, MJ | RDF flow, $m^3$ | RDF[b] flow, kg | RDF input, MJ | Total input, MJ | % RDF (heat input basis) |
|---|---|---|---|---|---|---|---|---|---|---|
| | | | | | | During | Test Period | | | |
| 10/18 | 1 EI/EO | 1630-1730 | 33.0 | 21795 | 526234[c] | 0 | 0 | 0 | 526234 | 0 |
| 10/19 | 2 EI/EO | 1100-1200 | 32.0 | 13517 | 326312 | 42.5 | 4422.5 | 62456[e] | 388768 | 16.1 |
| 10/25 | 3 EI/EO | 1400-1500 | 22.0 | 7620 | 183992 | 36.8 | 3832.8 | 54227 | 238219 | 22.7 |
| 10/26 | 4 EI/EO | 1000-1100 | 22.0 | 9389 | 226720 | 39.6 | 4127.7 | 58342 | 285061 | 20.5 |
| 10/27 | 5 EI/EO | 1000-1100 | 21.5 | 9208 | 222208 | 0 | 0 | 0 | 222208 | 0 |
| 10/27 | 6 EI/EO | 1400-1500 | 21.7 | 9934 | 239802 | 0 | 0 | 0 | 239802 | 0 |
| 10/30 | 7 EI/EO | 1100-1200 | 20.7 | 10342 | 249718 | 0 | 0 | 0 | 249718 | 0 |
| 10/30 | 8 EI/EO | 1430-1530 | 20.2 | 9707 | 234316 | 0 | 0 | 0 | 234316 | 0 |
| 10/31 | 9 EI/EO | 1030-1130 | 20.8 | 9843 | 237586 | 0 | 0 | 0 | 237586 | 0 |
| 11/28 | 20 EI/EO | 1130-1230 | 34.8 | 18030 | 422000[d] | 0 | 0 | 0 | 422000 | 0 |
| 11/28 | 21 EI/EO | 1430-1530 | 34.8 | 18370 | 429807 | 0 | 0 | 0 | 429807 | 0 |
| 11/29 | 22 EI/EO | 1130-1230 | 35.0 | 17826 | 417147 | 0 | 0 | 0 | 417147 | 0 |
| 11/29 | 23 EI/EO | 1430-1530 | 35.2 | 17055 | 399001 | 0 | 0 | 0 | 399001 | 0 |
| 11/30 | 24 EI/EO | 1030-1130 | 18.5 | 9072 | 212266 | 0 | 0 | 0 | 212266 | 0 |
| 11/30 | 25 EI/EO | 1330-1430 | 18.7 | 8958 | 209628 | 0 | 0 | 0 | 209628 | 0 |
| 12/1 | 26 EI/EO | 1000-1100 | 34.7 | 16057 | 375686 | 31.2 | 3243.2 | 54649[f] | 430334 | 12.7 |
| 12/1 | 27 EI/EO | 1400-1500 | 33.7 | 15694 | 367246 | 36.8 | 3832.8 | 64566 | 431812 | 15.0 |
| 12/1 | 28 EI/EO | 1500-1600 | 33.5 | 14832 | 347095 | 39.6 | 4127.7 | 69524 | 416620 | 16.7 |

a. Coal heating value is a composite average of the daily heating values used during the testing periods.

b. Average density of RDF over the entire test period was 104 $kg/m^3$ (6.5 $lb/ft^3$)

c. At 24.1 MJ/kg (10/18 through 10/31).

d. At 23.4 MJ/kg (11/28 through 12/1).

e. At 14.1 MJ/kg (10/19 through 10/26).

f. At 16.9 MJ/kg (12/1 only).

| To convert from | to | multiply by |
|---|---|---|
| kg | lb | 2.205 E + 00 |
| MJ | $10^6$ Btu | 9.470 E - 04 |
| $m^3$ | $ft^3$ | 3.531 E + 01 |

performed than ideal from an engineering analysis point of view. This limitation of data adversely affects full evaluation of the performance of the ESP.

Table 5-5 presents operating conditions of the mobile ESP during the test series. These data were documented by Acurex at the time of testing.

Table 5-6 presents a detailed listing of the emission concentrations that were determined on some collected samples by the analytical techniques noted. Specifically, particulate concentration is determined by using standard gravimetric procedures and relating total collected mass to measured volume of gas sampled. The halides (chloride, fluoride, and bromide) were measured by using an ion-specific electrode and relating the total amount measured to the total volume of gas sampled. Almost all of the halides were in gaseous form; almost none were detected on the particulate filters.

Atomic absorption (AA) analyses were made for five specific metals (Pb, Cd, Sb, Fe, Cu), which were also analyzed by SSMS. The concentrations determined by AA have a higher degree of reliability because this technique is quantitatively more accurate than SSMS. The spark source elemental composition analysis was performed to describe the emissions qualitatively.

Emission concentrations can be related to a number of variable conditions as a means of perceiving trends that may indicate methods of lowering emissions of potentially harmful pollutants. Comparison of inlet loading, outlet loading, or ESP

TABLE 5-5. MOBILE ESP OPERATING CONDITIONS

| Date | Run | Time (24-h clock) | % RDF (heat input basis) | Number of energized fields[a] | SCA,[a] $m^3$ per 1000 $m^3$/h | Actual gas flow rate,[a] $m^3$/h |
|---|---|---|---|---|---|---|
| 10/18 | 1 EI/EO | 1630-1730 | 0 | 4 | 7.33 | 4876.7 |
| 10/19 | 2 EI/EO | 1100-1200 | 16.1 | 4 | 16.40 | 2718.7 |
| 10/25 | 3 EI/EO | 1400-1500 | 22.7 | 5 | 16.40 | 2718.7 |
| 10/26 | 4 EI/EO | 1000-1100 | 20.5 | 5 | 16.40 | 2718.7 |
| 10/27 | 5 EI/EO | 1000-1100 | 0 | 5 | 16.40 | 2718.7 |
| 10/27 | 6 EI/EO | 1400-1500 | 0 | 5 | 16.40 | 2718.7 |
| 10/30 | 7 EI/EO | 1100-1200 | 0 | 5 | 21.87 | 2039.0 |
| 10/30 | 8 EI/EO | 1430-1530 | 0 | 5 | 21.87 | 2039.0 |
| 10/31 | 9 EI/EO | 1030-1130 | 0 | 5 | 21.87 | 2039.0 |
| 11/28 | 20 EI/EO | 1130-1230 | 0 | 5 | 27.34 | 1631.2 |
| 11/28 | 21 EI/EO | 1430-1530 | 0 | 5 | 16.40 | 2718.7 |
| 11/29 | 22 EI/EO | 1130-1230 | 0 | 5 | 16.40 | 2718.7 |
| 11/29 | 23 EI/EO | 1430-1530 | 0 | 5 | 16.40 | 2718.7 |
| 11/30 | 24 EI/EO | 1030-1130 | 0 | 3 | 10.90 | 2446.8 |
| 11/30 | 25 EI/EO | 1330-1430 | 0 | 3 | 10.90 | 2446.8 |
| 12/1 | 26 EI/EO | 1000-1100 | 12.7 | 5 | 16.40 | 2718.7 |
| 12/1 | 27 EI/EO | 1400-1500 | 15.0 | 5 | 16.40 | 2718.7 |
| 12/1 | 28 EI/EO | 1500-1600 | 16.7 | 5 | 16.40 | 2718.7 |

| To convert from | to | multiply by |
|---|---|---|
| $m^2$ per 1000 $m^3$/hr | $ft^2$ per 1000 $ft^3$/min | 1.829 E + 01 |
| $m^3$/hr | $ft^3$/min | 5.885 E - 01 |

[a] Reported by Acurex.

## TABLE 5-6. MOBILE ESP EMISSION CONCENTRATIONS

| OPERATING PARAMETERS (units as noted) | Primary | | | | | | | |
|---|---|---|---|---|---|---|---|---|
| Power generation, MW/h | 35.0 | 34.8 | 33.0 | 21.6 | 20.6 | 18.6 | 33.5 | 22.0 |
| SCA, $m^2$ per 1000 $m^3$/h | 16.4 | 27.34 | 7.33 | 16.4 | 21.87 | 10.93 | 16.4 | 16.4 |
| No. fields | 5 | 5 | 4 | 5 | 5 | 3 | 5 | 5 |
| Fuel | Coal | Coal | Coal | Coal | Coal | Coal | RDF[a] | RDF[a] |
| Run No. | 21,22,23 | 20 | 1 | 5,6 | 7,8,9 | 24,25 | 2,26,27,28 | 3,4 |
| ANALYTICAL RESULTS, mg/dscm | | | | | | | | |
| Gravimetric Analysis | | | | | | | | |
| T. particulate (in)[b] | 3119 | 3991 | 3235. | 2743. | 2004 | 3172. | 3697. | 2701. |
| (out) | 46.23 | 29.81 | 64.60 | 36.13 | 28.50 | 194.3 | 83.80 | 95.70 |
| Specific Ion Electrode Analysis | | | | | | | | |
| Cl (in)[c] | | | | 17.0 | | | | 170 |
| (out) | | | | 7.60 | | | | 160 |
| F (in)[d] | 10.6 | | | | 6.64 | 5.81 | 8.78 | |
| (out) | 6.66 | | | | 5.56 | 5.30 | 7.96 | |
| Br (in)[e] | ND[f] | ND | | | ND | ND | ND | |
| (out) | ND | ND | | | ND | ND | ND | |
| Atomic Absorption Analysis | | | | | | | | |
| Pb (in) | .31 | .53 | 2.7 | .51 | 8.2 | | 14 | 9.3 |
| (out) | .21 | .0070 | 1.1 | .017 | .022 | | .086 | 2.5 |
| Cd (in) | | | | .036 | | | | .092 |
| (out) | | | | .0028 | | | | .0077 |
| Sb (in) | | | | .073 | | | | 140 |
| (out) | | | | .0051 | | | | .0049 |
| Fe (in) | | | | 92 | | | | 140. |
| (out) | | | | 2.2 | | | | 2.1 |
| Cu (in) | | | | .20 | | | | .42 |
| (out) | | | | .012 | | | | .025 |
| Spark Source Mass Spectrometry Analysis | | | | | | | | |
| Li (in) | | | | | | | | |
| (out) (1)[g] | | | | | | | | |
| Be (in) | | | | | .04 | | .03 | .05 |
| (out) | | | | | .0003 | | .003 | .0001 |
| B (in) | | | | | | | | |
| (out) (1) | | | | | | | | |
| F (in) | | | | | 20 | | 10 | 10 |
| (out) | | | | | .7 | | .4 | .7 |
| Na (in) | | | | | | | | |
| (out) (2)[g] | | | | | | | | |

(continued)

TABLE 5-6 (continued)

| OPERATING PARAMETERS (units as noted) | Primary | | | | | | | |
|---|---|---|---|---|---|---|---|---|
| Power generation, MW/h | 35.0 | 34.8 | 33.0 | 21.6 | 20.6 | 18.6 | 33.5 | 22.0 |
| SCA, $m^2$ per 1000 $m^3$/h | 16.4 | 27.34 | 7.33 | 16.4 | 21.87 | 10.93 | 16.4 | 16.4 |
| No. fields | 5 | 5 | 4 | 5 | 5 | 3 | 5 | 5 |
| Fuel | Coal | Coal | Coal | Coal | Coal | Coal | RDF[a] | RDF[a] |
| Run No. | 21,22,23 | 20 | 1 | 5,6 | 7,8,9 | 24,25 | 2,26,27,28 | 3,4 |
| ANALYTICAL RESULTS, mg/dscm | | | | | | | | |
| SSMS | | | | | | | | |
| Ni (in) | | | | | 2 | | ≤2 | 2 |
| (out) | | | | | .07 | | ≤.07 | .2 |
| Cu (in) | | | | | .7 | | 3 | 8 |
| (out) | | | | | .02 | | .09 | .05 |
| Zn (in) | | | | | 2 | | 20 | 8 |
| (out) | | | | | .07 | | .7 | .07 |
| Ga (in) | | | | | .4 | | 2 | .1 |
| (out) | | | | | .003 | | .03 | <.004 |
| As (in) | | | | | <.1 | | .3 | .1 |
| (out) | | | | | <.001 | | .004 | <.001 |
| Br (in) | | | | | .05 | | <.03 | .03 |
| (out) | | | | | .001 | | <.0009 | .005 |
| Rb (in) | | | | | .1 | | 1 | .2 |
| (out) | | | | | .001 | | .04 | .001 |
| Sr (in) | | | | | 2 | | .4 | 2 |
| (out) | | | | | .02 | | .03 | .01 |
| Y (in) | | | | | .1 | | .04 | .1 |
| (out) | | | | | .0003 | | .003 | .0005 |
| Zr (in) | | | | | .4 | | .2 | .3 |
| (out) | | | | | .01 | | .007 | .007 |
| Nb (in) | | | | | .04 | | .03 | .01 |
| (out) | | | | | .0003 | | .0009 | <.0001 |
| Mo (in) | | | | | <.1 | | .3 | .05 |
| (out) | | | | | <.001 | | .009 | .01 |
| Ag (in)[g] | | | | | | | | |
| (out) | | | | | | | | |
| Cd (in) (3) | | | | | <.01 | | 2 | .02 |
| (out) | | | | | <.0003 | | .04 | <.0004 |

(continued)

TABLE 5-6 (continued)

| OPERATING PARAMETERS (units as noted) | Primary | | | | | | | |
|---|---|---|---|---|---|---|---|---|
| Power generation, MW/h | 35.0 | 34.8 | 33.0 | 21.6 | 20.6 | 18.6 | 33.5 | 22.0 |
| SCA, $m^2$ per 1000 $m^3/h$ | 16.4 | 27.34 | 7.33 | 16.4 | 21.87 | 10.93 | 16.4 | 16.4 |
| No. fields | 5 | 5 | 4 | 5 | 5 | 3 | 5 | 5 |
| Fuel | Coal | Coal | Coal | Coal | Coal | Coal | RDF[a] | RDF[a] |
| Run No. | 21,22,23 | 20 | 1 | 5,6 | 7,8,9 | 24,25 | 2,26,27,28 | 3,4 |
| **ANALYTICAL RESULTS** (mg/dscm) | | | | | | | | |
| SSMS | | | | | | | | |
| Mg (in) (2) | | | | | | | | |
| (out) | | | | | | | | |
| Al (in) (2) | | | | | | | | |
| (out) | | | | | | | | |
| Si (in) (2) | | | | | | | | |
| (out) | | | | | | | | |
| P (in) | | | | | 7 | | High | 5 |
| (out) | | | | | 1 | | High | .05 |
| S (in) (3)[9] | | | | | 20 | | 200 | 100 |
| (out) | | | | | .7 | | 9 | 5 |
| Cl (in) (1) | | | | | | | | |
| (out) | | | | | | | | |
| K (in) (2) | | | | | 20 | | | .7 |
| (out) | | | | | | | | |
| Ca (in) (2) | | | | | | | | |
| (out) | | | | | | | | |
| Sc (in) | | | | | 200 | | ≤.04 | .05 |
| (out) | | | | | <.001 | | .003 | <.0007 |
| Ti (in) | | | | | 40 | | 4 | 20 |
| (out) | | | | | .3 | | .3 | .1 |
| V (in) | | | | | .5 | | 4 | .2 |
| (out) | | | | | .003 | | .3 | .007 |
| Cr (in) | | | | | .5 | | 1 | 1 |
| (out) | | | | | .07 | | .09 | .1 |
| Mn (in) | | | | | 1 | | 3 | 5 |
| (out) | | | | | .01 | | .09 | .05 |
| Fe (in) (2) | | | | | 2 | | | |
| (out) | | | | | | | | |
| Co (in) | | | | | .07 | | .3 | .2 |
| (out) | | | | | .002 | | .004 | .005 |

(continued)

TABLE 5-6 (continued)

| OPERATING PARAMETERS (units as noted) | Primary | | | | | | | |
|---|---|---|---|---|---|---|---|---|
| Power generation, MW/h | 35.0 | 34.8 | 33.0 | 21.6 | 20.6 | 18.6 | 33.5 | 22.0 |
| SCA, $m^2$ per 1000 $m^3/h$ | 16.4 | 27.34 | 7.33 | 16.4 | 21.87 | 10.93 | 16.4 | 16.4 |
| No. fields | 5 | 5 | 4 | 5 | 5 | 3 | 5 | 5 |
| Fuel | Coal | Coal | Coal | Coal | Coal | Coal | RDF[a] | RDF[a] |
| Run No. | 21,22,23 | 20 | 1 | 5,6 | 7,8,9 | 24,25 | 2,26,27,28 | 3,4 |
| ANALYTICAL RESULTS, mg/dscm | | | | | | | | |
| SSMS | | | | | | | | |
| Sn (in) | | | | | <.04 | | .4 | .2 |
| (out) | | | | | <.001 | | .03 | .004 |
| Sb (in) | | | | | <.007 | | 1 | .1 |
| (out) | | | | | <.0002 | | .009 | .0004 |
| Cs (in) | | | | | <.01 | | .2 | .02 |
| (out) | | | | | <.0003 | | .009 | .00007 |
| Ba (in) | | | | | 4 | | 20 | 2 |
| (out) | | | | | .03 | | .4 | .01 |
| La (in) | | | | | .04 | | .04 | .05 |
| (out) | | | | | .0003 | | .003 | .0001 |
| Ce (in) | | | | | .1 | | .3 | .2 |
| (out) | | | | | .001 | | .009 | .0005 |
| Hg (in)[g] | | | | | | | | |
| (out) | | | | | | | | |
| Tl (in) (3) | | | | | <.1 | | .4 | <.005 |
| (out) | | | | | <.003 | | .007 | .0001 |
| Pb (in) (3) | | | | | .05 | | .6 | 1 |
| (out) | | | | | .001 | | .01 | .005 |
| Bi (in) | | | | | <.007 | | .2 | <.003 |
| (out) | | | | | <.0002 | | .003 | .00007 |

[a] RDF was co-fired with coal and ranged from 13 percent to 25 percent.

[b] Front half only.

[c] Detection limit for Cl is 1.8 mg/dry std. $m^3$.

[d] Detection limit for F is 0.05 mg/dry std. $m^3$.

[e] Detection limit for Br is 4.0 mg/dry std. $m^3$.

[f] Not detectable.

[g] Refer to Appendix A for further explanation of SSMS results.

(1) Element not observed in excess of background levels. (See Appendix B.)

(2) Concentration too high to be reliably estimated by SSMS. (See Appendix B.)

(3) May be low by a factor of 3 to 10 (or more for Cd). (See Appendix B.)

removal efficiency to power generation rate yields no useful trend. Boiler load in the range tested appears to have little or no effect on the pollutant removal efficiencies of the control devices.

Figure 5-2 shows the effect of specific collection area (SCA) and type of fuel (coal only vs. coal plus RDF) on particulate collection efficiency. At less than five energized fields and thus a lower SCA, the efficiency of particulate collection drops slightly in comparison with other coal only runs. Coal plus RDF also adversely affects the performance of the mobile ESP at a given SCA (16.4 $m^2$ per 1000 $m^3/h$). This does not appear to be proportional to an increase in the RDF input ratio. As shown in the data points on Figure 5-2, the average RDF input ratio for Runs 2, 26, 27, and 28 is greater than the average RDF input ratio for Runs 3 and 4; yet the average collection efficiency is greater for the higher of the two RDF ratios. Therefore, although RDF input may adversely affect ESP performance, the performance does not continue to decrease with further increases in RDF input.

Two conclusions that can be drawn from the particulate data:

1. When the number of energized fields and SCA are increased within reasonable design limits, particulate collection efficiency is enhanced, regardless of the coal and RDF mixture.
2. At a specific SCA, RDF input to the boiler tends to decrease ESP collection efficiency; however, a further increase in RDF input does not necessarily continue to decrease ESP performance.

The control of lead emissions, currently an environmental concern, can be evaluated in several ways. Figure 5-3 shows

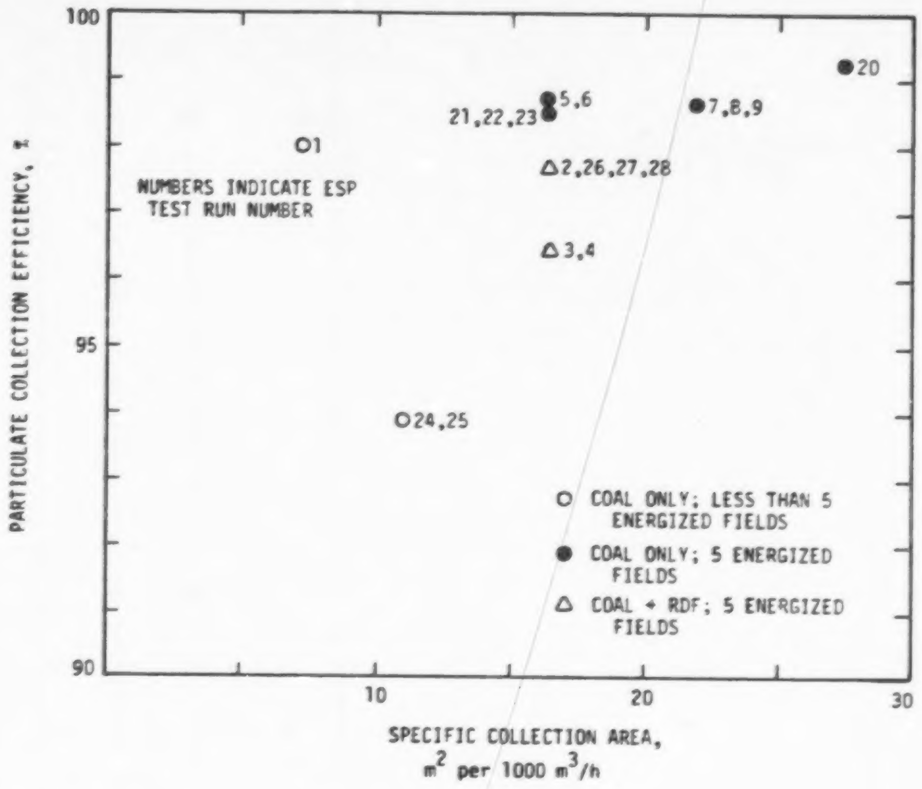

Figure 5-2. Particulate removal efficiency as a function of specific collection area.

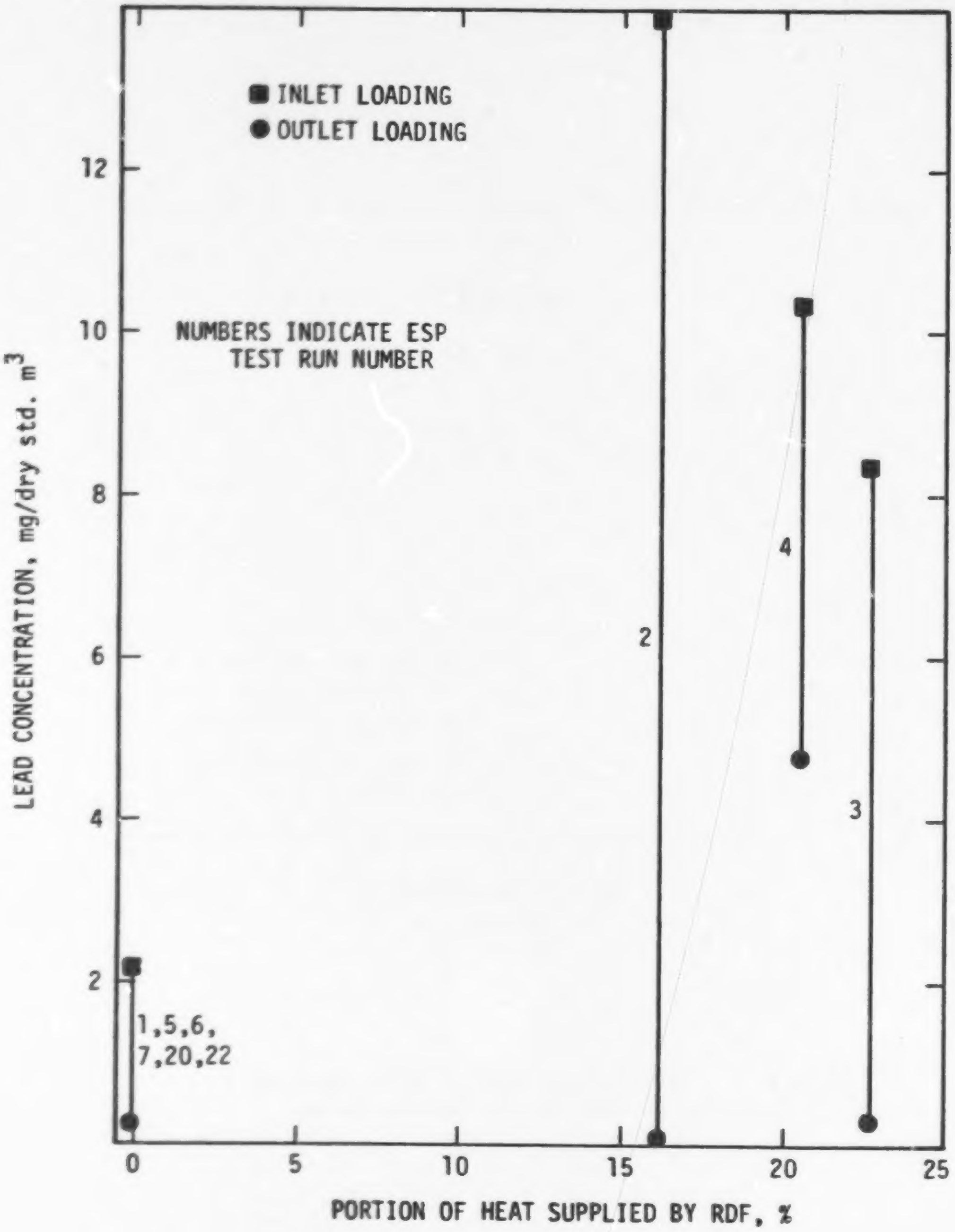

Figure 5-3. Lead concentration as a function of RDF input.

inlet and outlet lead concentrations measured during mobile ESP testing. Individual data points are not listed separately in Table 5-6; average emission concentrations are grouped according to runs having similar test conditions. Figure 5-3 shows that the highest controlled lead emission is less than 5 milligrams per dry standard cubic meter (see Run 4). The overall average of controlled lead emissions, including the coal-only runs, is 0.71 $mg/m^3$.

Figure 5-4 presents the lead composition of fly ash that was sampled at the inlet and outlet of the mobile ESP. The values shown indicate the composition of the fly ash, not the concentration of lead in the gas stream. In all cases but one, the finer particulate at the outlet was composed of a higher percentage of lead than the particulate at the inlet, which indicates the ESP is generally more efficient for particulate removal than for lead removal.

One theory is that lead volatilized in the boiler cools (as it passes from higher temperature regions) to the point where it condenses. As it does, it either adheres to particles or forms lead droplets. Lead emissions are difficult to control because lead exhibits small particle enrichment and is thus more difficult to collect. Figure 5-4 shows that the expected relationship (assuming the inlet particle size distribution is larger than the outlet) holds true in all observations except one (at 16% RDF).

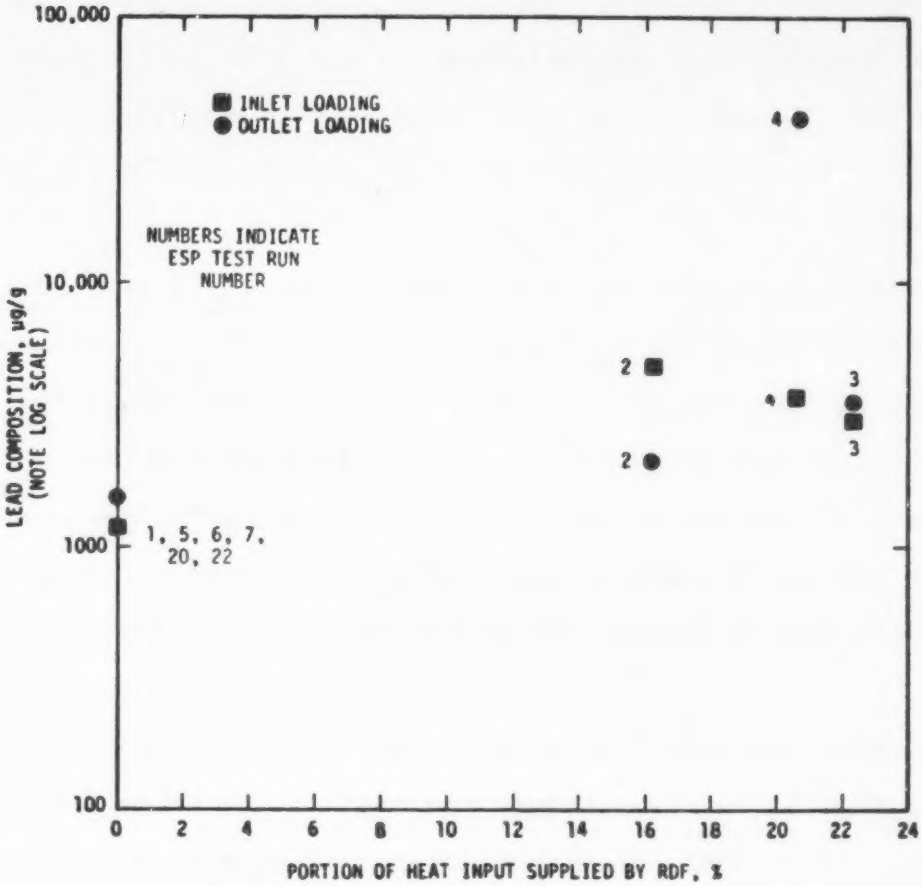

Figure 5-4. Lead composition as a function of RDF input.

## 5.3 MOBILE SCRUBBER

The mobile scrubber was operated at the Ames facility from October 11 through November 1, 1979. Table 5-7 shows the boiler operating conditions prevalent during scrubber tests. Most of the 17 test runs were performed when the boiler was firing coal and RDF.

The operating conditions of the scrubber, during each test run are shown in Table 5-8. As noted in Section 3, the scrubber test plan was structured to include slipstreams from two different locations: before and after the main ESP on Boiler 7. The term "primary device" or "1°" refers to test runs that slipstreamed gas ahead of the main ESP. "Secondary" or "2°" refers to a slipstream taken downstream of the main ESP.

Table 5-9 presents a detailed listing of the results reported from all mobile scrubber sampling and analytical efforts. As with the mobile ESP data, test runs having similar operating conditions are grouped and the corresponding individual data points are averaged. The Method 5 test performed at the scrubber inlet during Test Run 6 was voided because sampling methods did not meet with quality assurance criteria.

### 5.3.1 Mobile Scrubber - Primary Device Test Runs

Figure 5-5 shows particulate removal efficiency as a function of pressure drop across the venturi throat. Figure 5-6 shows particulate loading at the inlet and outlet of the mobile scrubber as a function of RDF input. During all primary device test runs, particulate removal efficiency exceeded 99 percent.

TABLE 5-7. BOILER NO. 7 OPERATING CONDITIONS DURING MOBILE SCRUBBER TESTING

| Date | Test No. | Time | Power generation rate, MW/h | Coal flow, kg | Coal input, MJ | RDF flow, $m^3$ | RDF flow,[b] kg | RDF input, MJ | Total input, MJ | RDF % (heat input basis) |
|---|---|---|---|---|---|---|---|---|---|---|
|  |  |  |  |  | During Test Period |  |  |  |  |  |
| 10/11 | 1 SI/SO | 1000-1200 | 35.0 | 29937 | 722780[a] | 90.62 | 8999 | 127233[c] | 850013 | 15.0 |
| 10/11 | 2 SI/SO | 1500-1700 | 35.0 | 27306 | 659270 | 99.12 | 9824 | 138838 | 798108 | 17.4 |
| 10/12 | 3 SI/SO | 1000-1200 | 35.0 | 29393 | 709593 | 116.11 | 12553 | 177451 | 887044 | 20.0 |
| 10/12 | 4 SI/SO | 1400-1600 | 35.0 | 28304 | 683324 | 124.61 | 13472 | 190428 | 873752 | 21.8 |
| 10/17 | 5 SI/SO | 1200-1330 | 33.0 | 21273 | 513574 | 53.81 | 5300 | 74905 | 588479 | 12.7 |
| 10/17 | 6 SI/SO | 1500-1630 | 31.0 | 22271 | 537628 | 62.30 | 6137 | 86721 | 624349 | 13.9 |
| 10/18 | 7 SI/SO | 1100-1230 | 32.0 | 19527 | 471374 | 62.30 | 7185 | 101491 | 572865 | 17.7 |
| 10/19 | 8 SI/SO | 1400-1500 | 33.0 | 13336 | 321986 | 42.48 | 4593 | 64882 | 386868 | 16.8 |
| 10/24 | 9 SI/SO | 1030-1130 | 22.0 | 8664 | 209101 | 36.82 | 4570 | 64566 | 273667 | 23.6 |
| 10/24 | 10 SI/SO | 1430-1600 | 22.0 | 14039 | 338972 | 55.22 | 6855 | 96849 | 435821 | 22.2 |
| 10/25 | 11 SI/SO | 1030-1230 | 22.0 | 8187 | 197707 | 43.90 | 5232 | 73956 | 271663 | 27.2 |
| 10/26 | 12 SI/SO | 1430-1530 | 22.0 | 9162 | 221234 | 39.65 | 4604 | 65094 | 286328 | 22.7 |
| 10/31 | 13 SI/SO | 1400-1500 | 27.5 | 14334 | 346040 | 0 | 0 | 0 | 346040 | 0 |
| 11/1 | 14 SI/SO | 1000-1100 | 29.0 | 15558 | 375580 | 0 | 0 | 0 | 375580 | 0 |
| 11/1 | 15 SI/SO | 1500-1600 | 29.0 | 15649 | 377796 | 0 | 0 | 0 | 377796 | 0 |
| 11/2 | 16 SI/SO | 1000-1100 | 30.0 | 17055 | 411766 | 0 | 0 | 0 | 411766 | 0 |
| 11/2 | 17 SI/SO | 1430-1530 | 32.3 | 16874 | 407336 | 0 | 0 | 0 | 407336 | 0 |

a. Coal heating value is a composite average of the daily heating values used during the test periods as 24.1 MJ/kg.

b. Average density of RDF over the entire test period was 104.1 kg/$m^3$ as measured by Ames and PEDCo personnel.

c. At 14.1 MJ/kg.

| To convert from | to | multiply by |
|---|---|---|
| kg | lb | 2.205 E + 00 |
| MJ | $10^6$ Btu | 9.470 E - 04 |
| $m^3$ | $ft^3$ | 3.531 E + 01 |

TABLE 5-8. MOBILE SCRUBBER OPERATING CONDITIONS

| Date | Run number | % RDF (heat input basis) | Device location, 1° or 2° | ΔP,[a] cm W.G. | Actual gas flow rate,[a] $m^3/h$ | Scrubbing liquor flow rate,[a] liters/min | L/G, liters/$m^3$ |
|---|---|---|---|---|---|---|---|
| 10/11 | 1 SI/SO | 15.0 | 2° | 76.2 | 781.5 | 29.3 | 2.25 |
| 10/11 | 2 SI/SO | 17.4 | 2° | 76.2 | 781.5 | 29.3 | 2.25 |
| 10/12 | 3 SI/SO | 20.0 | 2° | 76.2 | 920.9 | 30.2 | 1.98 |
| 10/12 | 4 SI/SO | 21.8 | 2° | 76.2 | 920.9 | 30.7 | 2.01 |
| 10/17 | 5 SI/SO | 12.7 | 1° | 76.2 | 852.9 | 30.2 | 2.13 |
| 10/17 | 6 SI/SO | 13.9 | 1° | 76.2 | 852.9 | 16.0 | 2.13 |
| 10/18 | 7 SI/SO | 17.7 | 1° | 25.4 | 485.9 | 16.0 | 1.98 |
| 10/19 | 8 SI/SO | 16.8 | 1° | 25.4 | 485.9 | 16.0 | 1.99 |
| 10/24 | 9 SI/SO | 23.6 | 1° | 76.2 | 835.9 | 29.2 | 2.10 |
| 10/24 | 10 SI/SO | 22.2 | 2° | 76.2 | 835.9 | 29.3 | 2.10 |
| 10/25 | 11 SI/SO | 27.2 | 2° | 25.4 | 487.6 | 16.6 | 2.05 |
| 10/26 | 12 SI/SO | 22.7 | 1° | 50.8 | 720.4 | 23.6 | 1.97 |
| 10/30 | 13 SI/SO | 0 | 1° | 25.4 | 433.2 | 14.3 | 1.99 |
| 11/1 | 14 SI/SO | 0 | 1° | 25.4 | 477.4 | 15.9 | 1.99 |
| 11/1 | 15 SI/SO | 0 | 1° | 76.2 | 854.6 | 28.3 | 1.99 |
| 11/1 | 16 SI/SO | 0 | 1° | 76.2 | 849.5 | 28.3 | 2.01 |
| 11/1 | 17 SI/SO | 0 | 1° | 76.2 | 886.9 | 28.4 | 1.93 |

| To convert from | to | multiply by |
|---|---|---|
| cm W.G. | in. W.G. | 3.937 E - 01 |
| liters/min | gal/hr | 1.585 E + 01 |
| liters/$m^3$ | gal/1000 $ft^3$ | 7.481 |
| $m^3$/hr | $ft^3$/min | 5.885 E - 01 |

[a] Reported by Acurex.

## TABLE 5-9. MOBILE SCRUBBER EMISSION CONCENTRATIONS

| OPERATING PARAMETERS (units as noted) | Primary | | | | | | | Secondary | | | |
|---|---|---|---|---|---|---|---|---|---|---|---|
| Power generation, MW/h | 30.4 | 28.3 | 32.5 | 33.0 | 31.0 | 22.0 | 22.0 | 35.0 | 35.0 | 22.0 | 22.0 |
| ΔP, cm W.G. | 76.2 | 25.4 | 25.4 | 76.2 | 76.2 | 76.2 | 50.8 | 76.2 | 76.2 | 76.2 | 25.4 |
| Gas flow rate, $m^3/h$ | 863.7 | 455.3 | 485.3 | 852.9 | 852.9 | 835.9 | 720.4 | 920.9 | 781.5 | 835.9 | 487.6 |
| S.I.[a] flow rate, liters/min | 28.3 | 15.1 | 16.0 | 30.2 | 16.0 | 29.2 | 23.6 | 30.5 | 29.3 | 29.3 | 16.6 |
| Fuel | Coal | Coal | RDF[b] | RDF[b] | RDF[b] | RDF[b] | RDF[b] | RDF[b] | RDF[b] | RDF[b] | RDF[b] |
| Run No. | 15,16,17 | 13,14 | 7,8 | 5 | 6 | 9 | 12 | 3,4 | 1,2 | 10 | 11 |
| ANALYTICAL RESULTS, mg/dry std. $m^3$ | | | | | | | | | | | |
| Gravemetric Analysis | | | | | | | | | | | |
| T. particulate (in)[c]<br>(out) | 12,210<br>106.0 | 12,770<br>92.26 | 18,130<br>89.88 | 9,945<br>51.54 | 49.21 | 11,610<br>56.09 | 18,520<br>54.20 | 396.0<br>12.62 | 423.9<br>24.19 | 107.9<br>25.92 | 103.9<br>28.23 |
| Specific Ion Electrode Analysis | | | | | | | | | | | |
| Cl (in)[d]<br>(out) | 10.0<br>ND[e] | | 91.0<br>ND | 120<br>5.00 | | 220<br>ND | 130<br>ND | | | 89.0<br>ND | 20.0<br>ND |
| F (in)[f]<br>(out) | 14.1<br>2.65 | 9.66<br>.350 | 5.51<br>.210 | 3.49<br>ND | | | 13.0<br>1.57 | .450<br>ND | | 8.94<br>.0900 | 7.98<br>.130 |
| Br (in)[g]<br>(out) | ND<br>ND | ND<br>ND | ND<br>ND | ND<br>ND | | | ND<br>ND | ND<br>ND | | ND<br>ND | ND<br>ND |
| Atomic Absorption Analysis | | | | | | | | | | | |
| Pb (in)<br>(out) | 1.7<br>.26 | 1.8<br>.22 | 9.1<br>.74 | | 1.3<br>.18 | 14.<br>2.2 | | | | | |
| Cd (in)<br>(out) | .034<br>.0026 | | | | | .14<br>.026 | | | | | |
| Sb (in)<br>(out) | .34<br>.0069 | | | | | .46<br>.017 | | | | | |
| Fe (in)<br>(out) | 260<br>2.1 | | | | | 460<br>1.5 | | | | | |
| Cu (in)<br>(out) | .25<br>.013 | | | | | .99<br>.025 | | | | | |
| Spark Source Mass Spectrometry Analysis | | | | | | | | | | | |
| Li (in) (1)[h]<br>(out) | | | | | | | | | | | |
| Be (in)<br>(out) | | .200<br>.005 | .100<br>.002 | | | .03<br>.002 | .100<br>.001 | | | .001<br>.001 | .001<br>.00003 |
| B (in) (1)<br>(out) | | | | | | | | | | | |
| F (in)<br>(out) | | 4<br>.4 | 50<br>.8 | | | 10<br>.6 | 20<br>.2 | | | 1<br>.5 | 2<br>.1 |

(continued)

TABLE 5-9 (continued).

| OPERATING PARAMETERS (units as noted) | Primary | | | | | | | Secondary | | | |
|---|---|---|---|---|---|---|---|---|---|---|---|
| Power generation, MW/h | 30.4 | 28.3 | 32.5 | 33.0 | 31.0 | 22.0 | 22.0 | 35.0 | 35.0 | 22.0 | 22.0 |
| ΔP, cm W.G. | 76.2 | 25.4 | 25.4 | 76.2 | 76.2 | 76.2 | 50.8 | 76.2 | 76.2 | 76.2 | 25.4 |
| Gas flow rate, $m^3/h$ | 863.7 | 455.3 | 485.3 | 852.9 | 852.9 | 835.9 | 720.4 | 920.9 | 781.5 | 835.9 | 487.6 |
| S.I.$^a$ flow rate, liters/min | 28.3 | 15.1 | 16.0 | 30.2 | 16.0 | 29.2 | 23.6 | 30.5 | 29.3 | 29.3 | 16.6 |
| Fuel | Coal | Coal | RDF$^b$ | RDF$^b$ | RDF$^b$ | RDF$^b$ | RDF$^b$ | RDF$^b$ | RDF$^b$ | RDF$^b$ | RDF$^b$ |
| Run No. | 15,16,17 | 13,14 | 7,8 | 5 | 6 | 9 | 12 | 3,4 | 1,2 | 10 | 11 |
| ANALYTICAL RESULTS mg/dry std. $m^3$ | | | | | | | | | | | |
| SSMS | | | | | | | | | | | |
| Na (in) (2)$^h$ | | | | | | | | | | | |
| (out) | | | | | | | | | | | |
| Mg (in) (2) | | | | | | | | | | | |
| (out) | | | | | | | | | | | |
| Al (in) (2) | | | | | | | | | | | |
| (out) | | | | | | | | | | | |
| Si (in) (2) | | | | | | | | | | | |
| (out) | | | | | | | | | | | |
| P (in) | | High | 30 | | | 9 | High | | | .1 | .6 |
| (out) | | High | .5 | | | .4 | High | | | .2 | .01 |
| S (in) (3) | | 20 | 100 | | | 70 | 200 | | | 3 | 20 |
| (out) | | 2 | 3 | | | .6 | High | | | High | .8 |
| Cl (in) (1) | | | | | | | | | | | |
| (out) | | | | | | | | | | | |
| K (in) (2) | | | | | | | | | | | |
| (out) | | | | | | | | | | | |
| Ca (in) (2) | | | | | | | | | | | |
| (out) | | | | | | | | | | | |
| Sc (in) | | .8 | 1 | | | .3 | 1 | | | <.003 | <.005 |
| (out) | | .005 | .02 | | | .02 | .001 | | | <.002 | <.0001 |
| Ti (in) | | 60 | 50 | | | 9 | 40 | | | .1 | <.4 |
| (out) | | 1 | .8 | | | .6 | .4 | | | .1 | <.008 |
| V (in) | | 2 | 1 | | | .9 | 1 | | | .01 | .01 |
| (out) | | .05 | .02 | | | .04 | .1 | | | .008 | .0003 |
| Cr (in) | | 2 | 2 | | | .7 | 2 | | | .1 | .1 |
| (out) | | .05 | .03 | | | .03 | .02 | | | .1 | .006 |
| Mn (in) | | 8 | 20 | | | 9 | 20 | | | .03 | .1 |
| (out) | | .05 | .08 | | | .4 | .1 | | | .02 | .003 |

(continued)

TABLE 5-9 (continued).

| OPERATING PARAMETERS (units as noted) | Primary | | | | | | | Secondary | | | |
|---|---|---|---|---|---|---|---|---|---|---|---|
| Power generation, MW/h | 30.4 | 28.3 | 32.5 | 33.0 | 31.0 | 22.0 | 22.0 | 35.0 | 35.0 | 22.0 | 22.0 |
| ΔP, cm W.G. | 76.2 | 25.4 | 25.4 | 76.2 | 76.2 | 76.2 | 50.8 | 76.2 | 76.2 | 76.2 | 25.4 |
| Gas flow rate, $m^3/h$ | 863.7 | 455.3 | 485.3 | 852.9 | 852.9 | 835.9 | 720.4 | 920.9 | 781.5 | 835.9 | 487.6 |
| S.I.[a] flow rate, liters/min | 28.3 | 15.1 | 16.0 | 30.2 | 16.0 | 29.2 | 23.6 | 30.5 | 29.3 | 29.3 | 16.6 |
| Fuel | Coal | Coal | RDF[b] | RDF[b] | RDF[b] | RDF[b] | RDF[b] | RDF[b] | RDF[b] | RDF[b] | RDF[b] |
| Run No. | 15,16,17 | 13,14 | 7,8 | 5 | 6 | 9 | 12 | 3,4 | 1,2 | 10 | 11 |
| ANALYTICAL RESULTS mg/dry std. $m^3$ | | | | | | | | | | | |
| SSMS | | | | | | | | | | | |
| Fe (in) (2)<br>(out) | | | | | | | | | | <br>2 | 4<br> |
| Co (in)<br>(out) | | .3<br>.002 | .5<br>.008 | | | .1<br>.006 | .2<br>.004 | | | .01<br>.01 | .01<br>.0003 |
| Ni (in)<br>(out) | | .8<br><.01 | <.5<br><.008 | | | <.1<br><.006 | .6<br><.004 | | | <.1<br><.05 | <.1<br>.003 |
| Cu (in)<br>(out) | | 3<br>.007 | 2<br>.03 | | | 1<br>.06 | 2<br>.04 | | | .03<br>.1 | .06<br>.003 |
| Zn (in)<br>(out) | | 2<br>.2 | 3<br>.2 | | | 3<br>.3 | 1<br>.2 | | | .06<br>.1 | .5<br>.006 |
| Ga (in)<br>(out) | | .8<br>.02 | .5<br>.008 | | | .1<br>.006 | <.2<br>.01 | | | .006<br>.003 | .02<br>.0006 |
| As (in)<br>(out) | | .3<br>.01 | .2<br>.003 | | | .1<br>.0002 | .2<br>.004 | | | .006<br><.002 | .004<br>.00008 |
| Br (in)<br>(out) | | <.07<br><.0007 | <.03<br><.0006 | | | <.01<br><.0006 | <.04<br><.0003 | | | .006<br>.003 | .002<br>.00003 |
| Rb (in)<br>(out) | | 2<br>.007 | .3<br>.02 | | | .9<br>.04 | 1<br>.03 | | | .03<br>.02 | .01<br>.0003 |
| Sr (in)<br>(out) | | 20<br>.1 | 5<br>.08 | | | 5<br>.2 | 6<br>.04 | | | .06<br>.03 | .04<br>.0008 |
| Y (in)<br>(out) | | .8<br>.002 | .2<br>.003 | | | .1<br>.006 | .6<br>.001 | | | .001<br>.0005 | .001<br>.00001 |
| Zr (in)<br>(out) | | 2<br>.004 | .2<br>.003 | | | .1<br>.006 | .2<br>.0004 | | | .003<br>.002 | .01<br>.0001 |
| Nb (in)<br>(out) | | .03<br>.0005 | .01<br>.0003 | | | .009<br>.0002 | .02<br>.0003 | | | <.0003<br><.0002 | <.0004<br><.00001 |
| Mo (in)<br>(out) | | <.2<br>.002 | <.1<br>.003 | | | <.03<br>.003 | <.1<br>.004 | | | .006<br>.003 | <.005<br>.0003 |

(continued)

TABLE 5-9 (continued).

| OPERATING PARAMETERS (units as noted) | Primary | | | | | | | Secondary | | | |
|---|---|---|---|---|---|---|---|---|---|---|---|
| Power generation, MW/h | 30.4 | 28.3 | 32.5 | 33.0 | 31.0 | 22.0 | 22.0 | 35.0 | 35.0 | 22.0 | 22.0 |
| ΔP, cm W.G. | 76.2 | 25.4 | 25.4 | 76.2 | 76.2 | 76.2 | 50.8 | 76.2 | 76.2 | 76.2 | 25.4 |
| Gas flow rate, $m^3$/h | 863.7 | 455.3 | 485.3 | 852.9 | 852.9 | 835.9 | 720.4 | 920.9 | 781.5 | 835.9 | 487.6 |
| S.I.[a] flow rate, liters/min | 28.3 | 15.1 | 16.0 | 30.2 | 16.0 | 29.2 | 23.6 | 30.5 | 29.3 | 29.3 | 16.6 |
| Fuel | Coal | Coal | RDF[b] | RDF[b] | RDF[b] | RDF[b] | RDF[b] | RDF[b] | RDF[b] | RDF[b] | RDF[b] |
| Run No. | 15,16,17 | 13,14 | 7,8 | 5 | 6 | 9 | 12 | 3,4 | 1,2 | 10 | 11 |
| ANALYTICAL RESULTS mg/dry std. $m^3$ | | | | | | | | | | | |
| SSMS | | | | | | | | | | | |
| Ag (in)[h] | | | | | | | | | | | |
| (out) | | | | | | | | | | | |
| Cd (in) (3) | | <.07 | <.03 | | | <.03 | <.04 | | | .001 | <.001 |
| (out) | | <.0007 | <.0006 | | | <.002 | .03 | | | .005 | .0003 |
| Sn (in) | | <.2 | .2 | | | .09 | .3 | | | .002 | .01 |
| (out) | | <.002 | .003 | | | .002 | .01 | | | .001 | .0008 |
| Sb (in) | | .07 | .3 | | | .7 | .2 | | | .006 | .007 |
| (out) | | .0005 | .006 | | | .01 | .02 | | | .005 | .00003 |
| Cs (in) | | .2 | <.03 | | | <.03 | .06 | | | .001 | <.001 |
| (out) | | .0007 | .002 | | | .004 | .003 | | | .0005 | <.00003 |
| Ba (in) | | 30 | 10 | | | 7 | 10 | | | .03 | .06 |
| (out) | | .4 | .2 | | | .3 | .1 | | | .02 | .003 |
| La (in) | | .6 | .2 | | | .09 | .1 | | | .0003 | <.0004 |
| (out) | | .0007 | .003 | | | .004 | .0002 | | | .00008 | <.00001 |
| Ce (in) | | 2 | .5 | | | .3 | .3 | | | .0006 | .001 |
| (out) | | .001 | .008 | | | .02 | .0004 | | | .0002 | <.00003 |
| Hg (in)[h] | | | | | | | | | | | |
| (out) | | | | | | | | | | | |
| Tl (in) (3) | | <.06 | <.03 | | | <.009 | <.04 | | | .0006 | <.001 |
| (out) | | .005 | .002 | | | .0006 | .01 | | | .0002 | <.00003 |
| Pb (in) (3) | | .5 | 3 | | | 3 | 1 | | | .6 | .02 |
| (out) | | .04 | .05 | | | .2 | .3 | | | .3 | .006 |
| Bi (in) | | <.03 | .02 | | | <.007 | <.02 | | | .0003 | <.001 |
| (out) | | .0005 | .0003 | | | <.0003 | .001 | | | .0002 | <.00003 |

[a] Scrubber liquor.

[b] RDF was co-fired with coal and ranged from 13 to 25 percent.

[c] Front half only.

[d] Detection limit for Cl is 1.8 mg/dry std. $m^3$.

[e] Not detectable.

[f] Detection limit for F is 0.05 mg/dry std. $m^3$.

[g] Detection limit for Br is 4.0 mg/dry std. $m^3$.

[h] Refer to Appendix A for further explanation of SSMS results.

(1) Element not observed in excess of background levels.

(2) Concentration too high to be estimated reliably by SSMS.

(3) May be low by a factor of 3 to 10 (or more for Cd).

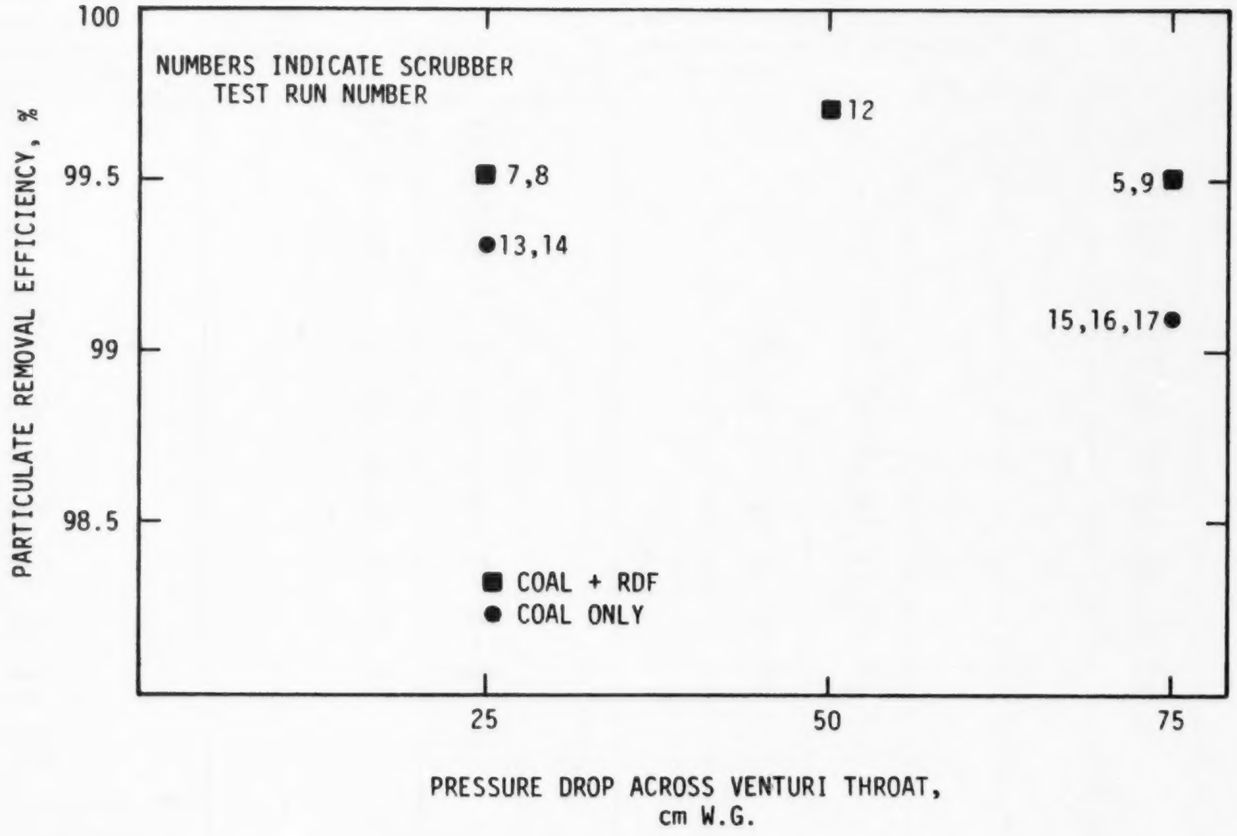

Figure 5-5. Mobile scrubber - primary device - particulate removal efficiency as a function of venturi throat pressure drop.

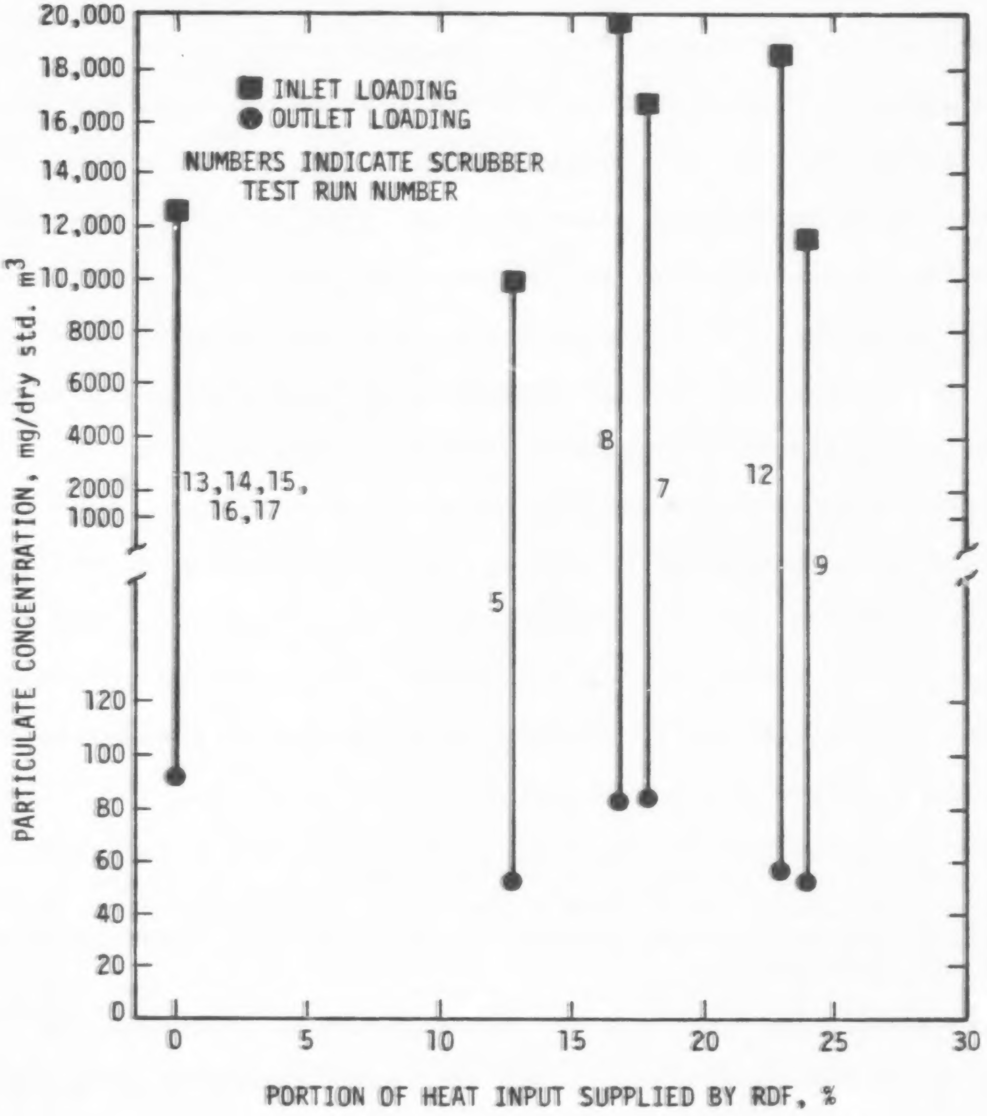

Figure 5-6. Particulate concentration as a function of RDF input.

The only test run at the medium pressure drop occurred when the boiler was firing coal plus RDF, during which the highest particulate collection efficiency (99.7%) was observed.

As shown in Figure 5-5, within the test conditions, the anticipated results show no increase in particulate collection efficiency with increasing pressure drop. The efficiency is the same on coal-plus-RDF tests at low and high pressure drops and actually decreases with increasing pressure drop on coal-only tests. The conclusion is that an operating parameter other than pressure drop affects particulate removal efficiency, and in these test runs, to a greater degree than pressure drop.

This was investigated by Midwest Research Institute (MRI), and their findings are found in Section 2 of Appendix C. The contradiction of the data with the normal relationships of pressure drop and collection efficiency is explained in the following closing remark from the MRI report:

> "The relationship of collection efficiency and pressure drop in the venturi scrubber performance data is due to the longer residence time created by a lower pressure drop and partly due to the fluctuation of particle size distribution in the flue gas."

This conclusion is based on the operational procedure that is used to change conditions in the scrubber. Pressure drop is varied by a change in gas flow rate, not in venturi throat size. The scrubber liquor flow rate is adjusted accordingly to keep the liquid-to-gas ratio constant for all test runs. The effect of this procedure on the results of the scrubber program was not anticipated. It is obvious, however, that the pressure drop/collection efficiency relationship experienced in this program is not what normally would be expected. Thus, the dominant operational parameter for the scrubber test series would appear to be residence time rather than pressure drop.

The data presented in Figure 5-6 also suggest that RDF input may enhance particulate collection in a venturi scrubber. At both low and high pressure drops, particulate collection efficiency was greater for the coal-plus-RDF tests than for the coal-only tests. This is somewhat misleading, however, inasmuch as inlet particulate loading appears to increase with RDF input. At constant inlet particulate loading, collection efficiency may not be enhanced by RDF input.

Figure 5-7 shows a comparison of lead concentrations at the device inlet and outlet versus percent RDF in the fuel. Lead emissions increase in test runs with an increasing percentage of RDF. A comparison of Figure 5-3 and 5-7 shows that the magnitude of both inlet and outlet lead concentrations for the mobile scrubber and the mobile ESP are about the same. Scrubber outlet emissions increase slightly, however, whereas ESP emissions remain very low.

The ability of a scrubber to remove chloride emissions is also of interest, since uncontrolled chloride emissions increase when RDF is burned. Uncontrolled chloride emissions are shown in Table 5-9. Controlled values are shown for only one test because of the lack of detectable amounts of chloride in outlet samples.

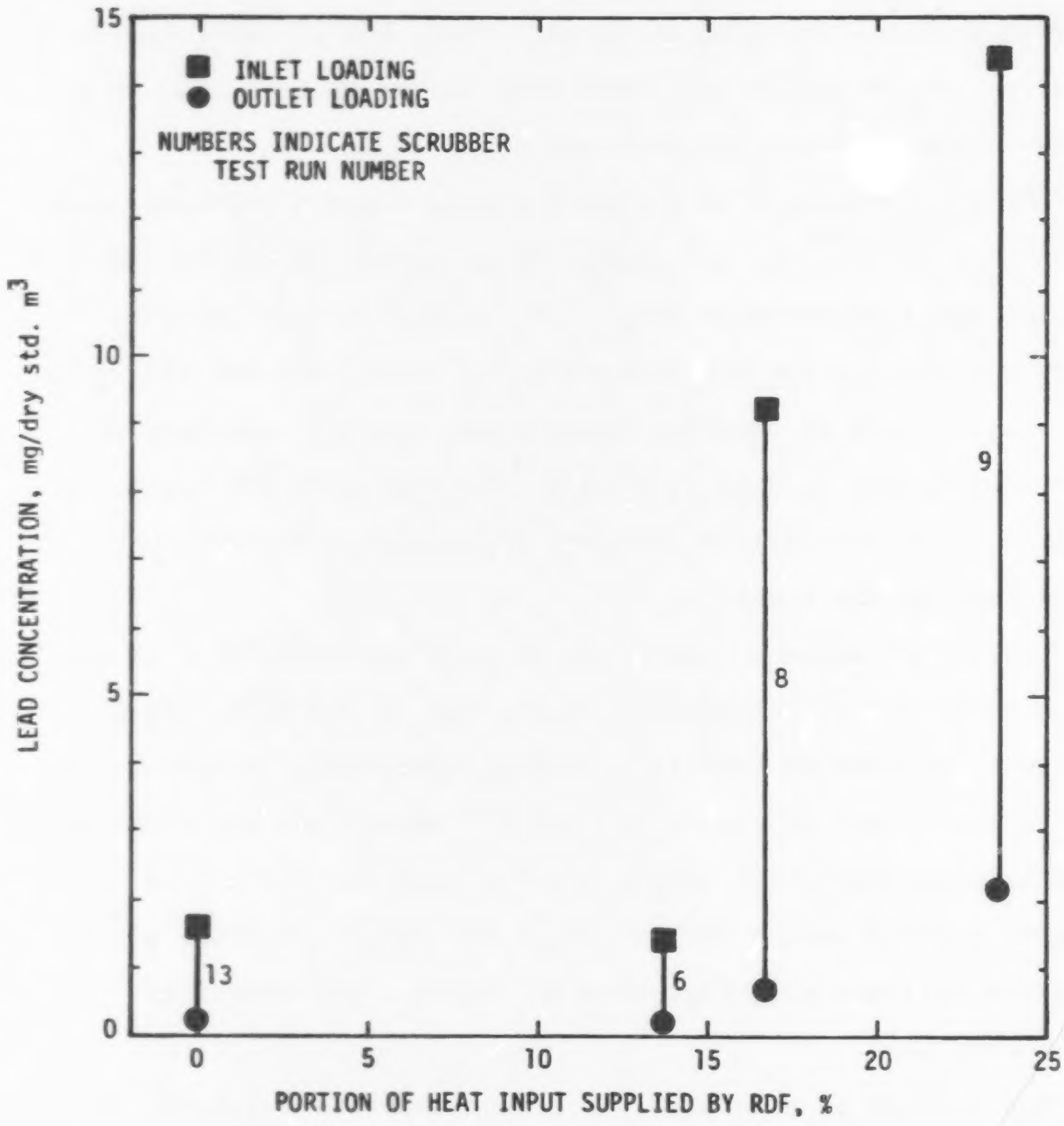

Figure 5-7. Lead concentration as a function of RDF input.

It is obvious that the coal-only test resulted in the lowest concentration of uncontrolled chlorides and that chloride concentrations increased significantly with RDF input. Chloride removal efficiency was 96 percent when the scrubber outlet chloride concentration was measured at 5 mg/dry std. $m^3$. Since the level of detectability of chloride with these sampling and analytical methods is 1.8 mg/dry std. $m^3$, the 96 percent removal efficiency probably represents worst-case conditions. Chloride analysis with the SSMS was not possible because of pre-digestion of particulate samples with hydrochloric acid.

Two conclusions can be drawn from the chloride discussion:

1. Uncontrolled chloride emissions increase when RDF is fired. This is also appears in the ESP emissions table (Table 5-6).
2. The control of chloride emissions appears highly effective when a water/lime solution is used in a venturi-type scrubber. The control of chloride emissions by the mobile ESP was poor. (See Table 5-6.)

### 5.3.2 Mobile Scrubber - Secondary Device Test Runs

Table 5-9 presented the results of sampling and analytical work done for "secondary device" test runs, along with the primary device results. The scrubber was operated for six test runs as a secondary device, all of which were coal-plus-RDF runs.

Figure 5-8 shows the particulate concentration results at inlet and outlet sample points as a function of venturi throat pressure drop. Five of the six test runs were at the higher pressure drop, and the data in the figure reflect an average of these runs. Only one test run was made at the low pressure drop.

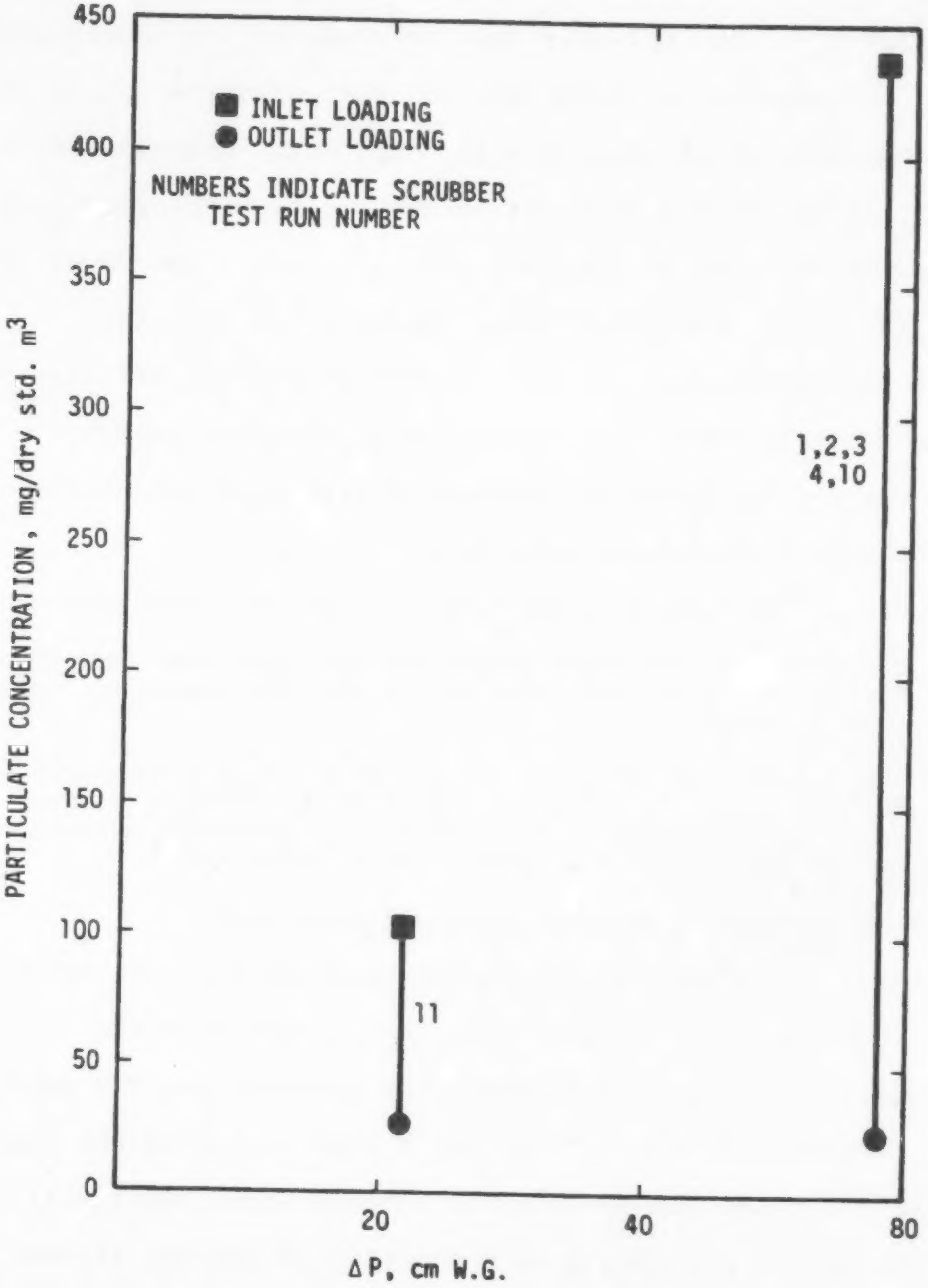

Figure 5-8. Mobile scrubber - secondary device - particulate concentration as a function of venturi throat pressure drop.

Outlet concentrations, which are very similar for both conditions, are consistent with expected values. The inlet particulate concentrations differ by a factor of 4, which may be due to a number of conditions. First, the power generation rate (boiler load) was much lower for the single data point at the low pressure drop condition. Although no correlation between particulate concentration and boiler load has been noted, one may exist in this instance.

Figure 5-9 shows the efficiency of particulate collection as a function of percent RDF input. Results appear consistent with expected values; i.e., a lower collection efficiency resulted from lower pressure drop conditions as compared with most of the runs under higher pressure drop conditions. No obvious trends emerged from a comparison of particulate removal efficiency with RDF input on secondary scrubber tests.

## 5.4 PILOT FABRIC FILTER

The mobile fabric filter, operated between June 19 and July 25, 1979, was tested in 53 runs. Table 5-10 presents boiler operating conditions during the fabric filter test series. The test runs are split almost evenly between firing coal only and coal plus RDF. This provides a better data base than that established for the mobile ESP or mobile scrubber.

Table 5-11 presents operating conditions for the mobile fabric filter. The air-to-cloth (A/C) ratios shown on this table are from the fabric filter operator log sheets (Section 4.3) used

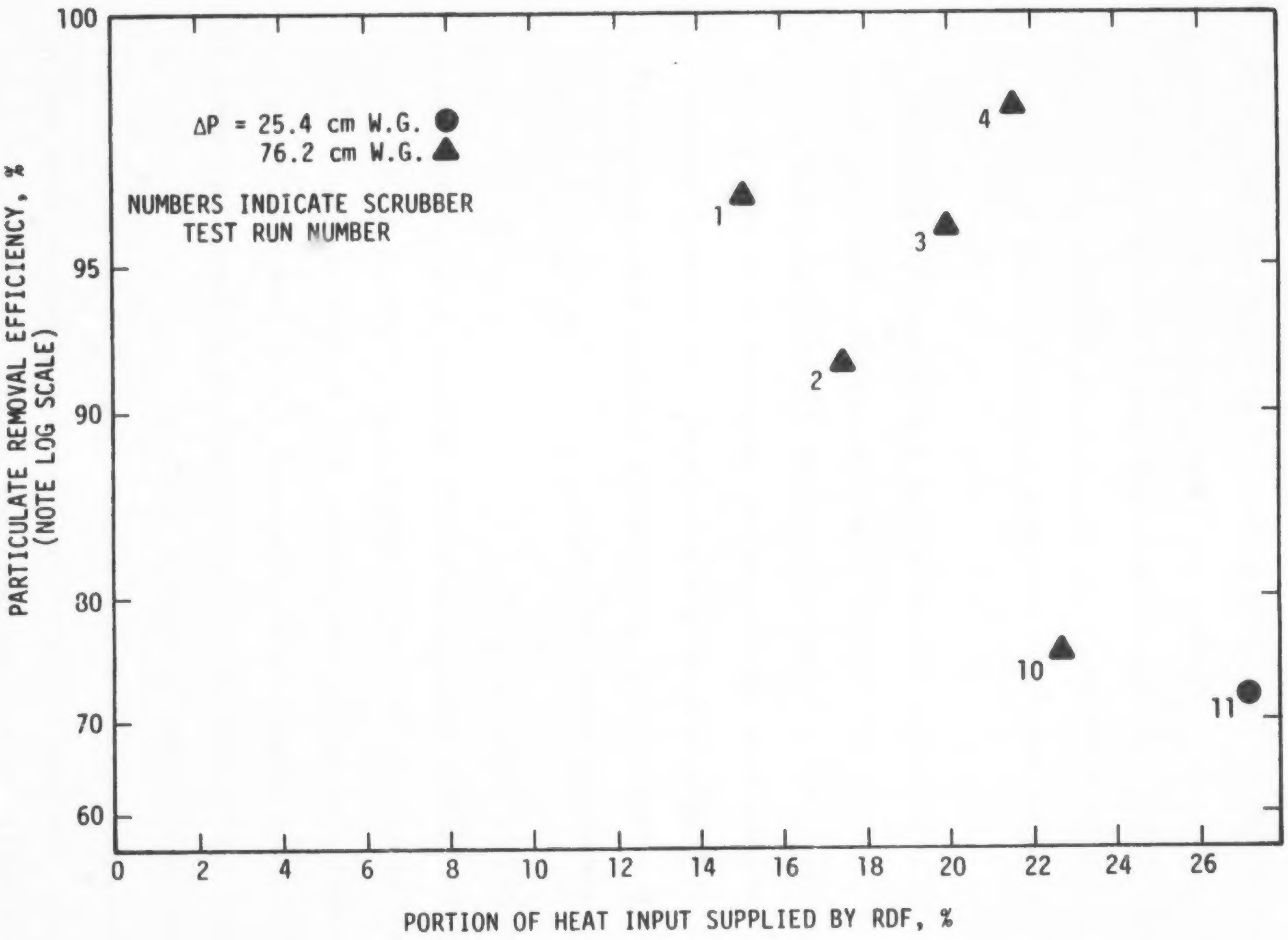

Figure 5-9. Mobile scrubber - secondary device - particulate removal efficiency as a function of RDF input.

## TABLE 5-10. BOILER NO. 7 OPERATING CONDITIONS DURING FABRIC FILTER TEST RUNS

| Date | Test No. | Time | Power generation rate, MW/h | Coal flow,[a] kg | Coal input, MJ | RDF flow,[b] $m^3$ | RDF flow, kg | RDF input, MJ | Total input, MJ | RDF, % (heat input basis) |
|---|---|---|---|---|---|---|---|---|---|---|
| 6/19 | 1 FI/FO | 2150-2250 | 29.5 | 13,605 | 289,242[c] | 0 | 0 | 0 | 289,242 | 0 |
| 6/20 | 2 FI/FO | 0200-0300 | 24.0 | 10,975 | 233,328 | 36.82 | 2241[d] | 39,356[e] | 272,684 | 14.4 |
| 6/20 | 3 FI/FO | 2020-2120 | 35.1 | 14,966 | 318,177 | 50.98 | 3103 | 54,491 | 372,668 | 14.6 |
| 6/20 | 4 FI/FO | 2300-2400 | 20.9 | 8,163 | 173,545 | 42.48 | 2586 | 45,406 | 218,951 | 20.7 |
| 6/21 | 5 FI/FO | 0100-0200 | 16.8 | 9,342 | 198,610 | 0 | 0 | 0 | 198,610 | 0 |
| 6/21 | 6 FI/FO | 2000-2105 | 34.9 | 19,298 | 410,275 | 0 | 0 | 0 | 410,275 | 0 |
| 6/21 | 7 FI/FO | 2215-2330 | 35.1 | 24,036 | 511,005 | 0 | 0 | 0 | 511,005 | 0 |
| 6/22 | 8 FI/FO | 0030-0130 | 20.7 | 11,429 | 242,980 | 0 | 0 | 0 | 242,980 | 0 |
| 6/22 | 9 FI/FO | 2105-2210 | 35.0 | 19,249 | 409,234 | 52.00 | 3165 | 55,581 | 464,815 | 11.9 |
| 6/23 | 10 FI/FO | 2349-0053 | 20.0 | 9,123 | 193,955 | 51.51 | 3135 | 55,058 | 249,013 | 22.1 |
| 6/23 | 11 FI/FO | 1953-2056 | 25.6 | 11,333 | 240,940 | 59.47 | 3620 | 63,566 | 304,506 | 20.9 |
| 6/23 | 12 FI/FO | 2212-2313 | 19.8 | 8,604 | 182,921 | 46.22 | 2813 | 49,404 | 232,324 | 21.3 |
| 6/25 | 13 FI/FO | 1249-1350 | 28.0 | 13,137 | 279,293 | 0 | 0 | 0 | 279,293 | 0 |
| 6/25 | 14 FI/FO | 1455-1605 | 30.6 | 17,033 | 362,122 | 0 | 0 | 0 | 362,122 | 0 |
| 6/25 | 15 FI/FO | 1710-1812 | 29.9 | 15,789 | 335,674 | 0 | 0 | 0 | 335,674 | 0 |
| 6/26 | 16 FI/FO | 1005-1107 | 26.1 | 14,995 | 318,794 | 0 | 0 | 0 | 318,794 | 0 |
| 6/26 | 17 FI/FO | 1214-1314 | 27.0 | 18,549 | 394,352 | 0 | 0 | 0 | 394,352 | 0 |
| 6/26 | 18 FI/FO | 1450-1550 | 35.4 | 20,045 | 426,157 | 0 | 0 | 0 | 426,157 | 0 |
| 6/27 | 19 FI/FO | 1055-1155 | 36.0 | 18,458 | 392,417 | 0 | 0 | 0 | 392,417 | 0 |
| 6/27 | 20 FI/FO | 1340-1440 | 35.6 | 19,456 | 413,634 | 0 | 0 | 0 | 413,634 | 0 |
| 6/27 | 21 FI/FO | 1600-1700 | 36.1 | 18,957 | 403,026 | 0 | 0 | 0 | 403,026 | 0 |
| 6/28 | 22 FI/FO | 1100-1200 | 35.0 | 17,778 | 377,960 | 0 | 0 | 0 | 377,960 | 0 |
| 6/28 | 23 FI/FO | 1350-1450 | 35.0 | 19,138 | 406,874 | 0 | 0 | 0 | 406,874 | 0 |
| 6/28 | 24 FI/FO | 1610-1710 | 34.8 | 20,000 | 425,200 | 0 | 0 | 0 | 425,200 | 0 |
| 7/10 | 25 FI/FO | 1545-1645 | 34.8 | 17,959 | 381,808 | 0 | 0 | 0 | 381,808 | 0 |
| 7/11 | 26 FI/FO | 1309-1409 | 35.5 | 19,229 | 408,808 | 0 | 0 | 0 | 408,808 | 0 |
| 7/11 | 27 FI/FO | 1615-1715 | 34.7 | 18,004 | 382,765 | 0 | 0 | 0 | 382,765 | 0 |
| 7/12 | 28 FI/FO | 1015-1115 | 34.9 | 18,639 | 396,265 | 0 | 0 | 0 | 396,265 | 0 |
| 7/12 | 29 FI/FO | 1300-1400 | 35.5 | 17,959 | 381,808 | 0 | 0 | 0 | 381,808 | 0 |
| 7/12 | 30 FI/FO | 1620-1720 | 35.2 | 18,141 | 385,678 | 0 | 0 | 0 | 385,678 | 0 |
| 7/13 | 31 FI/FO | 1138-1239 | 35.0 | 19,937 | 423,861 | 0 | 0 | 0 | 423,861 | 0 |
| 7/13 | 32 FI/FO | 1605-1712 | 35.0 | 14,599 | 310,375 | 0 | 0 | 0 | 310,375 | 0 |

(continued)

TABLE 5-10 (continued)

| Date | Test No. | Time | Power generation rate, MW/h | Coal flow,[a] kg | Coal input, MJ | RDF flow,[b] $m^3$ | RDF flow, kg | RDF input, MJ | Total input, MJ | RDF, % (heat input basis) |
|---|---|---|---|---|---|---|---|---|---|---|
| 7/16 | 33 FI/FO | 1105-1205 | 34.0 | 16,644 | 353,851 | 45.31 | 2758 | 48,431 | 402,282 | 12.0 |
| 7/16 | 34 FI/FO | 1405-1507 | 34.0 | 17,116 | 363,886 | 54.89 | 3341 | 58,670 | 422,557 | 13.9 |
| 7/16 | 35 FI/FO | 1645-1745 | 33.6 | 16,508 | 350,960 | 45.31 | 2758 | 48,431 | 399,391 | 12.1 |
| 7/17 | 36 FI/FO | 1030-1130 | 19.0 | 8,163 | 173,545 | 0 | 0 | 0 | 173,545 | 0 |
| 7/17 | 37 FI/FO | 1348-1448 | 23.7 | 10,658 | 226,589 | 65.14 | 3965 | 69,627 | 296,216 | 23.5 |
| 7/17 | 38 FI/FO | 1635-1735 | 34.4 | 17,007 | 361,569 | 70.80 | 4310 | 75,676 | 437,245 | 17.3 |
| 7/18 | 39 FI/FO | 1140-1240 | 35.2 | 17,642 | 375,068 | 76.47 | 4655 | 81,737 | 456,806 | 17.9 |
| 7/18 | 40 FI/FO | 1455-1555 | 35.1 | 15,601 | 331,677 | 87.79 | 5344 | 93,837 | 425,514 | 22.0 |
| 7/18 | 41 FI/FO | 1815-1915 | 33.5 | 15,147 | 322,025 | 82.13 | 4999 | 87,787 | 409,812 | 21.4 |
| 7/19 | 42 FI/FO | 1140-1240 | 33.1 | 16,825 | 357,700 | 0 | 0 | 0 | 357,700 | 0 |
| 7/19 | 43 FI/FO | 1435-1535 | 29.6 | 13,515 | 287,329 | 79.30 | 4827 | 84,762 | 372,091 | 22.8 |
| 7/19 | 44 FI/FO | 1725-1825 | 34.8 | 16,735 | 355,786 | 84.96 | 5172 | 90,812 | 446,598 | 20.3 |
| 7/20 | 45 FI/FO | 0625-0730 | 13.0 | 7,249 | 154,114 | 0 | 0 | 0 | 154,114 | 0 |
| 7/20 | 46 FI/FO | 1015-1115 | 34.6 | 18,005 | 382,786 | 0 | 0 | 0 | 382,786 | 0 |
| 7/20 | 47 FI/FO | 1418-1518 | 35.0 | 16,145 | 343,243 | 70.80 | 4310 | 75,676 | 418,919 | 18.1 |
| 7/21 | 48 FI/FO | 1207-1307 | 32.0 | 17,098 | 363,503 | 0 | 0 | 0 | 363,503 | 0 |
| 7/23 | 49 FI/FO | 1215-1315 | 33.9 | 16,145 | 343,243 | 56.64 | 3448 | 60,541 | 403,784 | 15.0 |
| 7/23 | 50 FI/FO | 1535-1635 | 35.0 | 16,735 | 355,786 | 42.86 | 2586 | 45,406 | 401,192 | 11.3 |
| 7/24 | 51 FI/FO | 1140-1240 | 22.3 | 18,322 | 389,526 | 0 | 0 | 0 | 389,526 | 0 |
| 7/25 | 52 FI/FO | 0670-0710 | 35.0 | 12,931 | 274,913 | 0 | 0 | 0 | 274,913 | 0 |
| 7/25 | 53 FI/FO | 1015-1115 | 35.2 | 14,875 | 316,242 | 0 | 0 | 0 | 316,242 | 0 |

[a] Read from integrator log sheet.

[b] Read from solid waste log sheet.

[c] Assumes 21.26 MJ/kg.

[d] Assumes 60.87 $kg/m^3$.

[e] Assumes 17.56 MJ/kg.

## TABLE 5-11. MOBILE FABRIC FILTER OPERATING CONDITIONS

| Date | Run No. | RDF, % | ΔP, cm W.G. | Air-to-cloth ratio, $m^3/h$ per $m^2$ | Cleaning mechanism[a] |
|---|---|---|---|---|---|
| 6/19 | 1 FI/FO | 0 | N.A.[b] | 27.4 | R |
| 6/20 | 2 FI/FO | 14.4 | N.A. | 27.4 | R |
| 6/20 | 3 FI/FO | 14.6 | N.A. | 27.4 | R |
| 6/20 | 4 FI/FO | 20.7 | N.A. | 27.4 | R |
| 6/21 | 5 FI/FO | 0 | N.A. | 27.4 | R |
| 6/21 | 6 FI/FO | 0 | N.A. | 27.4 | R |
| 6/21 | 7 FI/FO | 0 | N.A. | 27.4 | R |
| 6/22 | 8 FI/FO | 0 | N.A. | 27.4 | R |
| 6/22 | 9 FI/FO | 11.9 | 10.1 | 27.4 | R |
| 6/23 | 10 FI/FO | 22.1 | 10.1 | 27.4 | R |
| 6/23 | 11 FI/FO | 20.9 | 10.4 | 27.4 | R |
| 6/23 | 12 FI/FO | 21.3 | 10.7 | 27.4 | R |
| 6/25 | 13 FI/FO | 0 | 7.1 | 27.4 | S |
| 6/25 | 14 FI/FO | 0 | 8.4 | 27.4 | S |
| 6/25 | 15 FI/FO | 0 | 8.4 | 27.4 | S |
| 6/26 | 16 FI/FO | 0 | 11.4 | 27.4 | S |
| 6/26 | 17 FI/FO | 0 | 10.7 | 27.4 | S |
| 6/26 | 18 FI/FO | 0 | 10.7 | 27.4 | S |
| 6/27 | 19 FI/FO | 0 | 11.4 | 27.4 | S |
| 6/27 | 20 FI/FO | 0 | 11.4 | 27.4 | S |
| 6/27 | 21 FI/FO | 0 | 10.4 | 27.4 | S |
| 6/28 | 22 FI/FO | 0 | 11.4 | 27.4 | S |
| 6/28 | 23 FI/FO | 0 | 11.4 | 27.4 | S |
| 6/28 | 24 FI/FO | 0 | 9.4 | 27.4 | S |
| 7/10 | 25 FI/FO | 0 | 20.3 | 36.6 | S |
| 7/11 | 26 FI/FO | 0 | 25.9 | 32.9 | S |
| 7/11 | 27 FI/FO | 0 | 25.9 | 32.9 | S |
| 7/12 | 28 FI/FO | 0 | 29.2 | 27.4 | R&S |
| 7/12 | 29 FI/FO | 0 | 30.0 | 27.4 | R&S |
| 7/12 | 30 FI/FO | 0 | 30.5 | 27.4 | R&S |
| 7/13 | 31 FI/FO | 0 | 16.5 | 32.9 | R&S |

TABLE 5-11 (continued)

| Date | Run No. | RDF, % | ΔP, cm W.G. | Air-to-cloth ratio, $m^3/h$ per $m^2$ | Cleaning mechanism[a] |
|---|---|---|---|---|---|
| 7/13 | 32 FI/FO | 0 | 16.5 | 45.7 | R&S |
| 7/16 | 33 FI/FO | 12.0 | 13.7 | 43.9 | R&S |
| 7/16 | 34 FI/FO | 13.9 | 13.7 | 43.9 | R&S |
| 7/16 | 35 FI/FO | 12.1 | 13.7 | 43.9 | R&S |
| 7/17 | 36 FI/FO | 0 | 14.0 | 34.7 | R&S |
| 7/17 | 37 FI/FO | 23.5 | 16.2 | 34.7 | R&S |
| 7/17 | 38 FI/FO | 17.3 | 6.8 | 34.7 | R&S |
| 7/18 | 39 FI/FO | 17.9 | 5.8 | 36.6 | R&S |
| 7/18 | 40 FI/FO | 22.0 | 5.8 | 36.6 | R&S |
| 7/18 | 41 FI/FO | 21.4 | 5.8 | 36.6 | R&S |
| 7/19 | 42 FI/FO | 0 | 5.1 | 36.6 | R&S |
| 7/19 | 43 FI/FO | 22.8 | 8.9 | 36.6 | R&S |
| 7/19 | 44 FI/FO | 20.3 | 14.0 | 36.6 | R&S |
| 7/20 | 45 FI/FO | 0 | 7.1 | 36.6 | R&S |
| 7/20 | 46 FI/FO | 0 | 7.6 | 36.6 | R&S |
| 7/20 | 47 FI/FO | 18.1 | 5.1 | 36.6 | R&S |
| 7/21 | 48 FI/FO | 0 | 8.4 | 36.6 | R&S |
| 7/23 | 49 FI/FO | 0 | 13.0 | 36.6 | R&S |
| 7/23 | 50 FI/FO | 11.3 | 15.7 | 36.6 | R&S |
| 7/24 | 51 FI/FO | 0 | 7.3 | 36.6 | R&S |
| 7/25 | 52 FI/FO | 0 | 9.7 | 36.6 | R&S |
| 7/25 | 53 FI/FO | 0 | 9.7 | 36.6 | R&S |

[a] R = reserve air, S = shake, and R&S = reverse air and shake.

[b] N.A. = Not available.

| To convert from | to | Multiply by |
|---|---|---|
| $m^3/h$ per $m^2$ | $acfm/ft^2$ | 5.47 E-2 |
| cm W.G. | in. W.G. | 3.94 E-1 |

to document device operating conditions. The A/C ratio was determined by a flow measuring probe at the outlet of the fabric filter and the known size and number of bags that were on line throughout a test series.

A comprehensive evaluation of particulate removal efficiency and outlet particulate loading reveals two distinct groups, which will be termed "first-half" and "second-half." The average removal efficiencies, including the overall average, are shown on Table 5-12. The first-half group includes Test Runs 1 through 24, which took place on or before June 28, 1979. The second-half group includes Test Runs 25 through 53, which took place after July 10, 1979. Particulate removal efficiency increased markedly from the first-half group to the second-half group.

A closer examination and an evaluation of the two groups led to the conclusion that the first-half tests should not be included in further reduction of the data, based on the following premise: operational problems within the fabric filter, which were corrected the first week in July, prevented "representative" operation for the first half of the test program. Actually, first-half results were extremely erratic compared with second-half results. Figure 5-10 further illustrates this point. Operational problems resulted primarily from improper seals around a number of bag connections at the tube sheet (the floor of the baghouse). The unit was inspected, particulate leaks were isolated, and the bag connections were sealed.

TABLE 5-12. PARTICULATE REMOVAL EFFICIENCY AS A FUNCTION OF TEST GROUP

| Test group | Average efficiency ($\overline{x}$) | Standard deviation (s) |
|---|---|---|
| All particulate runs (46) | 97.1% | 2.6 |
| Runs 1-24 (first-half) | 95.1% | 2.2 |
| Runs 25-53 (second-half) (excluding 27, 47, 48, 49, 50, 52, 53)[a] | 99.3% | 0.6 |
| Coal only - all (29 runs) | 96.8% | 2.6 |
| RDF - all (17 runs) | 97.6% | 2.8 |
| Coal only (second-half) (25, 26, 28, 29, 30, 31, 32, 36, 42, 45, 46, 51) | 99.2% | 0.7 |
| RDF (second-half) (33, 34, 35, 37, 38, 39, 40, 41, 43, 44) | 99.5% | 0.1 |

[a] None of the excluded runs was a particulate sample run except Run 27, which did not meet quality assurance criteria.

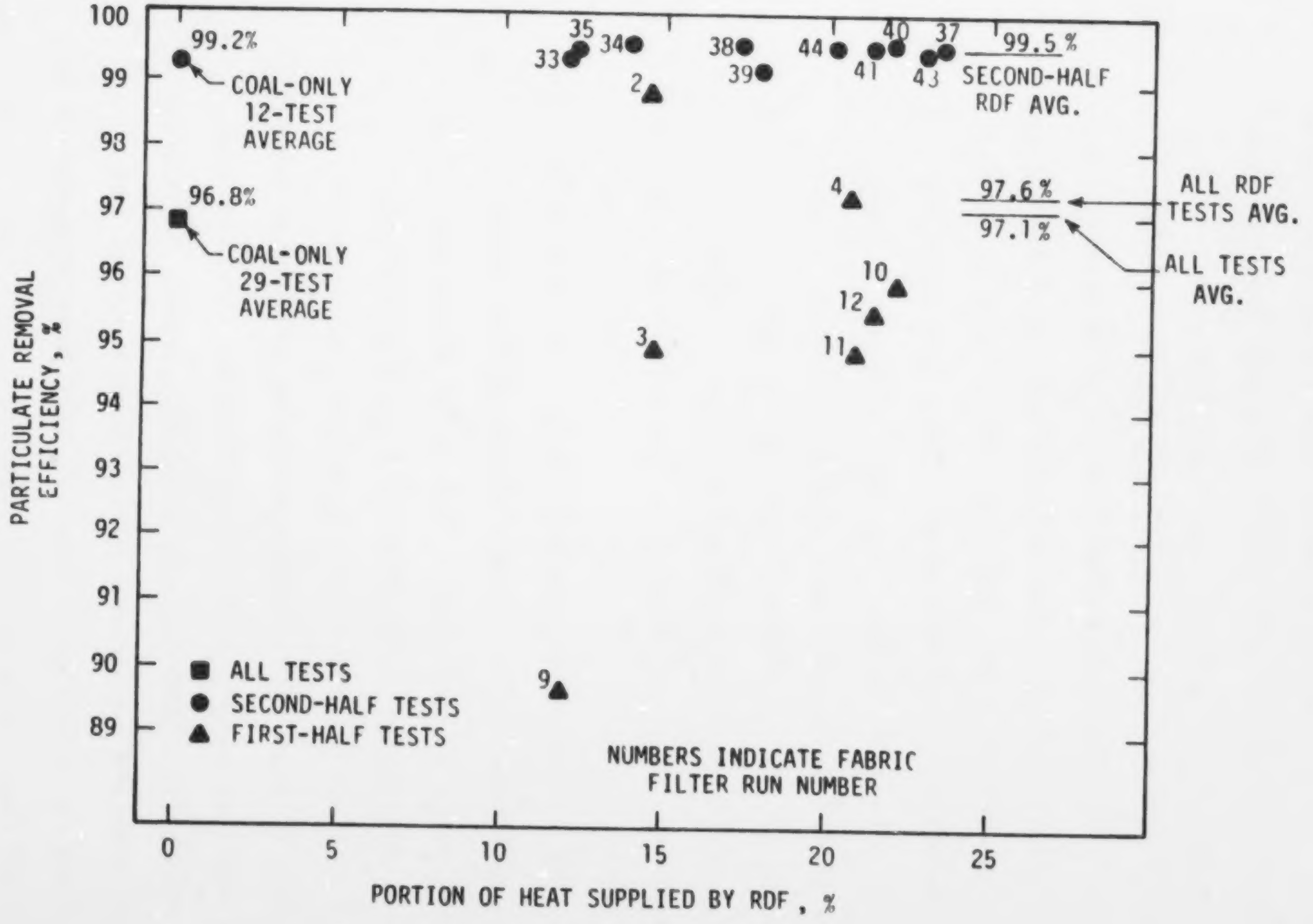

Figure 5-10. Particulate removal efficiency as a function of RDF input.

Because of the large difference in first-half and second-half results and because of the high confidence associated with second-half results, the entire first-half test group is considered invalid and has been dropped from further discussion.

Table 5-13 provides a detailed listing of emission concentrations calculated from the mobile fabric filter sampling and analytical test results. The organization of this table is similar to the emission concentration tables developed for the mobile ESP and mobile scrubber. All test runs are grouped according to similar operating and test conditions, and the analytical results are averaged. Test Run 27 was not analyzed for pollutant concentrations because it failed to meet quality assurance criteria. Test Runs 49, 50, 52, and 53 were not particulate sample runs.

Emission concentrations were graphically related to a number of variable conditions in an attempt to recognize trends which might indicate specific conditions that lower emissions of potentially harmful pollutants. Comparison of outlet loadings or fabric filter collection efficiency with power generation, air-to-cloth ratio, or type of cleaning mechanism yielded no useful trends. The data obtained in this test program indicate that these three operating parameters have minimal impact on outlet loading or particulate collection efficiency; however, the operating ranges in this program may not have been wide enough to represent actual full-scale design ranges.

# TABLE 5-13. PILOT FABRIC FILTER EMISSION CONCENTRATIONS

| OPERATING PARAMETERS (units as noted) | Primary | | | |
|---|---|---|---|---|
| PG, MW/h | 33.7 | 25.5 | 32.0 | 33.3 |
| A/C,[a] $m^3$/h per $m^2$ | 36.6 | 36.6 | 40.2 | 32.9 |
| ΔP, cm W.G. | 15.82 | 19.46 | 36.32 | 58.88 |
| Fuel | RDF[b] | Coal | RDF[b] | Coal |
| Run No. | 38, 39, 40, 41, 43, 47 | 42, 45, 46, 48, 51 | 33, 34, 35, 37, 44 | 25, 26, 27, 28, 29, 30, 31, 32, 36 |
| ANALYTICAL RESULTS (mg/dry std. $m^3$) | | | | |
| Gravimetric analysis[c] | | | | |
| T. particulate (in)[d]<br>(out) | 5209<br>27.59 | 5467<br>11.28 | 5963<br>29.88 | 5972<br>61.57 |
| Specific ion electrode analysis | | | | |
| Cl (in)[e]<br>(out) | 108<br>77.8 | | 126<br>98.2 | 29.2<br>23.0 |
| F (in)[f]<br>(out) | 16.9<br>16.4 | | 17.3<br>17.9 | 20.6<br>16.7 |

TABLE 5-13 (continued)

| OPERATING PARAMETERS (units as noted) | Primary | | | |
|---|---|---|---|---|
| PG, MW/h | 33.7 | 25.5 | 32.0 | 33.3 |
| A/C,[a] $m^3$/h per $m^2$ | 36.6 | 36.6 | 40.2 | 32.9 |
| ΔP, cm W.G. | 15.82 | 19.46 | 36.32 | 58.88 |
| Fuel | RDF[b] | Coal | RDF[b] | Coal |
| Run No. | 38, 39, 40, 41, 43, 47 | 42, 45, 46, 48, 51 | 33, 34, 35, 37, 44 | 25, 26, 27, 28, 29, 30, 31, 32, 36 |
| ANALYTICAL RESULTS (mg/dry std. $m^3$) | | | | |
| Atomic absorption analysis | | | | |
| Pb (in)[g]<br>(out) | 1.43<br>ND[h] | .570<br>.0297 | .979<br>ND | .551<br>ND |
| Zn (in)[i]<br>(out) | 15.5<br>.0169 | 5.10<br>.0200 | 4.61<br>.0124 | 4.88<br>.0465 |
| Fe (in)[j]<br>(out) | 162<br>.308 | 187<br>.848 | 244<br>.445 | 180<br>.372 |
| Cu (in)[k]<br>(out) | .198<br>.0264 | .190<br>.026 | .177<br>.0170 | .183<br>.0927 |
| Hg (in)[l]<br>(out) | .0008<br>.0008 | .006<br>ND | | |
| Cd (in)[m]<br>(out) | .106<br>.00526 | .0455<br>.00316 | .0609<br>ND | .0573<br>.00499 |
| $Ba(ClO_4)_2$ Titration | | | | |
| $SO_x$ (in)[n]<br>(out) | 17700<br>13500 | 18900<br>14500 | 16500<br>12400 | |

[a] Air to cloth.

[b] RDF was co-fired with coal and ranged from 11.3 to 23.5 percent.

[c] Particulate values are an average of the runs indicated above with the exception of run no. 27 which lacks inlet data. All other analyses are averages of selected runs within each group.

[d] Front half only.

[e] Detection limit for Cl is 1.8 mg/dry std. $m^3$.

[f] Detection limit for F is 0.05 mg/dry std. $m^3$.

[g] Detection limit for Pb is 0.007 mg/dry std. $m^3$.

[h] Not detectable.

[i] Detection limit for Zn is 0.003 mg/dry std. $m^3$.

[j] Detection limit for Fe is 0.0003 mg/dry std. $m^3$.

[k] Detection limit for Cu is 0.0003 mg/dry std. $m^3$.

[l] Detection limit for Hg is 0.0001 mg/dry std. $m^3$.

[m] Detection limit for Cd is 0.002 mg/dry std. $m^3$.

[n] Detection limit for $SO_2$ is 0.7 mg/dry std. $m^3$.

Figure 5-11 shows the effects of pressure drop and type of fuel on particulate collection efficiency. An increase in pressure drop showed increased collection efficiency. Figure 5-11, however, does not signal a significant trend within the collection efficiencies shown. Regardless of pressure drop or fuel type, the collection efficiency was 99 percent or greater.

The control of lead emissions by the fabric filter is difficult to evaluate quantitatively because lead concentrations were below the detectable limit in every outlet sample except one. Figure 5-12 shows concentrations of lead measured in fabric filter inlet samples as a function of RDF input. The figure shows that the inlet lead concentrations observed during fabric filter testing were significantly lower than those measured during the mobile ESP and scrubber test series. The highest measured inlet lead concentration for all fabric filter runs (2.59 mg/dry std. $m^3$) compares with the coal-only values measured during the ESP and scrubber test series. The reasons behind the observed reduction in lead emissions over the 8-month period are not apparent. Cadmium, copper, zinc, iron, and mercury concentrations were determined on selected samples only. Figures 5-13 through 5-16 show the inlet/outlet concentrations that were measured during fabric filter testing. Mercury concentrations are not shown graphically because data are limited. The specific run number from which each data point was obtained is noted on each graph. Where more than one run number is shown, the data point represents an average of those results. Where outlet

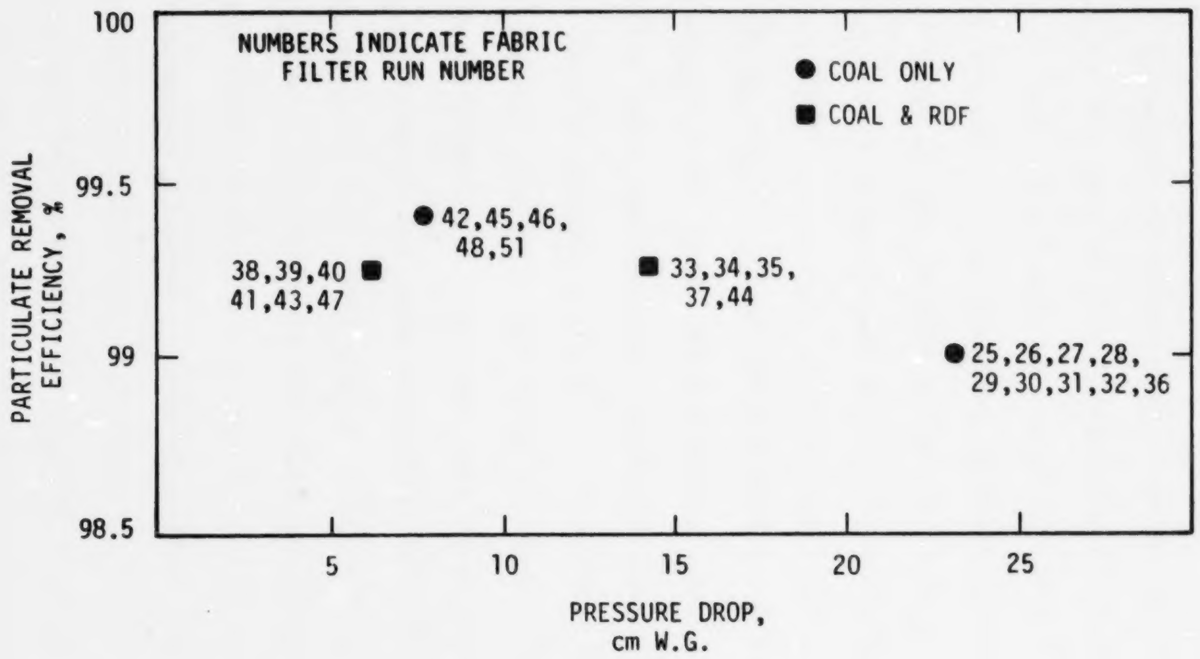

Figure 5-11. Particulate removal efficiency as a function of fabric filter pressure drop.

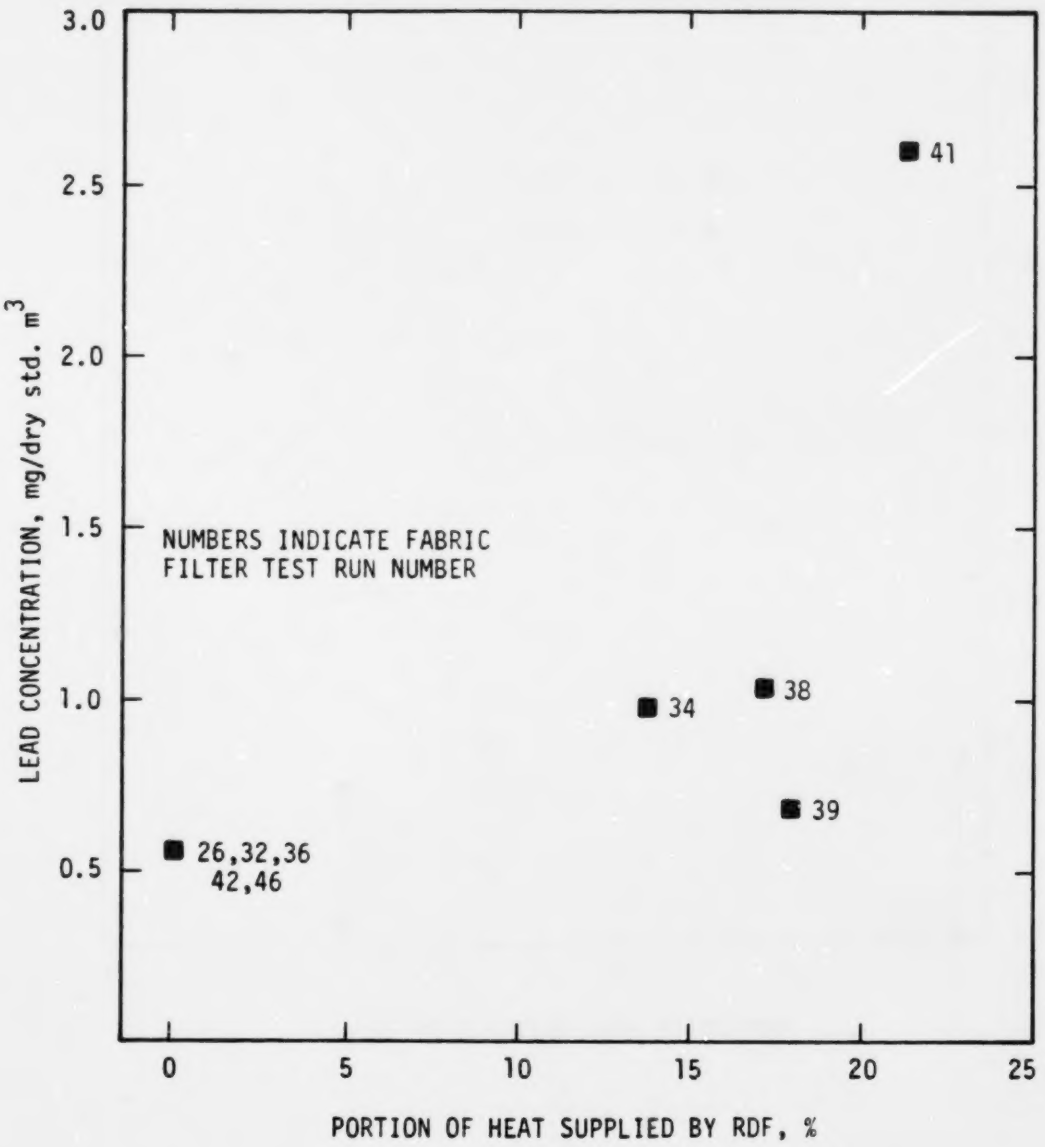

Figure 5-12. Uncontrolled lead concentration as a function of RDF input.

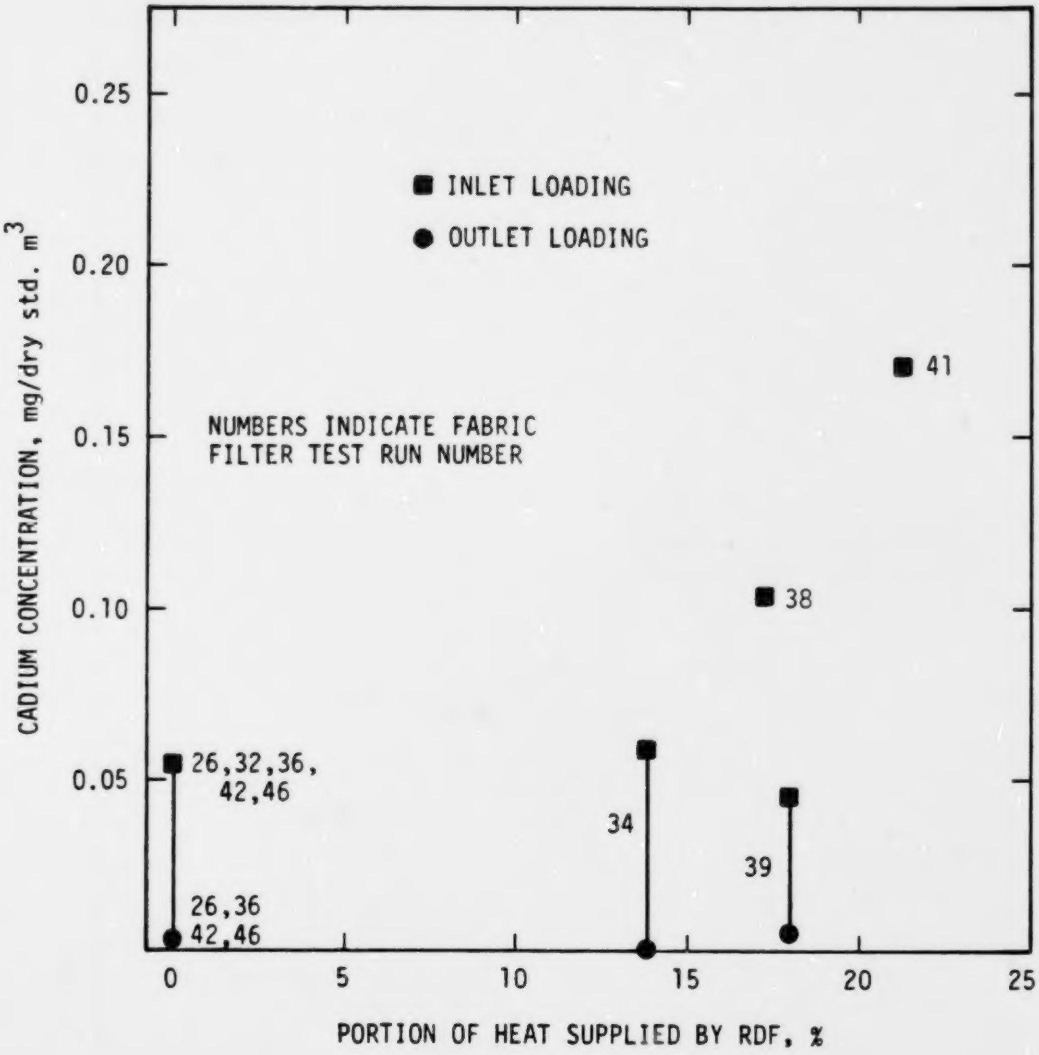

Figure 5-13. Cadmium concentration as a function of RDF input.

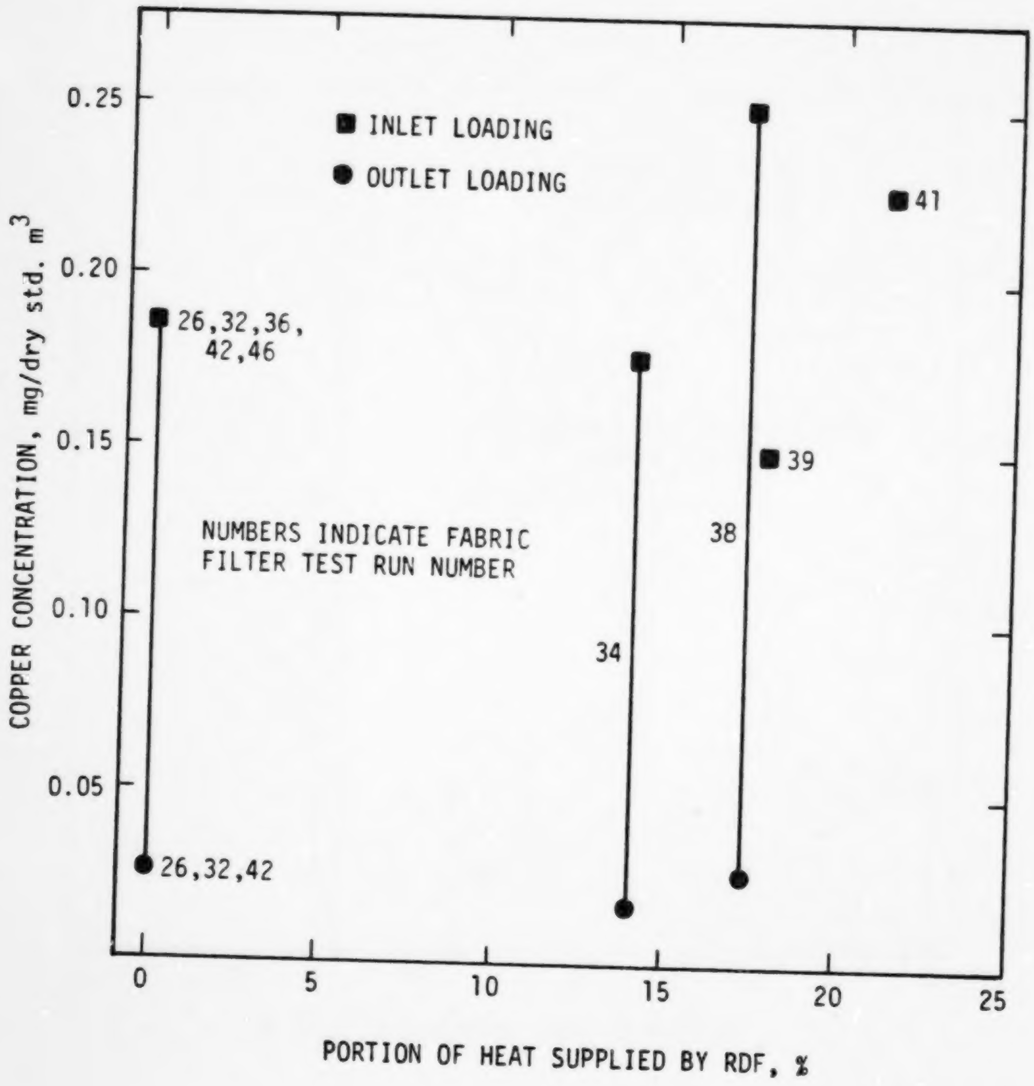

Figure 5-14. Copper concentration as a function of RDF input.

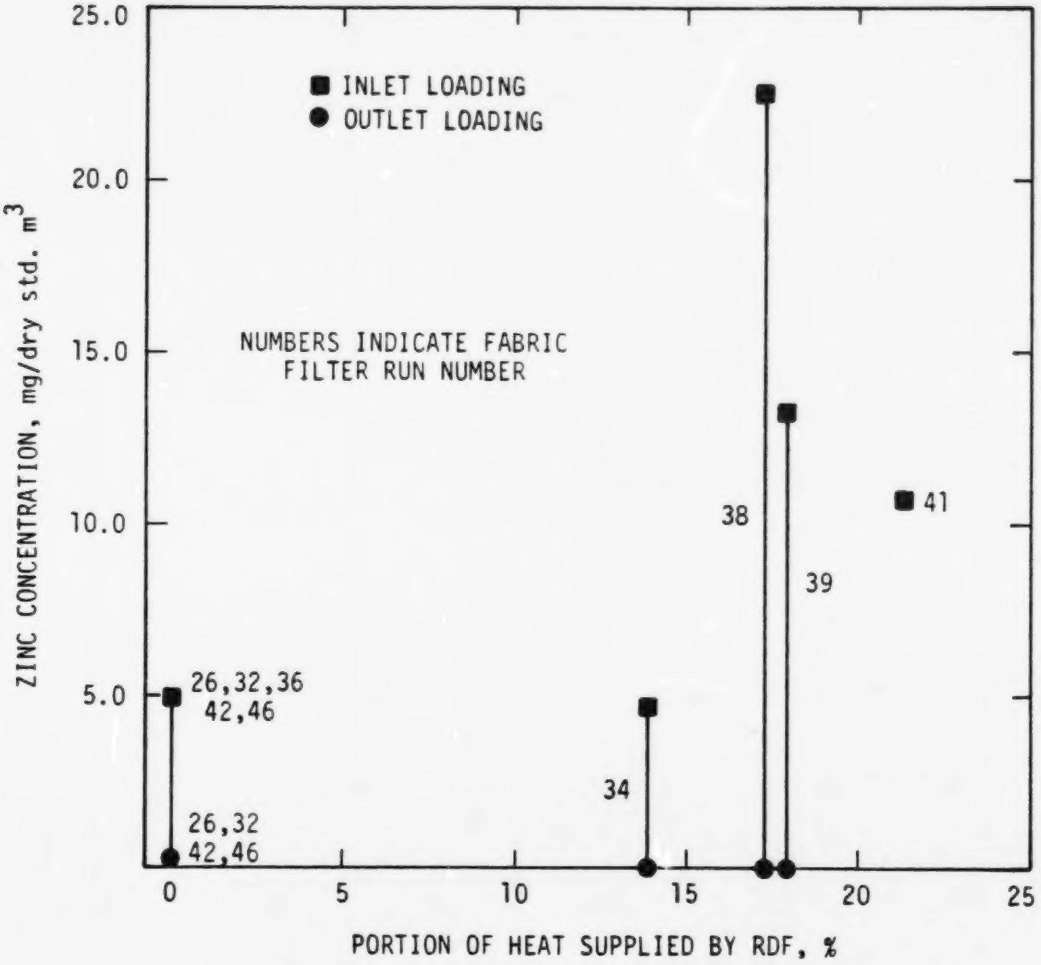

Figure 5-15. Zinc concentration as a function of RDF input.

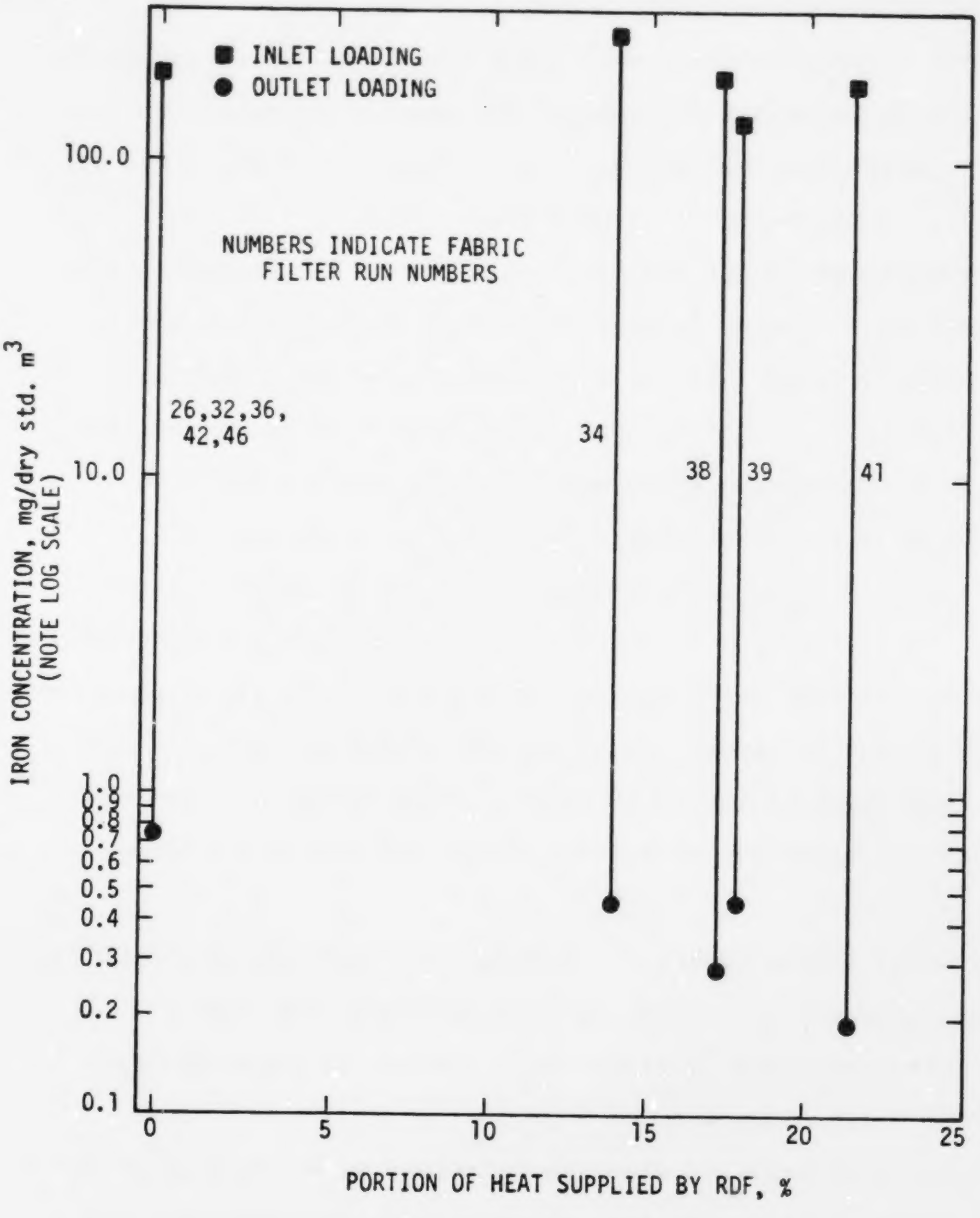

Figure 5-16. Iron concentration as a function of RDF input.

concentrations are not shown, the amount of the specific metal was lower than the detectable amount.

These figures indicate that cadmium and zinc inlet emissions increase with increased RDF input. The control of these two elements, which does not appear to be a function of RDF input (as expected), is maintained at a very high level.

Uncontrolled copper and iron emissions do not correlate with the amount of RDF being burned. Copper is controlled at about the 90 percent level, and the outlet emissions are somewhat higher than those of cadmium and zinc. Outlet emissions of iron appear to decrease with increased RDF input and are the highest among the metals investigated. It should be noted that all graphs except that for iron (Figure 5-16) are on linear scales. The iron concentrations are shown on a semilog plot because the differences between inlet and outlet emissions (and hence removal efficiency) are so large. Inlet concentrations of iron are much higher than those of the other metals, which probably accounts more than any other factor for the higher collection efficiencies.

As noted in the mobile ESP and scrubber test series, chloride emissions increase significantly with increased RDF input. Figure 5-17 shows this relationship. Control of chlorides with the fabric filter is poor.

Figure 5-18 presents fluoride emissions as a function of RDF input. Almost no fluoride removal efficiency was observed, and with the analytical measurement limitation, reported outlet

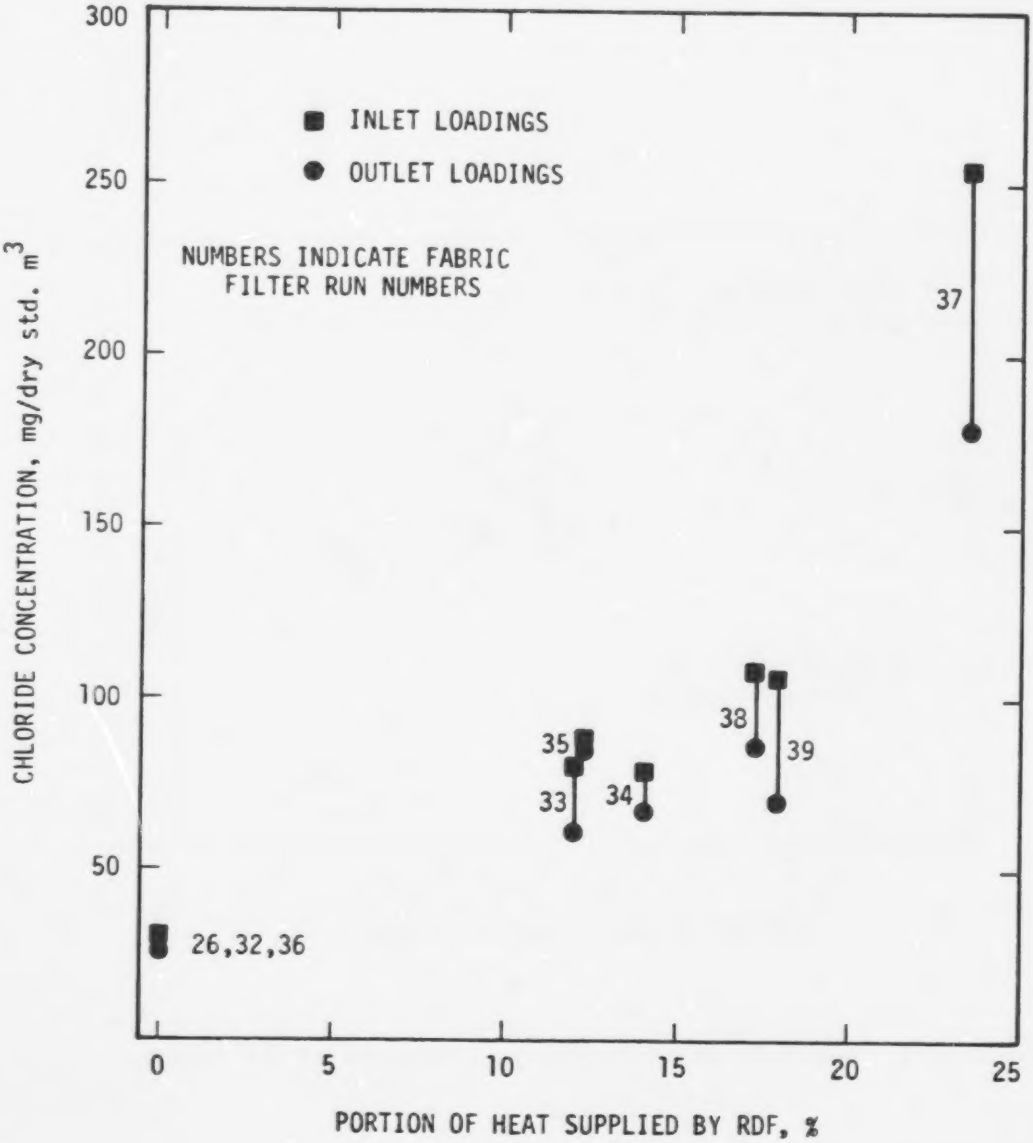

Figure 5-17. Chloride concentration as a function of RDF input.

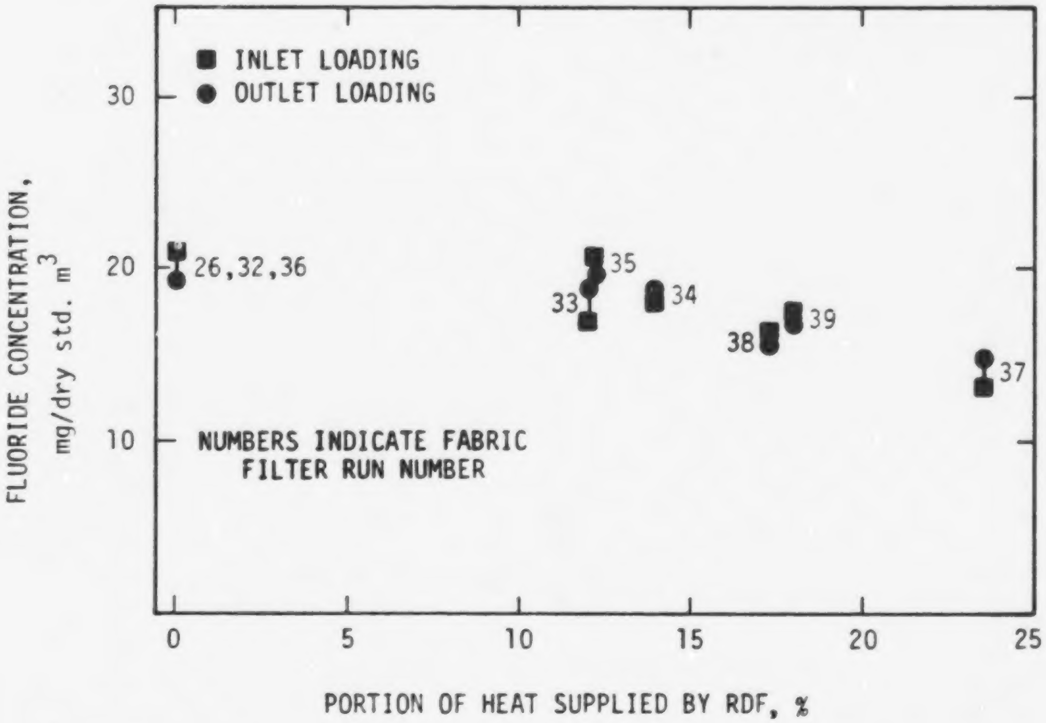

Figure 5-18. Fluoride concentration as a function of RDF input.

concentrations are sometimes greater than corresponding inlet concentrations. Fluoride emissions do not appear to change significantly with increased RDF.

Figure 5-19 presents concentrations of sulfur oxides ($SO_x$) as a function of RDF input. No reduction occurred in $SO_x$ emissions with increased RDF input. As expected, the control of $SO_x$ by the fabric filter was poor.

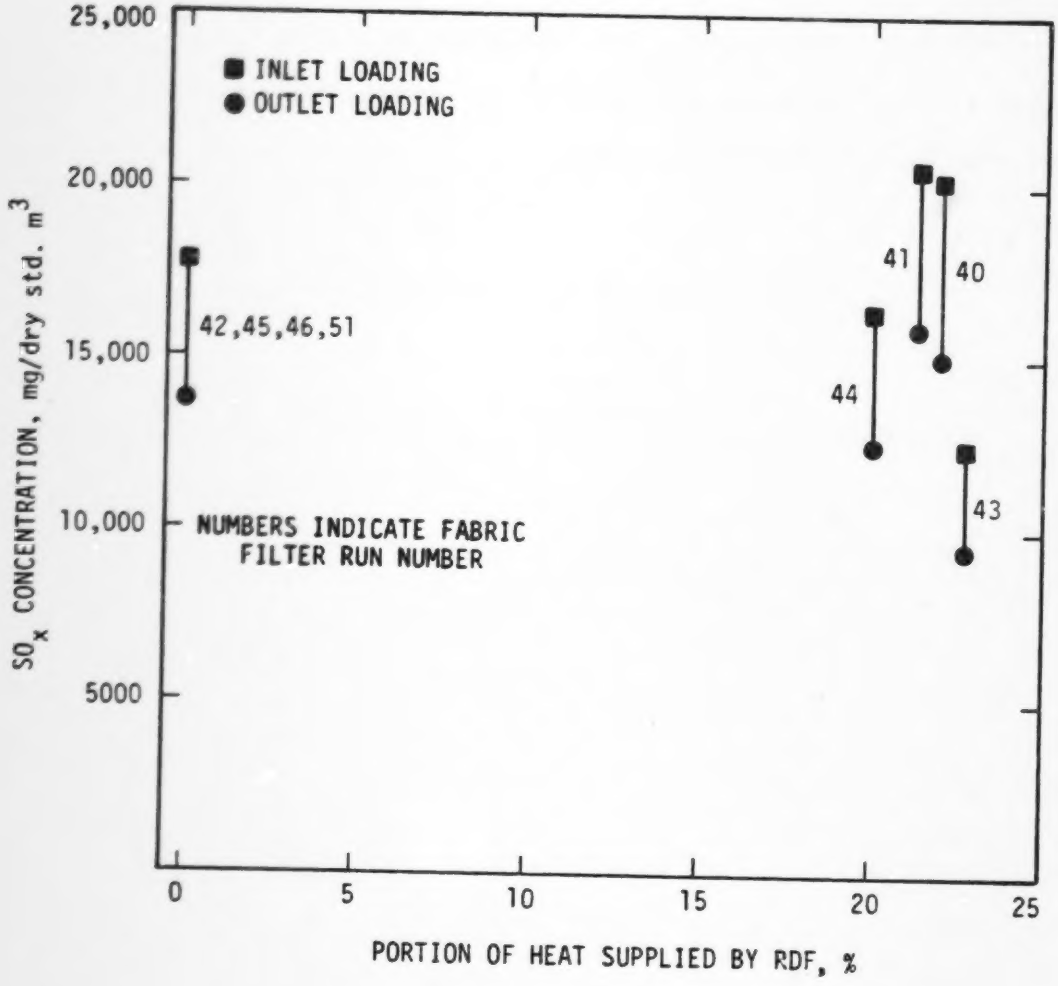

Figure 5-19. Sulfur oxide emissions as a function of RDF input.

# SECTION 6

# QUALITY ASSURANCE

An acceptable level of confidence in the analytical test data was achieved by implementation of a continuous quality assurance (QA) program, which became an integral part of all phases of sampling and analysis in this project. This section discusses the specific QA procedures applied, including standardized reference methods, equipment calibration, performance audits, maintenance of sample integrity, and data validation.

## 6.1 REFERENCE METHODS

The sampling and analytical methods used in this test program are discussed in detail in Appendix A. They are based on EPA reference methods in *Federal Register*, Vol. 42, No. 160, August 18, 1977, Methods 1-8; Annual Book of ASTM Standards, Part 26; and U.S. EPA, Methods for Chemical Analysis for Water and Wastes.

## 6.2 CALIBRATION PROCEDURES

Calibration procedures were applied to all sampling equipment and analytical instrumentation on a regularly scheduled basis. All sampling equipment was calibrated according to the procedures outlined in *Maintenance, Calibration, and Operation of Isokinetic Source-Sampling Equipment* by Office of Air Programs, Publication No. APTD-0576. All analytical instrumentation was calibrated either as recommended by manufacturers or, more frequently, as part of routine laboratory schedule. Specific details of calibration procedures are described in the following paragraphs.

Sampling equipment components that require routine calibration are nozzles, dry gas meter and orifice, thermocouples and temperature readout, and pitot tubes. The nozzles were calibrated by taking three separate measurements of the inside diameter with a micrometer and calculating the average. The measurements must agree within 0.051 mm (0.002 inches) for the nozzle to be considered acceptable. The dry gas meter and orifice are calibrated concurrently by use of the setup shown in Figure 6-1. They were calibrated against a wet test meter having ±1 percent accuracy. In such a calibration, six discrete comparisons are made with orifice pressure drops ranging from 1.3 to 10.2 cm (0.5 to 4.0 inches) W.G. and the information is recorded as shown on a form (Figure 6-2). The $\Delta H@$, orifice pressure differential that gives 0.021 $m^3$/min (0.75 cfm) of air at 21°C and 760 mm Hg (70°F and 29.92 in. Hg), is calculated, and each of the six readings must not deviate from the average by more than ±0.38 cm (0.15 inch). The $\gamma$ factor, which is the ratio of the volume measurement of the wet test meter to the dry gas meter, is calculated, and the allowable tolerance is ±1 percent.

All temperature measuring devices, such as thermocouples with potentiometers and thermometers, are calibrated against a

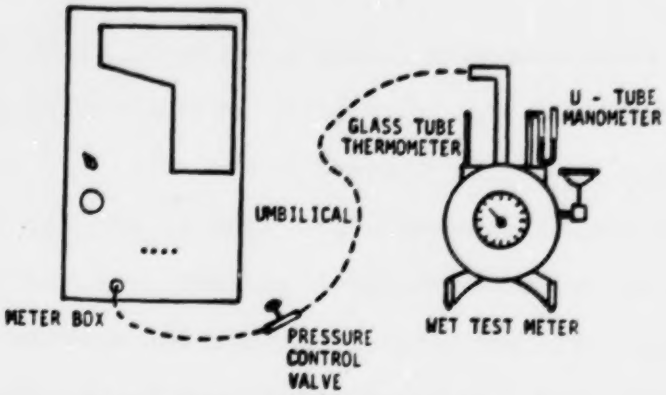
GLASS TUBE THERMOMETER
U - TUBE MANOMETER
UMBILICAL
METER BOX
PRESSURE CONTROL VALVE
WET TEST METER

Figure 6-1. Calibration setup.

**DATE**____________________

**METER BOX NO.**____________________

**BAROMETRIC PRESSURE,** $P_b$ **=** _____**in. Hg.**

**DRY GAS METER NO.**____________________

| Orifice manometer setting $\Delta H$ in. $H_2O$ | Gas volume wet test meter $V_w$, $ft_3$ | Gas volume dry gas meter $V_d$, $ft_3$ | Wet test meter $t_w$, °F | Dry gas meter Inlet $t_{di}$, °F | Outlet $t_{dn}$, °F | Average $t_d$, °F | Time θ, min | γ | ΔH@ |
|---|---|---|---|---|---|---|---|---|---|
| 0.5 | 5 | | | | | | | | |
| 1.0 | 5 | | | | | | | | |
| 1.5 | 10 | | | | | | | | |
| 2.0 | 10 | | | | | | | | |
| 3.0 | 10 | | | | | | | | |
| 4.0 | 10 | | | | | | | | |

**Average** __________

| $\Delta H$ | $\frac{\Delta H}{13.6}$ | γ: $\frac{V_w P_h (t_d + 400)}{V_d (P_b + \frac{\Delta H}{13.6}) (t_w + 460)}$ | ΔH@: $\frac{0.0317 \Delta H}{P_b (t_d + 460)} \left[ \frac{(t_w + 460) \theta}{V_w} \right]^2$ |
|---|---|---|---|
| 0.5 | 0.0368 | | |
| 1.0 | 0.0737 | | |
| 1.5 | 0.110 | | |
| 2.0 | 0.147 | | |
| 3.0 | 0.221 | | |
| 4.0 | 0.294 | | |

γ = Ratio of accuracy of wet test meter to dry test meter. Tolerance = ± 0.01

ΔH@ = Orifice of pressure differential that gives 0.75 cfm of air at 70°F and 29.92 inches of mercury, in $H_2$). Tolerance = +0.15.

Figure 6-2. Calibration data sheet.

glass mercury thermometer of known accuracy. Pitot tubes are checked to verify that design specifications outlined in EPA Reference Method 2 are met (Figure 6-3).

All analytical instrumentation used in the lab was calibrated according to manufacturers' instructions, and the results were documented. The analytical balance was checked daily with standard weights, and a log was maintained to document its calibration. The specific ion probe and the millivolt meter were calibrated before each use with calibration standards. Control samples were run throughout the analysis to assure that there was no drift in the calibration curve. The atomic absorption spectrophotometer was calibrated with each use, and control samples were also run periodically throughout the analyses.

## 6.3 PERFORMANCE AUDITS

In addition to the original calibration of all sampling equipment, periodic spot checks were performed for calibration verification or for rapid detection of out-of-control conditions. These checks are referred to as performance audits.

Performance audits were performed on the dry gas meter and orifice. After approximately 10 test runs, or whenever sampling equipment was transported or severely jolted, a calibration check was performed by pulling ambient air through the dry gas meter at an orifice pressure differential equivalent to the $\Delta H@$ and calculating the volumetric flow rate at 21°C and 760 mm Hg (ambient conditions). The $\Delta H@$ is the orifice pressure differential that

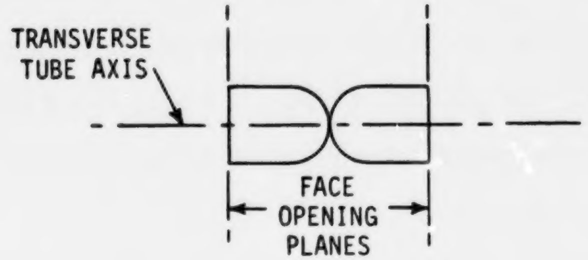
TRANSVERSE
TUBE AXIS
FACE
OPENING
PLANES

(a) ENDVIEW

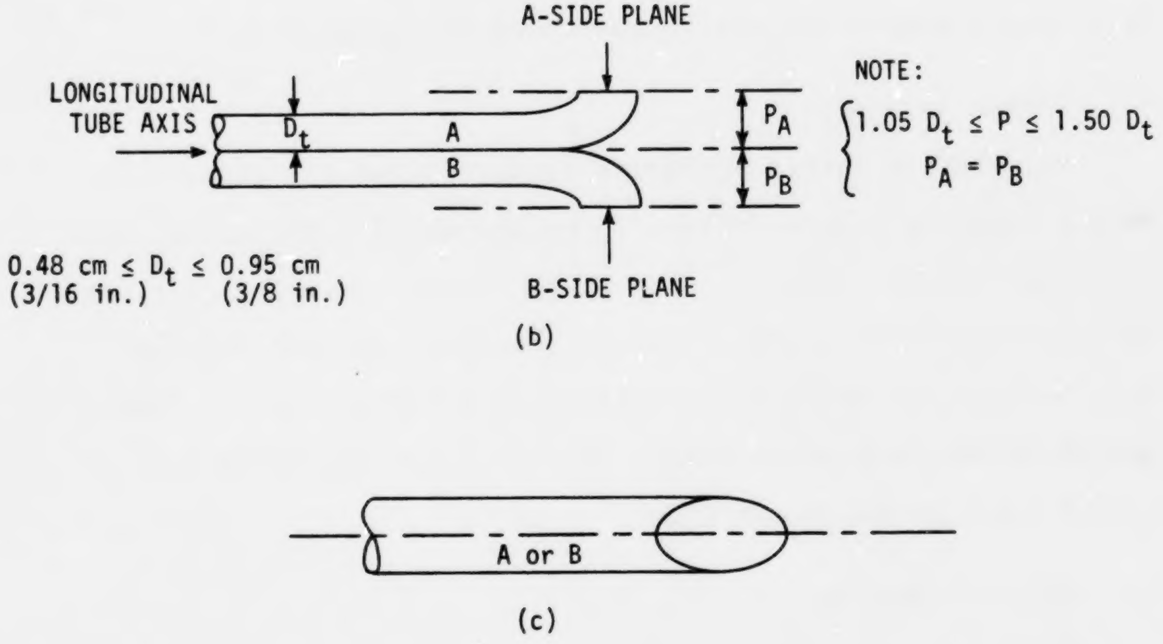
A-SIDE PLANE
LONGITUDINAL
TUBE AXIS
$D_t$
A
B
$P_A$
$P_B$
NOTE:
$1.05\ D_t \leq P \leq 1.50\ D_t$
$P_A = P_B$
$0.48\text{ cm} \leq D_t \leq 0.95\text{ cm}$
(3/16 in.) (3/8 in.)
B-SIDE PLANE
(b)
A or B
(c)

Figure 6-3. Properly constructed Type S pitot tube, shown in: (a) end view; face opening planes perpendicular to transverse axis; (b) top view; face opening planes parallel to longitudinal axis; (c) side view; both legs of equal length and centerlines coincident, when viewed from both sides. Baseline coefficient values of 0.84 may be assigned to pitot tubes constructed this way.

was determined at the time of calibration, which gives 0.021 $m^3$/min (0.75 cfm) of air at these conditions. The acceptance limits were 0.021 $m^3$/min ±0.001 $m^3$/min. If these limits were not met, the equipment was returned to the laboratory for remedial maintenance and recalibration.

For maintenance of quality control, a number of field activities were audited. Field data forms were routinely checked for completeness and accuracy, isokinetic sampling rates were verified, and a sample log system was carefully checked daily.

## 6.4 SAMPLE INTEGRITY

Maintaining sample integrity requires that all aspects of sample handling and recordkeeping be addressed. Basically, this involves thorough documentation of all sample activity, including labeling, chain of custody, sample preservation, and storage. This insures proper handling of samples and avoidance of sample contamination, ambiguous sample labeling, and the collection of insufficient sample quantities.

## 6.5 DATA VALIDATION

Precision is defined as the reproducibility of results when replicate measurements are made on a homogeneous sample when the same technique, reagents, instruments, and preferably the same analyst are used. Accuracy is defined as the closeness of a measurement to an accepted or true value.

Randomly selected samples were split after sampling and analyzed by the laboratory as separate, discrete samples. Precision values given in Table 6-1 were calculated as follows:

$$\%d = \left[\frac{A-B}{(A+B)/2}\right] \times 100$$

where %d = percent difference between values A and B

A = results of analysis of split sample aliquot A

B = results of analysis of split sample aliquot B

Also, randomly selected samples were split and spiked. One portion of the split sample was analyzed as received, and a known amount of "spike" solution was added to the other portion. The accuracy values shown in Table 6-1 were determined by the following equation:

$$\%A = 100 - \left(\frac{m - a}{a}\right) 100$$

%A = percent accuracy

m = measured value

a = actual value

Another means of quantifying accuracy is to analyze a standard reference material (SRM), obtainable from the National Bureau of Standards, along with the samples. One SRM was analyzed; the results are reported in Table 6-1.

## 6.6 SOURCE REPRESENTATIVENESS

One obvious objective in a program of this type is to withdraw a slipstream from the process source in a manner that will be as representative as possible. Several considerations come into play, including isokinetics at the point of slipstream, slipstream

## TABLE 6-1. RESULTS OF RANDOMLY SPLITTING AND SPIKING SAMPLES FOR ANALYSIS

| Precision | |
|---|---|
| Test | % d |
| Cl | 7.6% |
| F | 13.0%[a] |
| $SO_x$ | 3.1% |
| Heating value | 1.0% |
| **Accuracy** | |
| Test | % A |
| Cl | 94% |
| F | 104% |
| Pb[b] | 71% |
| Zn[b] | 36% |
| Fe[b] | 100% |

[a] Based on three duplicate runs, one of which was significantly higher than the other two.

[b] Based on NBS fly ash standard.

nozzle configuration, inleakage of ambient air and gas cooling prior to the inlet sampling location.

Determination of the representativeness of a slipstream requires the definition of a number of design and operating variables. Since the slipstream nozzle and ductwork required for the mobile ESP and fabric filter were the same size and test program scheduling permitted, the same nozzle was used in each program. Figure 6-4 is a detailed drawing of the nozzle. Fabrication of the nozzle simply involved cutting a 25.4-cm (10-in.) i.d. steel pipe on about a 27-degree angle with the outside edge of the pipe. The dimensions shown in the detail are scaled from a photograph of the nozzle.

The inlet nozzle used for the mobile scrubber was a 15.2-cm (6-in.) i.d. rounded elbow. The leading edge of the elbow was cut off slightly to allow insertion into the main breeching, but the cross-sectional area exposed to the inlet flow was circular.

For calculation of the isokinetic ratio of the slipstream, the total flow rate and cross-sectional area of the main breeching are used to determine the velocity of flue gas in the main breeching. The flow rate used to calculate the velocity, which is assumed constant for this purpose, was taken from the Ames Boiler 7 Compliance Test.[4] Table 6-2 shows the calculation of isokinetics for each device, and Figure 6-5 shows the isokinetic range for each device.

A direct comparison of measured inlet particulate concentrations for the mobile ESP and mobile scrubber could reasonably

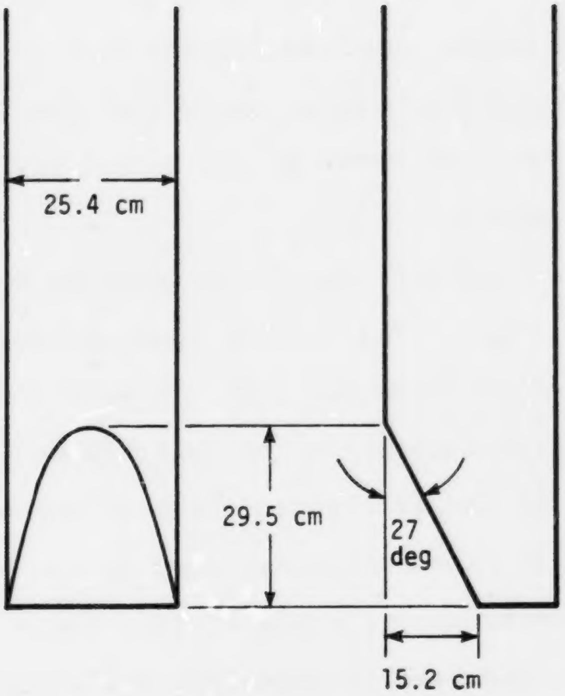
25.4 cm
29.5 cm
27
deg
15.2 cm

Figure 6-4. Mobile ESP and fabric filter slipstream nozzle detail.

TABLE 6-2. ISOKINETIC COMPARISON OF EACH SLIPSTREAM

| | Main breeching | Mobile ESP | Mobile scrubber | Mobile fabric filter |
|---|---|---|---|---|
| Ductwork inner dimensions,<br>m<br>(ft) | 6.4 x 1.2<br>(21 x 4) | See Figure 6-4 | 0.15 diameter<br>(0.5) | See Figure 6-4 |
| Cross sectional area,<br>$m^2$<br>($ft^2$) | 7.7<br>(84) | 0.07<br>(0.76)<br>by integration of partial ellipse | 0.02<br>(0.20) | 0.07<br>(0.76)<br>by integration of partial ellipse |
| Gas flow rate,<br>$m^3/s$<br>(acfm) | 83.4<br>(176,650) | 0.56 - 1.09<br>(1180 - 2310) | 0.14 - 0.30<br>(309 - 613) | 0.67 - 1.29<br>(1428 - 2726) |
| Gas velocity,<br>m/s<br>(fpm) | 10.7<br>(2100) | 8.0 - 15.6<br>(1550 - 3040) | 8.0 - 15.7<br>(1574 - 3123) | 9.5 - 18.2<br>(1879 - 3587) |
| Isokinetic ratio | NA[a] | 74% - 145% | 75% - 149% | 89% - 171% |

[a] Not applicable.

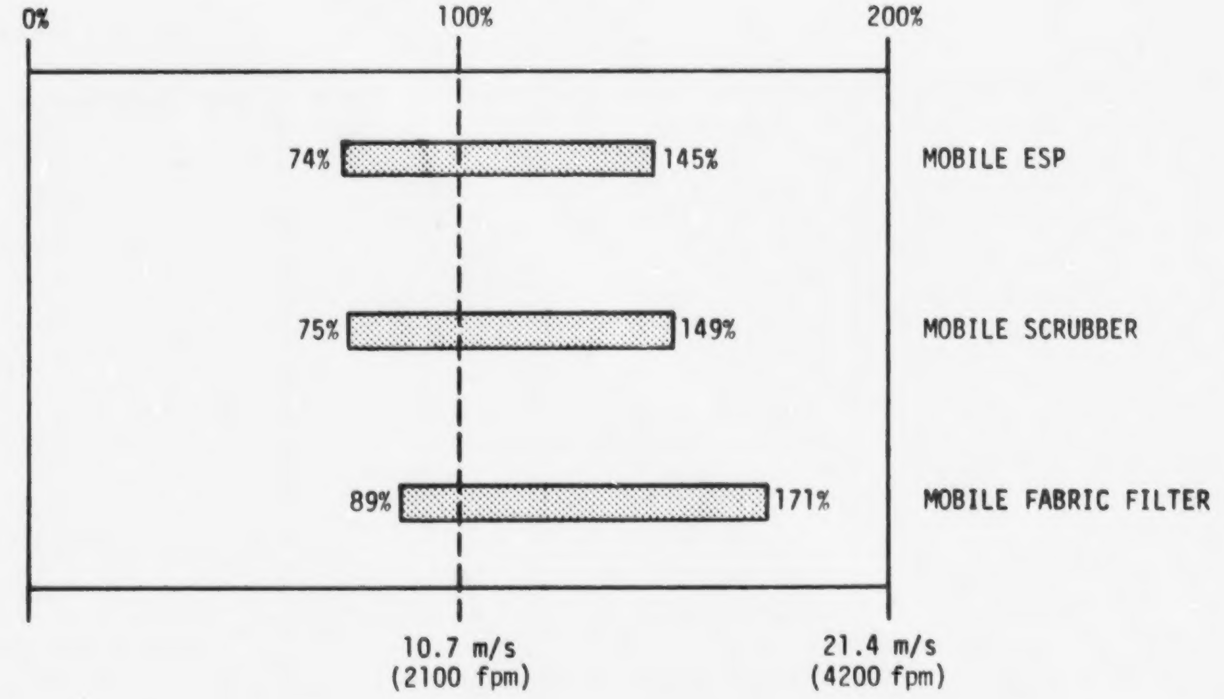

Figure 6-5. Slipstream isokinetic ranges for each mobile device operating range (velocity at point of slipstream/velocity in main duct).

be expected to yield similar values. So that observed values would be as comparable as possible, only the test runs occurring on the same day were compared. Table 6-3 presents a same-day listing of inlet sampling conditions for the test runs. The data show that the theoretically comparable values differ by as much as a factor of 9.6. Sampling conditions are given along with the measured particulate concentrations to demonstrate the similarity in all gas characteristics except particulate concentration.

Several factors could have contributed to the large difference in inlet particulate concentrations. Flow stratification in the main breeching is a possibility; however, the mobile ESP and scrubber inlet nozzles were placed on a "perpendicular to flow" centerline and at the same depth in the duct [0.9 m (35 in.)]. The two nozzles were about 0.76 m (30 in.) apart. Flow-straightening baffles in the main breeching, just upstream of the point of slipstreaming, should have prevented flow stratification. It is therefore believed that this factor played a small part, if any, in the difference between the inlet particulate concentrations.

Cooling of the slipstreamed gas and ambient inleakage are two possible causes that are discounted on the basis of temperature and similarities between oxygen ($O_2$) and carbon dioxide ($CO_2$) readings at the inlet sample locations. These values are shown on Table 6-3.

The physical shape of the flow nozzles used for the separate devices is considered the most significant factor in the difference between inlet particulate concentrations. The mobile ESP

TABLE 6-3. SAME-DAY COMPARISONS MOBILE ESP/SCRUBBER INLET PARTICULATE CONCENTRATIONS

| Run | Temp., °F | Part. conc., mg/dry std. $m^3$ | % $O_2$ | % $CO_2$ | Run | Temp., °F | Part. conc., mg/dry std. $m^3$ | % $O_2$ | % $CO_2$ |
|---|---|---|---|---|---|---|---|---|---|
| 7SI | 353 | 16,572 | 8.0 | 12.0 | 1EI | 382 | 3235 | 7.0 | 12.0 |
| 8SI | 356 | 19,685 | 5.0 | 12.5 | 2EI | 364 | 2775 | 6.0 | 13.5 |
| 12SI | 365 | 18,520 | 13.7 | 13.5 | 4EI | 335 | 2746 | 4.7 | 11.7 |
| 13SI | 357 | 17,304 | 5.0 | 14.4 | 8EI | 319 | 1798 | 6.3 | 11.7 |

inlet nozzle may not have provided a completely representative slipstream. Figure 6-6 shows the reasoning behind this conjecture.

Because of the aerodynamic shape of the mobile ESP slipstream inlet nozzle, a significant amount of mechanical separation of larger particulate may have occurred, thus decreasing the overall particulate concentration. For comparison, the figure also shows the aerodynamic design of the mobile scrubber inlet nozzle. As shown, mechanical separation should have been minimal at the inlet opening of the scrubber nozzle.

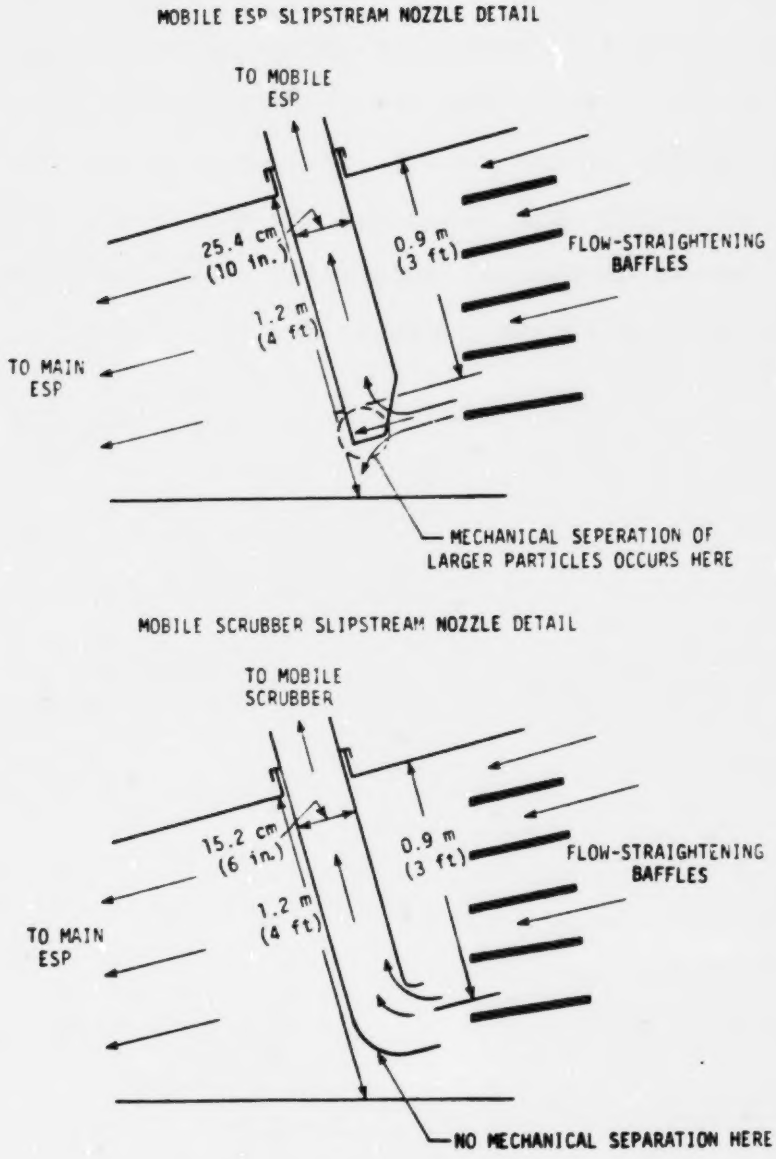
MOBILE ESP SLIPSTREAM NOZZLE DETAIL
TO MOBILE ESP
25.4 cm (10 in.)
0.9 m (3 ft)
FLOW-STRAIGHTENING BAFFLES
1.2 m (4 ft)
TO MAIN ESP
MECHANICAL SEPERATION OF LARGER PARTICLES OCCURS HERE
MOBILE SCRUBBER SLIPSTREAM NOZZLE DETAIL
TO MOBILE SCRUBBER
15.2 cm (6 in.)
0.9 m (3 ft)
FLOW-STRAIGHTENING BAFFLES
1.2 m (4 ft)
TO MAIN ESP
NO MECHANICAL SEPARATION HERE

Figure 6-6. Slipstream nozzle details.

# SECTION 7

# TEST SUMMARY

The Ames, Iowa, test program for the mobile ESP and scrubber took place October 11 through December 1, 1978; for the fabric filter, June 19 through July 25, 1979. As shown in Table 5-1, both the RDF and coal characteristics differed during each time period because of improvements made in the preprocessing plant and possibly the use of a different blend of coal. For each series of tests, however, the coal and RDF characteristics were relatively constant. While overall emission rates during the ESP and scrubber test series cannot be compared with those during the fabric filter test series, a confident comparison can be made between emissions when coal only was burned versus coal plus RDF for each control device.

An elemental analysis was performed on composite samples of the coal and RDF taken during the ESP and scrubber test series. The analysis showed that concentrations of copper, lead, bromine, fluorine, zinc, and manganese were more than 10 times greater in the RDF than in the coal, whereas concentrations of vanadium and beryllium were greater in the coal than in the RDF.

## 7.1 MOBILE ESP

Eighteen test runs were made with the mobile ESP between October 18 and December 1, 1978. The emission concentrations were related to a number of variable conditions so that trends could be noted that might indicate methods of lowering emissions of potentially harmful pollutants. A comparison of inlet loading and outlet loading (or ESP removal efficiency) with power generation rate yielded no useful trend. Boiler load in the range tested seemed to have little or no effect on emission concentrations.

A study of the effect of specific collection area and type of fuel (coal only vs. coal plus RDF) on particulate collection efficiency showed the following. When less than five energized fields were used (and thus a lower SCA), the efficiency of particulate collection dropped slightly on coal-only runs. It was also noticed that the use of coal plus RDF adversely affected the performance of the mobile ESP at a given SCA [16.4 $m^2$ per 1000 $m^3$/h (300 $ft^2$/1000 acfm)]; however, the effect did not appear to be directly proportional to the increase in the RDF input ratio. In other words, ESP performance did not decrease more with greater RDF input.

The control of lead emissions, currently a significant environmental concern, can be evaluated in a number of ways. Inlet and outlet lead concentrations measured during mobile ESP testing showed the highest controlled lead emission to be about 5 mg/dry std. $m^3$ when the fuel was approximately 20 percent RDF, whereas the overall average of controlled lead emissions, including the coal-only runs, was 0.71 mg/dry std. $m^3$. The lead composition of the fly ash sampled at the ESP inlet and outlet showed higher concentrations of lead in the finer particulate at the outlet than in the particulate at the inlet. This indicates that lead is more concentrated in the smaller, harder-to-collect size fraction and explains why the ESP is more efficient for particulate removal than for lead removal. This study showed an ESP particulate collection efficiency range of 94 to 98 percent and an average lead removal efficiency of greater than 95 percent.

## 7.2 MOBILE SCRUBBER

The mobile venturi scrubber was operated from October 11 through November 1, 1979. Most of 17 test runs were performed when the boiler was firing coal plus RDF.

The scrubber test plan was structured to include slipstreams from two different locations: before (primary) and after (secondary) the main ESP on Boiler 7.

### 7.2.1 Primary Device Test Runs

During all primary device test runs the particulate removal efficiency was in excess of 99 percent. Tests were run with different pressure drops across the venturi throat [25.4, 50.8, and 76.2 cm W.G. (10, 20, and 30 in. W.G., respectively)], but contrary to expectations, particulate collection efficiency did not increase with increasing pressure drop. In fact, the efficiency was the same on the coal-plus-RDF tests at low and high pressure drops, and efficiency decreased slightly with increasing pressure drop on the coal-only tests. This observation led to an investigation of other scrubber operating parameters to explain this apparent contradiction. During the test program, the pressure drop was varied by a change in gas flow rate, not venturi throat size, and the scrubber liquor flow rate was adjusted to keep the liquid-to-gas ratio constant. This resulted in a longer residence time in the venturi throat during lower-pressure-drop tests. The longer residence time in the throat appeared to affect the particulate removal efficiency more than the decreased pressure drop so that the efficiency did not drop appreciably when the scrubber was operated at 25.4 and 50.8 cm W.G. versus 70.2 cm W.G.

At both low and high pressure drops, particulate collection efficiency was greater during the coal-plus-RDF tests than during the coal-only tests. This is somewhat misleading, however, because inlet particulate loading appears to increase with RDF input. At constant inlet particulate loading, collection efficiency may not be enhanced by RDF input. During the test runs, lead emissions increased as RDF was increased. When coal only was burned, lead emissions were 0.22 mg/dry std. $m^3$ and increased to as high as 14 mg/dry std. $m^3$ when RDF was burned. Fuel input conditions, however, did not substantially affect the lead-removal efficiency of the scrubber. Lead-removal efficiencies ran about 90 percent, significantly less than overall particulate-removal efficiencies, which were more than 99 percent.

This again indicates that lead tends to be concentrated on smaller size fractions of particulate matter.

The ability of a scrubber to remove chloride emissions was also of interest because uncontrolled chloride emissions increase when RDF is burned. Controlled values are shown for only one test, as the other outlet samples were below the detectable limit of 1.8 mg/dry std. $m^3$. The chloride-removal efficiency was 96 percent when the scrubber outlet chloride concentration was measured at 5 mg/dry std. $m^3$.

### 7.2.2 Secondary Device Test Runs

Six runs were made with the scrubber operating as a secondary device; all were coal-plus-RDF runs. Particulate-removal efficiencies ranged from 72 to 97 percent. The lowest scrubber efficiency occurred on the only run in which the scrubber pressure drop was 25.4 cm W.G. (10 in. W.G.) and RDF heat input to the boiler was the highest (approximately 27 percent). On this test, however, the boiler load and inlet particulate grain loading were much lower (i.e., 22 MW and 104 mg/dry std. $m^3$ compared with 35 MW and approximately 400 mg/dry std. $m^3$ on tests in which scrubber efficiencies were greater than 90 percent). There were no detectable outlet chloride concentrations during the secondary scrubber tests.

## 7.3 PILOT FABRIC FILTER

Fifty-three test runs were made with the mobile fabric filter between June 19 and July 25, 1979.

The runs are split almost evenly between tests run while the boiler was firing coal only and those while firing coal plus RDF, which provided a better data base than did either the mobile ESP or mobile scrubber tests. The RDF heat input to the boiler ranged from 9 to 24 percent, and air-to-cloth ratios varied from 27.4 to 45.7 $m^3/h$ per $m^2$ (1.1 to 2.0 $acfm/ft^2$).

Emission concentrations were graphically related to a number of variable conditions in an attempt to recognize trends that might indicate specific conditions which would lower emissions of potentially harmful pollutants.

Improper seals around several bag connections caused particulate leaks during the first half of the fabric filter test series. The results of these tests are included in this report but were not considered in the data evaluation. A comparison of outlet loadings and fabric filter collection efficiency with power generation, air-to-cloth ratio, or type of cleaning mechanism yielded no apparent trends in pollution control efficiency. Data from this test program indicate that these three operating parameters, within their testing ranges, have minimal impact on outlet loading or particulate collection efficiency; however, the operating ranges used in this program may not have been wide enough to represent full-scale design ranges.

The effects of pressure drop and type of fuel on particulate collection efficiency were investigated, but fabric filter efficiencies consistently remained greater than 99 percent. When the boiler burned coal only, efficiencies averaged 99.4 percent during five tests at 8 cm W.G. (3 in. W.G.) and 99.0 percent during nine tests at 23 cm W.G. (9 in. W.G.). When coal plus RDF was burned, average particulate removal efficiency was 99.3 percent during five tests at 7 cm W.G. (2.5 in. W.G.) and five tests at 14 cm W.G. (5.5 in. W.G.).

Evaluation of the control of lead emissions by the fabric filter was difficult because only one outlet lead sample had a lead concentration above the detectable limit of 0.007 mg/dry std. $m^3$. Inlet lead concentrations averaged 0.56 mg/dry std. $m^3$ when the boiler burned coal only and 1.2 mg/dry std. $m^3$ when coal plus RDF was burned. The only detectable outlet concentration (0.03 mg/dry std. $m^3$) was measured when the boiler was burning coal only. The lead removal efficiency during this run was 94.8 percent. Assuming outlet lead concentrations equal to the detectable limit (which is a conservative estimation), lead-removal efficiencies averaged at least 99 percent during the other runs.

Cadmium, copper, zinc, iron, and mercury concentrations were determined for selected samples. Although the data are variable, uncontrolled concentrations of zinc and cadmium appear to increase when RDF is burned, but detectable concentrations in controlled emissions were about the same regardless of the fuel burned. The fabric filter controlled zinc emissions with an efficiency of greater than 99 percent, but the removal efficiency for cadmium ranged from 90 to 95 percent. Copper and iron emissions did not vary significantly with changes in RDF input. The fabric filter controlled iron emissions with an average removal efficiency of 99.7 percent and copper emissions with an efficiency of about 90 percent. Because only two test runs were analyzed for mercury emissions, the data are too limited to lead to any conclusions. The mercury samples taken while the boiler was burning coal plus RDF resulted in a concentration of 0.0008 mg/dry std. $m^3$ at both the inlet and outlet of the fabric filter, whereas samples taken while the boiler was burning coal only show an inlet concentration of 0.006 mg/dry std. $m^3$ and an outlet concentration below the detectable limit of 0.0001 mg/dry std. $m^3$. Further testing is needed to confirm or reject these results.

Uncontrolled chloride emissions averaged about 120 mg/dry std. $m^3$ while the boiler was burning coal plus RDF and 30 mg/dry std. $m^3$ while it was burning coal only, a fourfold increase in gaseous chlorides. The fabric filter removed approximately 20 percent of these chlorides during both coal-only and coal-plus-RDF test runs.

## 7.4 OVERALL EVALUATION

The tests at Ames showed no significant difference between total uncontrolled particulate emissions during coal firing and those during coal-plus-RDF firing. Some uncontrolled trace elements (such as lead, zinc, and cadmium) and gaseous chlorides increased significantly during coal-plus-RDF firing. On the other hand, $SO_x$ emissions did not change appreciably with increased RDF input to the boiler.

The particulate removal efficiencies of the control devices (scrubber, the ESP, or fabric filter) did not change appreciably with an increase in RDF heat input. The elemental removal efficiency was typically less with the scrubber than with the ESP or fabric filter. For example, lead removal efficiency was about 90 percent with the scrubber, but greater than 95 percent with both the ESP and the fabric filter. On the other hand, gaseous chloride removal efficiency was greater than 95 percent with the scrubber, but negligible with the ESP and about 20 percent with the fabric filter.

## SECTION 8

## REFERENCES

1. PEDCo Environmental, Inc. Evaluation of Fabric Filter Performance at Ames Solid Waste Recovery System, Ames, Iowa. (Draft Report) Prepared for the U.S. Environmental Protection Agency, Industrial Environmental Research Laboratory, under Contract No. 68-02-2509, November 1979.

2. Brumfield, J. L., and F. Crowson. Design and Fabrication of a Mobile Electrostatic Precipitator. Naval Surface Weapons Center, Dahlgren, Virginia.

3. Opferkuch, R. E. Particulate Control Mobile Test Units: First Year's Operation. Monsanto Research Corp., Dayton, Ohio. Prepared for the U.S. Environmental Protection Agency under Contract No. 68-02-1861, February 1976.

4. Hall, J. L., et. al. Compliance Tests of Steam Generator Unit 7 for Particulate Effluent, City of Ames, Iowa, July 17-25, 1978. University of Iowa, Ames, Iowa, 1978.

# APPENDIX A

# SAMPLING AND ANALYTICAL PROCEDURES

## SAMPLING PROCEDURE FOR PARTICULATE, HALIDES, $SO_x$, TRACE METALS

In this test program, sampling procedures followed those described in Method 5 of the Federal Register.*

## SAMPLING APPARATUS

The source sampling train used in these tests at inlet/outlet sampling sites meets design specifications established by the Federal EPA and was assembled by PEDCo personnel. It consisted of:

Nozzle - Stainless steel (316) with sharp, tapered leading edge and accurately measured round opening.

Probe - Pyrex glass with a heating system capable of maintaining a minimum gas temperature of 120°C (250°F) at the exit end during sampling.

Pitot tube - Type S pitot tube that meets all geometry standards and is attached to the probe to monitor stack gas velocity.

Filter holder - Pyrex glass with heating system capable of maintaining a filter temperature of approximately 120°C (250°F).

Draft gauge - An inclined manometer made by Dwyer with a readability of 0.025 cm (0.01 inch) $H_2O$ in the 0 to 2.54 cm (1-inch) range is used.

---

*Federal Register, Vol. 42, No. 160, August 18, 1977.

Impingers - Four impingers connected in series with glass ball joints. The first, third, and fourth impingers are of the Greenburg-Smith design, modified by replacing the tip with a 1.27 cm (1/2-inch) i.d. glass tube extending to 1.27 cm (1/2 inch) from the bottom of the flask.

Metering system - Vacuum gauge, leak-free pump, thermometers capable of measuring temperature to within -15°C (5°F), dry gas meter with 2 percent accuracy, and related equipment to maintain an isokinetic sampling rate and to determine sample volume. The dry gas meter is made by Rockwell and the fiber vane pump is made by Gast.

Barometer - Bourden tube type to measure atmospheric pressure to ±0.25 cm (0.1 inch) Hg.

## SAMPLING PROCEDURE

The stack pressure, temperature, moisture, and range of velocity head were measured according to procedures described in the Federal Register.* An average velocity point in the duct was chosen as the single sampling point.

Approximately 200 grams of silica gel was weighed in a sealed impinger prior to each test. Glass fiber filters** 7.62 cm (3-in. diameter) were desiccated for at least 24 hours and weighed to the nearest 0.1 milligram on an analytical balance. One hundred ml of distilled water was placed in each of the first two impingers; for $SO_x$ collection distilled deionized water was replaced by 3 percent $H_2O_2$. The third impinger was initially empty; and the impinger containing the silica gel was placed next in series. The train was set up with the probe as shown in Figure A-1. The sampling train was checked for leaks at the sampling site before each test run by plugging the inlet to the

---

* Federal Register, Vol. 42, No. 160, August 18, 1977.

** Gelman Type A.

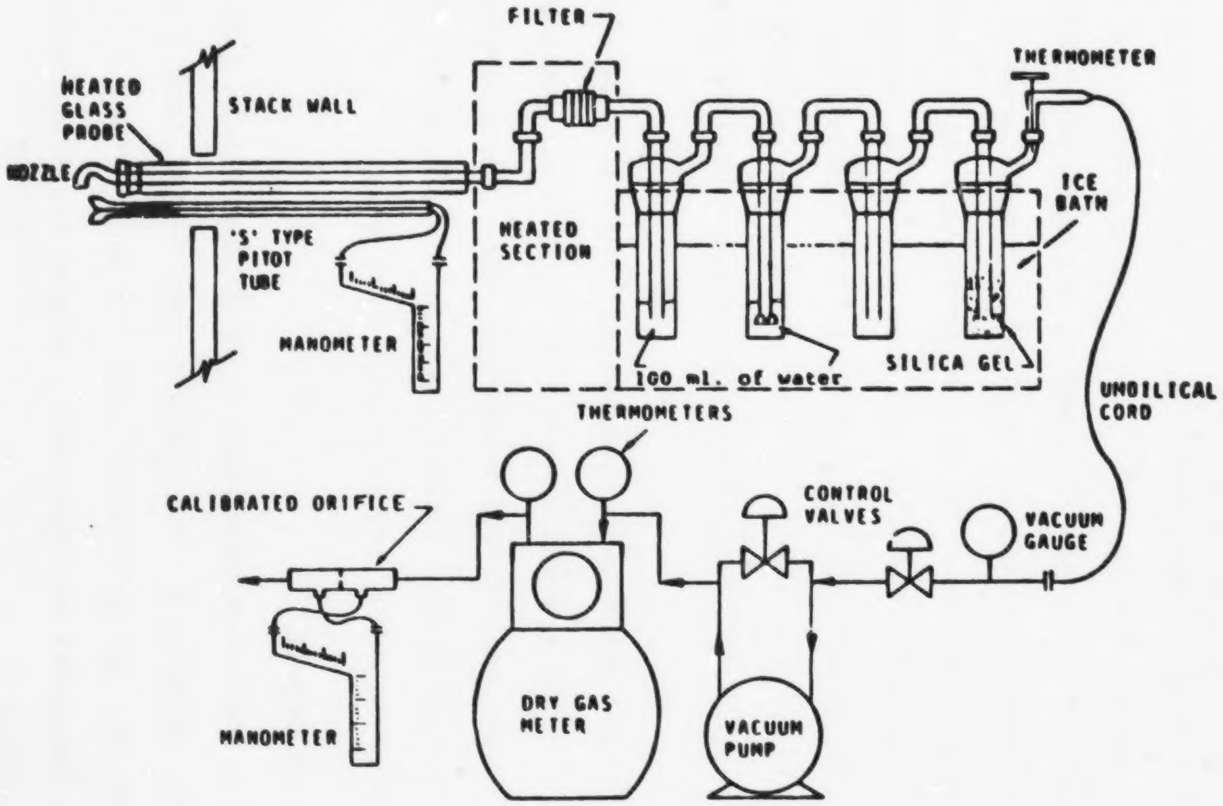
FILTER
THERMOMETER
HEATED GLASS PROBE
STACK WALL
NOZZLE
'S' TYPE PITOT TUBE
MANOMETER
HEATED SECTION
ICE BATH
100 ml. of water
SILICA GEL
UMBILICAL CORD
THERMOMETERS
CALIBRATED ORIFICE
CONTROL VALVES
VACUUM GAUGE
DRY GAS METER
VACUUM PUMP
MANOMETER

Figure A-1. Sample train.

nozzle and pulling a 38.1 cm (15-in.)-Hg vacuum, and at the conclusion of the test by plugging the inlet to the nozzle and pulling a vacuum equal to the highest vacuum reached during the test run. The pitot tube and lines were checked for leaks at the test site before and after each test run. The check was made by blowing into the impact opening of the pitot tube until 7.62 cm (3 inches) or more of water was recorded on the manometer and then capping the impact opening and holding it for 15 seconds to assure that it was leak-free. The static pressure side of the pitot tube was checked for leaks by the same procedure, except suction was used to obtain the 7.62 cm (3-in.)-$H_2O$ manometer reading. Crushed ice was placed around the impingers to keep the temperature of the gases leaving the last impinger at 20°C (68°F) or less.

During sampling, stack gas and sampling train data were recorded every 10 minutes and when stack flow conditions changed significantly. With the aid of a nomograph, isokinetic sampling rates were set throughout the sampling period. All sampling data were recorded on an emission testing field data sheet.

## SAMPLE RECOVERY PROCEDURE

The sampling train was carefully moved from the test site to the cleanup area. Samples of the acetone used in the sample recovery were taken for use as blanks. The volume of water from the first three impingers was measured. Sample fractions were recovered as follows:

Container No. 1 - The filter was removed from its holder, placed in a petri dish, and sealed.

Container No. 2 - Loose particulate and acetone washings from all sample-exposed surfaces prior to the filter were placed in a glass jar, sealed, and labeled. Particulate was removed from the probe with the aid of a brush and acetone rinsing. The liquid level was marked after the container was sealed.

Container No. 3 - The collected volume of liquid in the impingers was measured and recorded. The total catch was placed in a plastic bottle along with distilled deionized water rinse of all glassware following the filter. The liquid level was marked after the bottle was sealed.

Container No. 4 - A minimum of 200 ml of acetone was taken for the blank analysis. The blank was obtained and treated in a similar manner as the acetone washing.

Container No. 5 - 200 ml of 3 percent $H_2O_2$ was taken from the same batch of $H_2O_2$ solution used in sampling. This was labled the $H_2O_2$ Blank for $SO_x$ analysis with the samples.

The silica gel from the fourth impinger was weighed and recorded on the sample recovery and integrity data sheet with other pertinent data.

## ANALYTICAL PROCEDURES

The procedures used follow the methods described in the Federal Register.*

Container No. 1 - The filter and any loose particulate matter from this sample container were placed into a tared glass weighing dish, desiccated for 24 hours to a constant weight, and weighed to the nearest 0.1 mg. The filter was then sectioned with a template. One section of the filter was digested in concentrated $HNO_3$ and analyzed for various metals by atomic absorption analysis.** The other section was stored for later use.*

---

* Federal Register, Vol. 42, No. 160, August 18, 1977.

** Analysis was performed initially on front and back halves of the total catch from the sampling train. The back half contained a $HNO_3$ solution to collect vaporous trace metals, particularly lead; however, analysis showed that more than 99% of the lead was collected with the particulate. Consequently, in all the samples collected in the rest of the test program, only the particulate was analyzed for metals by atomic absorption.

Container No. 2 - The acetone washings were transferred to a tared beaker and evaporated to dryness at ambient temperature and pressure, desiccated for 24 hours to a constant weight, and weighed to the nearest 0.1 mg.

Container No. 3 - The impinger catch was brought to a total volume of 1000 ml with distilled deionized water. The impinger catch was analyzed for either halides or $SO_x$. For halides, the samples were split, and one portion was analyzed for fluoride (analysis procedure in Method 13B of the Federal Register**). The remaining portion was analyzed for chloride and bromide (ESP and scrubber only) by use of a specific ion electrode in conjunction with a millivolt meter. The analytical procedure for analyzing for $SO_x$ was a barium perchlorate titration (Method 6 of the Federal Register**).

Container No. 4 - The acetone blank was transferred to a tared beaker and evaporated to dryness at ambient temperature and pressure. The blank was then desiccated for 24 hours to a constant weight and weighed to the nearest 0.1 mg.

Container No. 5 - The $H_2O_2$ blank was brought to a total volume of 1000 ml with distilled deionized water. The sample blank was analyzed along with the samples for $SO_x$.

The term "constant weight" means a difference of no more than 0.5 mg or 1 percent of total weight less tare weight, whichever is greater in two consecutive readings, with no less than 6 hours of desiccation between weighings. All analytical data were recorded on analytical particulate data sheets. Acetone blank data were recorded on sheets supplied for this purpose.

---

* Elemental analysis by spark source mass spectometry was also performed (see Appendix B) on the particulate catch of samples collected by Acurex, a subcontractor on this project; however, only the ESP and scrubber samples were analyzed by this technique.

** Federal Register, Vol. 42, No. 160, August 18, 1977.

## SAMPLING PROCEDURE FOR Hg EMISSIONS

The following method was used for collection of mercury samples at inlet/outlet sites of the control devices. The sampling procedure is based on Method 101 of National Emissions Standards for Hazardous Air Pollutants.

### SAMPLING APPARATUS

The Hg sampling train used in these tests meets design specifications established by the Federal EPA and was assembled by PEDCo personnel. It consists of:

Nozzle - Stainless steel (316) with sharp, tapered leading edge and accurately measured round opening.

Probe - Pyrex glass with a heating system capable of maintaining a minimum gas temperature of 120°C (250°F) at the exit end during sampling.

Pitot tube - Type S pitot tube that meets all geometry standards, attached to the probe to monitor stack gas velocity.

Filter holder - Pyrex glass with heating system capable of maintaining a filter temperature of approximately 120°C (250°F).

Draft gauge - An inclined manometer, made by Dwyer, with a readability of 0.025 cm (0.01 inches) $H_2O$ in the 0 to 2.54 cm (1-inch) range.

Impingers - Four impingers connected in series with glass ball joints. The first, third, and fourth impingers are of the Greenburg-Smith design, modified by replacing the tip with a 1.27 cm (1/2-inch) i.d. glass tube extending to 1.27 cm (1/2 inch) from the bottom of the flask.

Metering system - Vacuum gauge, leak-free pump, thermometers capable of measuring temperature to within -15°C (5°F), dry gas meter with 2 percent accuracy, and related equipment to maintain an isokinetic sampling rate and to determine sample volume. The dry gas meter is made by Rockwell and the fiber vane pump is made by Gast.

Barometer - Bourden tube type to measure atmospheric pressures to ±0.25 cm (0.1 inch) Hg.

## SAMPLING PROCEDURE

The stack pressure, temperature, moisture, and range of velocity head were measured according to procedures described in the Federal Register.*

Approximately 200 grams of silica gel are weighed in a sealed impinger prior to each test. A hi-purity glass fiber filter** 7.62 cm (3-in.) diameter was placed ahead of the impingers. One hundred ml of 4 percent $KMnO_4$/10 percent $H_2SO_4$ was placed in each of the three impingers; and the impinger containing the silica gel was placed next in series. The train was set up with the probe as shown in Figure A-2. The sampling train was checked for leaks at the sampling site before each test run by plugging the inlet to the nozzle and pulling a 38.1 cm (15-inch)-Hg vacuum, and at the conclusion of the test by plugging the inlet to the nozzle and pulling a vacuum equal to the highest vacuum reached during the test run.

The pitot tube and lines were checked for leaks at the test site before and after each test run. The check was made by blowing into the impact opening of the pitot tube until 7.62 cm

---

*Federal Register, Vol. 42, No. 160, August 18, 1977.

**Gelman Spectrograde.

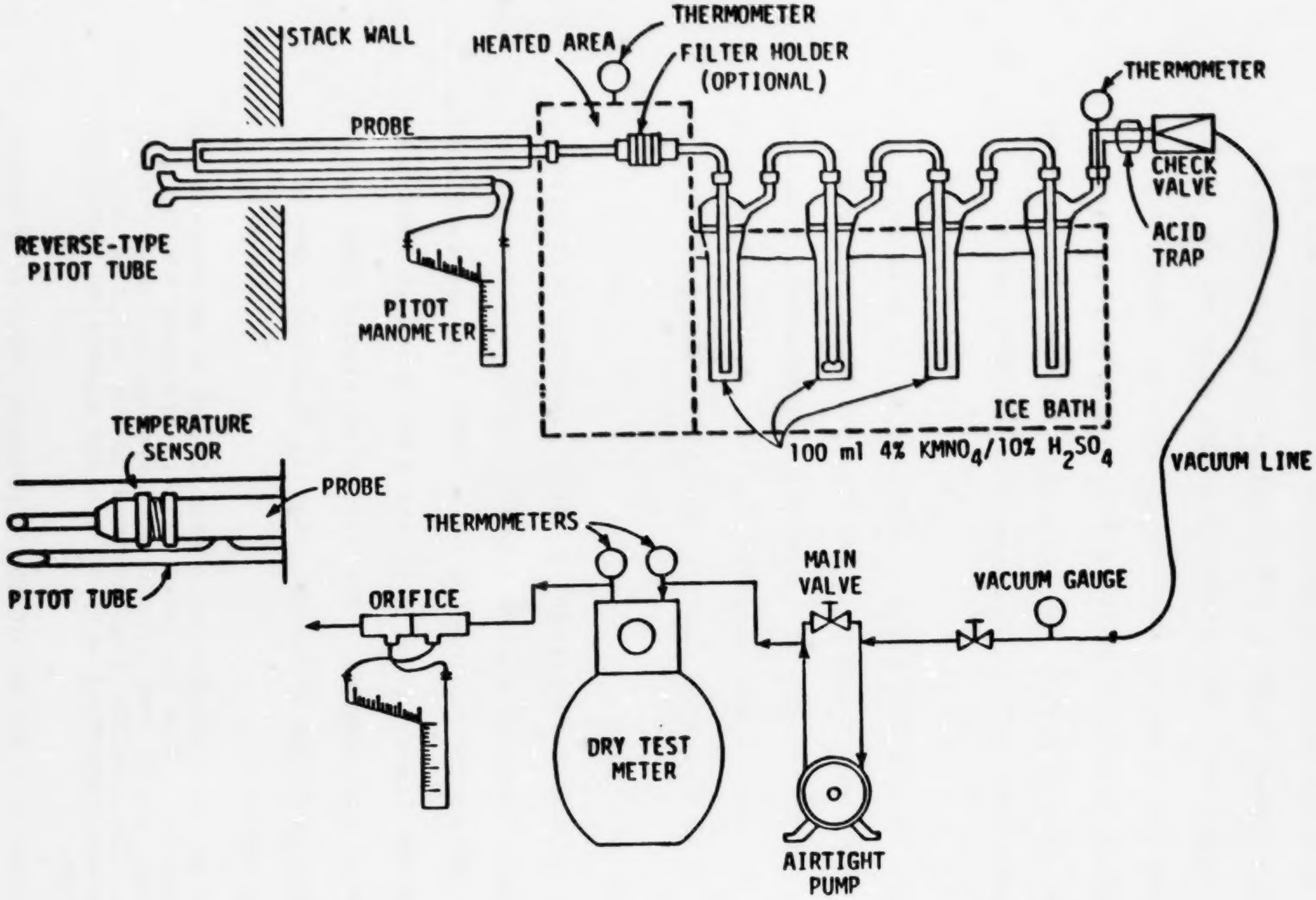
STACK WALL
HEATED AREA
THERMOMETER
FILTER HOLDER (OPTIONAL)
THERMOMETER
PROBE
CHECK VALVE
ACID TRAP
REVERSE-TYPE PITOT TUBE
PITOT MANOMETER
ICE BATH
100 ml 4% KMNO$_4$/10% H$_2$SO$_4$
VACUUM LINE
TEMPERATURE SENSOR
PROBE
THERMOMETERS
MAIN VALVE
VACUUM GAUGE
PITOT TUBE
ORIFICE
DRY TEST METER
AIRTIGHT PUMP

Figure A-2. Sample train for mercury.

(3 inches) or more of water was recorded on the manometer and then capping the impact opening and holding it for 15 seconds to assure it was leak-free. The static pressure side of the pitot tube was checked for leaks by the same procedure, except suction was used to obtain the 7.62 cm (3-in.)-$H_2O$ manometer reading. Crushed ice was placed around the impingers to keep the temperature of the gases leaving the last impinger at 20°C (68°F) or less.

During sampling, stack gas and sampling train data were recorded every 10 minutes and when stack flow conditions changed significantly. With the aid of a nomograph, isokinetic sampling rates are set throughout the sampling period. All sampling data were recorded on an emission testing field data sheet.

## SAMPLE RECOVERY PROCEDURE

The sampling train is carefully moved from the test site to the cleanup area. Samples of the 4 percent $KMnO_4$/10 percent $H_2SO_4$ used in the sample collection were taken for use as blanks, along with a glass fiber filter from the same batch as that used for collection of the samples. The volume of liquid from the first three impingers was measured. Sample fractions are recovered as follows:

> Container No. 1 - Entire catch was placed in an acid-washed Wheaton bottle. This included filter, impinger catch, and probe rinse, which were rinsed with the oxidative impinger solution. The residue that adhered to the walls of the glassware was recovered with 8N HCL and distilled deionized water rinse.
>
> Container No. 2 - 300 ml of the 4 percent $KMnO_4$/10 percent $H_2SO_4$ impinger solution and a blank filter were placed in an

acid-washed Wheaton bottle. The filter must be from the same batch as the filters used in sampling.

The silica gel from the fourth impinger is weighed and recorded on the sample recovery and integrity data sheets, along with other pertinent data.

## ANALYTICAL PROCEDURES

Both Containers 1 and 2 were analyzed for mercury by flameless atomic absorption (FAA). Sample preparation requires filtering the sample, digesting the filterable residue with concentrated nitric acid, filtering the digested sample, combining the filtrates, bringing the sample to a known volume, and analyzing with cold vapor atomic absorption. Method of standard addition is required to confirm that matrix effects have not interfered with analysis.

## SAMPLING PROCEDURE FOR COAL, RDF, ASH, AND SCRUBBER LIQUOR

The following methods were used for various grab samples taken in this test program.

### COAL

For each test run, a discrete grab sample of coal was taken from one of the integrators. The sampling location was before the pulverizer and within 1 minute of the coal's entry into the boiler. The coal sample was put into a wide-mouth plastic bottle, labeled, and transferred to the laboratory. Here the samples were first analyzed for air-dry loss, which was done by air-drying the samples for 24 hours and then determining the loss in weight. Next, all samples were pulverized to less than a 60-mesh size. A composite coal sample was made by extracting equal aliquots from each individual coal sample and combining them into one composite sample. Certain discrete coal samples were selected for analyses along with the composite sample.

The samples were analyzed for air-dry loss, moisture, ash, total sulfur, heating value, volatile matter, fixed carbon, carbon, hydrogen, nitrogen, oxygen, chlorides, and some trace metals.

RDF

For each test run, a discrete grab sample of RDF was taken from the Atlas storage bin. One cubic foot of RDF was extracted from the end of the conveyor as the RDF drops to a screw feeder to a pneumatic transfer system, which transported it to the boiler. At the point of sampling, the RDF was within 5 minutes of the boiler. The cubic foot of RDF was weighed to determine its density. The sample was then halved and quartered to a smaller sample size (nominally 1 liter), put in a wide-mouth plastic bottle, and labeled. All the samples were transported back to the laboratory for analysis. Each sample was air-dried for 24 hours, and the air-dry loss was determined. The samples were then put through a Wiley mill to prepare them for analysis. An aliquot was extracted from each milled individual RDF sample, and these were combined to make an RDF composite sample. Selected test run samples and the composite sample were analyzed for air-dry loss, moisture, ash, total sulfur, heating value, volatile matter, fixed carbon, carbon, hydrogen, nitrogen, oxygen, chlorides, and some trace metals.

ASH

At the completion of each test run, fly ash samples were taken from both the ESP catch and the fabric filter hopper. The ash samples were then separated between coal-only tests and coal-plus-RDF tests and stored for possible future analysis.

## SCRUBBER LIQUOR

An unfiltered scrubber liquor sample was taken for each test run. At the time of the sampling, temperature and pH were measured and recorded. All scrubber liquor samples were put in plastic bottles, sealed, labeled, and sent to Montgomery Engineering.*

---

*Montgomery Engineering was investigating wastewater resulting from waste-as-fuel processes.

APPENDIX B

# REPORT ON ANALYSES OF PARTICULATE EMISSIONS FROM A COAL-REFUSE DERIVED FUEL (RDF) - FIRED BOILER

Accomplished for PEDCo Environmental, Cincinnati, Ohio
Under Purchase Order No. 6373-3284

Prepared by

Brehm Laboratory
Wright State University
Dayton, Ohio 45435

Submitted to

Ms. Diane Albrink
PEDCo Environmental
Chester Towers
11499 Chester Road
Cincinnati, Ohio 45246

February 8, 1979

## INTRODUCTION

This report describes the results of Spark-Source-Mass Spectrographic (SSMS) analyses of particulates emitted by a coal-refuse derived fuel-(RDF) fired boiler at the Ames, Iowa power plant. These particulates were collected on glass fiber filters. The overall objective of the program under which these analyses were accomplished was to evaluate the effectiveness of various control devices in removing particulates from the emissions resulting from the combustion of the combined fuels. Obviously, such data is important in assessing the potential impact of using such fuels on air pollution considerations. This emission assessment program has been coordinated by PEDCo Environmental, under contract with the U. S. Environmental Protection Agency. PEDCo was responsible for the collection of all emission particulate samples, and has submitted these to the Brehm Laboratory, Wright State University for elemental analysis.

## ANALYTICAL PROCEDURES

Boiler emissions were sampled simultaneously at two points, one ahead of, and one following each of two pilot control devices. The two devices evaluated were an electrostatic precipitator, and a wet chemical scrubber. Collection of all samples, and observation of boiler operating parameters were accomplished by PEDCo personnel. The particulate samples, collected on glass fiber filters, were submitted to Wright State University for Spark Source Mass

Spectrographic (SSMS) analysis. Preparation of the filter samples for SSMS involved application of an acid extraction ($HCl-HNO_3$) method, which is known to be effective and reliable, on the basis of previous studies in our laboratory, in which such filters were spiked with known levels of selected elements and analyzed to determine recoveries. Briefly, the sample preparation entails the following:

1. Rapid extraction of particulates at moderate temperatures (Acid mixture, B.P. = $70^{\circ}C$) and atmospheric pressure, thereby facilitating retention of potentially volatile elements such as sulfur, cadmium, lead, tin, antimony, and arsenic.

2. Removal of glass fibers from the disintegrated filter using a teflon filter, which also retains insoluble particles (for example, fly ash).

3. Addition of a standard quantity of high purity graphite which yields a homogeneous mixture with the particulates, when the liquid is removed by evaporating the solution to dryness. The graphite also serves as an electrically conductive binder which is necessary for pelletizing the metal oxide sample.

4. Evaporation of the graphite-metal oxide solution to dryness in a clean acid hood at mild (~40°C) temperature with frequent stirring, followed by compression of the dried material in a press to produce a solid pellet.

The samples, prepared as described, are inserted into the Spark Source Mass Spectrograph, and spectra for each sample are recorded on photographic plates. Standard procedures are employed in obtaining the spark-source spectra.

Blank filters corresponding to two different batch numbers were submitted and analyzed by the above procedure to determine background levels of impurities.

In addition to the two blank samples, two doped standard filters (prepared at Wright State University), 18 sample filters, one coal sample, and one RDF sample, were analyzed. The coal sample was pulverized, briquetted, and analyzed so as to yield a detection limit approximately 1 part-per-million (weight basis). The RDF material was thoroughly mixed, and a small portion of the sample was low-temperature ashed to eliminate hydrocarbons. It should be noted that ashing of organic materials, which is necessary for SSMS analysis, results in loss of volatile metals, the extent of loss being dependent upon the molecular structure. Mercury and cadmium are probably lost quantitatively during low-temperature ashing.

# RESULTS

The data derived from the spark source mass spectrographic analyses accomplished during this program are reported in Tables 1 through 4. The values in Table 1 are reported as parts-per-million by weight (μg/g) in the materials as received. All other data is reported as total micrograms per filter. In most cases, two filters were submitted for each sampling run, and these were combined for particulate extraction and analysis. Other notations which appear in the Tables are (by letter designation):

(a) Elements not observed in excess of background levels.

(b) Concentrations are too high to be reliably estimated by this technique.

(c) The reported values for these elements in samples which are marked with an asterisk (7 SI, 9 SI, 12 SI, and 14 SI) may be low by a factor of 3 - 10 (or more for Cd), as a result of high organic content which necessitated low temperature ashing of these samples.

Elements not reported, such as Se, I, Ti, and the rare earth metals were not detected, and if present, are in quantities less than approximately 1 microgram.

## Table 1.

## SPARK SOURCE MASS SPECTROGRAPHIC ANALYSES OF COAL AND RDF (ppmw)

SAMPLE DESIGNATION

| Element | Coal | RDF* | Element | Coal | RDF* |
|---|---|---|---|---|---|
| Li(a) | | | Zn | 10 | 100 |
| Be | 5 | 0.2 | Ga | <1 | 1(c) |
| B(a) | | | As | 1 | < 1 |
| F | 4 | 100 | Br | <0.4 | 10 |
| Na(b) | | | Rb | 5 | 20 |
| Mg(b) | | | Sr | 50 | 100 |
| Al(b) | | | Y | 3 | 0.5 |
| Si(b) | | | Zr | 30 | 20 |
| P | 100 | 200 | Nb | <1 | 0.3 |
| S | ~10,000 | 2,000(c) | Mo | <10 | < 2 |
| Cl(a) | | | Ag | <1 | 3 |
| K (b) | | | Cd | <4 | < 1(c) |
| Ca (b) | | | Sn | < 1 | 10 |
| Sc | 20 | 3 | Sb | <2 | 10 |
| Ti | 500 | 1000 | Cs | <1 | 1 |
| V | 100 | 2 | Ba | 30 | 100 |
| Cr | 20 | 100 | La | 1 | 0.6 |
| Mn | 30 | 300 | Ce | 2 | 1 |
| Fe(b) | | | Tl | <3 | < 1 |
| Co | 2 | 10 | Pb | <1 | 100(c) |
| Ni | < 10 | < 5 | Bi | <2 | <2 |
| Cu | 1 | 100 | | | |

* See Report Text

## Table 2.

## SPARK SOURCE MASS SPECTOGRAPHIC ANALYSES OF BLANK FILTERS

(Total micrograms filter)

Sample Designation

| Element | Batch 7854 | Batch 8164 | Element | Batch 7854 | Batch 8164 |
|---|---|---|---|---|---|
| Li | 5 | 5 | Cu | 10 | 10 |
| Be | < 0.01 | < 0.01 | Zn | 2 | 2 |
| B | 1000 | 1000 | Ga | < 1 | < 1 |
| F | 50 | 50 | As | < 0.6 | <0.6 |
| Na(a) | High | High | Br | <0.2 | <0.2 |
| Mg(a) | High | High | Rb | 0.3 | 0.3 |
| Al(a) | High | High | Sr | 1 | 1 |
| Si(a) | High | High | Y | <0.1 | <0.1 |
| P | 3 | 3 | Zr | <0.06 | <0.06 |
| S | 100 | 100 | Nb | <0.03 | <0.02 |
| Cl(a) | High | High | Mo | 0.4 | 0.4 |
| K | 50 | 50 | Cd | <0.1 | <0.1 |
| Ca | 1000 | 1000 | Sn | <0.1 | <0.1 |
| Sc | <0.4 | <0.4 | Sb | <0.06 | <0.06 |
| Ti | 30 | 30 | Cs | <0.03 | <0.03 |
| V | 0.1 | 0.1 | Ba | 0.4 | 0.4 |
| Cr | 1 | 1 | La | <0.03 | <0.03 |
| Mn | 0.5 | 0.5 | Ce | <0.03 | <0.03 |
| Fe | 30 | 30 | Tl | <0.01 | <0.01 |
| Co | <0.2 | <0.2 | Pb | <0.1 | <0.1 |
| Ni | 0.3 | 0.3 | Bi | <0.06 | <0.06 |

## TABLE 3

## SPARK SOURCE MASS SPECTROGRAPHIC ANALYSIS OF BOILER PARTICULATE EMISSIONS FOLLOWING ELECTROSTATIC PRECIPITATION

(Total micrograms/filter)

| | Sample Designation | | | | | |
|---|---|---|---|---|---|---|
| Element | 3 EI | 3 EO | 9 EI | 9 EO | 121 EI | 121 EO |
| Li (A) | | | | | | |
| Be | 1 | 0.1 | 0.3 | 0.1 | 0.5 | 1 |
| B (A) | | | | | | |
| F | 200 | 500 | 200 | 200 | 200 | 200 |
| Na (B) | | | | | | |
| Mg (B) | | | | | | |
| Al (B) | | | | | | |
| Si (B) | | | | | | |
| P | 100 | 30 | 50 | 30 | High | High |
| S | 2000 | 2000 | 200 | 200 | 4000 | 4000 |
| Cl (A) | | | | | | |
| K (B) | | 500 | 200 | | | |
| Ca (B) | | | | | | |
| Sc | 1 | <0.4 | 2 | <0.4 | <1 | 1 |
| Ti | 300 | 100 | 300 | 100 | 100 | 100 |
| V | 4 | 4 | 4 | 1 | 100 | 100 |
| Cr | 20 | 100 | 4 | 20 | 20 | 50 |
| Mn | 100 | 30 | 10 | 3 | 50 | 50 |
| Fe | (B) | (B) | (B) | 500 | (B) | (B) |
| Co | 3 | 3 | 0.5 | 0.5 | 5 | 2 |
| Ni | 30 | 100 | 20 | 20 | ≤30 | ≤30 |
| Cu | 150 | 30 | 5 | 5 | 50 | 50 |
| Zn | 150 | 50 | 20 | 20 | 300 | 300 |
| Ga | 2 | <2 | 3 | 1 | 40 | 10 |
| As | 2 | <0.6 | <1 | <0.3 | 5 | 2 |

### TABLE 3 (CONT'D)

| ELEMENT | 3 EI | 3 EO | 9 EI | 9 EO | 121 EI | 121 EO |
|---|---|---|---|---|---|---|
| Br | 0.5 | 3 | 0.4 | 0.4 | <0.5 | <0.5 |
| Rb | 3 | 1 | 1 | 0.3 | 20 | 20 |
| Sr | 30 | 10 | 20 | 5 | 10 | 10 |
| Y | 2 | 0.3 | 1 | 0.1 | 1 | 1 |
| Zr | 5 | 5 | 3 | 3 | 3 | 3 |
| Nb | 0.2 | <0.1 | 0.3 | 0.1 | 0.5 | 0.5 |
| Mo | 1 | 10 | <1 | <0.4 | 5 | 5 |
| Cd | 0.4 | <0.2 | <0.1 | <0.1 | 40 | 20 |
| Sn | 3 | 2 | <0.3 | <0.3 | 10 | 10 |
| Sb | 2 | 0.2 | <0.06 | <0.06 | 20 | 5 |
| Cs | 0.3 | 0.05 | <0.1 | <0.1 | 3 | 5 |
| Ba | 30 | 10 | 30 | 10 | 400 | 200 |
| La | 1 | 0.1 | 0.3 | 0.1 | 1 | 1 |
| Ce | 3 | 0.3 | 1 | 0.3 | 5 | 5 |
| Tl | <0.1 | <0.1 | <1 | <1 | 10 | 3 |
| Pb | 20 | 3 | <0.4 | <0.4 | 200 | 200 |
| Bi | <0.06 | <0.06 | <0.06 | <0.06 | 3 | 1 |

## Table 4

## SPARK SOURCE MASS SPECTROGRAPHIC ANALYSIS OF BOILER PARTICULATE EMISSION AFTER SCRUBBING (Total Micrograms/filter)

Sample Designation

| Element | 7 SI* | 7 SO | 9 SI* | 9 SO | 10 SI | 10 SO | 11 SI | 11 SO | 12 SI* | 12 SO | 14 SI* | 14 SO |
|---|---|---|---|---|---|---|---|---|---|---|---|---|
| Li (a) | | | | | | | | | | | | |
| Be | 1 | 1 | 1 | 1 | 0.5 | 0.5 | 0.1 | 0.1 | 1 | 1 | 1 | 2 |
| B (a) | | | | | | | | | | | | |
| F | 500 | 500 | 500 | 500 | 300 | 300 | 200 | 500 | 200 | 200 | 200 | 200 |
| Na (b) | | | | | | | | | | | | |
| Mg (b) | | | | | | | | | | | | |
| Al (b) | | | | | | | | | | | | |
| Si (b) | | | | | | | | | | | | |
| P | 300 | 300 | 300 | 300 | 50 | 100 | 50 | 50 | High | High | High | High |
| S (c) | 1000 | 2000 | 2000 | 500 | 1000 | High | 1500 | 3000 | 2000 | High | 100 | 1000 |
| Cl (a) | | | | | | | | | | | | |
| K (b) | | | | | | | | | | | | |
| Ca (b) | | | | | | | | | | | | |
| Sc | 10 | 10 | 10 | 10 | <1 | <1 | <0.4 | <0.4 | 10 | <1 | 5 | 2 |
| Ti | 500 | 500 | 300 | 500 | 50 | 50 | <30 | <30 | 300 | 500 | 300 | 500 |
| V | 10 | 10 | 30 | 30 | 4 | 4 | 1 | 1 | 10 | 150 | 10 | 20 |

## Table 4 (Cont'd)

| Element | 7 SI* | 7 SO | 9 SI* | 9 SO | 10 SI | 10 SO | 11 SI | 11 SO | 12 SI* | 12 SO | 14 SI* | 14 SO |
|---|---|---|---|---|---|---|---|---|---|---|---|---|
| Cr | 20 | 20 | 20 | 20 | 50 | 50 | 10 | 20 | 20 | 20 | 10 | 20 |
| Mn | 200 | 50 | 300 | 300 | 10 | 10 | 10 | 10 | 200 | 100 | 50 | 20 |
| Fe | (b) | (b) | (b) | (b) | (b) | 1000 | 300 | (b) | (b) | (b) | (b) | (b) |
| Co | 5 | 5 | 5 | 5 | 5 | 5 | 1 | 1 | 2 | 5 | 2 | 1 |
| Ni | <5 | <5 | <5 | <5 | <30 | ≤30 | ≤10 | ≤10 | <5 | <5 | <5 | <5 |
| Cu | 20 | 20 | 50 | 50 | 10 | 50 | 5 | 15 | 20 | 50 | 20 | 20 |
| Zn | 30 | 100 | 100 | 200 | 20 | 50 | 40 | 20 | 10 | 200 | 10 | 100 |
| Ga (c) | 5 | 5 | 5 | 5 | 2 | 2 | 2 | 2 | <2 | 10 | 5 | 10 |
| As | 2 | 2 | 5 | 0.1 | 2 | <1 | 0.3 | 0.3 | 2 | 5 | 2 | 5 |
| Br | <0.4 | <0.4 | <0.4 | <0.4 | 2 | 2 | 0.2 | 0.1 | <0.4 | <0.4 | <0.4 | < 0.4 |
| Rb | 3 | 10 | 30 | 30 | 10 | 10 | 1 | 1 | 10 | 30 | 10 | 3 |
| Sr | 50 | 50 | 150 | 150 | 20 | 20 | 3 | 3 | 50 | 50 | 100 | 50 |
| Y | 2 | 2 | 5 | 5 | 0.3 | 0.3 | 0.1 | 0.03 | 5 | 1 | 5 | 1 |
| Zr | 2 | 2 | 5 | 5 | 1 | 1 | 1 | 0.5 | 2 | 0.5 | 10 | 2 |
| Nb | 0.1 | 0.2 | 0.3 | 1 | <0.1 | <0.1 | <0.03 | <0.03 | 0.2 | 0.3 | 0.2 | 0.2 |
| Mo | <1 | 2 | <1 | 2 | 2 | 2 | <0.4 | 1 | <1 | 5 | <1 | 1 |
| Ag | | | | | | | | | | | | |
| Cd (c) | <0.4 | <0.4 | <1 | <1 | 0.4 | 3 | ≤0.1 | 1 | <0.4 | 30 | <0.4 | <0.4 |
| Sn | 2 | 2 | 3 | 1 | 0.6 | 0.6 | 1 | 3 | 3 | 10 | ≤1 | ≤ 1 |
| Sb | 4 | 4 | 20 | 6 | 2 | 3 | 0.6 | 1 | 2 | 20 | 0.4 | 0.2 |
| Cs | <0.3 | 1 | 1 | 3 | 0.3 | 0.3 | <0.1 | <0.1 | 0.5 | 3 | 1 | 0.3 |
| Ba | 100 | 100 | 200 | 200 | 10 | 10 | 5 | 10 | 100 | 100 | 200 | 200 |

## Table 4 (Cont'd)

| Element | 7 SI* | 7 SO | 9 SI* | 9 SO | 10 SI | 10 SO | 11 SI | 11 SO | 12 SI* | 12 SO | 14 SI* | 14 SO |
|---|---|---|---|---|---|---|---|---|---|---|---|---|
| La | 2 | 2 | 3 | 3 | 0.1 | 0.04 | ≤0.03 | ≤ 0.03 | 1 | 0.2 | 3 | 0.3 |
| Ce | 5 | 5 | 10 | 10 | 0.2 | 0.1 | 0.1 | <0.1 | 3 | 0.5 | 10 | 0.5 |
| Tl (c) | <0.3 | 1 | <0.3 | 0.5 | 0.2 | 0.1 | <0.1 | <0.1 | <0.3 | 10 | <0.3 | 2 |
| Pb (c) | 30 | 30 | 100 | 100 | 200 | 200 | 2 | 20 | 10 | 400 | 3 | 20 |
| Bi | <0.2 | <0.2 | <0.2 | <0.2 | 0.1 | 0.1 | <0.1 | <0.1 | <0.2 | 1 | <0.2 | 0.2 |

# APPENDIX C

# EVALUATION OF THE PERFORMANCE OF MOBILE AIR POLLUTION CONTROL DEVICES

MIDWEST RESEARCH INSTITUTE

MRI REPORT

# EVALUATION OF THE PERFORMANCE OF MOBILE AIR POLLUTION CONTROL DEVICES

FINAL REPORT
August 21, 1979

MRI Project No. 4415-L

Prepared by

Midwest Research Institute
425 Volker Boulevard
Kansas City, Missouri 64110

For

PEDCo Environmental
11499 Chester Road
Cincinnati, Ohio 45246

MIDWEST RESEARCH INSTITUTE 425 VOLKER BOULEVARD, KANSAS CITY, MISSOURI 64110 • 816 753-7600

# EVALUATION OF THE PERFORMANCE OF MOBILE AIR POLLUTION CONTROL DEVICES

by

T. Sutikno

FINAL REPORT
August 21, 1979

MRI Project No. 4415-L

Prepared by

Midwest Research Institute
425 Volker Boulevard
Kansas City, Missouri 64110

For

PEDCo Environmental
11499 Chester Road
Cincinnati, Ohio 45246

## PREFACE

This special interim report was prepared to explain the performance of mobile air pollution control devices by simulation of field data with selected theoretical performance models.

This report was written by Mr. T. Sutikno. Questions concerning the technical aspects of this report should be directed to Mr. Sutikno or to Dr. K. P. Ananth.

Approved for:

MIDWEST RESEARCH INSTITUTE

for L. J. Shannon, Executive Director
Environmental and Materials
Sciences Division

August 21, 1979

# SUMMARY

This report presents theoretical verification and data analysis for performance data of a mobile venturi scrubber and a mobile electrostatic precipitator. The performance data of the mobile venturi scrubber indicate, in some cases with varying exhaust flow rate, high pressure drops collect particulates less efficiently than low pressure drops; this report also theoretically explains this relationship of $\Delta P$ with the collection efficiency ($\eta$).

Evaluation of three selected equations for estimation of $\Delta P$ are conducted to examine the validity of each. A theoretical equation developed by Yung et al. is shown to give the best agreement between calculated $\Delta P$ and measured $\Delta P$. Simulations of $\eta$s at various operating conditions are made with Yung's model to investigate the effect of residence time ($\tau$) on $\eta$. It is shown that a longer residence time, which is caused by a decrease in $\Delta P$ or by a slower gas throat velocity, compensates the expected reduction of $\eta$ due to the decrease in $\Delta P$. This compensation of $\eta$ is more significant for collection of large particles ($> 1\ \mu m$) than of small particles ($< 1\ \mu m$). The relationship of $\eta$ and $\Delta P$ in the measured performance data of the mobile venturi scrubber is due to longer residence time and due to the fluctuation in the inlet particle size distribution.

Regression analysis electrostatic precipitator performance data points using a modified Deutsch equation gives a correlation coefficient of 0.8102. Effect of RDF burning on the performance of the electrostatic precipitator cannot statistically be analyzed due to the limited number of data points; however, comparison of computed migration velocity ($\omega$) from each individual data point in coal burning operation and in coal and RDF burning operation indicates no significant difference in the performance of the electrostatic precipitator in these two operations.

# CONTENTS

Summary . . . . . . . . . . . . . . . . . . . . . . . . . . . . iii

1. Introduction . . . . . . . . . . . . . . . . . . . . . . . . 1
2. Mobile Venturi Scrubber. . . . . . . . . . . . . . . . . . . 5
    - Model selection . . . . . . . . . . . . . . . . . . . 5
    - Simulations . . . . . . . . . . . . . . . . . . . . . 6
3. Mobile Electrostatic Precipitator. . . . . . . . . . . . . . 17
    - Regression analysis . . . . . . . . . . . . . . . . . 20
    - Comparison of migration velocities. . . . . . . . . . 23
4. Conclusion . . . . . . . . . . . . . . . . . . . . . . . . . 24
    - Scrubber. . . . . . . . . . . . . . . . . . . . . . . 24
    - ESP . . . . . . . . . . . . . . . . . . . . . . . . . 24

References. . . . . . . . . . . . . . . . . . . . . . . . . . . 25

Appendices

A. Sample calculation of $\Delta P$ . . . . . . . . . . . . . . . . . 26
B. Sample calculation of collection efficiency. . . . . . . . 31
C. Analysis of ESP performance data . . . . . . . . . . . . . 35

Glossary. . . . . . . . . . . . . . . . . . . . . . . . . . . . 38

# SECTION 1

# INTRODUCTION

The objective of this report is to theoretically verify the performance data of a mobile venturi scrubber and a mobile electrostatic precipitator. The performance data of both mobile control devices are summarized in Table 1 and Table 2, and theoretical verification of performance is based on these data. The verification was conducted by simulations with selected theoretical or mathematical models. Selection of theoretical or mathematical models for each control device is discussed in detail in the following sections.

As shown in Figure 1 (plotted from Table 1), the particulate collection efficiency ($\eta$) of the mobile venturi scrubber is not significantly affected by the change in pressure drop across the venturi throat ($\Delta P$). According to Semrau Power Law, high pressure drops should collect particulate more efficiently than low pressure drops if other pertinent operating parameters (e.g., liquid flow rate/gas flow rate ratio) remain constant. However, Figure 1 indicates that, in some cases, higher $\eta$ can be obtained with lower $\Delta P$ (see * in Figure 1); it is also the purpose of this report to theoretically explain this relationship of $\eta$ and $\Delta P$ in the performance data of the mobile venturi scrubber. The following two sections will analyze the performance data of the mobile venturi scrubber and the mobile electrostatic precipitator.

## TABLE 1. MOBILE SCRUBBER EMISSION CONCENTRATION
(mg/dscm)

| | Primary | | | | | | | Secondary | | | |
|---|---|---|---|---|---|---|---|---|---|---|---|
| Power generation, mw/hr | 30.4 | 28.3 | 32.5 | 33.0 | 31.0 | 22.0 | 22.0 | 35.0 | 35.0 | 22.0 | 22.0 |
| ΔP cm., W.G. | 76.2 | 25.4 | 25.4 | 76.2 | 76.2 | 76.2 | 50.8 | 76.2 | 76.2 | 76.2 | 25.4 |
| Gas flow rate, $m^3/hr$ | 863.7 | 455.3 | 485.3 | 852.9 | 852.9 | 835.9 | 720.4 | 920.9 | 781.5 | 835.9 | 487.6 |
| S.l.[a] flow rate, l pm | 28.3 | 15.1 | 16.0 | 30.2 | 16.0 | 29.2 | 23.6 | 30.5 | 29.3 | 29.3 | 16.6 |
| Fuel | Coal | Coal | RDF[b] | RDF[b] | RDF[b] | RDF[b] | RDF[b] | RDF[b] | RDF[b] | RDF[b] | RDF[b] |
| Run No. | 15,16,17 | 13,14 | 7,8 | 5 | 6 | 9 | 12 | 3,4 | 1,2 | 10 | 11 |
| Total particulate | | | | | | | | | | | |
| (in)[c] | 12,210 | 12,770 | 18,130 | 9,945 | - | 11,610 | 18,520 | 396.0 | 423.9 | 107.9 | 103.9 |
| (out) | 106.0 | 92.26 | 89.88 | 51.54 | 49.21 | 56.09 | 54.20 | 12.62 | 24.19 | 25.92 | 28.23 |
| Efficiency, % | 99.1 | 99.3 | 99.5 | 99.5 | - | 99.5 | 99.7 | 96.8 | 94.3 | 78.0 | 72.8 |

[a] Scrubber liquor.

[b] RDF was co-fired with coal and ranged from 13 to 25%.

[c] Front half only.

## TABLE 2. MOBILE ESP EMISSION CONCENTRATION
(mg/dscm)

| | Primary | | | | | | | |
|---|---|---|---|---|---|---|---|---|
| Power generation, mw/hr | 35.0 | 34.8 | 33.0 | 21.6 | 20.6 | 18.6 | 33.5 | 22.0 |
| SCA | 16.4 | 27.34 | 7.33 | 16.4 | 21.87 | 10.9 | 16.4 | 16.4 |
| No. fields | 5 | 5 | 4 | 5 | 5 | 3 | 5 | 5 |
| Fuel | Coal | Coal | Coal | Coal | Coal | Coal | RDF[a] | RDF[a] |
| Run No. | 21,22,23 | 20 | 1 | 5,6 | 7,8,9 | 24,25 | 2,26,27,28 | 3,4 |
| Gas flow rate, $m^3$/hr | 2,718.7 | 1,631.2 | 4,876.7 | 2,718.7 | 2,039.0 | 2,446.8 | 2,718.7 | 2,718.7 |
| Total particulate | | | | | | | | |
| (in)[b] | 3,119.0 | 3,990.5 | 3,235.0 | 2,743.0 | 2,003.5 | 3,172.0 | 3,697.0 | 2,701.0 |
| (out) | 46.23 | 29.80 | 64.60 | 36.13 | 28.5 | 194.3 | 83.80 | 95.70 |
| Efficiency, % | 98.5 | 99.2 | 98.0 | 98.7 | 98.7 | 93.9 | 97.7 | 96.5 |

[a] RDF was co-fired with coal and ranged from 13 to 25%.

[b] Front half only.

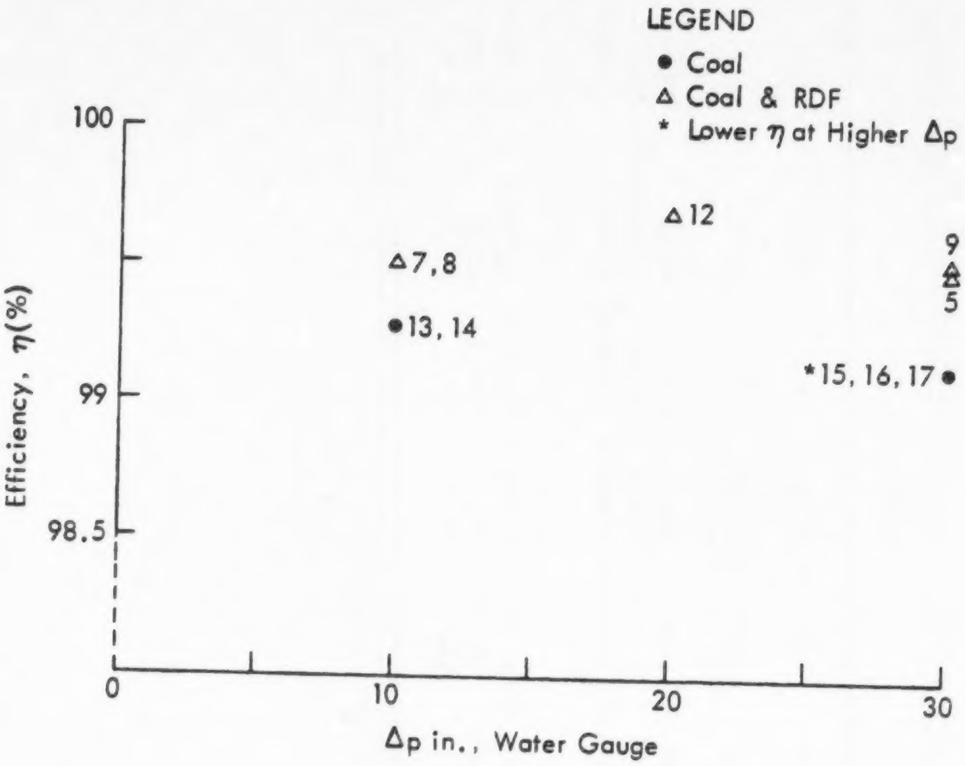

Figure 1. Efficiency of venturi scrubber (primary) as a function of pressure drop.

# SECTION 2

# MOBILE VENTURI SCRUBBER

To accomplish the objective of theoretically verifying the performance data of the mobile venturi scrubber, the following tasks have been performed.

1. Selection of an appropriate performance model for theoretical estimation of $\eta$ and $\Delta P$.

2. Simulation of the measured performance data with the selected performance model.

The methodology of each task is discussed as follows:

## MODEL SELECTION

Selection of an appropriate performance model for venturi scrubber is based on the availability of the measured operating parameters, agreement between the calculated results and measured data, and the ability of the model to identify the effect of each measured operating parameter on the estimation of $\eta$.

To examine the effect of each operating parameter available in Table 1 on estimations of $\Delta P$ and $\eta$, only those performance models that are able to simulate the effect of each available operating parameter on estimations of $\Delta P$ and $\eta$ are considered; hence, any model that requires an unknown empirical constant which is dependent upon the operating conditions is excluded. However, because of the following factors: (a) some of the data in Table 1 represent average value from several measurements; (b) other analytically necessary operating data (e.g., velocity and pressure profiles in the axial direction of the venturi throat) are not measured; and (c) physical properties of the fluids in the venturi have to be estimated; the use of a highly analytical performance model cannot be justified.

Therefore the selected model should contain the appropriate parameters to analyze the effect of each available operating parameter on the estimations of $\Delta P$ and $\eta$, and the model can only be an approximate one rather than an analytical one.

## SIMULATIONS

Based on the above considerations, three equations are selected for theoretical estimations of $\Delta P$ across the venturi throat. Theoretical estimation of $\Delta P$ by the selected equation are conducted first, for $\Delta P$ data in Table 1 have larger deviations compared to relatively constant $\eta$; agreement between the measured $\Delta P$ and calculated $\Delta P$ by each selected equation can be assessed to select the best descriptive equation and to determine if all theoretical assumptions made in the derivation of each model are reasonable. Once such an equation has been selected, it is used to theoretically predict $\eta$ and investigate the relationship between $\eta$ and $\Delta P$ as shown in Figure 1. Three equations to estimate $\Delta P$ are selected and listed below.

Calvert's equation[1]

$$\Delta P = 1.03(10^{-3})(U_G)^2 \frac{Q_L}{Q_G} \qquad \text{Equation 1}$$

where:

$U_G$ = gas linear velocity (cm/sec)
$Q_L$ = liquid volumetric flow rate (cm$^3$/sec)
$Q_G$ = gas volumetric flow rate (cm$^3$/sec)

Hesketh's equation[2]

$$\Delta P = \frac{U_G{}^2 \rho_G A^{0.133}}{507} \left[0.56 + 0.125L' + 2.3(10^{-3})L'^2\right] \qquad \text{Equation 2}$$

where:

$A$ = throat cross-sectional area (ft$^2$)
$\rho_G$ = gas density (lb/ft$^3$)
$L' = Q_L/Q_G$, gal/1,000 ft$^3$

Yung's equation[3]

$$\Delta P = \frac{-2\rho_L\ U_G^2}{g_c} \frac{Q_L}{Q_G} \left[1-x^2 + \sqrt{x^4 - x^2}\right] \qquad \text{Equation 3}$$

where:

$\rho_L$ = liquid density (8/cm$^3$)
g = conversion factor

$$x = \frac{3\ l_t C_{D1}\ \rho_G}{16\ d_d \rho_L} + 1$$

and: $l_t$ = throat length (cm)
$C_{D1}$ = drag coefficient at throat entrance (dimensionless)
$d_d$ = drop diameter (cm)

Sample calculations using the operating data in Table are described below.

Operating data: run Nos. 13, 14

$Q_L$ (scrubber liquid flow rate) = 15.1 liter/min
$Q_G$ (gas flow rate) = 455.3 m$^3$/hr
$\Delta P$ (pressure drops across venturi throat) = 25.4 cm WG
Throat diameter = 2.3 in.
Cross-sectional area = A = 28.7 cm$^2$
Gas velocity in the venturi throat = $U_G \cong \frac{Q_G}{A}$ = 4,406.7 cm/sec

Based on the above data, the calculated $\Delta P$ from the three equations are (details of calculation are given in Appendix A):

Measured $\Delta P$ = 25.4 cm WG
Calvert's equation: $\Delta P$ = 39.8 cm WG
Hesketh's equation: $\Delta P$ = 12.8 cm WG
Yung's equation: $\Delta P$ = 27.0 cm WG

Hence, Yung's equation gives the best agreement between the measured $\Delta P$ and calculated $\Delta P$. To verify the validity of Equation 3 at various operating conditions, further calculations are made, and the results are summarized as follows (see Appendix A for detailed calculations).

Operating data: Run Nos. 15, 16, 17

$Q_L$ = 28.3 liter/min
$Q_G$ = 863.7 m$^3$/hr
Measured $\Delta P$ = 76.4 cm WG
Calvert's equation: $\Delta P$ = 141.5 cm
Hesketh's equation: $\Delta P$ = 45.34 cm
Yung's equation: $\Delta P$ = 103 cm

Operating data: Run No. 12

$Q_L$ = 23.6 liter/min
$Q_G$ = 720.4 $m^3$/hr
Measured $\Delta P$ = 50.8 cm WG
Calvert's equation: $\Delta P$ = 98.4 cm WG
Hesketh's equation: $\Delta P$ = 31.0 cm WG
Yung's equation: $\Delta P$ = 70.9 cm WG

Note:

| $U_G$ (cm/sec) | Calculated $\Delta P$ (cm WG) by Equation 3 | Measured $\Delta P$ (cm WG) | Difference in $\Delta P$ |
|---|---|---|---|
| 4,407 | 27.0 | 25.4 | 1.6 |
| 8,259 | 103.0 | 76.2 | 26.8 |
| 6,973 | 70.9 | 50.8 | 20.1 |

To analyze the deviation of calculated $\Delta P$ from the measured $\Delta P$, the derivation of each equation is discussed. The derivation of Equation 1 is based on the assumption that all energy is used to accelerate the liquid droplets to throat velocity of the gas and that none of the drop momentum was converted to pressure in the diffuser. Yung et al. suggest that, in industrial venturi scrubbers, due to insufficient residence time during which liquid droplets accelerate to the gas throat velocity, Equation 1 predicts a higher $\Delta P$ than measured $\Delta P$; calculation result of Equation 1 indicates the validity of Yung's suggestion. Hesketh's equation (Equation 2), on the other hand, is an empirically-derived equation based on evaluation of experimental data obtained from many fixed throat venturi scrubbers. The accuracy of Equation 2 is dependent upon the operating condition, for all the empirical constants in Equation 2 are obtained from several specific ranges of operating conditions. As shown in the calculation results, Equation 2 gives better agreement between calculated and measured pressure drops at high gas throat velocities than at low throat velocities (see run Nos. 13, 14, and 15, 16, 17). However, Equation 2 was not further developed theoretically to predict the collection efficiency, but only a statistically derived equation relating collection efficiency with $\Delta P$ was developed; effect of particle size ($d_p$), particle density ($\rho_p$), and $\tau$ on $\eta$ cannot be simulated by the Hesketh's model. Due to that the dependency of $\eta$ on these parameters cannot be neglected, Hesketh's equation is not suitable for the simulation of the measured performance data. Alternately, even though Equation 3 overestimates $\Delta P$ more at high gas throat velocities than low gas throat velocities as shown in the above calculation, it can be observed that Equation 3 gives better agreement between calculated and measured pressure drops despite uncertainties in the estimated physical constants and the average temperature used in the calculations. It is concluded that Equation 3 describes fairly well the momentum transport of the fluids in the venturi throat, and all the assumptions made in the derivation of Equation 3 are, for practical purposes, reasonable. Assumptions made in the derivation of Equation 3 are as follows:

1. Pressure loss due to wall friction and pressure recovery by the gas in the divergent section are both neglected. (Note: The author suggested that this assumption causes overestimation of $\Delta P$ at high liquid flow rates and underestimation of $\Delta P$ at low liquid flow rates.)
2. Liquid is introduced at throat entrance with no axial velocity.
3. Liquid is atomized at injection point and is uniform in size with Sauter mean diameter as calculated in Appendix A.
4. The flow is one-dimensional, incompressible, and adiabatic.
5. Liquid fraction at cross-section is small.

With additional assumptions for the mechanism of particle collection in the venturi throat, Equation 3 was further developed by Yung et al. to Equation 4 to estimate the collection efficiency $\eta$.[4]

$$\begin{aligned}\ln Pt = \frac{B}{K_{p1}(1-U^*_{d1}) + 0.7} & \left\{ 4K_{p1}(1-U^*_{d1})^{1.5} + 4.2(1-U^*_{d1})^{0.5} - 5.02K_{p1}^{0.5} \right. \\ & \left. (1-U^*_{d1} + \frac{0.7}{K_{p1}}) \tan^{-1}\left(\frac{(1-U^*_{d1})K_{p1}}{0.7}\right)^{0.5} \right\} - \frac{B}{K_{p1} + 0.7} \left\{ 4K_{p1} + \right. \\ & \left. 4.2 - 5.02K_{p1}^{0.5}(1 + \frac{0.7}{K_{p1}}) \tan^{-1}(\frac{K_{p1}}{0.7})^{0.5} \right\} \qquad \text{Equation 4}\end{aligned}$$

where:

$$B = \frac{Q_L \rho_L}{Q_G \rho_G C_{D1}}$$

$C_{D1}$ = drag coefficient at the injection point

$$U^*_{d1} = 2[1 - x^2 + (x^4 - x^2)^{0.5}]$$

$$K_{p1} = \frac{C' \rho_p d_p^2 / U_{p1} - U_{d1} /}{9 \mu_G d_d}$$

$C'$ = Cunningham's correction factor (dimensionless)
$\rho_p$ = particle density (g/cm )
$d_p$ = particle diameter (cm)
$U_{p1}$ = particle velocity at injection point (cm/sec)
$U_{d1}$ = drop velocity at injection point (cm/sec)
$\mu_G$ = gas viscosity (g/cm sec)
$Pt = \frac{C_o}{C_i}$
$C_o$ = outlet concentration
$C_i$ = inlet concentration

The additional assumptions are listed below:

6. Particles are collected only by atomized liquid drops. The drop diameter is the Sauter mean diameter calculated in Appendix A.

7. Liquid drops are uniformly spread across the duct, and the drop diameter is invariant with axial distance.

8. Drag coefficient is governed by the following relationship as suggested by Equation 5.

$$C_{D1} = 0.22 + \frac{24}{N_{Re1}} (1 + 0.15 \, N_{Re1}^{\,0.6}) \qquad \text{Equation 5}$$

where:

$$N_{Re1} = \frac{d_d U_G \rho_G}{\mu_G}$$

9. Particle collection in primarily due to inertial impaction.

10. Particles are flowing at the same velocity as the gas.

11. The only force acting on the drops is the drag due to the relative motion of the gas and the drops.

Since none of the assumptions made in the derivation of Equation 3 (assumptions 1 through 6) is changed or violated by the additional assumptions, Equation 4 is selected to estimate the collection efficiency $\eta$ and to mathematically examine the irresponsive change of $\eta$ due to change in $\Delta P$. It is difficult, if not impossible, to justify the validity of each assumption made in Equation 4 without elaborate experimental study. However, accuracy of Equation 4 in estimating $\eta$ can be used as the basis to approximately verify the validity of each assumption. A sample calculation using an assumed mean particle diameter is given in Appendix B. Calculation results are shown on the following page:

Operating condition = run Nos. 15, 16, 17

assuming $d_p = 10\ \mu m$,
$\eta = 99.84\%$

Reported $\eta$ at 50% cutoff particulate diameter of > 10 $\mu m$ is 99.132%. Hence, agreement between the calculated $\eta$ and measured $\eta$ is reasonably good, and Equation 4 adequately describes the particles collection mechanism of the mobile venturi scrubber.

Equation 4 is used to investigate the effect of larger $\tau$ on the collection efficiency. Yung et al. has concluded that, under a specific condition, the performance of a venturi scrubber depends on the throat length as revealed by Figure 2. The longer the throat, the more efficient the scrubber. This dependence is more profound for large particles. However, sample calculations using the operating data in Table 1 are necessary to verify the enhancement of $\eta$ because of larger $\tau$, since the increase of $\tau$ in Table 1 is not caused by a longer throat length but by a lower gas flow rate. In other words, the larger $\tau$ in Table 1 is caused by lower $\Delta P$ while Yung's conclusion on the effect of $\tau$ on $\eta$ is based on the direct proportionality between $\tau$ and $\Delta P$. To clarify which factor ($\Delta P$ or $\tau$) predominantly affects $\eta$, sample calculations are made in Appendix B, and the results are summarized in Figure 3 in terms of $\Delta P$ and $\eta$.

It can be observed that $\partial\eta/\partial(\Delta P)$ is smaller with particle diameter of 10 $\mu m$ than with particle diameter of 1 $\mu m$. Mathematically,

$$\left.\frac{\partial\eta}{\partial\Delta P}\right|_{d_p = 10\ \mu m} < < \left.\frac{\partial\eta}{\partial\Delta P}\right|_{d_p = 1\ \mu m}, \text{ where } \left.\frac{\partial\eta}{\partial\Delta P}\right|_{d_p} > 0$$

$$\text{and } \left.\frac{\partial\frac{\partial\eta}{\partial\Delta P}}{\partial(d_p)}\right|_{d_p = 1 \text{ to } 10\ \mu m} < 0$$

Since low $\Delta P$ in this specific case (fixed throat length) was obtained by decreasing gas throat velocity, lower $\Delta P$ implies longer residence time. Therefore, for large particulate diameters (> 1 $\mu m$), the impairment of collection efficiency due to low $\Delta P$ is significantly compensated by the improvement of collection efficiency due to longer residence time, and this compensation is less significant for small particle sizes. It has been reported that 50% cutoff diameter of the inlet particle in Table 1 is larger than 10 $\mu m$; hence, enhancement of $\eta$ due to large $\tau$ in the measured performance data (see Figure 1) can theoretically be justified. Furthermore, since fluctuation in the particle size distribution of the inlet particulates is usually significant in actual

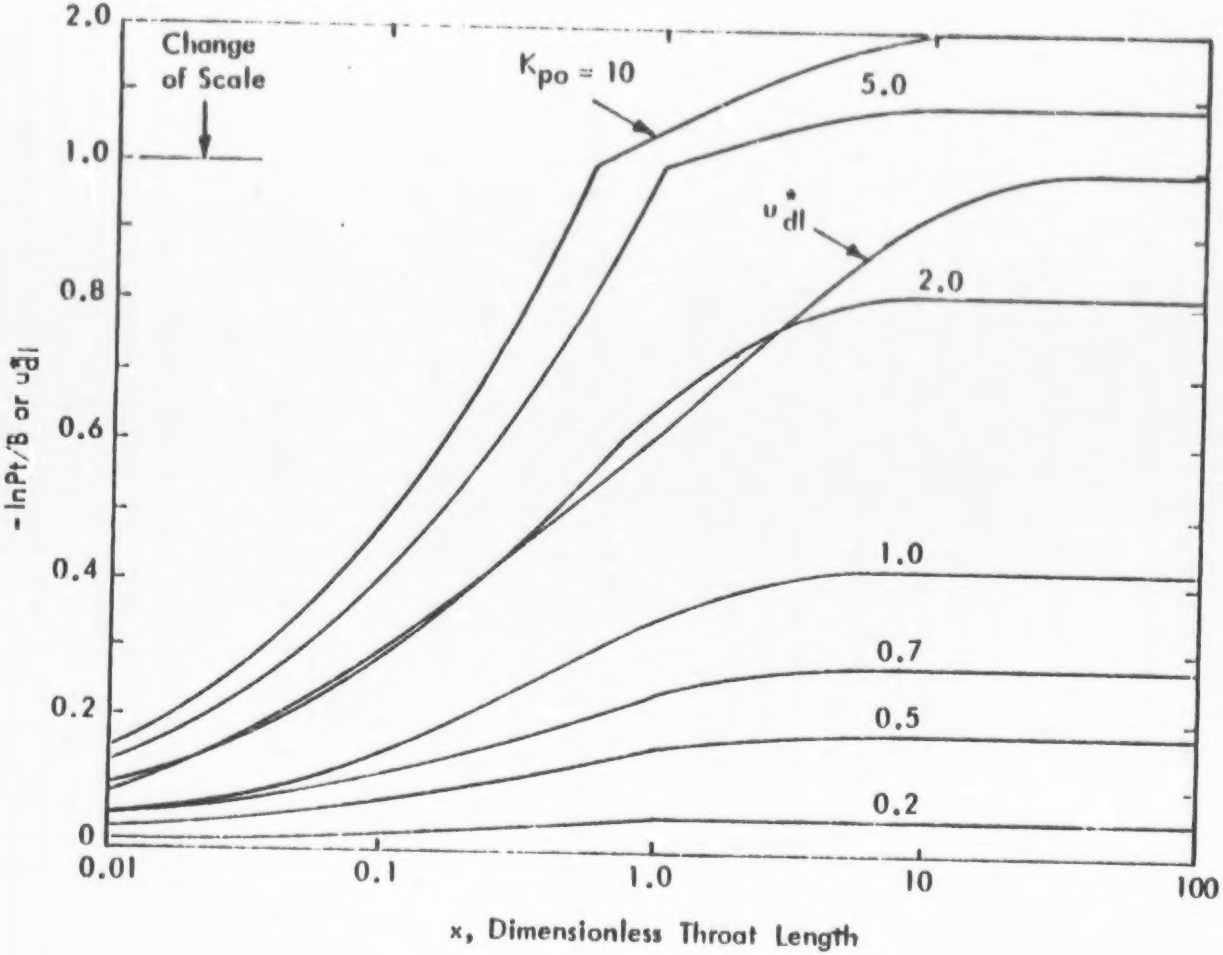

Figure 2. Theoretical Particle Penetration and Drop Velocity as a Function of Dimensionless Throat Length

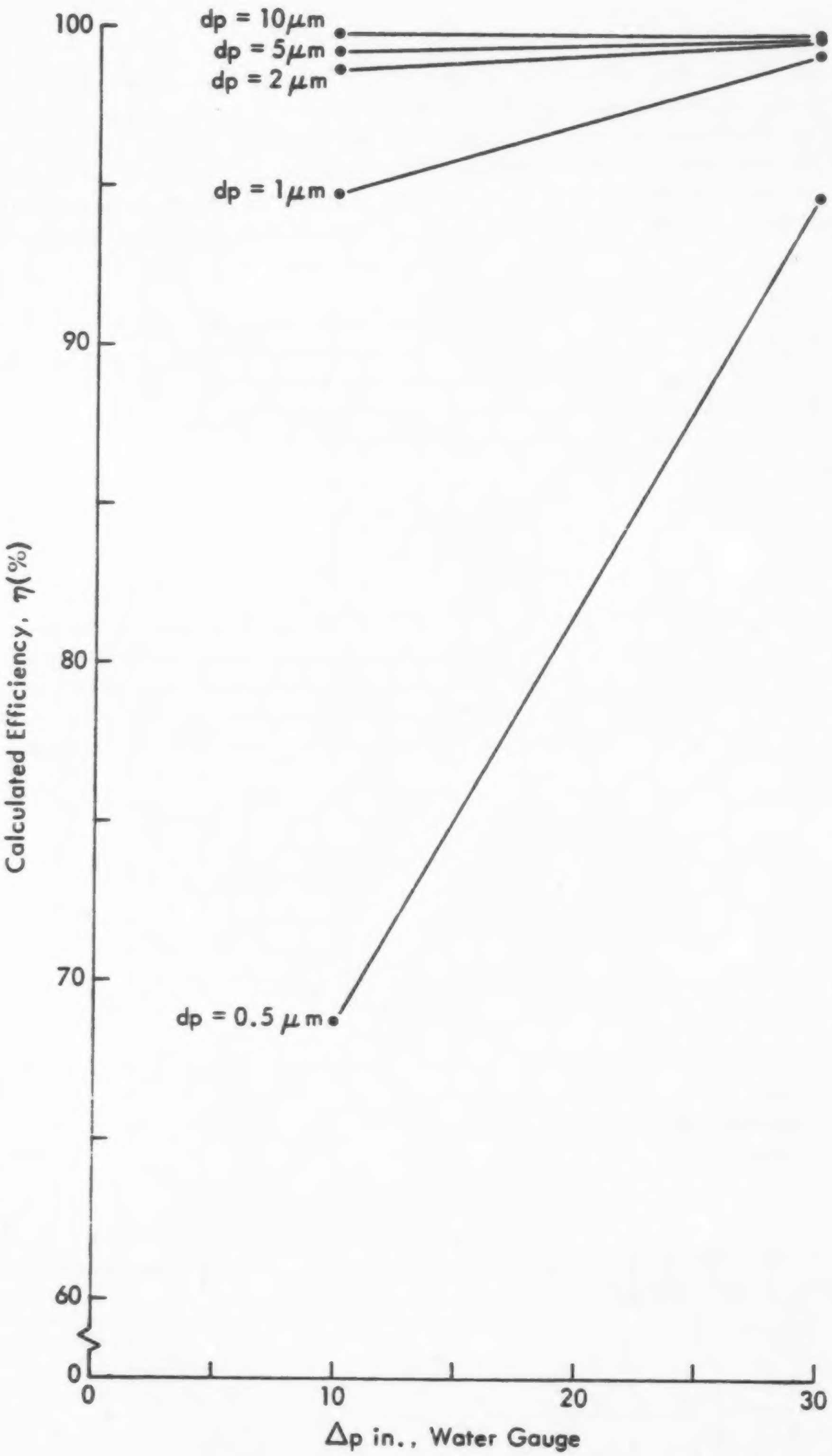

Figure 3. Calculated efficiency at various particle diameters as a function of pressure drop.

operating conditions, and since the effects of $\tau$ and $\Delta P$ on $\eta$ are very susceptible to particle diameter, the paradoxical trend of $\eta$ with respect to $\Delta P$ in Figure 1 is likely caused by the $\tau$ effect and by the variation in inlet particle size distributions. Specifically, data points in Figure 1 which indicate lower $\eta$ at $\Delta P = 30$ than at $\Delta P = 20$ or 10, are due to the higher percentage of smaller particles ($< 1\ \mu m$) and due to large $\tau$ caused by the decrease in $\Delta P$ itself.

Figure 1 also indicates than $\eta$ is higher with coal and RDF burning than with coal burning only. This can perhaps be explained by the inertial impaction parameter ($K_p$); high $K_p$s improve $\eta$. If fly ashes from the burning of RDF are assumed to have larger diameters ($d_p$) and smaller density ($\rho_p$) than the fly ashes of coal burning, then from the expression of

$$K_p = \left( \frac{C' \rho_p d_p^2 / U_p - U_d /}{9\ U_G\ d_d} \right),$$

improvement of the impaction (increase in the value of $K_p$) due to larger $d_p$ is, in a specific range of $d_p$ and $\rho_p$, more significant than impairment of impaction (decrease in the value of $K_p$) due to smaller $\rho_p$ for $K_p$ varies with the first order function of $\rho_p$ and with second order function of $d_p$. The particle size diameter $d_p$, therefore, predominantly affects $K_p$ and thus $\eta$. Mathematically,

$$K_p = f( d_p^2 \rho_p )$$

$$\left. \frac{\partial K_p}{\partial d_p} \right|_{\rho_p} = f( 2\ d_p \rho_p )$$

$$\left. \frac{\partial K_p}{\partial \rho_p} \right|_{d_p} = f( d_p^2 )$$

Since $0 < d_p < 1$ cm (the unit of $d_p$ is in centimeter for the computation of $K_p$), and if $0 < \rho_p \leq 2.6\ g/cm^3$,

then
$$\left. \frac{\partial K_p}{\partial d_p} \right|_{\rho_p} > \left. \frac{\partial K_p}{\partial \rho_p} \right|_{d_p}$$

However, only particulate size analysis at ESP inlet (see Figure 4) suggests that fly ash from coal plus RDF burning is larger than fly ash from coal burning, and at the venturi scrubber inlet there is no significant difference in the diameters of fly ashes from coal and coal plus RDF burnings. Further investigations are necessary to verify the enhancement of venturi scrubber efficiency in removing fly ashes from coal plus RDF burning as indicated in Figure 1.

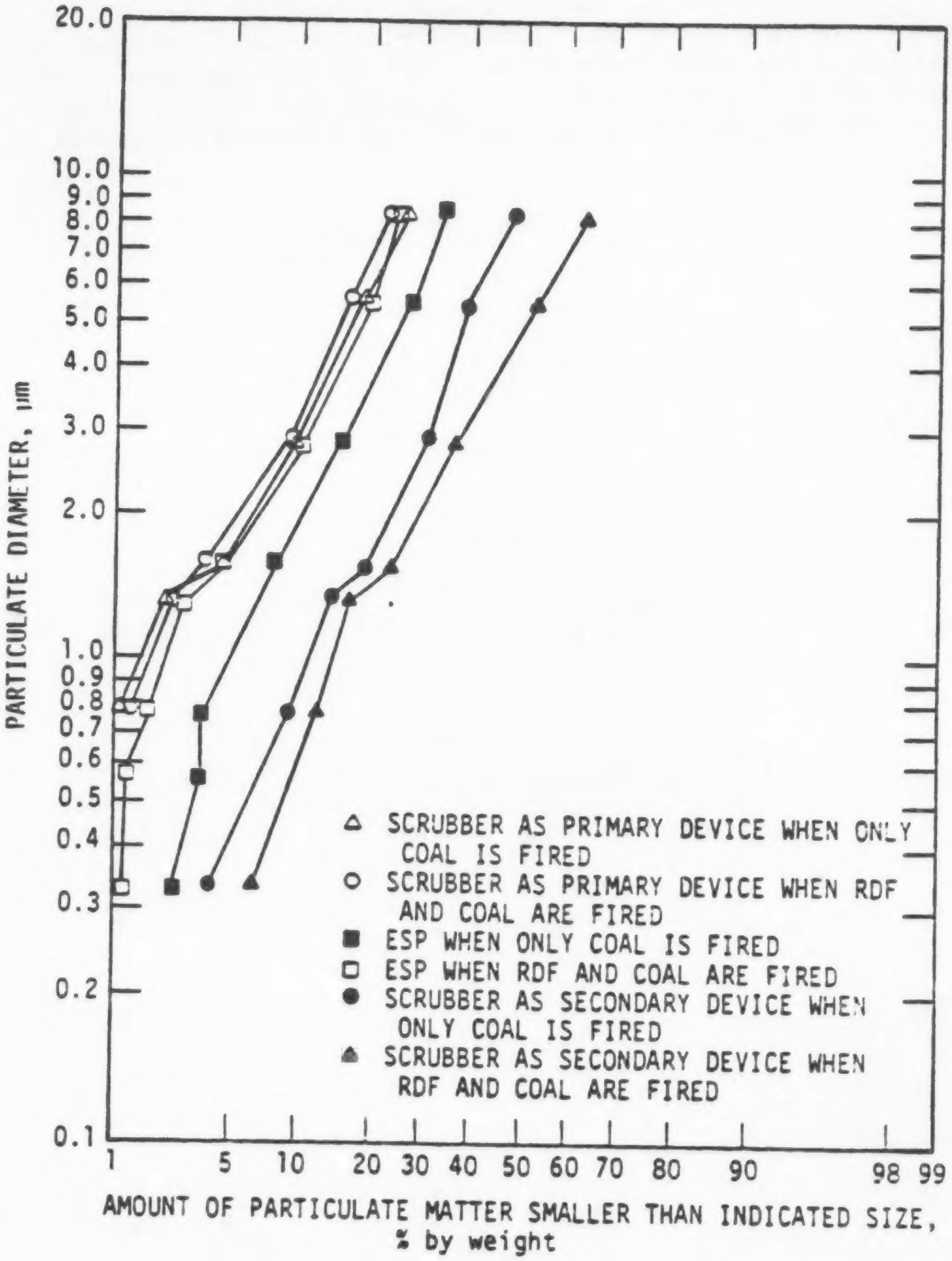

Figure 4. Particulate size distribution at control device inlets.

# SECTION 3

# MOBILE ELECTROSTATIC PRECIPITATOR

To theoretically verify the performance data of the mobile ESP, the conventional Deutsch equation (Equation 5) is used to simulate the measured performance data for no other descriptive theoretical ESP performance model has been found in literature.[8]

$$\eta = 1 - e^{-SCA\omega} \qquad \text{Equation 5}$$

where:

$SCA$ = specific collection area
$\omega$ = migration velocity

The Deutsch equation is not strictly a theoretical model but merely a mathematical model, for it contains a constant $\omega$ (the migration velocity) which is empirically determined by operating conditions. $\omega$ includes the effects of rapping losses, gas flow distribution, particle size distribution, and dust resistivity. Therefore, simulation of the ESP performance data with Equation 5 will only give a mathematical representation and cannot theoretically identify the effect of each pertinent parameter on $\eta$. To simulate the measured performance data of the ESP, the following data analyses are made.

The performance data in Table 2 are plotted in Figure 5. Data points obtained with number of electric fields in ESP less than 5 or with the use of coal and RDF as fuels are neglected in the analysis of the performance data. It is expected that the number of electric fields affects the collecting mechanism of the ESP; however, the effect of the number of electric fields on $\eta$ has already been represented by the effect of specific collection area (SCA) on $\eta$. Due to the limited performance data at different numbers of electric fields and at a constant gas flow rate, no statistical analysis is made, but Figure 6 presented to show the probable effect of the number of electric fields on $\eta$. It is desirable to analyze the effect of burning RDF on the performance of ESP; this can be done by comparing the migration velocities computed from performance cata with coal burning and with coal plus RDF burning. However, due to limited data obtained from the burning of coal plus RDF, a legitimate statistical or mathematical analysis cannot be made. Thus, $\omega$ will be computed by Equation 5 using two data points obtained from coal plus RDF burning. These computed $\omega$s will be compared with the $\omega$s calculated from the performance data of coal burning to assess the effect of the burning of RDF on the performance of ESP.

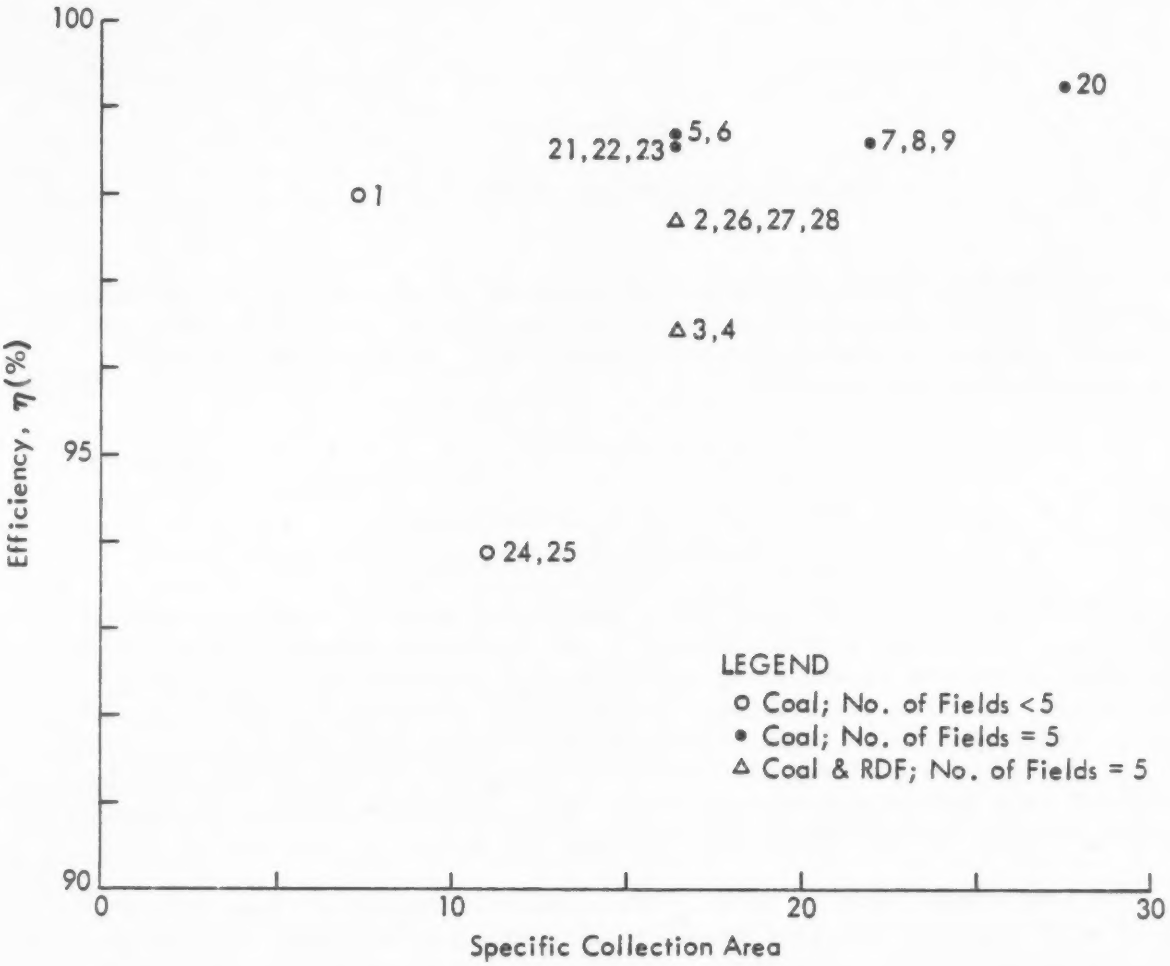

Figure 5. Efficiency of electrostatic precipitator as a function of specific collection area.

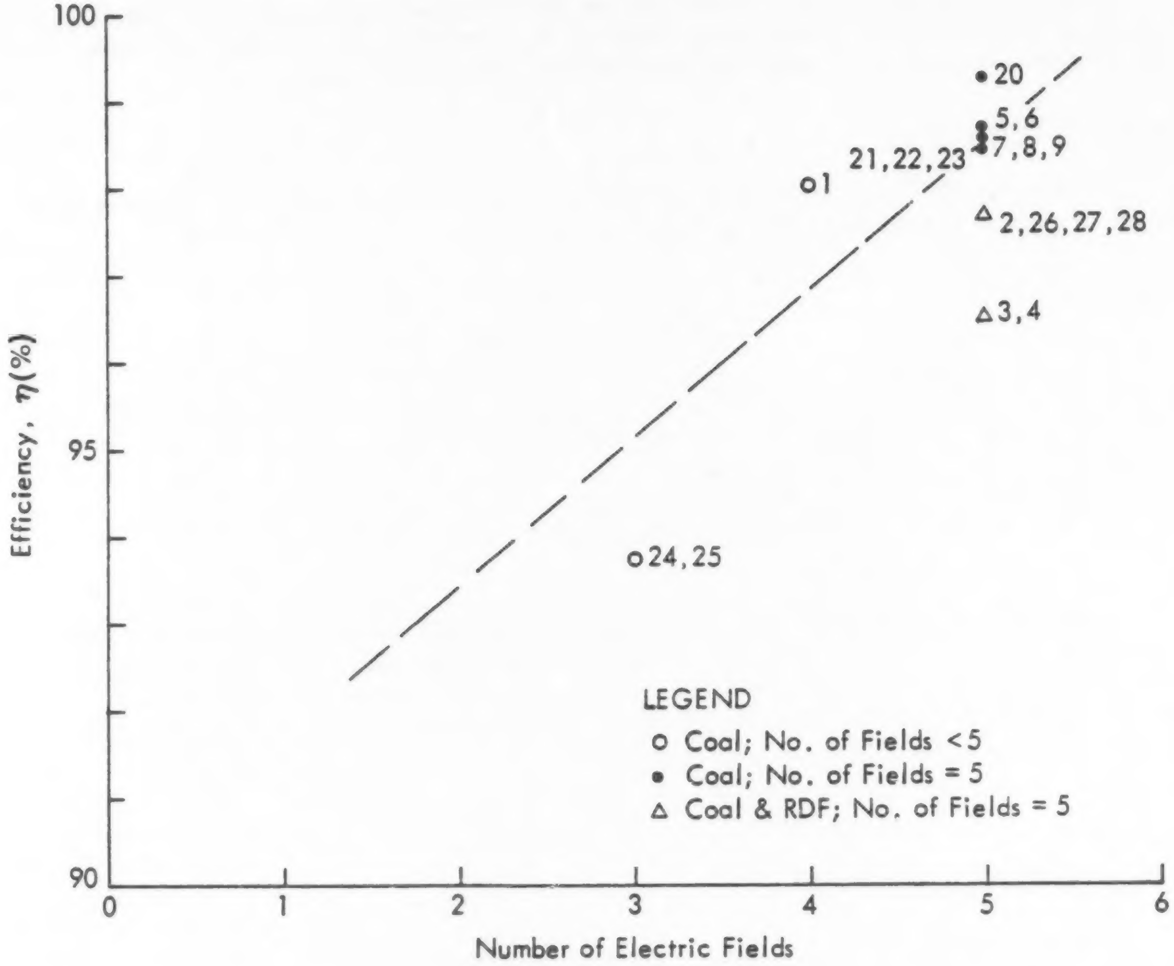

Figure 6. Efficiency of electrostatic precipitator as a function of number of electric fields.

Regression analysis of $\eta$ with SCA in coal burning operation and comparison of $\omega$ computed from performance data of coal burning and $\omega$ computed from performance data of coal plus RDF burning are presented below.

REGRESSION ANALYSIS

According to Equation 5, a plot of ln $(C_o/C_i)$ versus SCA $\left(= \frac{A}{Q_G}\right)$ (see Figure 7) should give a straight line. Mathematically,

$$\frac{C_i - C_o}{C_i} = 1 - e^{-SCA\omega}$$

$$\frac{C_o}{C_i} = e^{-SCA\omega}$$

$$\text{and,} \quad \ln\left(\frac{C_o}{C_i}\right) = -SCA\omega$$

Linear regression analysis of $\ln(C_o/C_i)$ with SCA gives a correlation coefficient of 0.8467 (data points with "o" and $\Delta$ are not included in this regression analysis) which indicates unsatisfactory linear relationship between $\ln(C_o/C_i)$ and SCA. Details of regression analysis are presented in Appendix C, and the regression line is represented by

$$\ln(C_o/C_i) = -3.3696 - 0.0513 \text{ SCA} \qquad \text{Equation 6}$$

and $\omega = 0.0513$ (length/time).

Theoretically, $\ln(C_o/C_i)$ should equal to zero at zero SCA. However, Eqaation 6 does not give zero $\ln(C_o/C_i)$ at zero SCA. To overcome this imperfection, the modified Deutsch equation [Equation 7 below (by Matt and Ohnfeld[5])] is used to simulate the performance data.

$$\eta = 1 - e^{-(SCA\omega_k)^k} \qquad \text{Equation 7}$$

$$\text{or,} \quad \ln[-\ln(C_o/C_i)] = k \ln\omega_k + k \ln \text{SCA} \qquad \text{Equation 8}$$

A plot of $\ln[-\ln(C_o/C_i)]$ versus ln SCA is presented in Figure 8. Regression analysis of $\ln[-\ln(C_o/C_i)]$ with ln SCA gives a correlation coefficient of 0.8102. The regression line is represented by:

$$\ln[-\ln(C_o/C_i)] = 0.8032 + 0.2274 \ln \text{SCA} \qquad \text{Equation 9}$$

$$\text{or,} \quad \eta = 1 - e^{-[34.19(SCA)]^{0.2274}} \qquad \text{Equation 10}$$

It can be observed that Equation 10 gives zero $\eta$ at zero SCA.

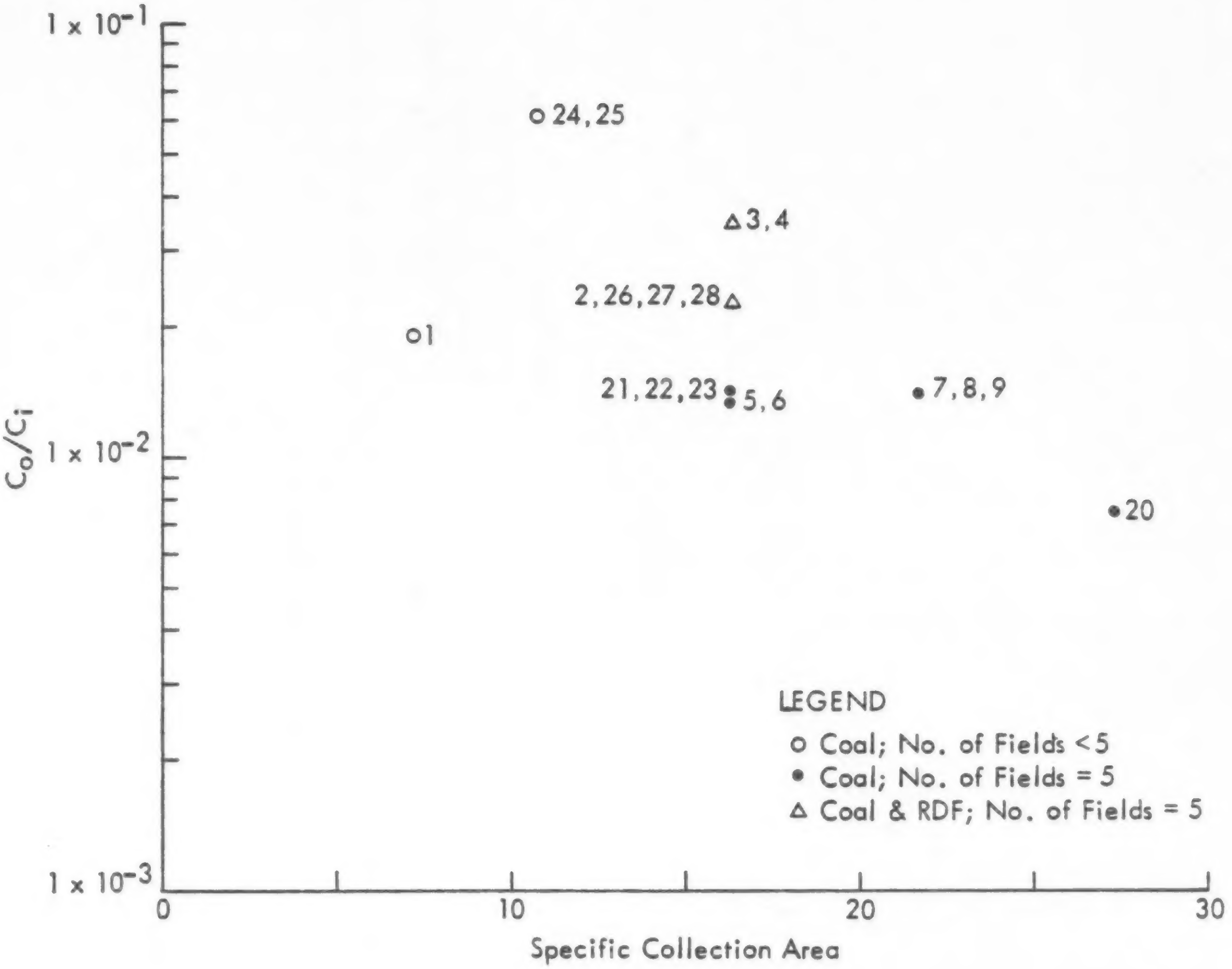

Figure 7. $\mathrm{Ln}\left(\frac{Co}{Ci}\right)$ versus specific collection area (SCA).

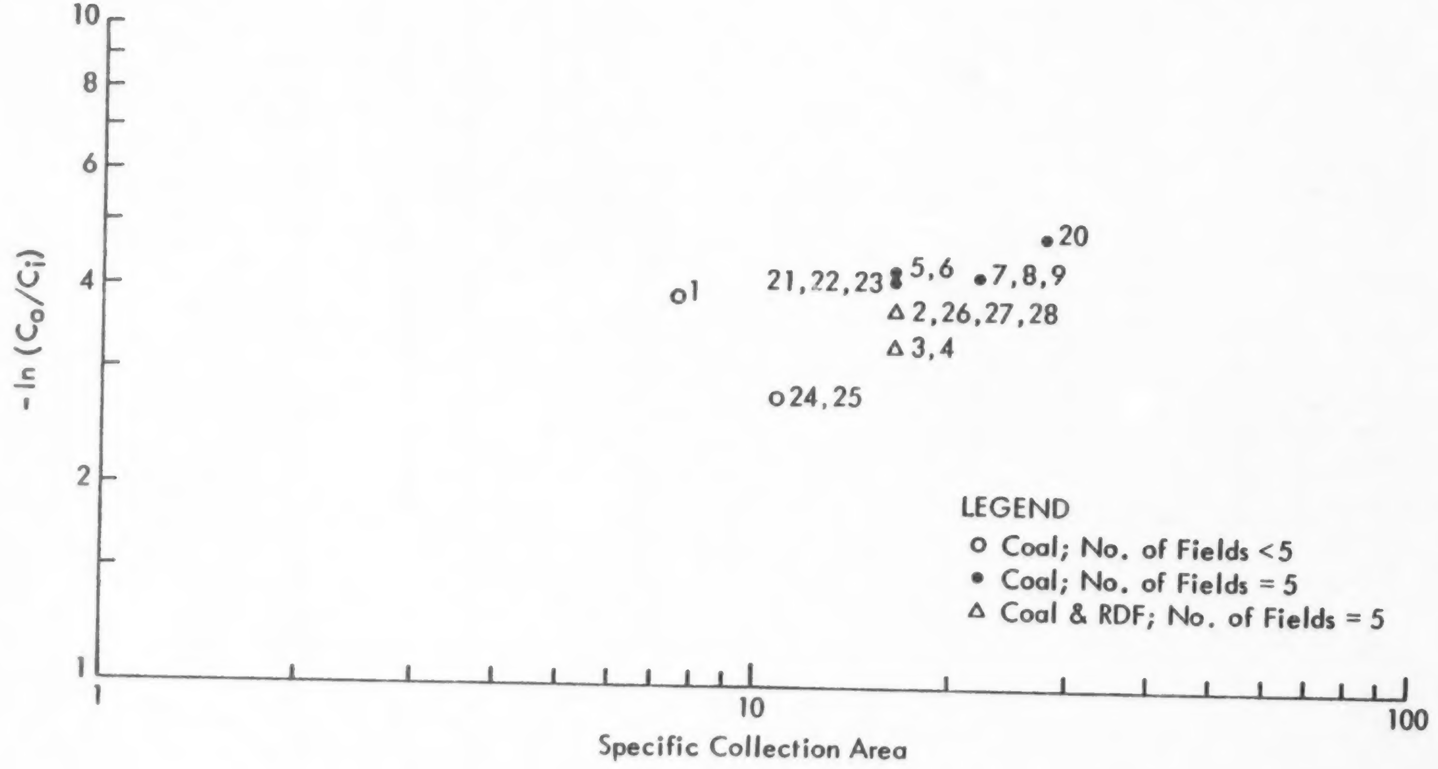

Figure 8. $\mathrm{Ln}\left[-\ln\left(\frac{Co}{Ci}\right)\right]$ as a function of ln SCA.

## COMPARISON OF MIGRATION VELOCITIES

Equation 5 is used to calculate $\omega$ from each individual data point. Since the purpose of this comparison of $\omega$s is to assess the effect of burning RDF on the performance of an ESP, data points obtained with number of electric fields less than five are excluded in this comparison, for data points of RDF burning were obtained with five electric fields. A sample calculation of $\omega$ is presented in Appendix C, and the computed $\omega$s are tabulated below:

| Run numbers | Fuels | |
|---|---|---|
| 21, 22, 23 | coal | 0.2569 |
| 20 | coal | 0.1794 |
| 5, 6 | coal | 0.2640 |
| 7, 8, 9 | coal | 0.1945 |
| 2, 26, 27, 28 | coal and RDF | 0.2309 |
| 3, 4 | coal and RDF | 0.2036 |

The range of $\omega$ computed from the performance data of coal burning is 0.1794 to 0.2332 with an average of 0.2237. Since the computed $\omega$s from the performance data of RDF burning fall within the range of $\omega$s computed from the performance data of coal burning, and since $\omega$ includes the effect of rapping losses, gas flow distribution, particle size distribution, and dust resistivity, there is no significant evidence of the effect of burning RDF on the performance of the ESP from this comparison of $\omega$. However, Figure 5 suggests $\eta$ with burning RDF is lower than $\eta$ with burning only coal, both at an SCA of 16.4. Further samplings with RDF burning at different values of SCA should be taken.

# SECTION 4

# CONCLUSION

## SCRUBBER

A mathematical model of venturi scrubber developed by Yung et al. has been shown to simulate the performance data of a mobile venturi scrubber better than Calvert's or Hesketh's equation. At high gas throat velocity, Yung's model tends to overestimate the pressure drop across the venturi throat as indicated in the calculation. Simulation results of the Yung model indicate:

- The effect of long residence time on the enhancement of the collection efficiency of a venturi scrubber is more profound for large particle sizes than for small particle sizes. Even though a decrease in $\Delta P$ will impair the collection efficiency of the venturi scrubber, longer residence time caused by slower gas throat velocity (thus implies reduction of $\Delta P$ if $\frac{Q_L}{Q_G}$ is constant) can compensate the reduction in collection efficiency which is supposedly caused by the decrease in $\Delta P$. This compensation, however, is directly dependent upon the particle size.

- The relationship of $\eta$ and $\Delta P$ in the venturi scrubber performance data is due to the longer resistence time created by a lower $\Delta P$ and partly due to the fluctuation of particle size distribution in the flue gas.

## ESP

A modified Deutsch equation has been used to simulate the performance data of the mobile ESP. Due to limited data, effects of the number of fields and of the burning RDF on the performance of ESP cannot satisfactorily be analyzed.

# REFERENCES

1. Calvert, S. Scrubber Handbook. Ambient Purification Technology, Inc. July 1972.
2. Hesketh, H. E. "Fine Particle Collection Efficiency Related to Pressure Design, Scrubbant and Particle Properties, and Contact Mechanism." Journal of the Air Pollution Control Association. Vol. 24, No. 10. October 1974.
3. Yung, S. C., H. F. Barbarika, and S. Calvert. "Pressure Loss in Venturi Scrubbers." Journal of the Air Pollution Control Association. Vol. 27, No. 24. April 1977.
4. Yung, S. C., S. Calvert, and H. F. Barbarika. "Venturi Scrubber Performance Model." Environmental Science and Technology. Vol. 12, No. 4. April 1978.
5. Matta, S., and P. Ohnfield. "Efficient Gas Cleaning with SF Electrostatic Precipitator." Bulletin of A. B. Svenska Flaktfabriken, Stockholm, Sweden.
6. Nakiyama, S., and Y. Tanasawa. "An Experiment on the Atomization of Liquid." Transactions of Japan Society of Mechanical Engineers. 5(18): 68. 1939.
7. Galeski, J. B. "Particle Size Definitions for Particulate Data Analysis." EPA-600/7-77-129, November 1977.
8. White, H. J. "Electrostatic Precipitation of Fly Ash." Journal of the Air Pollution Control Association. Vol. 27, No. 1. January 1977.

# APPENDIX A

## SAMPLE CALCULATION OF $\Delta P$

# APPENDIX A

## SAMPLE CALCULATION OF $\Delta P$

Operating Data: Run Nos. 13, 14
$Q_L$: 15.1 liter/min
$Q_G$: 455.3 $m^3/hr$
Measured $\Delta P$: 25.4 cm water gauge

Gas Throat Velocity: $U_G = \frac{Q_G}{A} = 4406.7$ cm/sec

(a) Calvert's Equation

$$\Delta P = 1.03(10^{-3})\ (\ U_G\ )^2\ \frac{Q_L}{Q_G}$$

Unit Conversion

$$Q_G = \frac{455.3\ m^3}{hr} \times \frac{hr}{3{,}600\ sec} \times \frac{(100\ cm)^3}{m^3} = \frac{126{,}472\ cm^3}{sec}$$

$$Q_L = \frac{15\ 1}{min} \times \frac{1{,}000\ cm}{e} \times \frac{min}{60\ sec} = 251.67\ cm^3/sec$$

$$\Delta P = 1.03(10^{-3})\ (\ U_G\ )^2\ \frac{Q_L}{Q_G}$$

$$= 1.03(10^{-3})(4{,}406.7)^2\ \frac{251.67}{126{,}472} = 39.8\ \text{cm WG}$$

(b) Hesketh's Equation

$$P = \frac{U_G{}^2\ \rho_G A^{0.133}}{507}\left[(0.56 + 0.125\ L' + 2.3(10^{-3})\ L'^2)\right]$$

where: $\rho_G = \frac{PMW}{RT}$, $L' = \frac{\text{Liquid flow rate}}{\text{Gas flow rate}}\ \frac{\text{Gal.}}{1{,}000\ ft^3}$

Average Temperature = 140°F
Pressure = 1 atm

$$\rho_G = \frac{1\ atm\ \ 29\ \frac{g}{g\ mole}}{82.057\ \frac{atm\ cm^3}{g\ mole\ {}^\circ K}\ 330^\circ K} = 0.00106\ \frac{g}{cm^3}$$

Unit Conversion

$$A = 28.7\ \text{cm}^2 = 28.7\ \text{cm}^2\left(\frac{\text{in}}{2.54\ \text{cm}}\right)^2\left(\frac{\text{ft}}{12\ \text{in}}\right)^2 = 0.031\ \text{ft}^2$$

$$\rho_G = 0.00106\ \frac{\text{g}}{\text{cm}^3} \times \frac{\text{lb}}{454\ \text{g}} \times\left(\frac{2.54\ \text{cm}}{\text{in}}\right)^3\times\left(\frac{12\ \text{in}}{\text{ft}}\right)^3 = 0.066\ \text{lb/ft}^3$$

$$U_G = 4{,}406.7\ \frac{\text{cm}}{\text{sec}}\left(\frac{\text{in.}}{2.54\ \text{cm}}\right)\left(\frac{\text{ft}}{12\ \text{in.}}\right) = 144.58\ \text{ft/sec}$$

$$Q_G = \frac{15.1\ \text{liter}}{\text{min}} \times \frac{0.264\ \text{gal.}}{\text{liter}} = 3.986\ \text{gal/min}$$

$$Q_G = \frac{455.3\ \text{m}^3}{\text{hr}} \times \frac{\text{hr}}{60\ \text{min}} \times \frac{35.314\ \text{ft}^3}{\text{m}^3} = 267.98\ \frac{\text{ft}^3}{\text{min}}$$

$$L' = \frac{3.986}{267.98} = \frac{0.0149\ \text{gal.}}{\text{ft}^3} = \frac{14.9\ \text{gal.}}{1{,}000\ \text{ft}^3}$$

$$\begin{aligned}\Delta P &= \frac{(144.58)^2\ (0.066)\ (0.031)^{0.133}}{507}\left[0.56 + 0.125(14.9) + 2.3(10^{-3})(14.9)^2\right]\\ &= 5.04\ \text{in. WG}\\ &= 12.8\ \text{cm WG}\end{aligned}$$

(c) Yung's Equation

$$\Delta P = \frac{-2\rho_L\ U_G^2}{g_c}\ \frac{Q_L}{Q_G}\left[\ 1 - x^2 + \sqrt{x^4 - x^2}\right]$$

$$\text{where:}\quad x = \frac{3\ l_t C_{D1}\ \rho_G}{16\ d_d \rho_L} + 1$$

Throat length $l_t$ = 12 in.

Point of injection = 2 in. from throat entrance

Estimated physical properties: at T = 140°F

Liquid surface tension $\sigma$ = 66.15 dyne/cm
Gas viscosity $\mu_G$ = 0.02 centipoise
Liquid viscosity $\mu_L$ = 0.5 centipoise

The sauter mean drop diameter ($d_d$) can be calculated as follows:6/

$$d_d = \frac{585}{U_G}\left(\frac{\sigma}{\rho_L}\right)^{0.5} + 597\left(\frac{\mu_L}{\sqrt{\sigma\rho_L}}\right)^{0.45}\left(1{,}000\,\frac{Q_L}{Q_G}\right)^{1.5}$$

$$= \frac{585}{44.07\text{ cm/sec}}\left(\frac{66.15\text{ dyne/cm}}{0.983\text{ g/cm}^3}\right)^{0.5} + 597\left(\frac{0.005\,\frac{\text{dyne-sec}}{\text{cm}^2}}{\sqrt{66.15\,\frac{\text{dyne}}{\text{cm}} \times 0.983\,\frac{\text{g}}{\text{cm}^3}}}\right)^{0.45}$$

$$\times\left(\frac{15.1(10)^6\text{ cm /min}}{7.588(10)^6\text{ cm/min}}\right)^{1.5}$$

$$= 109.89 + 60.37 = 169.26\text{ mm}$$

Reynold's number based on the $d_d$ at the injection point is: (drop axial velocity at injection point is assumed to be zero.)

$$N_{Rel} = \frac{d_d\, U_G\, \rho_G}{\mu_G} = \frac{0.01693\text{ cm} \times 4{,}407\text{ cm/sec} \times 0.00106\text{ g/cm}^3}{0.02(0.01)\text{ g/sec cm}}$$

$$= 395$$

The drag coefficient at the injection point is:

$$C_{D1} = 0.22 + \frac{24}{N_{Rel}}\left(1 + 0.15\, N_{Rel}^{0.6}\right)$$

$$= 0.61$$

then: $$x = \frac{3(25.4)(0.61)(0.00106)}{(16)(0.01693)(0.983)} + 1$$

$$= 1.185$$

$$\Delta P = \frac{-2(0.983)(4{,}407)^2}{1}\left[\frac{15.1(10^3)}{7.588(10^6)}\right]\left[1 - (1.185)^2 + \sqrt{(1.185)^4 - (1.185)^2}\right]$$

$$= 26{,}532\,\frac{\text{dyne}}{\text{cm}^2} = \frac{27\text{ g}}{\text{cm}^2} = 27\text{ cm WG}$$

Similarly:

At run No. = 15, 16, 17
$Q_G$ = 863.7 m$^3$/hr
$Q_L$ = 28.3 liter/min
Measured $\Delta P$ = 76.2 cm WG

Calvert's Equation: $\Delta P$ = 141.5 cm
Hesketh's Equation: $\Delta P$ = 45.34 cm
Yung's Equation: $\Delta P$ = 103.0 cm WG

At run No. 12:

$Q_G$ = 720.4 $m^3$/hr
$Q_L$ = 23.6 l/min
Measured $\Delta P$ = 50.8 cm WG
$U_G$ = 6,972.5 cm/HC

Calvert's Equation: $\Delta P$ = 98.4 cm WG
Hesketh's Equation: $\Delta P$ = 31.0 cm WG
Yung's Equation: $\Delta P$ = 70.9 cm WG

# APPENDIX B

## SAMPLE CALCULATION OF COLLECTION EFFICIENCY

# APPENDIX B

## SAMPLE CALCULATION OF COLLECTION EFFICIENCY

(1) Operating conditions: Run Nos. 15, 16, 17

$Q_G = 863.7\ m^3/hr$
$Q_L = 28.3$ liter/min
$P = 76.2$ cm WG
$\eta = 99.132\ \%$

To compute $\eta$ from equation 5, the following parameters have to be calculated:

Cunningham's correction factor C': $C' \cong 1 + 2A \frac{\lambda}{dp}$ [7]

where: $A = 1.246 + 0.42\ e^{-\left(\frac{0.87\ d_p}{2\lambda}\right)}$
$d_p$ = particle diameter
$\lambda$ = mean free path at the operating condition
$= \lambda o \left(\frac{U_G}{U_{Go}}\right)\left(\frac{T}{T_o}\right)^{1/2}\left(\frac{Po}{P}\right)$

$\lambda_o = 0.0653\ \mu m$ at $T_o = 23°C$, $Po = 1$ atm
$\mu_{Go} = 0.018$ centipoise
$\mu_G$ (at $T = 333°K$) $= 0.019$ centipoise

$$\lambda = 0.0653\ \mu m \left(\frac{0.019}{0.018}\right)\left(\frac{333}{296}\right)^{1/2}\left(\frac{1}{1}\right) = 0.0731\ \mu m$$

Assuming particle diameter ($d_p$) = 10 $\mu m$ (reported 50% cut-off diameter is > 10 $\mu m$)

$$C' = 1 + 2\left[1.246 + 0.42\ e^{-\left(\frac{0.87(10)}{2(0.073)}\right)}\right]\left[\frac{0.0731}{10}\right]$$
$$= 1.0182$$

For run Nos. 15, 16, 17

$d_d = 0.0116$ cm
$C_{D1} = 0.5625$
(calculated in Appendix A)

$$B = \frac{Q_L \rho_L}{Q_G \rho_G C_{D1}} = \frac{28.3(10^3)\ \text{cm}^3/\text{min} \times 0.983\ \text{g/cm}^3}{14.39(10^6)\ \text{cm}^3/\text{min} \times 0.00106 \times 0.5625}$$

$$= 3.2411$$

$$U_G = \frac{Q_G}{A} = 8{,}359.5\ \text{cm/sec}$$

$$x = \frac{3\ l_t C_{D1}\ G}{16\ d_d\ L} + 1 = \frac{3(25.4)(0.5625)(0.00106)}{16(0.0116)(0.98)} = 1$$

$$= 1.2480$$

$$K_{po} = \frac{C'\rho_p d_p{}^2/U_{p1} - \overset{0}{U_{d1}}/}{9\ \mu_G d_d}$$

$$= \frac{(1.0182)(2)(0.001)\ /8{,}359 - 0/}{9(0.02)(0.01)(0.01165)}$$

$$= 811.7$$

$$\overset{*}{U}_{d1} = 2(1 - x^2 + \sqrt{x^4 - x^2}) = 0.74866$$

$$1 - \overset{*}{U}_{d1} = 0.2513$$

$$\ln Pt = \frac{B}{K_{p1}(1-\overset{*}{U}_{d1}) + 0.7} \left\{ 4K_{p1}(1-\overset{*}{U}_{d1})^{1.5} + 4.2(1-\overset{*}{U}_{d1})^{0.5} - 5.02K_{p1}^{0.5} \right.$$

$$\left. (1-\overset{*}{U}_{d1} + \frac{0.7}{K_{p1}}) \tan^{-1}\left(\frac{(1-\overset{*}{U}_{d1})K_{p1}}{0.7}\right)^{0.5} \right\} - \frac{B}{K_{p1} + 0.7} \left\{ 4K_{p1} + \right.$$

$$\left. 4.2 - 5.02K_{p1}^{0.5}(1 + \frac{0.7}{K_{p1}}) \tan^{-1}( \frac{K_{p1}}{0.7} )^{0.5} \right\}$$

$$= \frac{3.2411}{(811.7)(0.2513) + 0.7} \Big[ 4(811.7)(0.2513)^{1.5} + 4.2(0.2513)^{0.5}$$

$$- 5.02(811.7)^{0.5} \times \left(0.2513 + \frac{0.7}{811.7}\right) \tan^{-1}\left(\frac{(0.2513)(811.7)}{0.7}\right)^{0.5} \Big]$$

$$\frac{-3.2411}{811.7 + 0.7} \Big[ 4(811.7) + 4.2 - 5.02(811.7)^{0.5}\left(1 + \frac{0.7}{811.7}\right)$$

$$\tan^{-1}\left(\frac{811.7}{0.7}\right)^{0.5} \Big]$$

$$= -6.4432$$

$Pt = 1.59(10^{-3})$ $\qquad$ $\eta = 99.84\%$

Similarly:

| $d_p$ | $\eta$, % |
|---|---|
| 5 | 99.83 |
| 2 | 99.79 |
| 1 | 99.28 |
| 0.5 | 94.88 |

(2) Operating data: Run Nos. 13, 14

$Q_G$ = 455.3 $m^3$/hr
$Q_L$ = 15.1 liter/min
Measured $\Delta P$ = 25.4 cm

With the same calculation procedure described above, the computed $\eta$ at different assumed $d_p$ are:

| $d_p$ | $\eta$, % |
|---|---|
| 10 | 99.55 |
| 5 | 99.49 |
| 2 | 98.84 |
| 1 | 94.88 |
| 0.5 | 68.69 |

# APPENDIX C

## ANALYSIS OF ESP PERFORMANCE DATA

# APPENDIX C

## ANALYSIS OF ESP PERFORMANCE DATA

The efficiency of ESP in Table 2 can be tabulated as follows:

| SCA | $C_o/C_i$ | Number of Fields | Run Number | Number of Runs | Fuel |
|---|---|---|---|---|---|
| 16.4 | 0.0148 | 5 | 21, 22, 23 | 3 | Coal |
| 27.34 | 0.0075 | 5 | 20 | 1 | Coal |
| 7.33 | 0.0199 | 4 | 1 | 1 | Coal |
| 16.4 | 0.0131 | 5 | 5, 6 | 2 | Coal |
| 21.87 | 0.0142 | 5 | 7, 8, 9 | 3 | Coal |
| 10.9 | 0.0613 | 3 | 24, 25 | 2 | Coal |
| 16.4 | 0.0226 | 5 | 2, 26, 27, 28 | 4 | Coal and RDF |
| 16.4 | 0.0354 | 5 | 3, 4 | 2 | Coal and RDF |

### (a) Regression Analysis

Data points obtained with number of electric fields less than five and with the burning of coal and RDF are excluded in the regression analysis. For the first regression of $\ln(C_o/C_i)$ with SCA, the following four data points are used:

| SCA | $\ln(C_o/C_i)$ | Run Number |
|---|---|---|
| 16.4 | -4.213 | 21, 22, 23 |
| 27.34 | -4.893 | 20 |
| 16.4 | -4.329 | 5, 6 |
| 21.87 | -4.253 | 7, 8, 9 |

The data points for regression analysis of $\ln[-\ln(C_o/C_i)]$ with ln SCA are:

| ln SCA | $\ln\left(-\ln\frac{C_o}{C_i}\right)$ | Run Number |
|---|---|---|
| 2.797 | 1.4382 | 21, 22, 23 |
| 3.307 | 1.5878 | 20 |
| 3.085 | 1.4476 | 7, 8, 9 |
| 2.797 | 1.4655 | 5, 6 |

### (b) Calculation of $\omega$ from Equation 6

$$\eta = 1 - e^{-SCA\omega}$$

$$\frac{Ci - Co}{Ci} = 1 - e^{-SCA\omega}$$

$$\ln\left(\frac{Co}{Ci}\right) = -SCA\omega$$

$$W = -\ln\left(\frac{Co}{Ci}\right)\frac{1}{SCA}$$

## GLOSSARY

Nomenclatures (Latin)

$A$ = cross-sectional area, cm$^2$

$C$ = concentration, g/cm$^3$

$C'$ = Cunningham's correction factor, dimensionless

$C_D$ = drag coefficient, dimensionless

$d$ = drop or particle diameter, cm or mm

$D_e$ = equivalent diameter of venturi, 4A divided by the flow perimeter, ft

$g_c$ = conversion factor

$K_p$ = impaction parameter, dimensionless

$L'$ = $Q_L/Q_G$, gal/1,000 ft$^3$

$l_t$ = throat length, cm

$m$ = liquid-to-gas flow ratio, pounds of liquid to pounds of gas

$MW$ = molecular weight, g/gml

$N_{Re}$ = Reynolds number, dimensionless

$P$ = pressure, cm WG

$Q$ = volumetric flow rate, cm$^3$/min

$R$ = gas constant

SCA = specific collection area, time/length

$T$ = temperature

$U$ = linear velocity, cm/sec or m/sec

$y$ = position along the venturi throat

Nomenclatures (Greek)

$\psi$ = Moody friction factor for venturi, dimensionless

$\lambda$ = mean free path, $\mu$m

$\rho$ = density, g/cm$^3$

$\sigma$ = surface tension, dyne/cm

$\mu$ = viscosity, centipoise

$\tau$ = residence time, sec

$\eta$ = efficiency, %

$\omega$ = migration velocity, length/time

$\omega_k$ = modified migration velocity, length/time

Subscripts

a = air

d = liquid drop

G = gas

L = liquid

t = at throat exit or distance $l_t$ from throat entrance

P = particle

Re = Reynolds number

1 = injection point or throat entrance

2 = throat exit

o = outlet

i = inlet

# APPENDIX D

## HALIDE AND TRACE METAL EMISSIONS FROM RDF COMBUSTION

# HALIDE AND TRACE METAL EMISSIONS FROM RDF COMBUSTION

by

T. Sutikno

SPECIAL INTERIM REPORT
November 5, 1979

MRI Project No. 4415-L

Prepared by

Midwest Research Institute
425 Volker Boulevard
Kansas City, Missouri 64110

For

PEDCo Environmental
11499 Chester Road
Cincinnati, Ohio 45246

MRI

**MIDWEST RESEARCH INSTITUTE**
425 Volker Boulevar
Kansas City, Missouri 6411
Telephone (816) 753-760

November 5, 1979

RECEIVED
NOV 1979
PEDCO ENVIRONMENTAL
By

Mr. Fred Hall
PEDCo Environmental, Inc.
11499 Chester Road
Cincinnati, Ohio 45256

Subject: Final Report, "Halide and Trace Metal Emissions From RDF Combustion," MRI Project No. 4415-L.

Dear Mr. Hall:

Enclosed please find a copy of the final report on analyses of the halide and trace metal emission data.

Please call me or Dr. K. P. Ananth if you have any questions.

Sincerely,

MIDWEST RESEARCH INSTITUTE

Tek Sutikno
Assistant Engineer

TS/sp

Enclosure

## PREFACE

This report analyzes the emission data of selected elements from a coal-fired power plant. These analyses evaluate the effect of cofiring refuse-derived fuel (RDF) on the quantitative emissions of the selected elements and on the elemental removal efficiencies of two mobile pollution control devices.

This report was written by Mr. T. Sutikno under the direction of Dr. K. P. Ananth. Questions concerning the technical aspects of this report should be directed to Mr. T. Sutikno or to Dr. K. P. Ananth.

Approved for:

MIDWEST RESEARCH INSTITUTE

L. J. Shannon

L. J. Shannon, Executive Director
Environmental and Materials
  Sciences Division

November 5, 1979

## CONTENTS

Preface . . . . . . . . . . . . . . . . . . . . . . . . . . . . . . . . ii
Figures . . . . . . . . . . . . . . . . . . . . . . . . . . . . . . . . iv
Tables. . . . . . . . . . . . . . . . . . . . . . . . . . . . . . . . . v
Summary . . . . . . . . . . . . . . . . . . . . . . . . . . . . . . . . vi

1. Introduction. . . . . . . . . . . . . . . . . . . . . . . . . . . 1
2. Methods of Evaluation . . . . . . . . . . . . . . . . . . . . . . 2
3. Halides . . . . . . . . . . . . . . . . . . . . . . . . . . . . . 6
    Chloride . . . . . . . . . . . . . . . . . . . . . . . . . . . . 6
    Fluoride . . . . . . . . . . . . . . . . . . . . . . . . . . . . 11
4. Metals (Pb, Cd, Sb, Fe, and Cu) . . . . . . . . . . . . . . . . . 17
    Lead . . . . . . . . . . . . . . . . . . . . . . . . . . . . . . 17
    Cd, Sb, Fe, Cu . . . . . . . . . . . . . . . . . . . . . . . . . 19
5. Conclusions . . . . . . . . . . . . . . . . . . . . . . . . . . . 24
    Halides. . . . . . . . . . . . . . . . . . . . . . . . . . . . . 24
    Metals (Pb, Cd, Sb, Fe, and Cu). . . . . . . . . . . . . . . . . 24

References. . . . . . . . . . . . . . . . . . . . . . . . . . . . . . 26
Appendix - Calculation Procedure. . . . . . . . . . . . . . . . . . . 27
Glossary. . . . . . . . . . . . . . . . . . . . . . . . . . . . . . . 28

## FIGURES

Number Page

1 Chloride removal efficiency of the venturi scrubber as a function of pressure drop across the venturi. . . . . . . . . 7

2 Chloride removal efficiency of the venturi scrubber as a function of percentage of RDF burned. . . . . . . . . . . . . 8

3 Chloride removal efficiency of ESP as a function of specific collection area . . . . . . . . . . . . . . . . . . . . . . . 12

4 Fluoride removal efficiency of the venturi scrubber as a function of pressure drop across the venturi. . . . . . . . . 14

5 Fluoride removal efficiency of the ESP as a function of specific collection area. . . . . . . . . . . . . . . . . . . . 16

6 Lead removal efficiency of the venturi scrubber as a function of pressure drop across the venturi throat. . . . . . . . . . 18

7 Lead removal efficiency of the ESP as a function of specific collection area . . . . . . . . . . . . . . . . . . . . . . . 20

8 Removal efficiencies of the venturi scrubber for Cd, Sb, Fe, and Cu as a function of pressure drop across the venturi throat. . . . . . . . . . . . . . . . . . . . . . . . . . . . 21

9 Removal efficiencies of the ESP for Cd, Sb, Fe, and Cu as a function of specific collection area. . . . . . . . . . . . . . 23

# TABLES

| Number | | Page |
|---|---|---|
| 1 | Mobile Scrubber Emission Concentration | 3 |
| 2 | Mobile ESP Emission Concentration | 4 |
| 3 | Differences in Elemental Composition Between Coal and RDF Fuel Samples From All Tests | 5 |
| 4 | Emissions of Cd, Sb, Fe, and Cu at the Venturi Scrubber Outlet | 22 |
| 5 | Emissions of Cd, Sb, Fe, and Cu at the ESP Outlet | 22 |

# SUMMARY

The emissions of selected elements from a coal-fired power plant have been analyzed. These analyses evaluate the effects of cofiring RDF on the emissions of selected elements: halides (Cl, F) and metals (Pb, Cd, Sb, Fe, Cu). A mobile venturi scrubber and a mobile electrostatic precipitator (ESP) were used separately to control these elemental emissions. Effects of cofiring RDF on the elemental removal efficiencies of these two control devices are evaluated in this report.

## HALIDES (Cl, F): SECTION 3

### Chloride

RDF cofiring increases the emission of chloride. However, the chloride removal efficiency of the venturi scrubber improves when RDF is cofired. Because of this improvement, increases in the inlet concentrations of chloride due to RDF cofiring do not affect the atmospheric emission of chloride when controlled by the venturi scrubber. On the other hand, the chloride removal efficiency of the ESP significantly decreases with the increase in the inlet chloride concentration. Thus, if ESP is used as the control device, RDF cofiring adversely increases the atmospheric emission of chloride. Theoretical explanations for the changes in the chloride removal efficiencies of both control devices have been suggested.

### Fluoride

Most of the fluoride constituents in RDF after combustion are retained in the bottom ash. Because of this retention, RDF cofiring does not affect the emission of fluoride. The effect of RDF cofiring on the efficiencies of both control devices for fluoride removal cannot be analyzed since the data fluctuate so greatly.

## METALS (Pb, Cd, Sb, Fe, Cu): SECTION 4

The emissions of the subject metals increase in RDF cofiring. Higher concentrations of these metals in RDF and excessive masses of RDF burned per unit power output are the main reasons for the increases in metal emissions. The metal removal efficiencies of both control devices have not been theoretically analyzed because of the lack of elemental size distribution data. However, there is no notable effect of RDF cofiring on the metal removal efficiencies of both control devices.

# SECTION 1

# INTRODUCTION

PEDCo Environmental, Inc., has acquired emission data of halides (Cl, F) and metals (Pb, Cd, Sb, Fe, Cu) from a coal-fired power plant in Ames, Iowa. The coal-fired power plant was cofired with RDF to reduce coal consumption and to facilitate refuse disposal. Due to quantitatively distinct elemental composition, heat of combustion, and chemical property of RDF relative to coal, RDF cofiring results in a new characteristic of elemental emissions. To assess this new characteristic of the elemental emissions in the combined firing of coal plus RDF, the elemental emission data were taken when coal only was fired and when coal plus RDF was fired. Therefore, the main objective of this report is to evaluate the effects of RDF cofiring on the emissions of the selected elements.

A mobile venturi scrubber and a mobile ESP were used individually to control the selected elemental emissions. Effects of RDF cofiring on the elemental removal efficiencies of both control devices are evaluated in this report. Moreover, to assess the economic benefit of RDF cofiring, the controlled mass of each element emitted per unit of power output in the burnings of coal only is quantitatively compared to that of coal plus RDF.

The methods of evaluation are described in Section 2. The chloride and fluoride are analyzed in Section 3. The metal lead--for which extensive data are available--is discussed before a review of Cd, Sb, Fe, and Cu in Section 4. The conclusions are presented in Section 5.

# SECTION 2

# METHODS OF EVALUATION

Evaluation of RDF cofiring is based on the measured data in both coal and coal plus RDF burning operations. PEDCo Environmental Inc., has presented the measured data as shown in Tables 1 and 2, and compositional analyses of coal and RDF are given in Table 3. All elemental concentration data in Tables 1 and 2 were obtained from the total mass collected from the front and back halves of a Method 5 Source Sampling Train (SST).

The measured data from the two burning operations are compared to analyze the environmental impact of RDF cofiring. Engineering principles pertinent to the removal phenomena in the control devices are used as the rationale with which to analyze the elemental removal efficiency of each control device. Theoretical relationships between the measured operating parameters and removal efficiency are discussed when appropriate. Additionally, changes in the operating parameters of control devices because of RDF cofiring are identified, especially when the changes affect performance. No statistical analyses of the data are made because the number of the measured data is limited.

Approximately 90 wt % of the halides were collected from the back half of the SST, and virtually 100% of the metals were collected from the front half of the SST (1). Therefore, all the halides data are considered to be the gaseous halides data, and all the metals to be solid metal data. Because gaseous pollutants differ significantly from solid pollutants, the effects of RDF cofiring on the emissions of halides and metals must be evaluated separately. The next two sections of this report consecutively evaluate the halides and the metals. Each section reviews the elemental removal efficiency of the venturi scrubber; the venturi scrubber-controlled elemental emission; and the elemental removal efficiency of the ESP and the ESP-controlled elemental emission.

In addition, the mass of each element emitted per unit of power output is calculated on the assumption that the flue gas generated is linearly dependent upon the amount of heat input to the boiler; the calculation procedure is given in the Appendix.

## TABLE 1. MOBILE SCRUBBER EMISSION CONCENTRATION[a] (mg/dscm)

| | Primary | | | | | | |
|---|---|---|---|---|---|---|---|
| Power generation (MW/hr) | 30.4 | 28.3 | 32.5 | 33.0 | 31.0 | 22.0 | 22.0 |
| ΔP cm (W.G.) | 76.2 | 25.4 | 25.4 | 76.2 | 76.2 | 76.2 | 50.8 |
| Gas flow rate ($m^3$/hr) | 863.7 | 455.3 | 485.3 | 852.9 | 852.9 | 835.9 | 720.4 |
| S.L.[b] flow rate (liter/min) | 28.3 | 15.1 | 16.0 | 30.2 | 16.0 | 29.2 | 23.6 |
| Fuel | Coal | Coal | RDF | RDF | RDF | RDF | RDF |
| % RDF (heat input basis) | 0 | 0 | 17 | 13 | 14 | 24 | 23 |
| Run No. | 15,16,17 | 13,14 | 7,8 | 5 | 6 | 9 | 12 |
| T. particulate (in)[c] | 12,210 | 12,770 | 18,130 | 9,945 | | 11,610 | 18,520 |
| (out) | 106.0 | 92.26 | 89.88 | 51.54 | 49.21 | 56.09 | 54.00 |
| Cl (in)[d] | 10.0 | | 91.0 | 120 | | 220 | 130 |
| (out) | 2.4 | | ND[e] | 5.00 | | ND | ND |
| F (in)[f] | 14.1 | 9.66 | 5.51 | 3.49 | | | 13.0 |
| (out) | 2.65 | 0.350 | 0.210 | ND | | | 1.57 |
| Br (in)[g] | ND | ND | ND | ND | | | ND |
| (out) | ND | ND | ND | ND | | | ND |
| AA analysis | | | | | | | |
| Pb (in) | 1.7 | 1.8 | 9.1 | | 1.3 | 14.0 | |
| (out) | 0.26 | 0.22 | 0.74 | | 0.18 | 2.2 | |
| Cd (in) | 0.034 | | | | | 0.14 | |
| (out) | 0.0025 | | | | | 0.026 | |
| Sb (in) | 0.34 | | | | | 0.46 | |
| (out) | 0.0069 | | | | | 0.017 | |
| Fe (in) | 260 | | | | | 460 | |
| (out) | 2.1 | | | | | 1.5 | |
| Cu (in) | 0.25 | | | | | 0.99 | |
| (out) | 0.013 | | | | | 0.025 | |

---

[a] In case of an undetectable outlet concentration, the detection limit was used as the outlet concentration.

[b] Scrubber liquor.

[c] Front half only.

[d] Detection limit for Cl is 1.8 mg/dscm.

[e] Not detectable.

[f] Detection limit for F is 0.05 mg/dscm.

[g] Detection limit for Br is 4.0 mg/dscm.

## TABLE 2. MOBILE ESP EMISSION CONCENTRATION
(mg/dscm)

| | Primary | | | | | | | |
|---|---|---|---|---|---|---|---|---|
| Power generation (MW/hr) | 35.0 | 34.8 | 33.0 | 21.6 | 20.6 | 18.6 | 33.5 | 22.0 |
| SCA | 16.4 | 27.34 | 7.33 | 16.4 | 21.87 | 10.93 | 16.4 | 16.4 |
| No. Fields | 5 | 5 | 4 | 5 | 5 | 3 | 5 | 5 |
| Fuel | Coal | Coal | Coal | Coal | Coal | Coal | RDF | RDF |
| % RDF (Heat input basis) | 0 | 0 | 0 | 0 | 0 | 0 | 15 | 22 |
| Run No. | 21,22,23 | 20 | 1 | 5,6 | 7.8,9 | 24,25 | 2,26,27<br>28 | 3,4 |
| T. particulate (in)[a] | 3,119 | 3,991 | 3,235 | 2,743 | 2,004 | 3,172 | 3,697 | 2,701 |
| (out) | 46.23 | 29.81 | 64.60 | 36.13 | 28.50 | 194.3 | 83.80 | 95.70 |
| Cl (in)[b] | | | | 17.0 | | | | 170 |
| (out) | | | | 7.60 | | | | 160 |
| F (in)[c] | 10.6 | | | | 6.64 | 5.81 | 8.78 | |
| (out) | 6.66 | | | | 5.56 | 5.30 | 7.96 | |
| Br (in)[d] | ND[e] | ND | | | ND | ND | ND | |
| (out) | ND | ND | | | ND | ND | ND | |
| AA Analysis | | | | | | | | |
| Pb (in) | 0.31 | 0.53 | 2.7 | 0.51 | 8.2 | | 14 | 9.3 |
| (out) | 0.21 | 0.0070 | 1.1 | 0.017 | 0.022 | | 0.086 | 2.5 |
| Cd (in) | | | | 0.36 | | | | 0.092 |
| (out) | | | | 0.0028 | | | | 0.0077 |
| Sb (in) | | | | 0.073 | | | | 140 |
| (out) | | | | 0.0051 | | | | 0.0049 |
| Fe (in) | | | | 92 | | | | 140 |
| (out) | | | | 2.2 | | | | 2.1 |
| Cu (in) | | | | 0.20 | | | | 0.42 |
| | | | | 0.012 | | | | 0.025 |

[a] Front half only.

[b] Detection limit for Cl is 1.8 mg/dscm.

[c] Detection limit for F is 0.05 mg/dscm.

[d] Detection limit for Br is 4.0 mg/dscm.

[e] Not detectable.

## Table 3. DIFFERENCES IN ELEMENTAL COMPOSITION BETWEEN COAL AND RDF FUEL SAMPLES FROM ALL TESTS[a]

| | Factor by which elemental concentration in RDF differs from elemental concentration in coal |
|---|---|
| Elements more concentrated in RDF than in coal | |
| Copper[b] | 120 |
| Lead[b] | 40 |
| Bromine | 25 |
| Fluorine | 25 |
| Zinc | 10 |
| Manganese | 10 |
| Antimony | 5 |
| Chromium | 5 |
| Cobalt | 5 |
| Rubidium | 4 |
| Tin | 3 |
| Barium | 3 |
| Silver | 3 |
| Cadmium[b] | 2 |
| Titanium | 2 |
| Strontium | 2 |
| Phosphorus | 2 |
| Elements less concentrated in RDF than in coal | |
| Vanadium | 50 |
| Beryllium | 25 |
| Scandium | 7 |
| Yttrium | 6 |
| Sulfur[c] | 5 |
| Molybdenum | 5 |
| Iron[b] | 4 |
| Thallium | 3 |
| Nickel | 2 |
| Cerium | 2 |
| Lanthanum | 2 |
| Zirconium | 2 |

[a] Based on SSMS analysis unless otherwise stated.

[b] Based on AAS.

[c] The initial determination of sulfur concentration might have been low by a factor of 3-10 because of high organic content, which necessitated low-temperature ashing of the samples.

# SECTION 3

# HALIDES

Since chloride and fluoride do not have the same chemical properties, discussions of these two halides are necessarily separated.

## CHLORIDE

### Venturi Scrubber

Removal Efficiency--

The performance of the mobile venturi scrubber for chloride removal is plotted in Figure 1.

1. Uncontrolled gaseous chloride emissions are about 9 to 20 times greater when coal plus RDF is burned than when only coal is burned.

2. The efficiency of venturi scrubber is higher in coal plus RDF burning than in coal burning.

Observation (1) strongly suggests that the elemental concentration of chloride is higher in RDF than it is in coal. Because of the lack of chloride elemental data in coal and RDF, analyses are necessary to confirm the high concentration of chloride in RDF.

Despite the limited data points of chloride removal in coal burning, the chloride removal efficiency of the venturi scrubber did improve significantly when coal was cofired with RDF. The chloride removal efficiency increases with the increase in the percentage of RDF cofired (see Figure 2).

To explain the improvement, the removal phenomena of gaseous chloride in the venturi scrubber must be discussed. As mentioned previously, the obvious difference between the chloride data for coal and for coal plus RDF is significantly higher inlet chloride concentrations in coal plus RDF burning. Theoretically, in the case of a dilute chloride concentration in the flue gas, a high inlet concentration ($C_i$) should not affect the overall removal efficiency if the mass transfer coefficient is independent of concentration. It should increase the inital rate of diffusional mass transfer because of a larger concentration difference. Provided that all pertinent operating parameters are kept constant, a higher inlet concentration increases the amount of

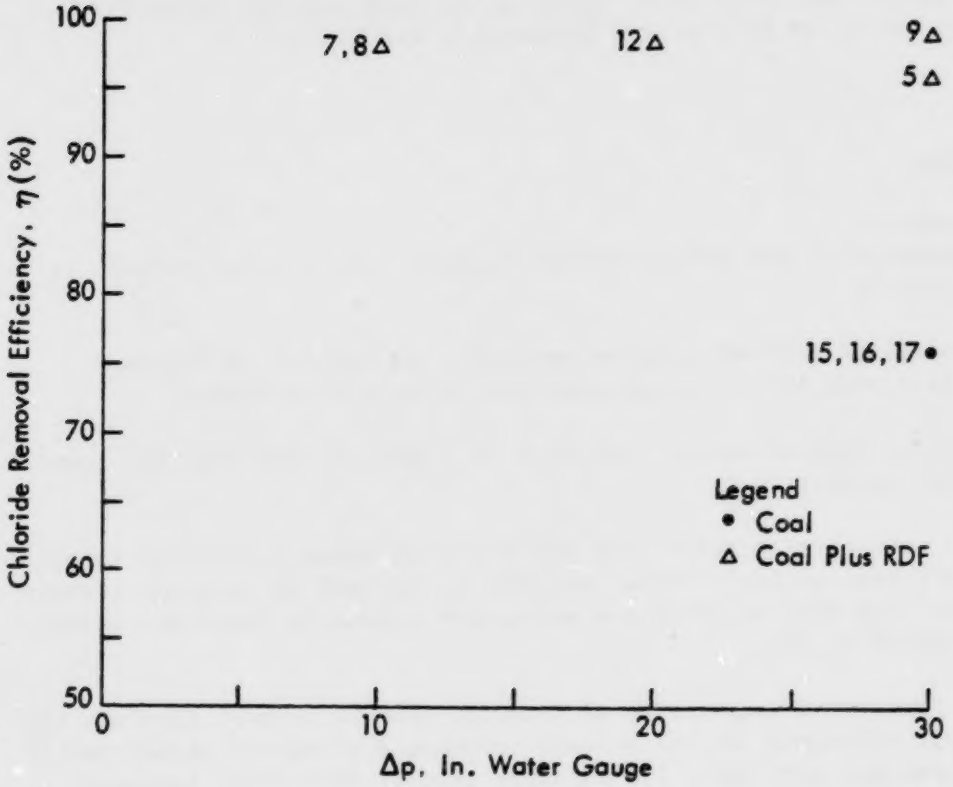

Figure 1. Chloride removal efficiency of the venturi scrubber as a function of pressure drop across the venturi.

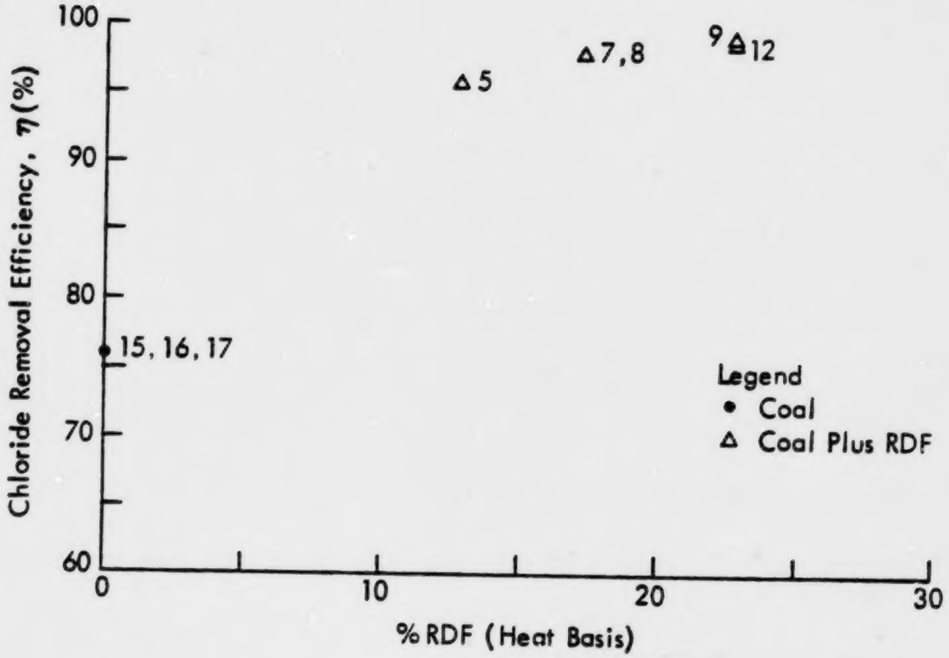

Figure 2. Chloride removal efficiency of the venturi scrubber as a function of percentage of RDF burned.

chloride removed. It also increases the outlet concentration (Co) at a given efficiency.

The predominant mechanism of mass transfer for gaseous chloride from the flue gas stream to the scrubbing liquor in the venturi throat is absorption by droplet. A mass balance of gaseous chloride across a small section of the venturi throat can be written as:

$$-G\,dy = K_{OG}a'AP\,(y-y^*)\,dz \qquad (1)$$

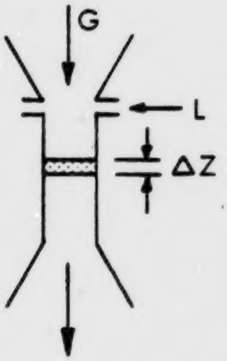

where G = molar flow rate of gas (gmole/sec)

a' = surface area of liquid droplet per unit volume of the throat ($cm^2/cm^3$)

A = throat cross-sectional area ($cm^2$)

P = pressure (atm)

$K_{OG}$ = overall gas phase mass transfer coefficient (gmole/sec $cm^2$ atm)

y = gas soluble component mole fraction (dimensionless)

$y^*$ = gas phase soluble component mole fraction that would be in equilibrium with the bulk liquid concentration of the soluble component

dz = differential element of the venturi length in which gas phase concentration of soluble component changes by "dy" (cm)

Several solutions of Eq. (1) for various diffusional cases have been summarized by Calvert (2). However, the controlling step and other characteristics of diffusional transfer of the soluble component must be known prior to the application of these solutions. Since the diffusional characteristics of the chloride are unknown in this case, these solutions are not used to analyze the operating parameters attributable to the improvement of $\eta$ in the burning of coal plus RDF. However, in the case of dilute gas--with the mole fraction of the soluble component within 5%--Eq. (1) can be integrated to give the number of overall gas phase transfer units:

$$N_{OG} = \int_{P_o}^{P} \frac{dp}{P-Hx} = \frac{K_{OG}a'AZP}{G} \tag{2}$$

where $N_{OG}$ = number of overall gas phase transfer units (dimensionless)

$p$ = partial pressure of the soluble component (atm)

$H$ = Henry's Law constant (atm/mole fraction)

$Z$ = venturi throat length (cm)

$x$ = liquid phase mole fraction (dimensionless)

For constants L/G and H , and in case of cocurrent flow, the overall efficiency can be written as (3):

$$\eta = \frac{P_i - P_o}{P_i} = \frac{1}{\left(1 + \frac{HG}{PL}\right)} \left(1 - \text{Exp} - \left(\frac{K_{OG}a'ZP}{G}\right)\left(1 + \frac{HP}{PL}\right)\right) \tag{3}$$

The diffusional properties of the soluble component (e.g., H, $K_{OG}$) have significant effects on the removal efficiency $\eta$ . If all the operating conditions (a', Z, G/L, P) remain unchanged (see runs 5 and 15, 16 and 17), the gaseous chloro compound with a high $K_{OG}$ will be removed more efficiently than a chloro compound with a low $K_{OG}$. It is realistic to expect that the chemical properties of the gaseous chlorides from RDF burning and from coal burning are different; therefore, the enhancement of the venturi scrubber performance in the gaseous chloride removal in RDF burning can be explained by the more favorable diffusional properties of gaseous chloride emitted from RDF burning. Moreover, RDF cofiring will affect the performance of the venturi scrubber if the following parameters are somehow varied.

L/G ratio - High L/G ratios increase the number of liquid droplets per unit volume of venturi throat, and increase the amount of soluble gas component that can be dissolved. A high L/G increases $\eta$ .

Gas-throat velocity - At a constant L/G, high gas-throat velocities increase mass transfer areas because smaller droplet diameters are the result of higher gas-throat velocities.

Throat length - $\eta$ can be improved by increasing the throat length (Z) as shown by Eq. (1). A longer throat length gives a longer residence time (contact time) for diffusion. However, if the increase in residence time is not due to a longer throat length but rather to a slower gas velocity, $\eta$ may not be improved: i.e., the mass transfer surface area is reduced because of a slower gas velocity.

Performance of the venturi scrubber in gaseous chloride removal in coal and coal plus RDF burnings cannot be compared meaningfully unless the above operating parameters are kept constant.

Emission--

The average venturi scrubber-controlled emission of chloride to the atmosphere is 1.00 ($10^{-2}$) g/MW for coal burning and about 7.58 ($10^{-3}$) g/MW (average) for coal plus RDF burning. Because of the substantial increase in chloride removal efficiency when coal plus RDF is burned, an increase in the uncontrolled chloride emission from RDF cofiring does not significantly affect the atmospheric emission of chloride.

## ESP

Removal Efficiency--

The performance of the ESP in gaseous chloride removal is plotted in Figure 3. The efficiency decreases significantly when RDF is cofired for the following reason.

The efficiency of the ESP in gaseous chloride removal is expected to be low because the primary function of ESP is to collect particulates. The removal of gaseous chloride in the ESP is not well understood; an ESP is not expected to be capable of capturing gaseous pollutants. Absorption of gaseous chloride by moisture condensation in the ESP is unlikely because of the high temperature (350°F) of the flue gas. However, another hypothesis is as follows: since significant constituents of the solid particulate are alkali oxides ($Na_2O$, $K_2O$, CaO), the adsorption of gaseous halides or moisture on the solid particulate can be expected at the gas temperature of 350°F (4). Thus, it is likely that the removal of gaseous chloride in ESP is induced by adsorption on the solid particulates; these, in turn, are captured on the collection plate. The amounts of chloride removed in the ESP for the burning of coal and coal plus RDF are approximately the same. The removal of gaseous halides may be induced and limited by the amount of alkali in the flue gas, if the alkalinities of the flue gases in both burning operations are approximately the same.

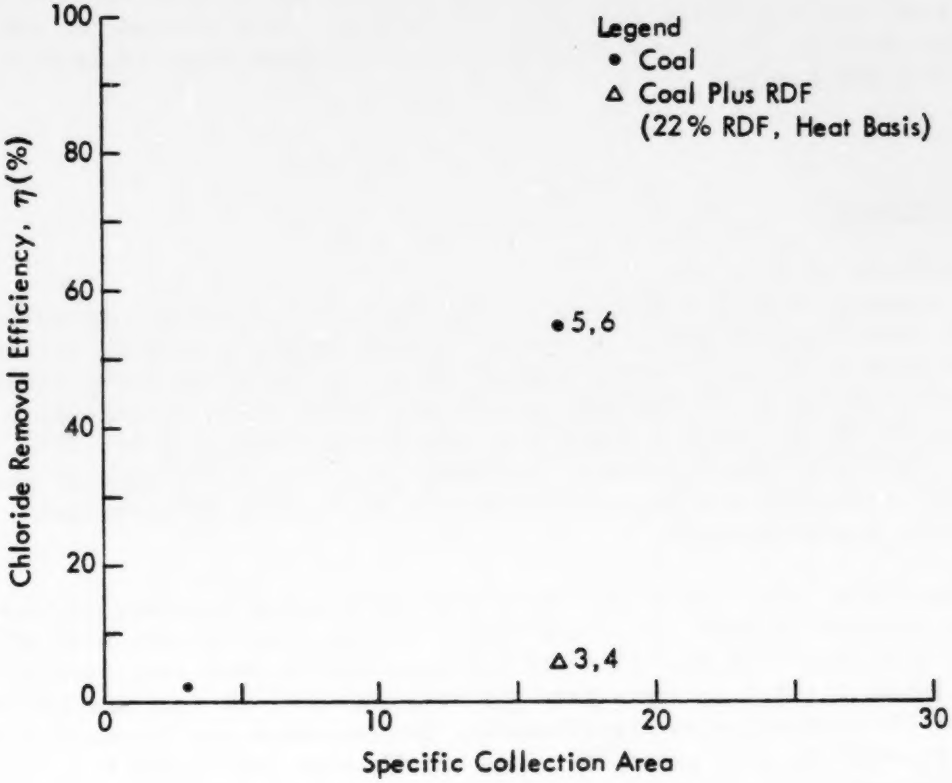

Figure 3. Chloride removal efficiency of ESP as a function of specific collection area.

The inlet chloride concentration of the ESP increases significantly when RDF is cofired; thus, in RDF cofiring, removal of gaseous chloride requires an excessive amount of alkali oxides in the particulate. If the alkalinity of the flue gas is not increased by the cofiring of RDF, RDF cofiring impairs the gaseous chloride removal of the ESP. This impairment is due to the substantial increase in the emission of gaseous chloride. The efficiency of ESP in removing higher concentrations of gaseous chloride, and of gaseous halides in general, decreases.

Emission--

ESP-controlled chloride emission is about 2.59 $(10^{-2})$ g/MW for coal burning and 5.98 $(10^{-1})$ g/MW for coal plus RDF burning. This increase in the ESP-controlled emission of gaseous chloride is due to higher inlet concentration emitted from RDF burning.

## FLUORIDE

### Venturi Scrubber

Removal Efficiency--

The fluoride removal efficiency of the venturi scrubber is plotted in Figure 4. The effect of RDF cofiring on fluoride removal cannot be directly evaluated because of significant fluctuations in the data. With the exception of their different diffusional properties, the collection mechanisms of the venturi scrubber for chloride and fluoride are basically the same. Therefore, the diffusional transfer of gaseous fluoride is the same as that of chloride. However, a unique characteristic of fluoride emission from the RDF cofiring should be noted.

Table 3 shows that elemental composition of fluoride is about 25 times higher in RDF than in coal. One would expect the uncontrolled emission of fluoride to be higher in coal plus RDF burning, than in only coal burning. However, Tables 1 and 2 indicate that RDF cofiring does not increase the uncontrolled fluoride emission significantly, but decreases the uncontrolled fluoride emission in most cases. Most of the fluoride constituents in the RDF are retained in the bottom ash after the combustion, and cofiring RDF in a coal-fired power plant does not affect the emission of fluoride.

Emission--

The average fluoride emission controlled by the venturi scrubber is 6.24 $(10^{-3})$ g/MW for coal burning and 2.56 $(10^{-3})$ g/MW for coal plus RDF burning. In this case, cofiring RDF reduces the atmospheric emission of fluoride from the power plant.

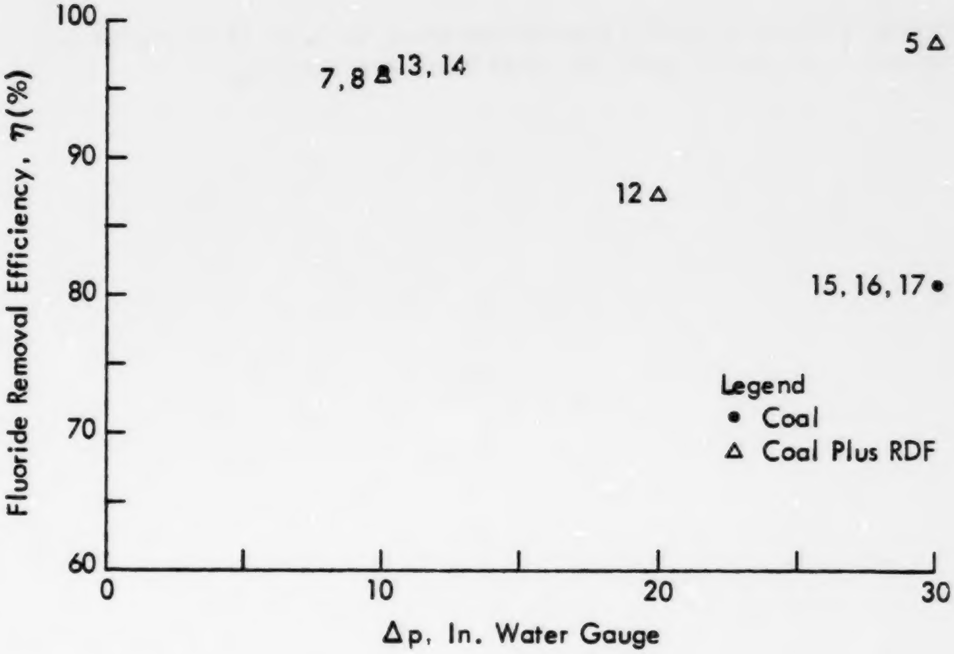

Figure 4. Fluoride removal efficiency of the venturi scrubber as a function of pressure drop across the venturi.

## ESP

### Removal Efficiency--

Figure 5 shows the fluoride removal efficiency of the ESP. Due to randowm fluctuation of the efficiency data in coal burning, the effect of RDF cofiring on the fluoride removal efficiency of ESP cannot be observed. Adsorption of the gaseous fluoride on the solid particulate is the expected phenomenon by which gaseous fluoride is collected in the ESP. Moreover, the amounts of fluoride removed in all data points, except for run Nos. 21, 22, and 23, are approximately the same as in the case of chloride removal in the ESP. These data indicate the limitation of gaseous halides removal by the alkalinity of the flue gas.

### Emission--

The average ESP-controlled fluoride emission is 2.16 ($10^{-2}$) g/MW for coal burning and 3.12 ($10^{-2}$) g/MW for coal plus RDF burning.

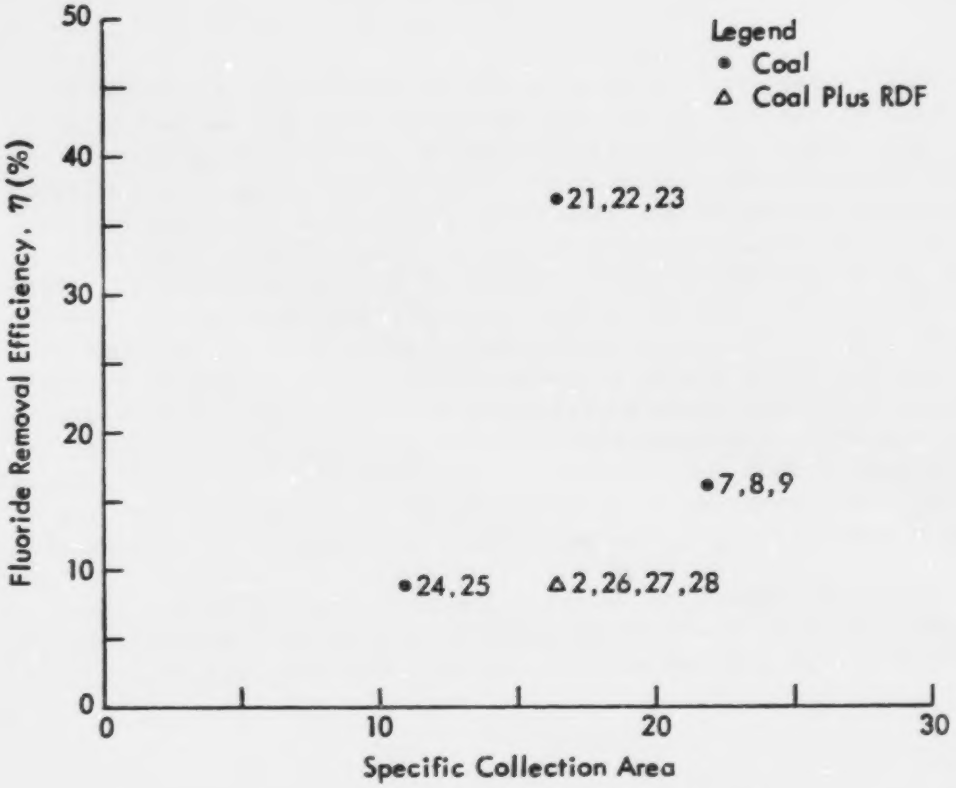

Figure 5. Fluoride removal efficiency of the ESP as a function of specific collection area.

# SECTION 4

## METALS (Pb, Cd, Sb, Fe, and Cu)

As mentioned in Section 2, virtually 100% of the metals were collected in the front half of the SST; hence, all the metals data are assumed to be in solid phase. The removal of solid particulate in both control devices is dependent upon particle size distribution. Because each element is contained or condensed on the surface of the particulate, elemental size distribution data (or elemental enrichment factors in various sizes of solid particulates) are necessary for an analysis of metal removal of both control devices. Furthermore, in the case of stack fly ash from a coal-fired power plant, enrichments of Pb, Cd, and Sb increase with decreasing particle size; enrichments of Fe and Cu are relatively small, or insignificant, with decreasing particle size (5). Hence, total particulate size distribution data do not necessarily correspond to individual elemental size distribution data (enrichment factor). Because of the lack of analysis of elemental enrichments in the inlet particulate, the removal efficiency data for metals cannot be analyzed. Only the direct effect of RDF cofiring on the performance is evaluated in this report.

The following two subsections describe the evaluation of lead and the remaining metals. Lead is discussed separately because, as presented in Tables 2 and 3, lead was analyzed more extensively than the remaining metals.

### LEAD

### Venturi Scrubber

#### Removal Efficiency--

The lead removal efficiency of the venturi scrubber is plotted in Figure 6 as a function of pressure drops across the venturi throat. RDF burning has no significant effect on the lead removal efficiency of the venturi scrubber, in spite of unknown size distribution data for lead.

#### Emission--

As expected, the uncontrolled lead emission is higher in the burning of coal plus RDF than it is in coal only; RDF has a higher lead composition than coal. The average venturi scrubber controlled lead emission to the atmosphere

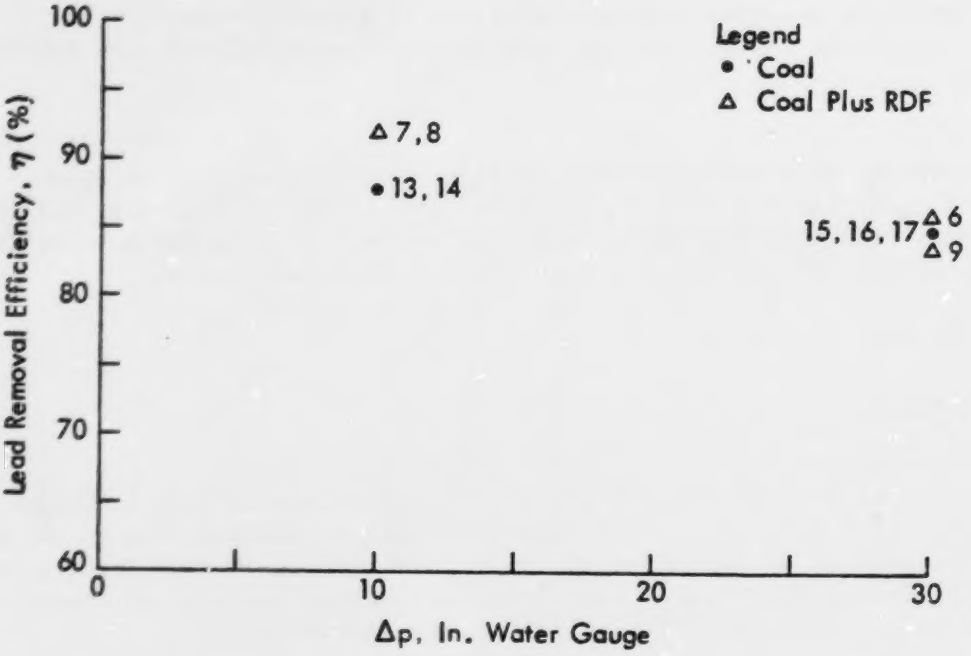

Figure 6. Lead removal efficiency of the venturi scrubber as a function of pressure drop across the venturi throat.

is 9.89 ($10^{-4}$) g/MW for coal burning and 4.39 ($10^{-3}$) g/MW for coal plus RDF burning; the high concentration of lead in the RDF explains why atmospheric lead emission increases in RDF cofiring.

## ESP

### Removal Efficiency--

The lead removal efficiency of the ESP is plotted in Figure 7; this figure shows significant variation in the performance at a fixed specific collection area (see, in particular, the data on the specific collection area of 16.4). A possible explanation for the variation is the difference in lead enrichment factors in the particulates of several samplings. Because of this variation, the effect of RDF cofiring on lead removal efficiency of the ESP cannot be analyzed with precision; it is probably insignificant if the lead enrichment factors are the same in the burning of both coal and coal plus RDF.

### Emission--

The average ESP-controlled lead emission to the atmosphere is about 1.31 ($10^{-3}$) g/MW for coal burning and 4.84 ($10^{-3}$) g/MW for coal plus RDF burning. Again, high lead atmospheric emission in the coal plus RDF burning is expected because RDF has a higher lead concentration than coal.

## Cd, Sb, Fe, Cu

## Venturi Scrubber

### Removal Efficiency--

The removal efficiencies for Cd, Sb, Fe, and Cu are plotted in Figure 8. As in the case of lead, there is no notable effect of RDF cofiring on the removal efficiency of the venturi scrubber for the above elements, despite (a) the limited data points, and (b) the possible variation in the enrichment factor of each element in different particulate samplings.

### Emission--

Inlet concentrations of Cd, Sb, Fe, and Cu increase when coal is cofired with RDF; these increases are mostly due to the higher compositions of these elements in RDF relative to coal. In the case of Fe--which shows less concentration in RDF than in coal by a factor of 1/4--the excessive mass of RDF burned per unit of power output is the likely explanation for the increase in uncontrolled emission of Fe.

The venturi scrubber-controlled emissions of the above elements in both coal and coal plus RDF burning may be compared in Table 4.

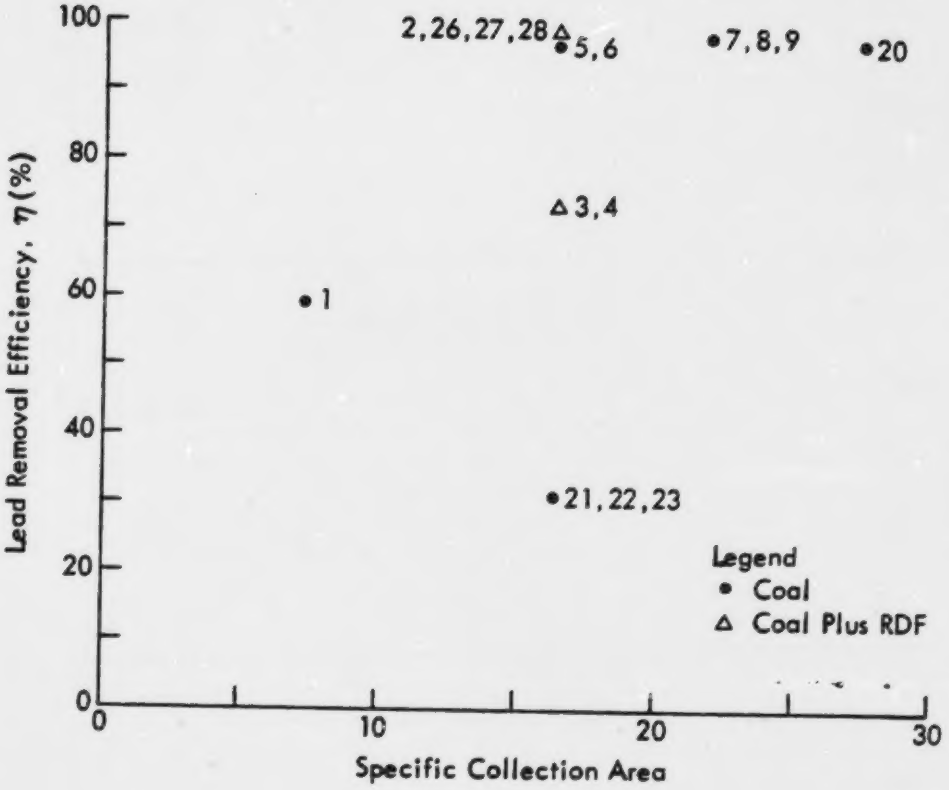

Figure 7. Lead removal efficiency of the ESP as a function of specific collection area.

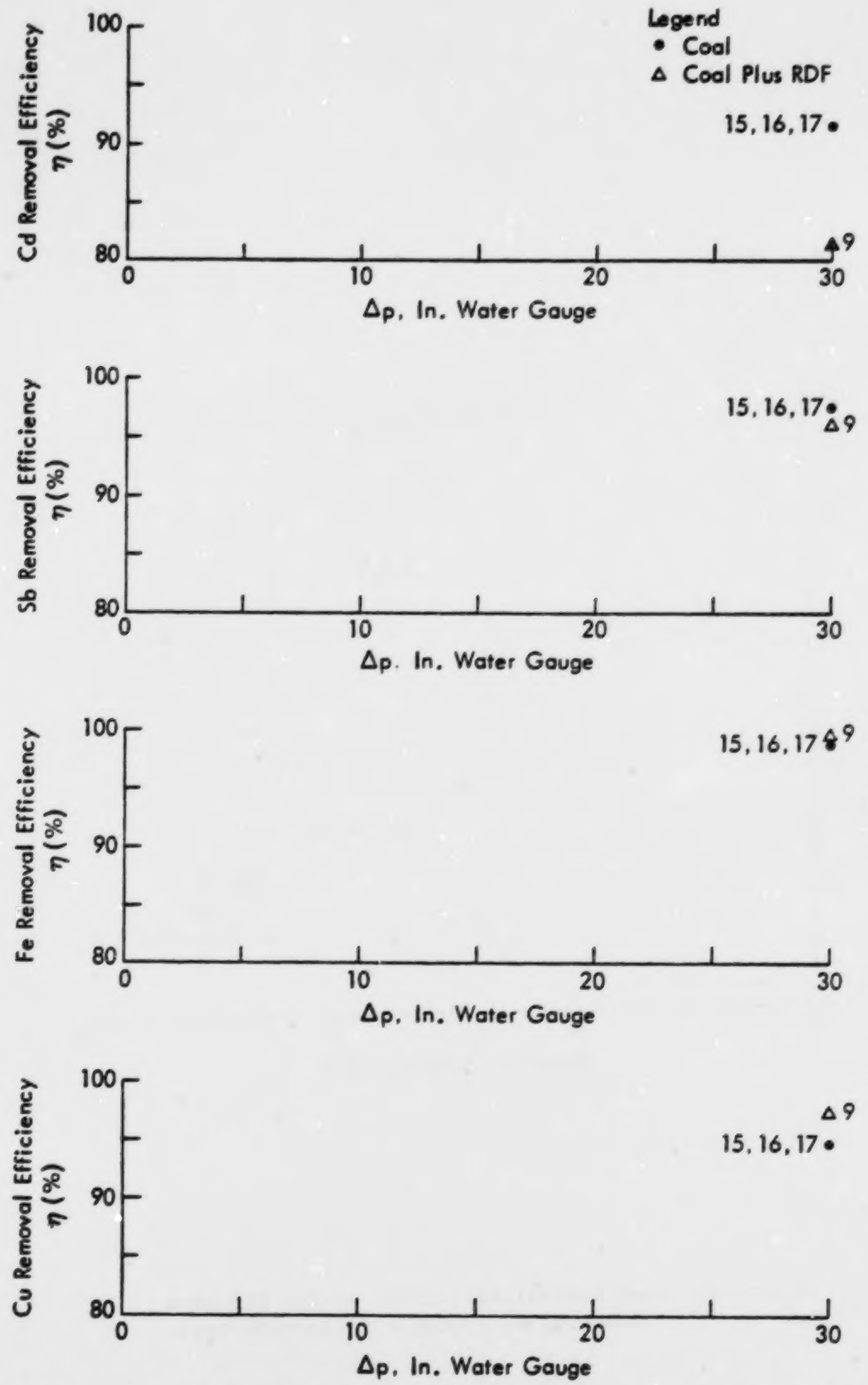

Figure 8. Removal efficiencies of the venturi scrubber for Cd, Sb, Fe, and Cu as a function of pressure drop across the venturi throat.

TABLE 4. EMISSIONS OF Cd, Sb, Fe, AND Cu AT THE VENTURI SCRUBBER OUTLET

| | Coal (g/MW) | Coal plus RDF (g/MW) |
|---|---|---|
| Cd | 1.10 $(10^{-5})$ | 1.01 $(10^{-4})$ |
| Sb | 2.90 $(10^{-5})$ | 6.60 $(10^{-5})$ |
| Fe | 8.77 $(10^{-3})$ | 5.85 $(10^{-3})$ |
| Cu | 5.40 $(10^{-5})$ | 9.80 $(10^{-5})$ |

### ESP

Removal Efficiency--

The removal efficiencies for Cd, Sb, Fe, and Cu are plotted in Figure 9. RDF cofiring has virtually no effect on the removal efficiencies of those elements.

Emission--

The concentrations of these elements in the ESP inlet increase when RDF is cofired, as in the case of the venturi scrubber inlet (see p. 19).

The ESP-controlled emissions of Cd, Sb, Fe, and Cu for both coal and coal plus RDF burning may be compared in Table 5.

TABLE 5. EMISSIONS OF Cd, Sb, Fe, AND Cu AT THE ESP OUTLET

| | Coal (g/MW) | Coal plus RDF (g/MW) |
|---|---|---|
| Cd | 1.00 $(10^{-5})$ | 2.90 $(10^{-5})$ |
| Sb | 1.70 $(10^{-5})$ | 1.80 $(10^{-5})$ |
| Fe | 7.48 $(10^{-3})$ | 7.84 $(10^{-3})$ |
| Cu | 4.10 $(10^{-5})$ | 9.30 $(10^{-5})$ |

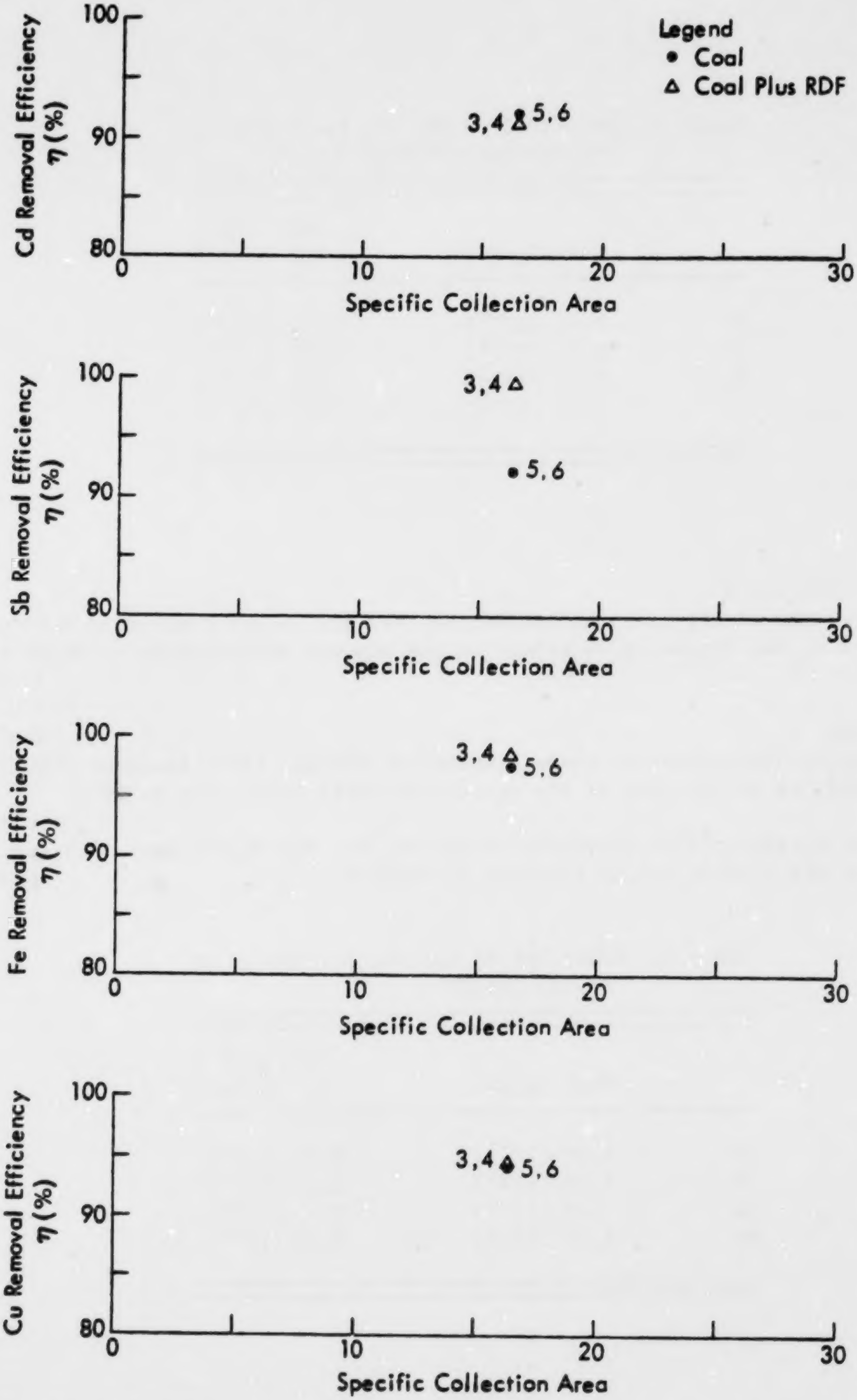

Figure 9. Removal efficiencies of the ESP for Cd, Sb, Fe, and Cu as a function of specific collection area.

# SECTION 5

# CONCLUSIONS

The following conclusions are presented to summarize the effect of RDF cofiring on the controlled emissions of the halides and the metals.

## HALIDES

### Chloride

RDF cofiring increases the chloride emission. However, the chloride removal efficiency of the venturi scrubber improves when RDF is cofired. Due to this improvement, RDF cofiring does not affect the atmospheric emission of chloride if controlled by the venturi scrubber. More favorable diffusional properties of chloride emitted from RDF may be responsible for the improvement.

The performance of ESP in chloride removal decreases with the increase in inlet chloride concentration. Thus, if an ESP is used as the control device, RDF cofiring increases the atmospheric emission of chloride.

### Fluoride

Most of the fluoride constituents in the RDF are retained in the bottom ash after the combustion. Because of this retention, RDF cofiring does not affect the controlled emission of fluoride. The effects of RDF cofiring on fluoride removals in the venturi scrubber and in the ESP cannot be evaluated because of data fluctuation.

## METALS (Pb, Cd, Sb, Fe, and Cu)

The atmospheric emissions of the subject metals, either controlled by the venturi scrubber or the ESP, generally increase when RDF is cofired. High elemental compositions of the metals in RDF is one reason for the increase in the atmospheric emission of the metals. Another reason is the low heating value of RDF compared to coal and the consequent increase in the trace metal content in the feedstock.

Because of the lack of elemental enrichment factors in the solid particulate, the effect of RDF cofiring on the removal of metals in the venturi scrubber and in the ESP cannot theoretically be analyzed. However, the performance data of both control devices indicate that RDF cofiring has no important effect on the removal of metals.

## REFERENCES

1. Private communication with PEDCo.

2. Calvert, S. Scrubber Handbook. Ambient Purification Technology, Inc., July 1972.

3. Stern, A. C. Air Pollution, Vol. III, 2nd Edition, Academic Press, Inc., 1968.

4. White, H. J. Electrostatic Precipitation of Fly Ash. Journal of the Air Pollution Control Association, Vol. 27, No. 2, February 1977.

5. Coles, D. G., R. C. Ragaimi, and J. M. Ondov. Chemical Studies of Stack Fly Ash From a Coal-Fired Power Plant. Environmental Science and Technology, Vol. 13, No. 4, April 1979.

# APPENDIX

## CALCULATION PROCEDURE

The mass of each element emitted per unit power generated is calculated as follows:

$$\text{Emission factor}\left(\frac{\text{g}}{\text{MW}}\right) = \text{elemental concentration}\left(\frac{\text{g}}{\text{dscm}}\ \text{in the flue gas}\right)$$

$$\times\ \text{amount of flue gas generated per unit of heat input}\left(\frac{\text{dscm}}{\text{M Btu}}\right)$$

$$\div\ \text{total power generated (MW)}$$

Data for the amount of flue gas generated per unit of heat input are tabulated below:

| % RDF (heat input basis) | Flue gas generated / Heat input $\left(\frac{\text{dscm}}{\text{M Btu}}\right)$ |
|---|---|
| 0 | 335.5 |
| 10 | 333.5 |
| 25 | 330.6 |

# GLOSSARY

## Nomenclature (Latin)

a' = surface area of liquid droplet per unit volume of the venturi throat ($cm^2/cm^3$)

A = throat cross-sectional area ($cm^2$)

C = concentration ($g/cm^3$)

G = molar flow rate of gas (gmole/sec)

H = Henry's Law constant (atm/mole fraction)

L = scrubbing liquid flow rate (gmole/sec)

$K_{OG}$ = overall gas phase mass transfer coefficient (gmole/sec $cm^2$ atm, dimensionless)

$N_{OG}$ = number of overall gas phase transfer units (dimensionless)

P = pressure (atm)

p = partial pressure (atm)

x = liquid phase mole fraction (dimensionless)

y = gas soluble component mole fraction (dimensionless)

$y^*$ = gas soluble component mole fraction that would be in equilibrium with the bulk liquid concentration of the soluble component (dimensionless)

Z = throat length (cm)

## Greek

$\eta$ = efficiency (dimensionless)